A comprehensive C/EBPβ interactome

Dissertation

zur Erlangung des akademischen Grades

doctor rerum naturalium

(Dr. rer. nat.)

im Fach Biologie / Molekularbiologie

eingereicht an der

Lebenswissenschaftlichen Fakultät

der Humboldt-Universität zu Berlin

von

Julia Wiebke Böhm, Dipl. Biologin

Präsident der Humboldt-Universität zu Berlin

Prof. Dr. Jan-Hendrik Olbertz

Dekan der der Lebenswissenschaftlichen Fakultät

Prof. Dr. Richard Lucius

Gutachter:

1. Prof. Dr. Achim Leutz

2. Prof. Dr. Udo Heinemann

3. Prof. Dr. Matthias Selbach

Eingereicht am: 29.01.2015

Tag der mündlichen Prüfung: 26.06.2015

Contents

ZUSAMMENFASSUNG

Der Transkriptionsfaktor CCAAT/enhancer-binding Protein β (C/EBPβ) reguliert die Expression zahlreicher Gene, welche die Proliferation, Differenzierung und Seneszenz in hämatopoietischen Zellen, Adipozyten, Hepatozyten und Leukämiezellen kontrollieren. Um diese mannigfaltigen Aufgaben zu erfüllen interagiert C/EBPβ mit zahlreichen Kofaktoren und Proteinen der Transkriptionsinitiations- und Transkriptionsrepressions-Maschinerie. Da das funktionale Netzwerk von C/EBPβ und seinen zahlreichen Kooperationspartnern bis heute nicht vollständig entziffert ist, ist es das Ziel dieser Arbeit das Netzwerk aus Interaktionspartnern und C/EBPβ regulierten Proteinen in Leukämiezelllinien und darüber hinaus zu erforschen und aufzudecken. Das Interaktom von C/EBPβ wurde mittels einer Kombination aus einem membranbasierten Peptid-Interaktions Testverfahrens (APS) und endogener Immunprezipitationen mit gekoppelter MS-Analyse untersucht. Außerdem wurde die Proteinmenge von C/EBPβ und die potentiell von C/EBPβ regulierten Proteine mittels proteomischer MS-Analyse in C/EBPβ Knock-out- und Leukämiezelllinien untersucht. Die Daten dieser Arbeit erweitern das Wissen über das Protein-Interaktom von C/EBPβ und zeigen zahlreiche neue Interaktoren, sowie potentielle Protein-komplexe als C/EBPβ Interaktoren auf. Die Protein-Interaktionsversuche ergaben epigenetische und allgemeine transkriptionsregulierende Proteine, sowie Chromatinstruktur modellierende Faktoren, die mit C/EBPβ interagieren. Überdies eröffnen die Versuchsergebnisse Interaktionen von C/EBPβ mit Proteinen, deren Aufgabe die Regulation von mitotischem Chromatin und des Zellzyklusses ist. Die Interaktionsdaten beinhalten auch Proteine, die in RNA-Polymerase Komplexen, dem SWI/SNF-Chromatinremodeling Komplex oder MLL-Histonemethyltransferase Komplexen vorkommen. Zusätzlich konnten neue Interaktionen von C/EBPβ mit Kondensin- und Kinetochorproteinen beobachtet werden. Die Daten dieser Studie eröffnen überdies neue Interaktionen von C/EBPβ mit DNA Reparatur (DNA damage response) und Apoptose assoziierten Proteinen. Interessanterweise konnten auch Komponenten des Spliceosomes und

Proteine, die mit RNA-Prozessierung assoziiert sind, als Interaktoren von C/EBPβ identifiziert werden. Diese Beobachtungen deuten auf Funktionen des Transkriptionsfaktors C/EBPβ hin, die über die Regulation von Genexpression und Chromatinorganisation hinausgehen. Mit Hilfe der proteomischen-MS Untersuchungen konnten überdies potentielle C/EBPβ regulierte Proteine identifiziert werden, die in Energie-Metabolismus und Kinase-Signalwegen involviert sind. Zusammenfassend ermöglicht diese Studie nicht nur die Verifikation von bereits bekannten Proteininteraktionen von C/EBPβ, sondern eröffnet zahlreiche weitere zukünftige Forschungsfelder bezüglich des funktionellen Netzwerkes des Transkriptionsfaktors C/EBPβ in Leukämien, sowie anderen Zellarten und Geweben.

Stichwörter: C/EBPβ, konservierte Proteindomänen/CRs, transkriptionelle Regulation, Protein-Protein Interaktionsnetzwerk, Leukämie, Metabolismus

SUMMARY

The basic leucine zipper transcription factor CCAAT/enhancer-binding protein β (C/EBPβ) regulates the expression of multitudinous genes that control the proliferation, differentiation and senescence of haematopoietic cells, adipocytes, hepatocytes and leukemia cells. To facilitate its multifaceted functions C/EBPβ interacts with a collection of cofactors and proteins of the transcription initiation as well as the gene repression machinery. Since the functional network of C/EBPβ and its numerous cooperation partners is still incomplete this study attempted to analyze interaction partners and downstream proteins of C/EBPβ in leukemia cells and beyond. A combinatory approach of an array based peptide-interaction screening (APS) and endogenous shotgun IP-MS from leukemia cell lines was applied to elucidate the interactome of C/EBPβ. Moreover, C/EBPβ abundance and potential C/EBPβ regulated proteins were determined by MS proteomics in C/EBPβ knockout and leukemia cell lines. The data presented here largely expands previous knowledge of the C/EBPβ interactome and discloses a plethora of novel C/EBPβ interactors and potential protein complexes. The interaction screenings revealed proteins associated with the general and epigenetic regulation of transcription, with chromatin remodeling and mitotic chromatin organization as well as cell cycle regulation. Among those interactors were members of the RNA-Polymerase complexes, the SWI/SNF chromatin remodeling complex or MLL histone methyltransferase complexes. Additionally, new interactions of C/EBPβ with condensin and kinetochore proteins could be elucidated. The data also reports of novel C/EBPβ interactors involved in DNA damage response and apoptosis. In addition, components of the spliceosome and RNA-processing were detected, suggesting extended functions of C/EBPβ beyond gene and chromatin regulation. Furthermore, potential C/EBPβ regulated proteins involved in energy metabolism and kinase pathways were discovered. Altogether this study verifies known and reveals various novel spheres of activity of the transcription factor C/EBPβ and augments the network of previous reported functions and cooperation partners. The here collected data discloses new

subjects for further research concerning the role and functional network of C/EBPβ during cell differentiation and in leukemia.

Keywords: C/EBPβ, conserved protein domains/CRs, transcriptional regulation, protein-protein interaction network, leukemia, metabolism.

INTRODUCTION

1.1 Transcription factors

The expression of genes is initiated and regulated by a multitude of cellular signaling pathways. Transcription factors act at the tip of these pathways recruiting components of the transcription machinery and associated co-factors to gene promoters.
Transcription factors are often characterized and grouped into families according to their highly conserved DNA-binding domains that recognize specific sites on DNA. The majority of those protein families possess either DNA recognizing helix-turn-helix motifs, helix-loop-helix motifs, homeodomains, leucine zippers, zinc fingers or other metal ion-binding domains (for overview see: Pabo and Sauer, 1992). Most of the DNA binding proteins attach to DNA at the major groove of the helical structure forming hydrogen bounds with the phosphodiesters of the DNA-backbone. Some DNA binding proteins interact with the sugar group of the nucleobases, preferably with purines such as guanine (for overview see: Pabo and Sauer, 1992). The number of possible binding sites on DNA is increased by the ability of homo and especially heterodimer formation between transcription factors.

1.2 Family of basic leucine zipper DNA-binding domain proteins

One of the families of transcription factors that are able to form homo- and heterodimers is the family of basic leucine zipper domain proteins. The basic leucine zipper consists of two subdomains: the DNA binding basic region and the leucine zipper domain. The leucine zipper facilitates homo- and hetero dimerization with other proteins carrying leucine zipper domains.

Basic leucine zipper domains are also called “bZIP”(basic-zipper) domains due to the before mentioned dual domain structure. BZIP domains are usually 60-80 amino acids long while the basic region covers about 30 amino acids (Hope and Struhl, 1986; Landschulz et al., 1988). The bZIP domain carries two α-helical structures forming a coiled-coil structure that contacts the major groove of B-helical DNA. The DNA affinity of the basic region arises mostly from its high content of charged arginine and lysine residues (Agre et al., 1989; Kerppola and Curran, 1991).

1.3 The CCAAT box and the family of CCAAT/enhancer-binding proteins

Mammalian promoters are characterized by several conserved sequence boxes that are identified and bound by specific transcriptional regulator proteins (Chodosh et al., 1988). One of those elements is the evolutionary highly conserved CCAAT box motif that is a common element in eukaryotic class 2 promoters and usually locates between -50 and -110 bp in front of the transcriptional start site (Bi et al., 1997; Chodosh et al., 1988; Dorn et al., 1987; Hatamochi et al., 1988; McKnight and Tjian, 1986; Raymondjean et al., 1988).

A protein family that was discovered to bind to CCAAT box motifs as well as enhancer core elements is the family of CCAAT/enhancer-binding proteins (C/EBPs) (Landschulz et al., 1988; Johnson et al., 1987). The family of CCAAT/enhancer-binding proteins consists of six transcription factors C/EBP α, β, δ, ε, γ and ζ that bind with their C-terminal DNA-binding domain (DBD) to homologous sites on DNA (Osada et al., 1996; Mahoney et al., 1992; Akira et al., 1990; Ryden and Beemon, 1989; Figure 1 and 2).

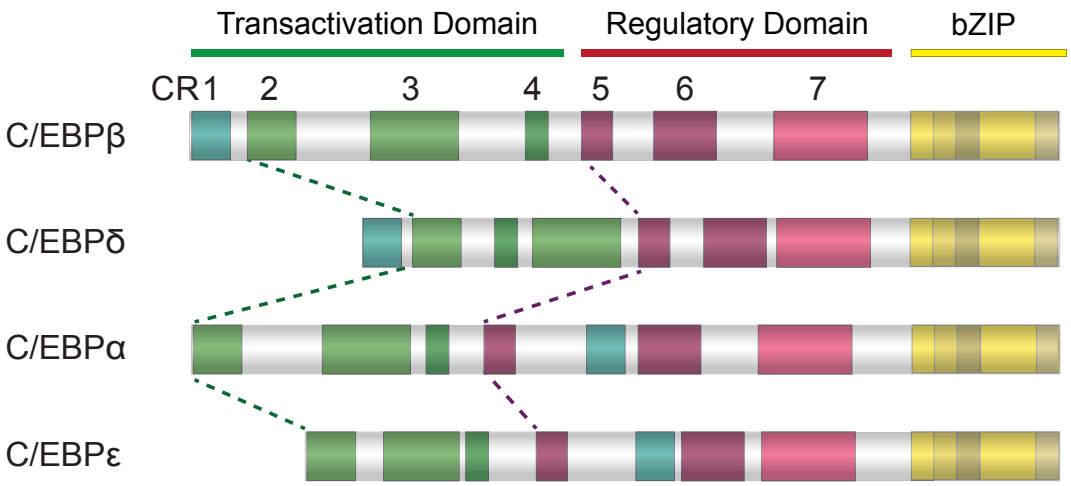

Figure 1: The C/EBP family members α, β, δ and ε share 9 highly conserved regions (CRs) forming a transactivation domain (TAD; depicted in green) that spans from CR1-4, a regulatory domain (RD; depicted in red) which encloses CR 5-7, a DNA binding domain and a basic leucine-zipper (bZIP; CR8-9; depicted in yellow) domain. The CRs are divided by interspersed low complexity regions (LCRs; depicted in grey). The scheme is modified after Ramji and Foka, 2002 and Leutz et al., 2011.

The C/EBP family members share a conserved C-terminal bZIP (Figure 1), which enables the formation of homo- and heterodimers among the C/EBP family members or with other bZIP transcription factors like those of the ATF family (Tsukada et al., 1994; 2011; Vallejo et al., 1993; Vinson et al., 1993; Landschulz et al., 1989). Homodimerization of two C/EBP proteins facilitates binding to the general C/EBP recognized CCAAT box DNA-sequence "A/GTTGCGC/TAAC/T" or the ideal "ATTGC-GCAAT" motif (Landschulz et al., 1988; Mahoney et al., 1992; Miller et al., 2003; Figure 2). The number of possible DNA motifs that could be recognized is extended even more by the possibility of heterodimerization of two different bZIP domain proteins (Huber et al., 2012; Podust et al., 2001; Tsukada et al., 1994; 2011).

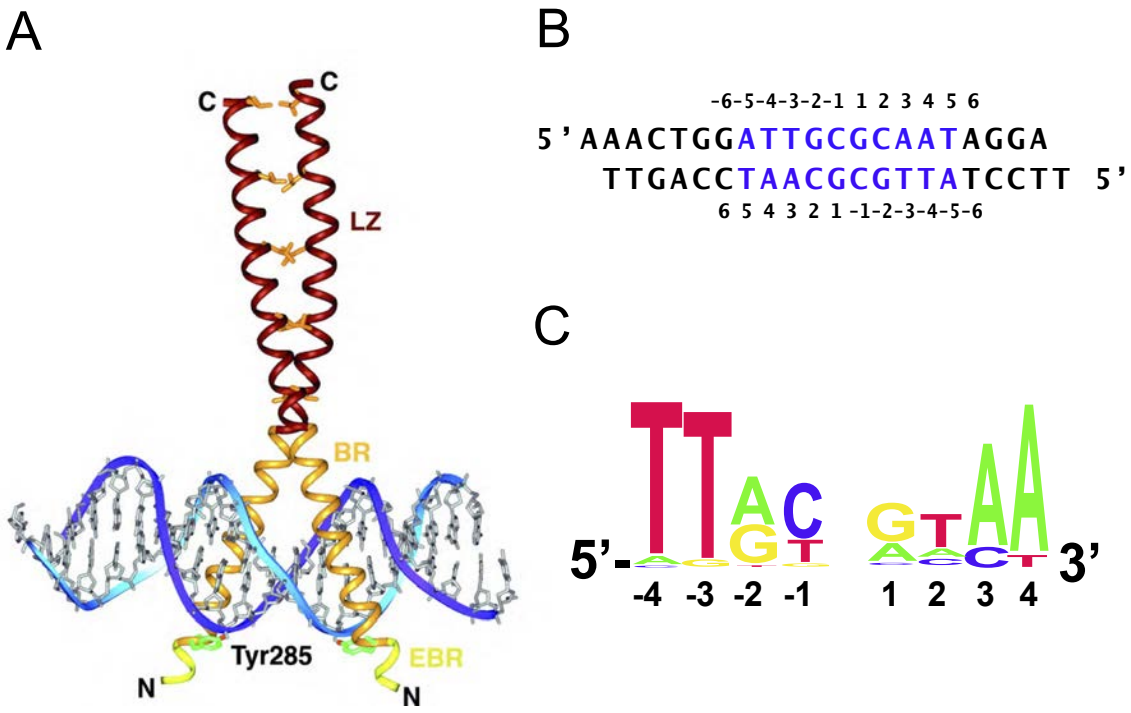

Figure 2: DNA binding domain and recognition motif of C/EBP family members. A) Depicted is the proposed structure of a C/EBPα homo-dimer with DNA. The leucine zipper (LZ) domains are depicted in red, the basic regions, which contact the DNA, are colored in orange and the extended basic regions (EBR) that span beyond the DNA are depicted in yellow (the DNA backbone is depicted in blue, the sugar structures in grey) (derived from Miller et al., 2003). B) Complement DNA sequence of the proposed binding site of C/EBPα (Miller et al., 2003). C) The general DNA sequence consensus motif proposed for the C/EBP family by Mahoney et al., 1992.

Knockout experiments suggest that C/EBPβ and α are the most essential members of the C/EBP family. Knockout of these two C/EBPs demonstrates early embryonic lethality and defective tissue specification (Begay et al., 2004). Besides partially redundant functions of the C/EBPα/β proteins, deletion mutants of either gene caused organ specific defects like disturbed skin functions, liver regeneration or innate immunity (Hirai et al., 2006; Screpanti et al., 1995; Tanaka et al., 1995).

The *CEBPB* gene encodes an intron-less transcript which is translated into three isoforms, namely the long LAP* and LAP and the short LIP isoform (Dey et al., 2012; Ramji and Foka, 2002; Descombes and Schibler, 1991; Figure 3). The *CEBPB* gene contains three in-frame start codons and an upstream open reading frame (uORF) that is located out

of frame between the initiation codons of the LAP* and LAP isoforms. The transcription of the short LIP isoform is mediated by the uORF element that induces leaky scanning after transcription initiation at the promoter followed by re-initiation of transcription at the ORF-internal third start codon (Wethmar et al., 2010; Xiong et al., 2001; Calkhoven et al., 2000). Alternative translation of the *CEBPB* gene depends on the activity of the translation initiation machinery and in particular on mTOR activity (Esteves et al., 2012; Calkhoven et al., 2000).

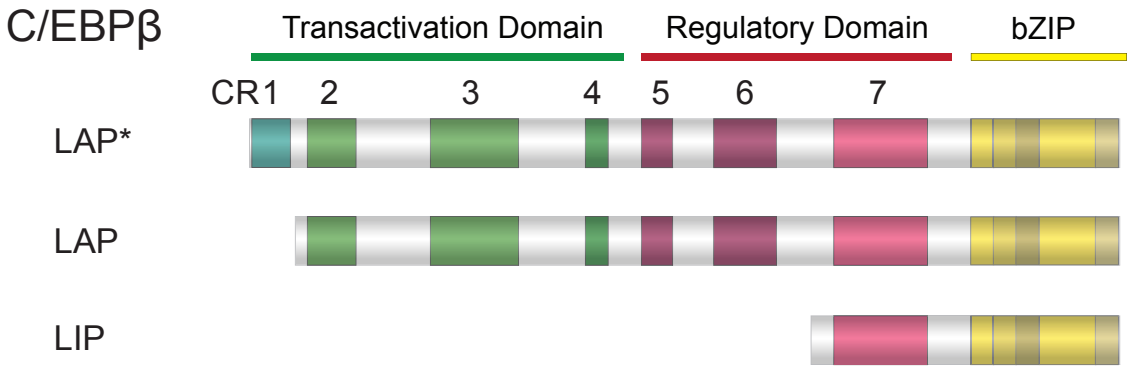

Figure 3: The C/EBPβ protein possesses 9 highly conserved regions (CRs) grouping into the transactivation domain (TAD; depicted in green; covering CR1-4) a regulatory domain (RD; depicted in red; enclosing CR 5-7) a DNA binding domain and a basic leucine-zipper domain (bZIP; depicted in yellow) (modified after Leutz et al., 2011). The conserved regions are intermitted by interspersed low complexity regions (LCRs; depicted in grey). Depicted are the three C/EBPβ isoforms LAP*, LAP and LIP. The LAP* and LAP isoforms share the last 8 C-terminal CRs, while the N-terminal CR1 is exclusively present in the LAP* isoform. The truncated LIP isoform shares the conserved region 7 of the regulatory domain and the bZIP domain with the other two isoforms, but lacks the complete transactivation domain (Scheme is modified after Ramji and Foka, 2002).

The long C/EBPβ LAP* and LAP isoforms harbor the transactivation domain (Figure 3) and are understood to be effective activators of target genes (Kowenz-Leutz and Leutz, 1999; Williams et al., 1995). The truncated LIP isoform completely lacks the transactivation domain (TAD) and part of the regulatory domain (RD) domain. LIP has been shown to act as a dominant negative regulator of the two long activating C/EBPβ isoforms (Zahnow, 2009; Ramji and Foka, 2002) and C/EBPβ target genes (Smink and Leutz, 2010; Smink et al., 2009). Moreover, the ratio between the long LAP* and LAP isoforms and the short LIP isoform affects the regulation of C/EBPβ target genes influencing various cell differentiation

processes and tumorigenesis (Seagroves et al., 1998; Luedde et al., 2004; Nerlov et al., 2007; Smink and Leutz, 2010; Smink et al., 2009).

1.4 C/EBP transcription factors share a modular structure

The C/EBP transcription factor family members C/EBPα, β, δ and ε share nine highly conserved regions. The conserved regions (CRs) of all family members form a transactivation domain (TAD), a regulatory domain (RD), a DNA binding domain and a basic leucine-zipper (bZIP) domain (Ramji and Foka, 2002; Figure 1). The TAD of C/EBPβ includes the N-terminal first four conserved regions (CR1-4, contained in the activating isoforms LAP* and CR2-4 present in LAP; Figure 3) and is understood to mediate the interaction with various proteins and protein-complexes. The TAD of C/EBPβ was shown to mediate the interaction with the SWI/SNF chromatin remodeling complex, which shuffles nucleosomes along the DNA and thereby facilitates the binding of the gene transcription machinery. In this context, the LAP*-isoform specific CR1 region is essential for granulocytic transdifferentiation by facilitating SWI/SNF recruitment (Stoilova et al., 2013). Moreover, the TAD CR1 region was suggested to mediate the interaction of LAP* with Myb facilitating the transactivation of myeloid genes like mim-1/ *LECT2* (Kowenz-Leutz et al., 1999). The TAD region of C/EBPβ was shown to be essential for the interaction with the histone acetyltransferases (HATs) CBP/p300 (Mink et al., 1997; Guo et al., 2001; Kovacs et al., 2003). The interplay between C/EBPβ and the HATs leads to target gene activation. C/EBPβ has been linked to gene repression as well (Di-Poi et al., 2005; Descombes and Schibler, 1991). In accordance with this the TAD of C/EBPβ not only mediates the interaction with proteins that positively regulate gene expression but also with transcriptional repressors. The TAD of C/EBPβ is known to interact with transcriptional co-repressors like NCOR2 that recruits histone deacetylases (HDACs) to gene promoters facilitating transcriptional silencing (Ki et al., 2005). Finally, the TAD containing LAP* and LAP isoforms, but not the truncated LIP isoform, have the ability to induce transdifferentiation of B-cells to myeloid cells (Stoilova et al., 2013).

The regulatory domain (RD) contained in all three isoforms (Figure 3) harbors the

conserved regions five, six and seven. The RD is considered to serve as a negative internal regulator sequence counteracting the activating function of the TAD (Williams et al., 1995). Indeed the deletion of the RD of C/EBPβ (CR5,6,7) entails an enhanced transdifferentiation potential concerning B-cell to myeloid transdifferentiation (Stoilova et al., 2013). This is emphasized by the observation that a deletion of the RD (CR5,6,7) or at least CR5 and CR7 amplifies the transactivation potential of C/EBPβ significantly. In contrast to this the CR6 domain appears to be opposing the repressive effect of the CR5 and 7 by stabilizing an active conformational state of C/EBPβ (Kowenz-Leutz et al., 1994). The RD is also known to be the target for posttranslational modifications that regulate C/EBPβ activity and protein-protein interactions (Leutz et al., 2010; Kowenz-Leutz and Leutz, 1999; Nakajima et al., 1993).

1.5 C/EBPβ is regulated by a multitude of PTMs

Numerous signaling pathways like the Ras, STAT, TNFα and TGFβ pathway regulate C/EBPβ functions through various posttranslational modifications (PTMs) like phosphorylation, acetylation or methylation (Leutz et al., 2011; Kowenz-Leutz et al., 2010; Ramji and Foka, 2002; Buck et al., 2001). Protein-protein interactions of C/EBPβ are influenced by PTMs. These PTMs can be subdivided into modifications that attract or repel protein-protein interactions or do not affect protein interplay at all. Multitudinous arginine and lysine methylations as well as lysine acetylations and SUMOylation of C/EBPβ have been described (Leutz et al., 2010; Berberich-Siebelt et al., 2006; Eaton et al., 2003; Kim et al., 2002).

The most extensively described PTMs of C/EBPβ are phosphorylations of serine or threonine residues. For example the phosphorylation of C/EBPβ CR7 at Thr235 (human; Thr-189 in rat; Thr-188 in mouse; RD) by the receptor tyrosine kinases ERK1/2, which is part of the Ras/MAPK signaling pathway (Nakajima et al., 1993; Figure 4). This modification was shown to influence further modifications of C/EBPβ as well as its activity. The C/EBPβ phosphorylation by ERK1/2 blocks the transcriptionally repressive methylation of C/EBPβ at Arg3 (R3) by CARM1/PRMT4. The C/EBPβ Thr235 phosphorylation leads to a conformational change enabling the interaction with transcriptional activators like the Mediator-

and the SWI/SNF-complexes (Kowenz-Leutz et al., 2010; Mo et al., 2004; Sato et al., 2004; Kowenz-Leutz and Leutz, 1999). The interaction with the SWI/SNF complex is essential for subsequent activation of myeloid and adipogenic C/EBPβ target genes, as well as adipogenic differentiation (Kowenz-Leutz et al., 2010).

In addition, TGFβ-signals induce the phosphorylation of C/EBPβ on Ser105 (rat) (Thr217 in mouse) by the MAPK-downstream kinase RSK2 and stimulate hepatocyte proliferation (Buck et al., 1999). The protein kinase C (PKC) was revealed to phosphorylate C/EBPβ at Ser105 as well, enhancing the transactivation activity of the LAP isoform (Trautwein et al., 1993). The phosphorylation of C/EBPβ by GSK-3 at Ser184 (mouse) is considered to be important concerning target gene activation by the LAP isoform (Piwien-Pilipuk et al., 2001). This GSK-3 phosphorylation marks increased C/EBPβ transcriptional activity, whereas the modification by the protein kinase C (PKC) especially on Ser299 is understood to prohibit C/EBPβ DNA binding ability (Mahoney et al., 1992). Modifications of C/EBPβ are also important for its cellular localization. The phosphorylation at Ser299 by protein kinase A (PKA) is essential for nuclear translocation of C/EBPβ (Chinery et al., 1997; Trautwein et al., 1994; 1993). C/EBPβ is also a target of the cell cycle kinases CDK2 and CDC2 that were shown to phosphorylate Ser-64 (rat) and the ERK1/2 target site Thr-189 (rat; Thr-188 mouse) in a cell cycle dependent manner (Shuman et al., 2004; Figure 4).

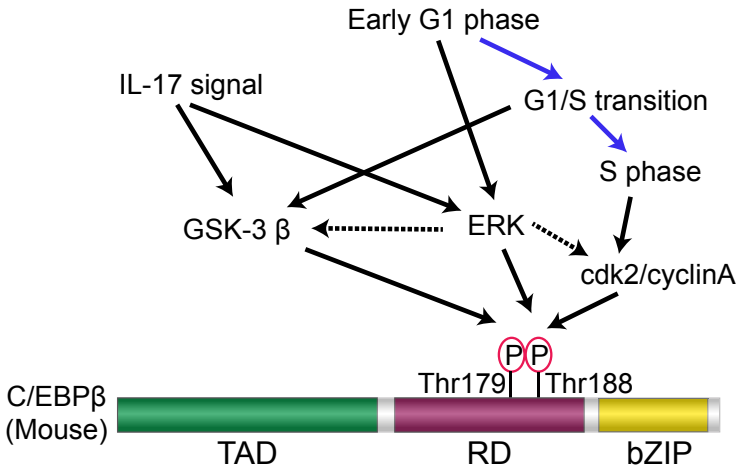

Figure 4: Different cellular signal transduction pathways induce the phosphorylation of C/EBPβ at threonine 179 and/or 188 (mouse) in the regulatory domain (RD). Depicted are exemplary interleukin involving pathways activating GSK-3β and the MAPKinase ERK1 as well as cell cycle associated signals inducing phosphorylation of C/EBPs by ERK1 or the Cyclin-dependent kinase 2 (cdk2). The scheme is modified after Tsukada et al., 2011.

The activity of C/EBPβ can be negatively regulated by methylation of lysines and arginines. The repressive arginine methylation at C/EBPβ R3 by CARM1/PRMT4 prohibits interaction of C/EBPβ with the SWI/SNF complex, as described before. The lysine methylation of K39 in the TAD of C/EBPβ by the histone H3K9 methyltransferase G9a was shown to repress C/EBPβ target gene activation as well. This mechanism was confirmed by a lysine-to-alanine exchange at K39 that prohibited this modification and simultaneously hyper-activated expression of the C/EBPβ target gene mim-1/*LECT2* (Pless et al., 2008).

1.6 C/EBPβ interacts with epigenetic modifiers to regulate gene expression

C/EBPβ plays a significant role in cell differentiation, proliferation and tumor development and promotion in various cell types suggesting a regulation of its activity by numerous PTMs and substantial cooperation with a multitude of different proteins. In particular C/EBPβ

was associated with myeloid differentiation, bone metabolism as well as with adipogenesis amongst others by regulating the expression of various genes (Esteves et al., 2013; 2012; Smink and Leutz, 2010; Smink et al., 2009; Zwergal et al., 2006; Gorgoni et al., 2002; Ramji and Foka, 2002; Screpanti et al., 1995). C/EBPβ was shown to interact with various epigenetic regulators like histone modifying proteins or chromatin remodeling complexes to fulfill its transcriptional regulatory tasks in cell differentiation and disease (Ki et al., 2005, Di-Poi et al., 2005). C/EBPβ is known to interact with the HATs CBP/p300 (Kovacs et al., 2003; Mink et al., 1997).

As mentioned before, C/EBPβ is capable of transcriptional repression as well (Descombes and Schibler, 1991; Di-Poi et al., 2005; Tsukada et al., 2011). Negative regulation of gene expression can be mediated by the removal of histone acetylations and activating histone tail methylations, followed by the establishment of transcriptionally repressive histone tail methylations. C/EBPβ was shown to repress PPARβ expression by recruiting a histone deacetylase 1 (HDAC-1) containing repressor complex to the PPARβ promoter (Di-Poi et al., 2005). The study of Ki et al. described the interaction of the C/EBPβ TAD with the histone deacetylase recruiting co-repressors NCOR2/SMRT and NCOR1 (Ki et al., 2005).

1.7 The role of C/EBPβ in differentiation

C/EBPβ plays a role in myelopoiesis and macrophage functions, emergency granulopoiesis and neoplastic transformation (Hirai et al., 2006; Tanaka et al., 1995; Natsuka et al., 1992). The three different isoforms of C/EBPβ, as well as the their ratio to each other, achieve different functions during mammary gland development (Seagroves et al., 1998), liver regeneration (Luedde et al., 2004) and bone metabolism (Smink and Leutz, 2010; Smink et al., 2009). C/EBPβ plays a vital role in osteogenesis by cooperating with the transcription factors Runx2 or ATF4 during osteoblast differentiation (Tominaga et al., 2008; Hata et al., 2005). The translation of the truncated C/EBPβ LIP isoform is upregulated during osteoblast differentiation and LIP interacts with RUNX2 to promote the differentiation of osteoblasts (Hata et al., 2005). C/EBPβ is a target gene of the mTOR pathway and low mTOR levels

lead to enhanced expression of the two long C/EBPβ isoforms simultaneously decreasing LIP transcription. This enhanced translation of the activating LAP* and LAP isoforms induces MafB expression, a transcription factor vital for different developmental processes. MafB suppresses osteoclastogenesis by interacting with several inhibiting transcription factors (Smink and Leutz, 2010; Smink et al., 2009).

C/EBPβ plays an important role in mammary gland development, proliferation and functional differentiation of mammary epithelial cells. The two studies of Robinson et al. and Seagroves et al. report impaired mammary ductual morphogenesis and inhibited expression of the characteristic milk proteins β-casein and WAP in the mammary gland of C/EBPβ knockout mice (Seagroves at al., 1998; Robinson et al., 1998). Female C/EBPβ knockout mice not only exhibit impaired mammary gland development but also present reproductive defects. The abundance of C/EBPβ is vital for ovarian follicle development and therefore plays an important role in female reproduction (Sterneck et al., 1997).

Enforced expression of C/EBPβ induces reprogramming or transdifferentiation of B-cell precursors to cells resembling inflammatory macrophages. Expression of C/EBPβ in B-cell precursors induces the expression of the granulocyte/monocyte marker Gr-1, Mac-1 and the mature macrophage marker F4/80 in about 60% of all transfected cells, whereas the expression of CD19 is downregulated (Xie et al., 2003). The study of Xie et al. showed that enforced expression of C/EBPβ, in contrast to C/EBPα, is associated with increased cell proliferation. Furthermore, the different isoforms of C/EBPβ exhibit distinctive functionality in transdifferentiation of blood cells. The long isoforms LAP* / LAP, but not the N-terminally truncated LIP isoform, are capable of transdifferentiating primary mouse B lymphoid progenitors into myeloid cells (Stoilova et al., 2013). The study of Stoilova et al. elucidated the requirement of the LAP* specific CR1 region for induced transdifferentiation of primary B-lymphocytes to the granulocytic lineage. In concordance with this C/EBPβ was shown to be required for C/EBPα independent emergency granulopoiesis after cytokine stimulation or fungal infection (Hirai et al., 2006). The survey of Hirai et al. revealed that C/EBPβ, in contrast to C/EBPα, facilitates proliferation of granulocytic progenitors accompanied or even benefited by delayed c-Myc downregulation. Summarizing, Hirai and colleagues suggested that C/EBPα is crucial for the maintainance of a stable number of

granulocytes, whereas C/EBPβ is mainly activated under emergency conditions to elevate the numbers of mature granulocytes. Another survey suggests that it is not necessarily the C/EBPα or β isoform itself that induces granulocytic differentiation of myeloid precursors, but the time point and the level of C/EBPα and β expression that regulates the differentiation process (Jones et al., 2002). The study by Jones et al. investigated myeloid differentiation in mice carrying the *CEBPB* gene sequence inside the deleted *CEBPA* gene locus. These mice showed an unusually elevated C/EBPβ expression in bone marrow cells that probably originated from the knockin sequence inside the *CEBPA* locus. In contrast to C/EBPα knockout mice, the bone marrow levels of myeloid proteins stayed unaffected in the C/EBPα knockout-C/EBPβ knockin mice and no effects on the hematopoietic system could be observed. According to these results the authors propose a redundant function of C/EBPα/β proteins in the myeloid lineage (Jones et al., 2002).

1.8 The role of C/EBPβ in cancer

The transcription factor C/EBPβ plays multifaceted roles in several types of cancer. Whereas some studies associate C/EBPβ with tumor cell proliferation, metastasis and survival others suggest a role in oncogene induced senescence and apoptosis (Pal et al., 2009; Piva et al., 2006; Robinson et al., 1998). C/EBPβ has also been suggested to regulate proliferation in different cancer and cell types by directly interfering with cell cycle regulators delaying S-phase entry (Gutsch et al., 2011; Luedde et al., 2004; Seagroves et al., 1998).

Increased expression of C/EBPβ mRNA appears especially in aggressive types of breast cancer. The upregulation of C/EBPβ correlates with poor prognosis, metastasis and high tumor grade (Van de Vijver et al., 2002; Zahnow, 2009). Estrogen-receptor-negative and highly proliferative breast cancers often show an increased ratio of C/EBPβ LIP:LAP isoforms (Zahnow, 2009; Arnal-Estape et al., 2010). This was also examined by the studies of Zahnow et al. showing that overexpression of LIP in mammary epithelial cells contributed to increased proliferation, hyperplasia and tumor formation. On top of that, decreasing the LIP:LAP ratio via enforced LAP expression reverted proliferation and malignant transformation of breast

cancer cells (Zahnow et. al., 2001; Zahnow, 2009). The same procedure induced senescence and reduced MYC expression in response to TGFβ in breast cancer cells (Arnal-Estape et al., 2010). Moreover, the study implicated that CUGBP1, a member of the HER2 receptor pathway, increases the translation of the LIP isoform. Based on this knowledge, the authors propose the suppression of LIP expression by the HER2 pathway inhibitor Trastuzumab as a potential breast cancer therapeutic.

C/EBPβ is associated with tumor invasiveness in colorectal cancer. The expression of the long C/EBPβ isoforms (LAP* and LAP) was shown to be significantly increased in colorectal cancer samples of Duke's stages A (submucosa invasion) and to a lesser degree in stages B (penetration of intestinal wall and invasion of adjacent organs) and C (lymph node invasion) compared with normal colon mucosa. Moreover, the short LIP isoform was markedly increased in colorectal tumors of Duke's stage B (Rask et a., 2000).

C/EBPβ is highly expressed in various types of leukemia. Several studies indicate C/EBPβ to stimulate proliferation and survival in Anaplastic large cell lymphoma (ALCL), multiple myeloma (MM) and myeloid lymphomas as well as in the leukemia derived cell lines SU-DHL-1 (ALCL), HL60 (premyelocytic leukemia), U937 (histiocytic lymphoma) and OPM2 (MM) (Studzinski et al., 2012; Anastasov et al., 2010; Piva et al., 2010; 2006; Pal et al., 2009; Blenk et al. 2008; Quintanilla-Martinez et al., 2006).

The proliferation of the anaplastic lymphoma kinase positive (ALK+) ALCL cell line SU-DHL-1 was shown to be vitally dependent on C/EBPβ, as its knockdown resulted in a total block of proliferation. Moreover, the study revealed that the proliferation of SU-DHL-1 cells partially depends on the activating Thr235 phosphorylation of C/EBPβ by the MAPK-pathway kinases ERK1/2 (Anastasov et al., 2010). Further studies showed that the NPM-ALK kinase as well as the STAT3 pathway positively regulate the transcription of C/EBPβ in SU-DHL-1 cells. On top of that, the authors suggested that C/EBPβ plays a significant role in the survival of SU-DHL-1 cells (Piva et al., 2006; 2010; Quintanilla-Martinez et al., 2006). Another study of the Quintanilla-Martinez group analyzed C/EBPβ regulated genes in the ALK+- ALCL cell lines SU-DHL-1, Karpas 299 and KiJK after shRNA knockdown of C/EBPβ (Bonzheim et al., 2013). They could identify more than 100 genes that were significant differentially regulated in SU-DHL-1 and KiJK cells after

C/EBPβ knockdown. The majority of genes shown to be regulated by C/EBPβ, grouped into the GO:terms immunity, apoptosis or cell proliferation. In addition to that, C/EBPβ was identified to bind to the promoters of the *BCL2A1, G0S2* and *DDX21* gene associated with cell proliferation, cell survival and the inflammatory response. The knowledge of the C/EBPβ regulatory network in ALCL cells is expanded by the observation of Bergalet et al. that demonstrated that C/EBPβ mRNA is posttranscriptionally controlled by NPM-ALK in SU-DHL-1 cells. NPM-ALK enhances the interaction of the mRNA binding protein HuR with the C/EBPβ mRNA, entailing increased mRNA stability and translation (Bergalet et al., 2011). Taken together, those results show a complex regulation of C/EBPβ expression in ALK+-ALCL cells and at the same time imply that C/EBPβ gene regulatory function is pivotal for the proliferation of these lymphomas.

C/EBPβ has not only been investigated concerning its earlier discussed functions in myeloid cells and their differentiation but also in myeloid leukemia. Monocytic differentiation of the premyelocytic leukemia cell lines HL60 (acute premyelocytic leukemia; AML) and U937 (Histiocytic / Non-Hodgkin lymphoma) can be initiated by the MAPK-pathway activator PMA/TPA and has been previously shown to be C/EBPβ dependent (Ji and Studzinski, 2004; Chen et al., 1996). Further studies revealed that 1,25-Dihydroxyvitamin D3 (1,25D3) and some of its analogs (deltanoids) can induce C/EBPβ dependent monocytic differentiation of premyelocytic leukemia and HL60 cells (Studzinski et al., 2005; Ji and Studzinski, 2004; Ji et al., 2002).

Moreover, C/EBPβ was reported to play a role in multiple myeloma (MM) proliferation and survival. Bone marrow samples of multiple myeloma patients exhibited high levels of C/EBPβ mRNA in MM cells expressing the plasma cell marker CD138. Additionally, MM cell lines like U226 and the OPM2 cell line were reported to express the activating C/EBPβ LAP isoform (Pal et al., 2009). The study of Pal et al. observed increased expression of anti-apoptotic BCL2 and IRF4, modulators of MM malignancy, after C/EBPβ binding to their gene promoters. The enforced expression of C/EBPβ enhances the proliferation of MM cells. Summarizing, the authors suggested an anti-apoptotic and proliferation enhancing function of C/EBPβ in MM malignancies.

MATERIAL AND METHODS

2.1 Materials

2.1.1 Chemicals

Acetonitrile hypergrade for MS (Merck Millipore, Billerica, MA, USA)

Ampicillin sodium salt (Carl Roth, Karlsruhe, Germany)

Chloramphenicol (Sigma-Aldrich, St. Louis, MO, USA)

1,4-Dithiothreitol DTT (Merck Millipore, Billerica, MA, USA)

Disodium hydrogen phosphate (Na_2HPO_4) (SERVA, Heidelberg, Germany)

Ethylenediaminetetraacetic acid (EDTA/Na_2EDTA-2H_2O) (Calbiochem/EMD/Merck Millipore, Billerica, MA, USA)

EGTA (Ethylenglycol-bis(aminoethylether)-N,N,N´,N´-tetraacetic acid) (Carl Roth, Karlsruhe, Germany)

Formic acid (Merck Millipore, Billerica, MA, USA)

Glacial acetic acid ($C_2H_4O_2$)(Carl Roth, Karlsruhe, Germany)

Glycerol ($C_3H_80_3$)(Carl Roth, Karlsruhe, Germany)

Hydrochloric acid (HCL), 37% (Carl Roth, Karlsruhe, Germany)

HEPES ([N-2- hydroxyethylpiperazine-N'-2-ethanesulfonic acid)(Merck Millipore, Billerica, MA, USA)

Magnesium chloride ($MgCl_2$) (Carl Roth, Karlsruhe, Germany)

Methanol (Carl Roth, Karlsruhe, Germany)

Monopotassium phosphate (KH_2PO_4) (Carl Roth, Karlsruhe, Germany)

Non-fat milk powder (Merck Millipore, Billerica, MA, USA)

Nonidet P40 Substitute (NP-40) (Sigma-Aldrich, St. Louis, MO, USA)

Protease-Inhibitor-Cocktail (complete, EDTA-free) (Roche, Penzberg, Germany)

PMSF (Sigma-Aldrich, St Louis, MO, USA)

Polybrene (Sigma-Aldrich, St Louis, MO, USA)

Potassium chloride (KCl) (Merck Millipore, Billerica, MA, USA)

Reprosil-Pur120 C18-AQ 3 µm beads (Dr. Maisch GmbH, Ammerbuch, Germany)

Sodium dodecyl sulfate (SDS) (Carl Roth, Karlsruhe, Germany)

Sodium chloride (NaCl) (Carl Roth, Karlsruhe, Germany)

Sodium hydroxide (NaOH) (Carl Roth, Karlsruhe, Germany)

SpikeTides TQL (JPT Peptide Technologies, Berlin, Germany)

Thiourea (Carl Roth, Karlsruhe, Germany)

Tris/tris(hydroxymethyl)aminomethane) (Sigma- Aldrich, St. Louis, MO, USA)

TurboFect (Thermo Fischer Scientific, Waltham, MA, USA)

Tween 20/ Polysorbate 20 (Sigma-Aldrich, St. Louis, MO, USA)

Universal Proteomics standard 2 (Sigma-Aldrich, St. Louis, MO, USA)

Urea (VWR International, Geldenaaksebaan, Belgium)

2.1.2 Enzymes

Anti-C/EBPβ antibody C19 rabbit polyclonal IgG (Santa Cruz; sc-150), was purchased from Santa Cruz Biotech (Santa Cruz, CA, USA).

Benzonase Nuclease, ultrapure (Sigma Aldrich; E8263), was purchased from Sigma Aldrich (St. Louis, MO, USA).

Lys-C was purchased from Wako (Osaka, Japan).

Modified trypsin, sequencing grade was purchased from Promega (Madison, WI, USA).

2.1.3 Peptides

C/EBP peptides

Murine C/EBP peptides (Swiss-Prot P28033) were purchased from PSL GmbH (PeptideSpecialtyLaboratories GmbH, Heidelberg, Germany) and obtained from Dr. Michael Beyermann (Leibniz-Institut für Molekulare Pharmakologie im Forschungsverbund Berlin e.V. (FMP), Berlin, Germany; vide Table 1).

Table 1: Sequences of murine C/EBP peptides used for the different APS approaches. The peptides were hybridized to UniPEx libraries as described in the method section.

Name (murine C/EBP peptide)	conserved region of C/EBP family	amino acid sequence
purchased from PSL		
C/EBPbeta aa1-41 "CR1-2"	CR1-2	MHRLLAWDAACLPPPPAAFRPMEVANFYYEPDCLAYGAKAA - Biotinyl
C/EBPbeta aa49-72 "CR3"	CR3	AAEPAIGEHERAIDFSPYLEPLAP - Biotinyl
C/EBPbeta aa153-173 "CR7"	N-terminus of CR7	MAAGFPFALRAYLGYQATPSG - Biotinyl
C/EBPepsilon aa1-62 "CR2-4"	CR2-4	MSHGTYYECEPRGGQQPLEFSGGRAGPGELGDMCEHEASIDLSAYIESGEEQLLSDLFAVGX - Biotinyl
purchased from AG Beyermann - applyed as mix		
C/EBPbeta aa 79-111	CR4-5	Biotinyl-APAHHDFLSDLFADDYGAKPSKKPADYGYVSLG
C/EBPbeta aa 128-172	CR6 - N-terminus of CR7	Biotinyl-PPAALKAEPGFEPADSKRADDAPAMAAGFPFALRAYLGYQATPSG
C/EBPbeta aa 152-196	CR7	Biotinyl-MAAGFPFALRAYLGYQATPSGSSGSLSTSSSSSPPGTPSPADAKA

2.1.4 Protein libraries

UniPEx protein expression libraries were purchased from imaGenes (Source BioScience, Berlin, Germany). A library set consisted of 2 Arrays (22 cm x 22 cm PVDF membranes, #9027/9028) on which 15,300 UniPEx E. coli colonies are spotted that express human in-frame ORF constructs of 7,390 human genes (on average each gene is expressed by 2.4 colonies = coverage of 2.4 of the 7,390 genes). The expression colonies of each gene are spotted in a double spot pattern inside one spotting scheme to reduce false positive signals during final signal evaluation.

2.1.5 Cell lines

cell line name	cell line / cancer classification	source
U937	histiocytic lymphoma	DSMZ no.:ACC 5; Deutsche Sammlung von Mikro-organismen und Zellkulturen (DSMZ), Braunschweig, Germany
SU-DHL-1	anaplastic large cell lymphoma (ALCL)	DSMZ no.: ACC 356; Deutsche Sammlung von Mikro-organismen und Zellkulturen (DSMZ), Braunschweig, Germany

HL60	acute myeloid leukemia (AML)	DSMZ no.: ACC 3; Deutsche Sammlung von Mikro-organismen und Zellkulturen (DSMZ), Braunschweig, Germany
JEKO-1	B-cell lymphoma	DSMZ no.: ACC 553; Deutsche Sammlung von Mikro-organismen und Zellkulturen (DSMZ) , Braunschweig, Germany
OPM2	multiple myeloma	The cell line was kindly provided by Prof. Dr. Bernd Doerken (MDC, Berlin).
PlatE/HEK	derived from human embryonal kidney-293T cell line	The cell line was generated by Morita et al. from HEK 293T cells as described by Morita et al., 2000
C/EBPβ$^{-/-}$ MEF	murine embryonal fibroblast	The cell line was derived from C/EBPβ$^{-/-}$ 129 Ola X C57Bl/6 animals (Sterneck et al., 1997).

2.1.6 Retroviral vectors

The C/EBPβ expression plasmids are based on the chicken sequence (gene bank # EMBLZ 21646) resembling the isoforms LAP* and LAP. The C/EBPβ LAP* start site was optimized to a Kozak consensus sequence by exchanging a glutamine at position 2 to glutamic acid. All C/EBPβ sequences are present in a MIEG3-vector (an improved murine stem cell virus (MSCV)-based bi-cistronic retroviral giving a very bright EGFP fluorescence (Williams et al., 2000)) and were described before in detail by Stoilova et al., 2013.

Additionally, vectors encoding the viral Gagpol and Envelope (Env) were used as described before in detail by Stoilova et al., 2013.

2.1.7 Equipments

AB Sciex Nano Spray II source (AB Sciex, Washington, DC, USA)

Avanti Centrifuge J-26 (Beckman Coulter, Brea, CA, USA)

Bachofer Sonoplus HD70 Ultrasonic device (Bachofer, Germnay)

Binder Inkubator (Binder, Tuttlingen, Germany)

Centrifuge Varifuge 3.0R (Heraeus, Hanau, Germany)

Centrifuge 5417R (Eppendorf, Hamburg, Germany)

FACS Canto II (BD DivaSoftware; BD Becton Dickinson, Franklin Lakes, NJ, USA)

Eksigent nano LC-ultra 1D (Eksigent, Dublin, CA, USA)

Odyssey Scanner (LI-COR, Lincoln, NE, USA)

Orbitrap electrospray ion source (Thermo Fischer Scientific, Odense, Denmark)

Proxeon EASY nLC II (Thermo Fischer Scientific, Odense, Denmark)

Q-Exactive mass spectrometer (Thermo Fischer Scientific, Waltham, MA, USA)

QTRAP 5500 (AB Sciex, Washington, DC, USA)

Rocking platform (Polymax 1040; Heidolph Instruments, Schwabach, Germany)

2.2 Methods

2.2.1 Array peptide screening (APS)

Hybridization of UniPEx protein macroarrays was performed as described before (Pless et al., 2011), except for using of 0,2 µM biotin coupled peptides, incubated with macroarrays for 2h at room temperature (RT) and the detection with 1 µg/ml streptavidin coupled IRDye800cw or IRDye680lt (LI-COR, Lincoln, NE, USA) with incubation for 1h. Detection was performed at 700 nm or 800 nm with LI-COR Odyssey CLx laser scan device (LI-COR, Lincoln, NE, USA). Briefly: Macroarrays were washed with 96% ethanol and subsequently several times with ddH_2O and equilibrated in TBS-T-T. Residual expression colony material was removed gently with a soft tissue (Kim-wipe). Macroarrays were rinsed 3 times, then washed twice for 10 min at RT in TBS-T-T and afterwards 3 times for 3 min and twice for 10 min at RT in TBS on a rocking platform at 30 r.p.m.. Macroarrays were blocked for 2 h at RT in blocking solution on a rocking platform at 10 r.p.m.. After removal of blocking solution macroarrays were incubated with 0,2 µbiotin coupled peptide bait for 2 h at RT on a rocking platform at 10 r.p.m. Afterwards macroarrays were washed 4 times for 10 min at RT in TBS-T and twice for 10 min at RT in TBS on a rocking platform at 30 r.p.m.. For detection macroarrays were incubated with 1 µ/ml streptavidin coupled IRDye800cw or IRDye680lt for 1 h on a rocking platform at 10 r.p.m.. Subsequently macroarrays were washed 4 times for 10 min at RT in TBS-T and twice for 10 min at RT in TBS on a rocking platform at 30 r.p.m.. The signal detection was acquired with an Odyssey Laser scan device (LI-COR, Lincoln, NE, USA)

at 800 nm or 700 nm wavelength. Image scan files were evaluated manually but software assisted using AIDA Image Analyzer software (Raytest, Straubenhardt, Germany).

Blocking solution

3 % non-fat milk powder (Merck Millipore, Billerica, MA, USA) in TBS-T (filtrated)

TAE (Tris-acetate-EDTA)

50M stock solution:

242 g Tris base

57.1 ml glacial acetic acid

37.2 g $Na_2EDTA\text{-}2H_2O$

add H_2O to 1 liter

Working solution, pH 8.5:

40 mM Tris-acetate

2 mM $Na_2EDTA\text{-}2H_2O$

Tris-HCl [tris(hydroxymethyl)aminomethane], 1 M

121 g Tris

add H_2O to 1 l

pH adjustment with HCl

Tris-buffered saline (TBS)

100 mM Tris-HCl, pH 7.5

0.9 % (150 mM) NaCl

Tris-buffered saline plus Tween (T-TBS)

0.1 % Tween 20 in Tris-buffered saline (TBS)

2.2.2 Cell culture

U937, SU-DHL1, HL60 and JEKO-1 and OPM2 cell lines were maintained at 5 ℅ CO_2, 37 ℃ and in RPMI 1640 (Invitrogen, Carlsbad, CA, USA), 10 ℅ heat-inactivated fetal calf serum (FCS), 1 ℅ penicillin/streptomycin in a Binder Inkubator (Binder, Tuttlingen, Germany). MEF and PlateE/HEK cell lines were maintained in DMEM (Invitrogen, Carlsbad, CA, USA) with 10 ℅ heat- inactivated fetal calf serum (FCS) and 1 ℅ penicillin/ streptomycin at 5 ℅ CO_2, 37 ℃ in a Binder Inkubator (Binder, Germany).

Cell culture solutions

Penicillin/Streptomycin (PAA/GE Healthcare, Little Chalfont, UK)

100 x Trypsin-EDTA (PAA/GE Healthcare, Little Chalfont, UK)

DMSO (Merck Millipore, Billerica, MA, USA)

Roswell Park Memorial Institute (RPMI) 1640 medium (Gibco, Life technologies/Thermo Fischer Scientific, CA, USA)

Dulbecco's modified Eagle medium (DMEM) + Glutamax (Gibco, Life technologies/Thermo Fischer Scientific, CA, USA)

Fetal Bovine Serum (FCS; PAA/GE Healthcare, Little Chalfont, UK)

2.2.3 Cell lysate preparation

Whole cell lysates

Whole cell lysates were prepared as triplicates from 1x10E7 cells per sample. Lysates were prepared from PBS washed 1x10E7 cells of SU-DHL-1, HL60, JEKO-1 or U937 cell lines in lysis-buffer 1. After 10 min incubation at 4 ℃ on a wheel at 10 r.p.m. the lysates were treated with an ultrasonic device twice on ice for 20 sec and centrifugated for 20 min at 13 000 r.p.m. and 4 ℃. Supernatants were used for immunoprecipitation.

Nuclear enrichment of cell lysates

Nuclear enriched lysates were prepared as triplicates from 1x10E7 cells per sample. Nuclear enrichment of lysates from 1x10E7 cells of SU-DHL-1 or OPM2 cell lines were prepared as previously described (Schreiber et al., 1989). Briefly: 1x10E7 SU-DHL-1 or OPM2 cells were

washed with PBS, resuspended in 400 µl buffer A per 1x10E6 cells and incubated for 15 min on ice. Nonident P-40 was added (final conc. 0.1%), lysates were vortexed for 2 sec and crude nuclei were pelleted by centrifugation for 30 sec at 13 000 r.p.m. Crude nuclei were resuspended in buffer C in 50 µl per 1x10E6 cells and incubated for 15 min at 4 ℃ on a shaker and subsequently treated with an ultrasonic device twice for 20 sec on ice followed by centrifugation for 5 min at 13 000 r.p.m. at 4 ℃. The supernatant was used for immunoprecipitations.

Dithiothreitol (DTT), 1 M

15.45 g DTT in 100 ml H_2O

stored at -20℃

EDTA (ethylenediamine tetraacetic acid), 0.5 M, pH 8.0

186.1 g $Na_2EDTA\text{-}2H_2O$ in 700 ml H_2O

pH adjustment with NaOH

add H_2O to 1 l

KCl, 1 M

74.6 g KCl

H_2O to 1 l

MgCl2, 1 M

20.3 g $MgCl_2\text{-}6H_2O$

H_2O to 100 ml

NaCl, 5 M

292 g NaCl

add H_2O to 1 l

10 X PBS

1.4 M NaCl

0.027 M KCl

0.018 M KH_2PO_4

0.1 M Na_2HPO_4

Dissolved in deionized water, autoclaved and stored at RT.

Buffer A (low salt)

10 mM HEPES, pH 7.5

0.1 mM EDTA, pH 8

0.1 mM EGTA, pH 8

10mM KCl

1mM DTT

0.5 mM PMSF

protease inhibitors (Roche, Penzberg, Germany)

Buffer C (high salt)

20 mM HEPES, pH 7.5

1 mM EDTA, pH 8

1 mM EGTA, pH 8

400 mM NaCl

1mM DTT

0.5 mM PMSF

protease inhibitors (Roche, Penzberg, Germany)

Lysis/IP buffer 1 (for whole cell lysates)

20 mM HEPES, pH 7.5

150 mM NaCl

1 mM EDTA, pH 8

1 mM EGTA, pH 8

20% Glycerol

1 U/ml Bezonase

1 mM dithiothreitol [DTT]

protease inhibitors (Roche, Penzberg, Germany)

IP buffer 2 (for nuclear enrichment)

20 mM HEPES, pH 7.5

200 mM NaCl

1 mM EDTA, pH 8

1 mM EGTA, pH 8

1 U/ml Bezonase

1 mM DTT

2.2.4 Immunoprecipitations (IP)

IPs of nuclear lysates of SU-DHL-1 or OPM2 cells or of whole cell lysates of HL60, JEKO-1, SU-DHL-1 or U937 cells were performed with 1 µg/ml anti-C/EBPβ antibody (C19; Santa Cruz) in IP-buffer 2 for 2 h at 4 ℃ on a wheel at 10 r.p.m.. Precipitations were collected with 3 mg protein G-coated Dynabeads (Life technologies/Thermo Fischer Scientific, CA, USA) for 5 min at 4 ℃ and washed twice afterwards. Beads were separated from the supernatant using a magnetic rack. Beads were stored at -80 ℃ and subjected to mass spectrometry analysis. Günther Kahlert (MDC) conducted the preparation and mass spectrometry measurements that followed. Briefly: Proteins were released from the beads by adding laemmli-SDS buffer and boiling the samples at 95 ℃ for 3 min. Then the proteins were methanol-chloroform precipitated (Wessel and Flügge, 1984) and reconstituted in urea buffer. Subsequently the samples were subjected to a two-step in-solution digest as described by Sury et al., 2014 using Lys-C and trypsin. The acquired peptides were desalted by StageTip purification (Rappsilber et al., 2007). The eluted peptides were subjected to mass spectrometric analysis on a Q Exactive.

Laemmli-SDS buffer

1.3 ⁒ (w/v) SDS

10 mM TRIS, pH 6.8

0.1 M DTT

Urea buffer

10 mM HEPES, pH 8.0

6 M urea

2 M thiourea

2.2.5 Retrovirus production

Viruses were produced by transfection of PlatE/HEK cells (Morita et al., 2000). 4 h before transfection 3x10E6 PlatE cells were seeded in a 10 cm dish in DMEM + Glutamax (Invitrogen, Carlsbad, CA, USA), 10⁒ Fetal Bovine Serum (Gibco), 1⁒ Penicillin-Streptomycin (PAA/GE Healthcare, Little Chalfont, UK) and incubated at 37 ℃ and 5⁒ CO_2 (Binder incubator). The transfection mix was prepared as follows:

- 15 ml DMEM + Glutamax, 10⁒ FCS, 1⁒ Penicillin-Streptomycin
- 5 µg retroviral vector pMSCV
- 10 µg plasmid encoding Gagpol
- 2 µg plasmid encoding Env
- 20 µl Turbofect

The mix was added drop wise to the PlatE cells and incubated for 12 h at 37 ℃, 5 ⁒ CO_2. Subsequently the supernatant was discarded and 15 ml DMEM (DMEM + Glutamax, 10⁒ FCS, 1⁒ Penicillin- Streptomycin) was added. After 24h the supernatants were harvested and replaced with 15 ml fresh DMEM (DMEM + Glutamax, 10⁒ FCS, 1⁒ Penicillin-Streptomycin). The harvested supernatants were sterile filtered (for removal of cellular and other contaminants) and used for infection of C/EBP$\beta^{-/-}$ MEF cells. The procedure of virus secretion

(PlatE cells) and subsequent supernatant harvest was repeated a second time resulting in two infection cycles

2.2.6 Infection and cell cultivation of MEF C/EBPβ$^{-/-}$ cells

For the virus infection, MEF C/EBPβ$^{-/-}$ cells were resuspended at 5x10E4 cells/ml in DMEM+ Glutamax (Invitrogen, Carlsbad, CA, USA) medium and 1⁒ penicillin/streptomycin and transferred into 6-well plates 12 h prior to infection. Cells were infected twice, by adding equal volume of sterile filtered retroviral supernatant (from PlatE cells) containing 8 µl Polybrene (Sigma Aldrich, St. Louis, MO, USA). Plates were centrifuged for 90 min at 2100 r.p.m. at 37 ℃ in an Eppendorf centrifuge followed by 24 h incubation at 5 ⁒ CO_2, 37 ℃.

2.2.7 FACS sorting

Cells were washed with 1 X PBS twice and resuspended in ice cold 1 X PBS. Samples were run in 1 X PBS on a FACS Canto II (BD Biosciences, BD DivaSoftware) and analyzed with the FlowJo software applying a sorting for GFP positive cells (FACS facility, Dr. Hans-Peter Rahn, MDC). For each probe 1x10E7 cells were sorted and stored at 4 ℃. Günther Kahlert (MDC) conducted the preparation and mass spectrometry measurements that followed. Briefly: Cells were lysed immediately after FACS sorting with laemmli-SDS buffer. Then the proteins were methanol-chloroform precipitated (Wessel and Flügge, 1984) and reconstituted in urea buffer. Subsequently the same amounts of proteins were subjected to a two-step in-solution digest as described by Sury et al., 2014 with the exception that only Lys-C was used as a cleavage enzyme. The acquired peptides were desalted by StageTip purification (Rappsilber et al., 2007). The eluted peptides were speed-vaced to dryness and subsequently isotypically dimethyl labeled (Boersema et al., 2009). The labeled peptides were combined and purified by StageTip purification. Thereafter the purified peptides were fractionated by anion-exchange based fractionation onto StageTips (Wisniewski et al., 2009). The eluted peptides were subjected to mass spectrometric analysis on a Q Exactive.

2.2.8 MS-iBAQ proteomics of SU-DHL-1 cells

SU-DHL-1 cells were grown in cell culture as described before. Günther Kahlert (MDC) conducted the preparation and mass spectrometry measurements that followed. Briefly: Cells were lysed immediately with laemmli-SDS buffer. Then the proteins were methanol-chloroform precipitated (Wessel and Flügge, 1984) and reconstituted in urea buffer. Universal Proteomics standard 2 (UPS2) was added to the sample. The proteins were subjected to a two-step in-solution digest as described by Sury et al., 2014 using Lys-C and trypsin. The acquired peptides were desalted by StageTip purification (Rappsilber et al., 2007). The eluted peptides were subjected to mass spectrometric analysis on a Q Exactive. UPS2 was used to compute iBAQ intensities with MaxQuant 1.2.2.5 for SU-DHL-1 cells.

2.2.9 Bioinformatic analysis

Extended data and network analysis was performed using the DAVID online tool (Huang et al., 2009; DAVID.abcc.ncifcrf.gov) to determine GO terms and functional domains (cutoff: Benjamini-Hochberg 0.05).

The Cytoscape software inclusive the BisoGenet plugin (Martin et al., 2010; Shannon et al., 2003) was used for network analysis and visualization.

Moreover the CORUM (Ruepp et al., 2008; 2010), UniProt (UniProt Consortium, 2013), HIPPIE (Schaefer et al., 2011) and STRING databases (Jensen et al., 2009) were used to determine functional associations, protein complexes and cellular networks of the here detected protein interactions.

For further data analysis and visualization the R statistical software package was used (R Core Team, 2013).

2.2.10 Mass spectrometry measurements and MS raw data evaluation

Mass spectrometry measurements and MS raw data evaluation was performed by Günther Kahlert, MDC, Berlin.

Mass spectrometry analysis of the FACS sorted infected MEF C/EBPβ $^{-/-}$ cells, C/EBPβ IPs and SU-DHL-1 MS-iBAQ

Briefly: A Proxeon EASY nLC II using a 5-50 % (v/v) acetonitrile gradient with 0.1 % formic acid with a flow rate of 200 nl/min was used for reversed-phase chromatography. In-house packed reversed-phase columns packed with Reprosil-Pur120 C18-AQ 3 µm beads were used for peptide separation. The SU-DHL-1 MS-iBAQ sample and the FACS sorted infected MEF C/EBPβ$^{-/-}$ cell samples were measured in 8-hour runs and the C/EBPβ IP measurements were conducted in 3-hour runs.

FACS sorted infected MEF C/EBPβ$^{-/-}$ cells, C/EBPβ IP samples from SUDHL-1, HL60, U937, JEKO-1 and OPM2 cells and the iBAQ quantification of SU-DHL-1 cell line were analyzed by MS and MS/MS acquisition on a Q Exactive mass spectrometer equipped with an Orbitrap electrospray ion source. The data dependent mode with a mass window of 300 to 1700 *m/z*, a resolution of 60,000, the isolation window of 2.1 Th and a target value of 1x10E6 ions was selected for data acquisition. Higher-energy C-trap dissociation with the normal collision energy of 25 was used for fragmentation. The 10 most abundant *m/z* with a charge state of +1 were selected with a dynamic exclusion of 60 sec. MS/MS fragments were collected using a fill time of 60 ms fort the SU-DHL-1 MS-iBAQ sample and the FACS sorted infected MEF C/EBPβ$^{-/-}$ cell samples and a fill time of 120 ms for the C/EBPβ IP measurements.

The MaxQuant Software Package Version 1.2.2.5 (Cox and Mann, 2008) using the Andromeda search engine was used for matching the MS data to the Homo sapiens database ipi.HUMAN.v3.72. Depending on the used cleavage enzyme Trypsin/P or Lys-C/P setting was selected permitting two missed cleavage sites per peptide. The main search mass tolerance was 6 ppm. The MS/MS search mass tolerance was set to 20 ppm selecting the top 10 MS/MS peaks per 100 Da. The MaxQuant iBAQ setting was selected for quantification of the iBAQ SU-DHL- 1 proteome and the MaxQuant label-free quantification setting was selected for the data quantification of the C/EBPβ IPs.

Perseus 1.2.0.17 was used for analysis of the C/EBPβ IPs. For anti-C/EBPβ IPs from whole cell lysates only proteins were chosen that were identified three times in one of the groups. For anti-C/EBPβ IPs of nuclear enriched lysates only proteins were selected that

were detected at least twice in one of the groups. Missing values were imputated. A cutoff for significant C/EBPβ protein-protein interactions of $p \leq 0.02$ for whole lysate IPs and FDR ≤ 0.05 for nuclear enriched IPs was determined (performed by Günther Kahlert, MDC, Berlin).

C/EBPβ quantity determination by SRM of SU-DHL-1 and U937

Briefly: For the C/EBPβ abundance determination in the SU-DHL-1 and the U937 whole cell lysates were used. The proteins were methanol-chloroform precipitated (Wessel and Flügge, 1984) and reconstituted in urea buffer. Heavy labeled peptides containing arginine^{10} (SpikeTides TQL) for C/EBPβ and ActinB were added before subjecting both cell lysates to a two-step in-solution digest as described by Sury et al., 2014 using Lys-C and trypsin. The acquired peptides were desalted by StageTip purification (Rappsilber et al., 2007). The eluted peptides were subjected to mass spectrometric analysis.

Peptides were separated in hourly runs by an Eksigent nanoLC-ultra 1D using a 10-50 % (v/v) acetonitrile gradient with 0.06 % formic acid. A flow rate of 250 nl/min was used. In-house packed reversed-phase columns packed with Reprosil-Pur120 C18-AQ 3 µm beads were used for peptide separation. Samples were measured on a QTRAP 5500 equipped with an AB Sciex Nano Spray II source using a positive ion spray voltage of 2300 V. See also table 2 for details on the SRM method.

The MultiQuant 1.2 software (AB Sciex, Washington, DC, USA) was used for data evaluation. C/EBPβ and Actin B heavy standards were used to verify the retention times and peptide ion fragmentation patterns of the naturally occurring peptides. C/EBPβ area counts were normalized to Actin B area counts for cell line comparison (performed by Günther Kahlert, MDC, Berlin).

Table 2: Selected reaction monitoring method for C/EBPβ abundance quantification. Table shows the protein names (Protein), the relevant masses for the first quadrupole (Q1) and the third quadrupole (Q3), the collision energy (CE) and the dwell time (Time) for both the transitions of the arginine[10] containing peptides and the naturally occurring peptides. The identification (ID) shows the peptide amino acid sequence targeted by SRM. Next to that, the mass-to-charge ration (m/z) and the fragment ion y-series are annotated in the ID section.

Protein	Q1 [Da]	Q3 [Da]	Time [msec]	ID	CE [Volts]
C/EBPβ	592.30	971.45	150	VLELTAENER (*m/z* +2) y8	31
	592.30	842.41	150	VLELTAENER (*m/z* +2) y7	31
	592.30	729.32	150	VLELTAENER (*m/z* +2) y6	31
	587.30	961.45	150	VLELTAENER (*m/z* +2) y8	31
	587.30	832.41	150	VLELTAENER (*m/z* +2) y7	31
	587.30	719.32	150	VLELTAENER (*m/z* +2) y6	31
ActinB	571.76	922.43	5	GYSFTTTAER (*m/z* +2) y8	30
	571.76	835.40	5	GYSFTTTAER (*m/z* +2) y7	30
	571.76	688.33	5	GYSFTTTAER (*m/z* +2) y6	30
	566.76	912.43	5	GYSFTTTAER (*m/z* +2) y8	30
	566.76	825.40	5	GYSFTTTAER (*m/z* +2) y7	30
	566.76	678.33	5	GYSFTTTAER (*m/z* +2) y6	30

RESULTS

3.1 Determination of the impact of C/EBPβ on the cellular proteome

The transcription factor C/EBPβ was described to regulate the expression of various genes during the differentiation of myeloid cells and adipocytes, as well as in proliferation and tumor progression in various cell types (Bonzheim et al., 2013; Esteves et al., 2012; 2013; Zwergal et al., 2006; Gorgoni et al., 2002; Ramji and Foka, 2002; Screpanti et al., 1995). In order to expand the knowledge of the cellular network regulated by the transcription factor C/EBPβ we attempted to elucidate the influence of C/EBPβ on the cellular proteome. Therefore, C/EBPβ$^{-/-}$ murine endothelial fibroblast (MEF) cells were retrovirally infected with C/EBPβ constructs expressing the two long isoforms LAP* or LAP (C/EBPβ LAP*, C/EBPβ LAP; Figure 5) that were previous analyzed concerning their trans-differentiation potential in C/EBPβ$^{-/-}$ murine B-cell progenitors (Stoilova et al., 2013). The study of Stoilova et al. showed a different outcome in the trans-differentiation of B-cell progenitors in which the LAP* isoform induced trans-differentiation into granulocytic, macrophage and dendrite-like cells while the LAP isoform failed to induce granulocyte differentiation. The survey showed also a partially differential activation of characteristic myeloid genes by the LAP* and LAP isoforms. As a fair amount of cells is necessary for the successful investigation of proteomes by mass spectrometry we chose a C/EBPβ$^{-/-}$ murine endothelial fibroblast (MEF) cell line instead of analyzing primary blood cell precursors from murine bone marrow as Stoilova et. al. had done.

The murine retro viruses were produced in the human PlatE cell line by transfection with vectors encoding the viral particles and the MIEG3 (MSCV-IRES-EGFP) C/EBPβ expression vectors (as control an empty MIEG3 vector was used). The C/EBPβ$^{-/-}$ MEFs

were infected with the murine retroviruses carrying C/EBPβ LAP* and LAP isoforms or a control plasmid in two rounds (2 x 24 h; see Figure 5 and for further details material and methods). After 48h of infection the MEF cells were harvested and GFP positive cells were obtained by FACS sorting (FACS facility, Dr. Hans-Peter Rahn, MDC). After sorting, whole cell lysates from GFP positive MEF cells were prepared immediately. The lysates were Lys-C digested, followed by dimethyl-labeling and MS-proteomic analysis (Günther Kahlert, MDC; Figure 5). Protein abundance was calculated as Log2 fold changes of proteins detected with the LAP*/LAP infected cells versus the cells infected with the empty control vector or between the LAP* and LAP infected cells. Proteins with a Log2 fold change ≥ 1 or ≤ -1 were considered as significantly regulated between the samples (MS analysis by Günther Kahlert, MDC).

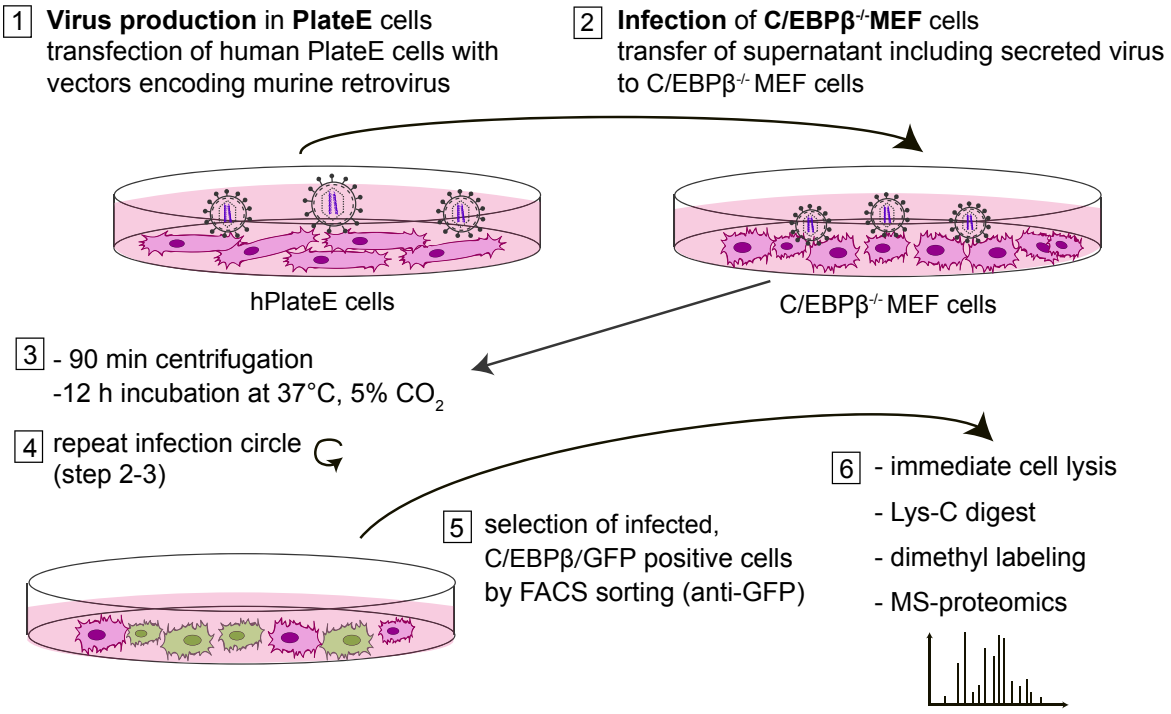

Figure 5: Workflow of the proteomics experiment with C/EBPβ$^{-/-}$ MEF cells. Depicted is a scheme of the production of the retroviruses carrying the C/EBPβ LAP* or LAP or control constructs in PlatE cells. The PlatE cells secrete the viruses after transfection with the vectors encoding the viral components and MIG3 vectors containing C/EBPβ LAP* or LAP or control sequences. The supernatants were used for 2 infection rounds of C/EBPβ$^{-/-}$ MEF cells. After two 24h-infection circles the MEF cells were harvested and GFP positive cells were obtained by FACS sorting and transmitted to MS proteomics analysis (for further details see material and methods section).

The analysis of the C/EBPβ$^{-/-}$ MEF cells infected with the LAP* isoform revealed 97 proteins that were upregulated more than 2 fold and 20 proteins that were downregulated more than 2 fold. The analysis of the cells infected with the LAP isoform revealed 122 proteins that were upregulated more than 2 fold and 107 proteins that were downregulated more than 2 fold. 16 proteins were downregulated 2 fold by both LAP* and LAP Isoforms and 67 significantly upregulated by both (Figure 6, Figure S1 and Table 3). The difference between the up- or downregulated proteins by the LAP* or LAP isoform was rarely significant ($\geq$ 2 fold; Figure 6 and Figure S1). Therefore it was not possible to reveal the functional difference between the two isoforms on a proteome level. This might be due to the fact that only the 2649 most abundant proteins of the infected C/EBPβ$^{-/-}$ MEF cells were detected with a ratio by this MS-proteomics approach.

Figure 6: The heatmap on the following page (page 42) depicts a selection of proteins detected in the proteomics experiment with C/EBPβ$^{-/-}$ MEF cells infected with the retroviral vectors carrying either C/EBPβ LAP*, LAP or a control vector. The first two columns of the heatmap show the Log2 fold change of the detected proteins (MS analysis by Günther Kahlert, MDC) from the cells infected with C/EBPβ LAP* and LAP constructs versus cells infected with the control construct. Signals with a Log2 fold change ≥ 1 or ≤ -1 were considered as significant. Proteins that were detected with a significant Log2 fold change of ≤ -1 after C/EBPβ infection compared to the control vector are depicted with a red scale. Proteins detected with a Log2 fold change of ≥ 1 after C/EBPβ infection compared to the control vector are depicted with a green scale. Protein signals with an insignificant Log2 fold change are depicted with a grey scale. The third column of the heatmap depicts the Log2 fold change of the cells infected with the C/EBPβ LAP isoform versus the cells infected with the LAP* isoform. Proteins that were detected with a significant log2 fold change of ≥ 1 after LAP infection compared to the LAP* isoform are depicted with a yellow scale. Proteins detected with a Log2 fold change of ≤ -1) after LAP* infection are depicted with a blue scale. Protein signals with an insignificant Log2 fold change are depicted with a grey scale. The DAVID online tool (DAVID.abcc.ncifcrf.gov; Huang et al., 2009) was used to determine GO:terms of the proteins that were 2 fold upregulated by LAP* and/or LAP infection and a selection of assigned GO:terms is annotated on the left side of the heatmap. A separate heatmap in Supplemental Figure S1 in the supplement section depicts all detected proteins of this proteomics approach.

MASS SPECTROMETRY PROTEOMICS OF C/EBPβ$^{-/-}$ MEF CELLS INFECTED WITH RETROVIRAL CONSTRUCTS OF HUMAN C/EBPβ LAP* OR HUMAN C/EBPβ LAP

- SELECTION OF MOST SIGNIFICANT DIFFERENTIAL EXPRESSED PROTEINS -

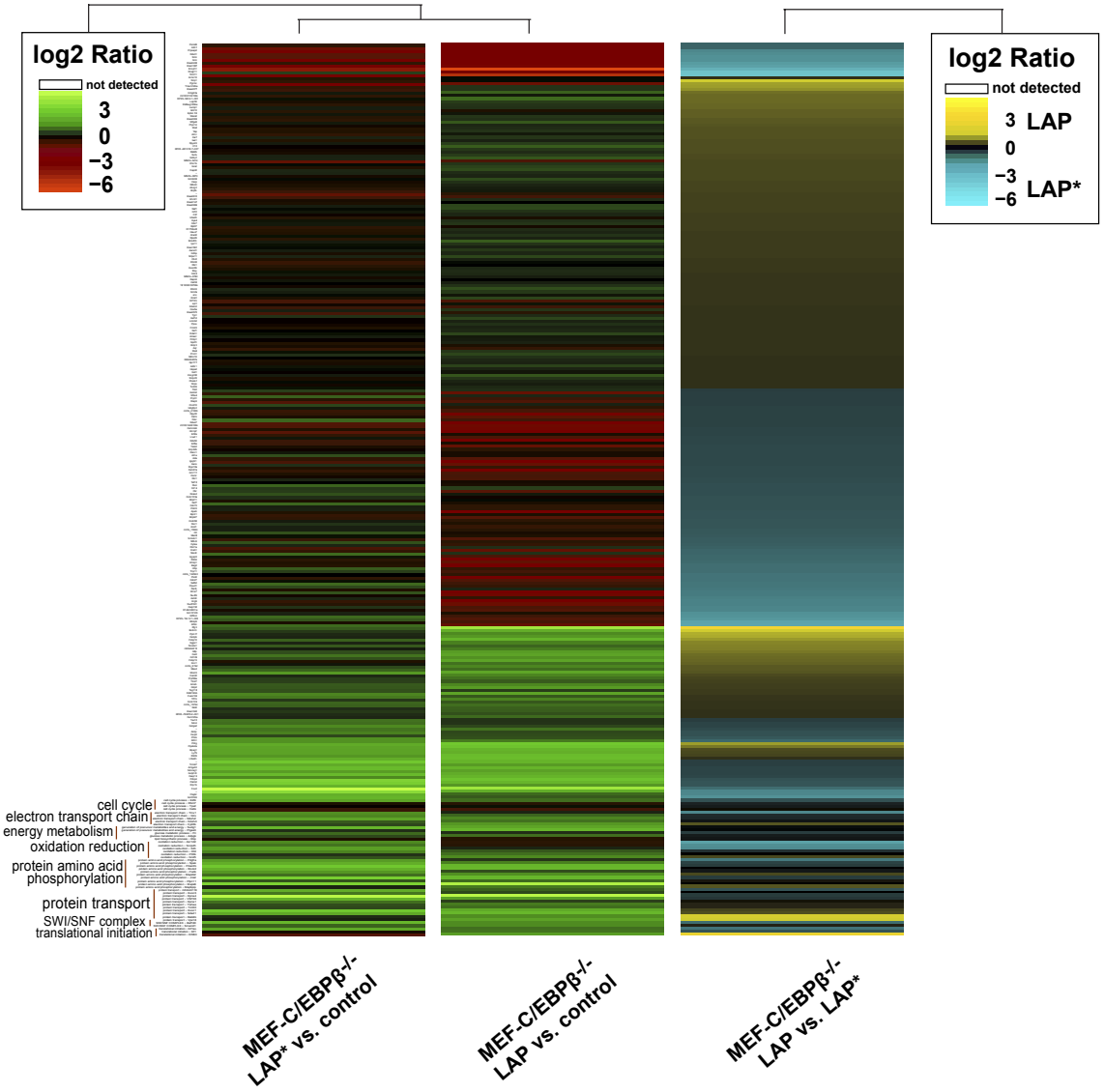

The DAVID online tool (DAVID.abcc.ncifcrf.gov; Huang et al., 2009) was used to determine GO:terms of the proteins that were 2 fold upregulated by LAP* and/or LAP infection. The main ranking terms were: "GO:0015031 protein transport", "GO:0055114 oxidation reduction", "GO:0006468 protein amino acid phosphorylation" and "GO:0006091 generation of precursor metabolites and energy" (Figure 6 and Table 3). The transport associated proteins could be grouped into several different intracellular transport mechanisms among

them the two nuclear importin subunits Importin subunit α-1 (Kpna1; upregulated 2 fold by LAP* and 1.5 fold by LAP) and Kpna4 (upregulated 29 fold by LAP* and LAP; Table 3). Interestingly the GO-terms "oxidation reduction" and "generation of precursor metabolites and energy" encompass proteins mainly involved in carbohydrate and amino acid metabolism like the NAD dehydrogenases Ndufv3 (upregulated 1.8 fold by LAP* and 2.1 fold by LAP; Table 3) and Ndufv2 (upregulated 3.5 fold by LAP* and 2.3 fold by LAP), the 1,5-anhydro-D-fructose reductase Akr1cl2 (upregulated 2.4 fold by LAP*), ADP-dependent glucokinase that phosphorylates D-glucose to D-glucose 6-phosphate (Adpgk; upregulated 1.6 fold by LAP* and 2 fold by LAP), or the Krebs cycle associated Succinyl-CoA synthetase subunit α (Suclg1; upregulated 5 fold by LAP* and 3.6 fold by LAP). Moreover, the gluconeogenesis promoting phosphatase Pp4r3b (upregulated 7 fold by LAP* and 4 fold by LAP; Table 3) and the cytochrome Cyb5b (upregulated 1.6 fold by LAP* and 2.9 fold by LAP; Table 3) are significantly upregulated after C/EBPβ infection (Figure 6, Figure S1 and Table 3).

Further proteins that were associated with metabolism and upregulated more than 2 fold by C/EBPβ were the Fructose metabolism associated p35b (upregulated 1.3 fold by LAP* and 2 fold by LAP; Table 3), the nucleotide metabolism associated 3(2),5-bisphosphate nucleotidase 1 (Bpnt1; upregulated 5.6 fold by LAP* and 4.8 fold by LAP), the Pyruvate carboxylase (Pc; upregulated 2 fold by LAP* and 1.3 fold by LAP; Table 3), the Pyruvate dehydrogenase phosphatase regulatory subunit (Pdpr; upregulated by 5 fold by LAP* and 7 fold by LAP) and Cytochrome b5 type B (Cyb5b; upregulated by LAP).

Proteins associated with fatty acid metabolism like Long-chain fatty acid acyl-CoA ligase 1 (Acsl1; upregulated by 2 fold LAP* and 1.4 fold by LAP) and Cpt1 (upregulated 3 fold by LAP* and 2 fold by LAP) that catalyzes the transfer of long-chain fatty acids between CoA and carnitine prior to mitochondrial uptake were upregulated as well (Nyman et al., 2011).

The GO-term "protein amino acid phosphorylation" includes several kinases of the MAPK- and further kinase pathways like Jnk2/Mapk9, Jnk1/Mapk8, Fadk/Ptk2, Rock2, Map2k2, Prkar2b, Pdgfra, the MAPKK activator Mapbpip as well as the Rock2 phosphatase Ptpn11 that were mostly upregulated by both isoforms (Figure 6, Figure S1 and Table 3). The MS proteomics also revealed a significant ($\geq$ 2 fold) up-regulation of the two

known C/EBPβ target genes Xdh and Glrx (Gery et al., 2005) in the MEF cells infected with the LAP* isoform. Findings that will be discussed later in this thesis will reveal that C/EBPβ interacts with several components of the SWI/SNF chromatin-remodeling complex like BAF180. Interestingly, the MS proteomics of the transfected MEF cells revealed the significant upregulation of the two SWI/SNF family members Baf180 (upregulated 5 fold by LAP* and 2.5 fold by LAP) and Smarcd1 (upregulated 1.9 fold by LAP* and 2.5 fold by LAP; Figure 6, Figure S1 and Table 3) after C/EBPβ infection as well.

Table 3: The table on the following page (page 45) lists a selection of proteins that were significantly up- or downregulated in C/EBPβ$^{-/-}$ MEF cells after C/EBPβ infection. The DAVID online tool (DAVID.abcc.ncifcrf.gov; Huang et al., 2009) was used to determine GO:terms (column 3-4; GO_BP_FAT, Benjamini-Hochberg $\leq$ 5 %) of the proteins that were $\geq$ 2 fold upregulated by LAP* and/or LAP over-expression (column 5-7).

UniProt AC.	Name	GO ID	GOterm (GO_BP_FAT)	log2 ratio LAP* vs. GFP	log2 ratio LAP vs. GFP	log2 ratio LAP vs. LAP*
A0AUM9	Eif2b3	GO:0006413	translational initiation	-0.85144329	1.66698377	2.48913185
P48024	Eif1	GO:0006413	translational initiation	-0.07514000	1.08290692	-0.76184904
Q8BMJ3	Eif1ax	GO:0006413	translational initiation	1.87589799	1.03513120	-1.07755855
Q61466	Baf60a	-	SWI/SNF complex	0.92014083	1.34101794	0.18052981
Q8BSQ9	Baf180	-	SWI/SNF complex	2.34457288	1.33233558	-1.01987231
Q8R307	Vps18	GO:0015031	protein transport	0.21636174	1.75928369	1.47674458
P61028	Rab8b	GO:0015031	protein transport	0.35907131	1.36013950	1.61725146
Q80UZ2	Sdad1	GO:0015031	protein transport	1.91704979	2.37183762	0.52446493
Q6P1Y9	Exoc1	GO:0015031	protein transport	2.86874602	1.94542043	0.45459706
Q9D880	Tim50	GO:0015031	protein transport	0.66884528	1.02474519	0.21138606
P62259	Ywhae	GO:0015031	protein transport	0.72071624	1.16008117	0.19547359
Q60960	Kpna1	GO:0015031	protein transport	1.04502352	0.59359281	0.06529657
Q91XD6	Vps36	GO:0015031	protein transport	2.16526881	1.72355856	-0.45987351
Q3UGH8	Kpna4	GO:0015031	protein transport	4.90967711	4.90631340	-0.52871888
Q6KAR6	Exoc3	GO:0015031	protein transport	1.12154595	0.67138396	-0.55968560
Q6A0C7	mKIAA0118	GO:0015031	protein transport	2.04896851	0.91249658	-0.76660274
Q9JHS3	Mapbpip	GO:0006468 / GO:0000165	protein amino acid phosphorylation / MAPK cascade	0.25592366	1.13835577	0.55924706
Q7TSJ7	Mapk8	GO:0006468 / GO:0000165	protein amino acid phosphorylation / MAPK cascade	3.28346253	4.62538740	0.32065796
P35235	Ptpn11	GO:0006468 / GO:0000165	protein amino acid phosphorylation / MAPK cascade	0.76544988	0.99617178	0.08515268
Q9WTU6	Jnk2	GO:0006468 / GO:0000165	protein amino acid phosphorylation / MAPK cascade	3.15613770	2.36832137	-0.52383609
Q63932	Map2k2	GO:0006468	protein amino acid phosphorylation	1.03836594	1.40930946	0.48336436
P34152	Fadk	GO:0006468	protein amino acid phosphorylation	1.53176821	0.72185384	-0.08100323
P70336	Rock2	GO:0006468	protein amino acid phosphorylation	2.15137178	2.39176772	-0.18023373
P31324	Prkar2b	GO:0006468	protein amino acid phosphorylation	2.93213678	2.33222099	-0.51062148
Q9Z1W9	Spak	GO:0006468	protein amino acid phosphorylation	2.11732934	1.21182212	-0.59795459
P26618	Pdgfra	GO:0006468	protein amino acid phosphorylation	1.64547110	0.47061495	-1.14025303
P97346	Gn25	GO:0055114	oxidation reduction	0.76884067	1.29048338	0.46811407
P23591	P35b	GO:0055114	oxidation reduction	0.43253188	1.05443175	0.01492654
P53395	Dbt	GO:0055114	oxidation reduction	1.22329897	0.81015515	-0.37909459
B2RUJ7	Xdh	GO:0055114	oxidation reduction	1.71158301	0.26963165	-1.41396069
Q8R127	Sccpdh	GO:0055114	oxidation reduction	1.08481264	-0.27979159	-1.47533449
Q9DCT1	Akr1cl2	GO:0055114	oxidation reduction	1.30264075	-0.34267097	-1.84425077
P70245	Ebp	GO:0008610	lipid biosynthetic process	-0.15346256	-0.25635578	-0.08263699
Q8VDL4	Adpgk	GO:0006006 / GO:0006091	glucose metabolic process /generation of precursor metabolites and energy	0.66329907	1.01163876	-0.12538400
Q05920	Pc	GO:0006006	glucose metabolic process	0.99523123	0.38879570	-0.53184421
Q9R0Q7	Ptges3	GO:0006091 / GO:0006006	generation of precursor metabolites and energy / glucose metabolic process	0.38261192	2.35656641	-0.00494247
Q9WUM5	Suclg1	GO:0006091	generation of precursor metabolites and energy	2.32716997	1.86266959	-0.02047214
Q9CQX2	Cyb5b	GO:0022900 / GO:0006091 / GO:0055114	electron transport chain / oxidation reduction /generation of precursor metabolites and energy	0.66475588	1.55586523	0.57056008
Q3U422	Ndufv3	GO:0022900 / GO:0006091 / GO:0055114	electron transport chain / oxidation reduction /generation of precursor metabolites and energy	0.83139086	1.05880135	-0.05844292
Q9D6J6	Ndufv2	GO:0022900 / GO:0006091 / GO:0055114	electron transport chain / oxidation reduction /generation of precursor metabolites and energy	1.80496219	1.25174939	-0.28275460
Q9QUH0	Glrx	GO:0022900 / GO:0006091 / GO:0055115	electron transport chain / oxidation reduction /generation of precursor metabolites and energy	1.26897328	0.96450953	-0.33508032
Q8VBT0	Tmx1	GO:0022900 / GO:0006091 / GO:0055114	electron transport chain / oxidation reduction /generation of precursor metabolites and energy	1.41213115	0.27572226	-1.31980169
Q922R5	Pp4r3b	GO:0045722 / GO:0019216	positive regulation of gluconeogenesis / regulation of lipid metabolic process	2.00834346	2.92512594	1.01870538
D3Z041	Acsl1	GO:0008152	metabolic process	1.02353925	0.45995614	-0.60651790
Q9Z0S1	Bpnt1	-	-	2.47910119	2.25951354	-0.59998678
Q7TSQ8	Pdpr	GO:0006546	glycine catabolic process	2.36086990	2.79333409	0.10339692
P97742	Cpt1	GO:0001676	long-chain fatty acid metabolic process	1.65122394	1.00180224	-0.43561208

3.2 APS - a method to explore the interactome of C/EBPβ in an expression independent manner

The cooperation with cofactors is essential to transcription factors in the course of gene regulation. Following the detection of downstream proteins whose expression is probably influenced by the transcription factor C/EBPβ, we attempted to expand the functional network of the transcription factor by elucidating potential cofactors that interacted with C/EBPβ and could assist the transcription factor during target gene regulation and further cellular tasks. Our group recently developed the array peptide screening (APS; Pless et al., 2011) to determine protein interactomes and it was employed here to detect direct protein interactions of conserved C/EBPβ TAD and RD regions. The APS technique is a high throughput in-vitro interaction screening that uses libraries of membrane expressed and fixated proteins that can be hybridized with the desired proteins or peptides. During this survey APS screenings were performed by incubation of UniPEx protein libraries (imaGenes, Source Bioscience) with chemically synthesized and C-terminally biotinylated C/EBP protein fragments/peptides (PSL GmbH and AG Beyermann). A UniPEx protein library encompasses 15,300 E. coli colonies expressing 7,390 full-length human proteins (7,390 human genes as ORF clones) that are spotted and fixated on two PVDF membranes (UniPEx libraries #9027/28, imaGenes, Source Bioscience). Positive interactions of the hybridized peptides with the membrane-expressed proteins were detected with fluorophore-labeled (IRDye, LI-COR, Lincoln, NE, USA) streptavidin applying a laser based scanning technique (LI-COR Odyssey CLx, LI-COR, Lincoln, NE, USA) (Figure 7; for further details vide the material and methods section). The bacterial, clonal expression of human proteins enables due to the lack of cellular cofactors the discovery of direct protein interactions and overcomes the limited availability of minor cellular components. The hybridization of peptides containing conserved peptide sequences facilitates a mapping of interactions to those regions.

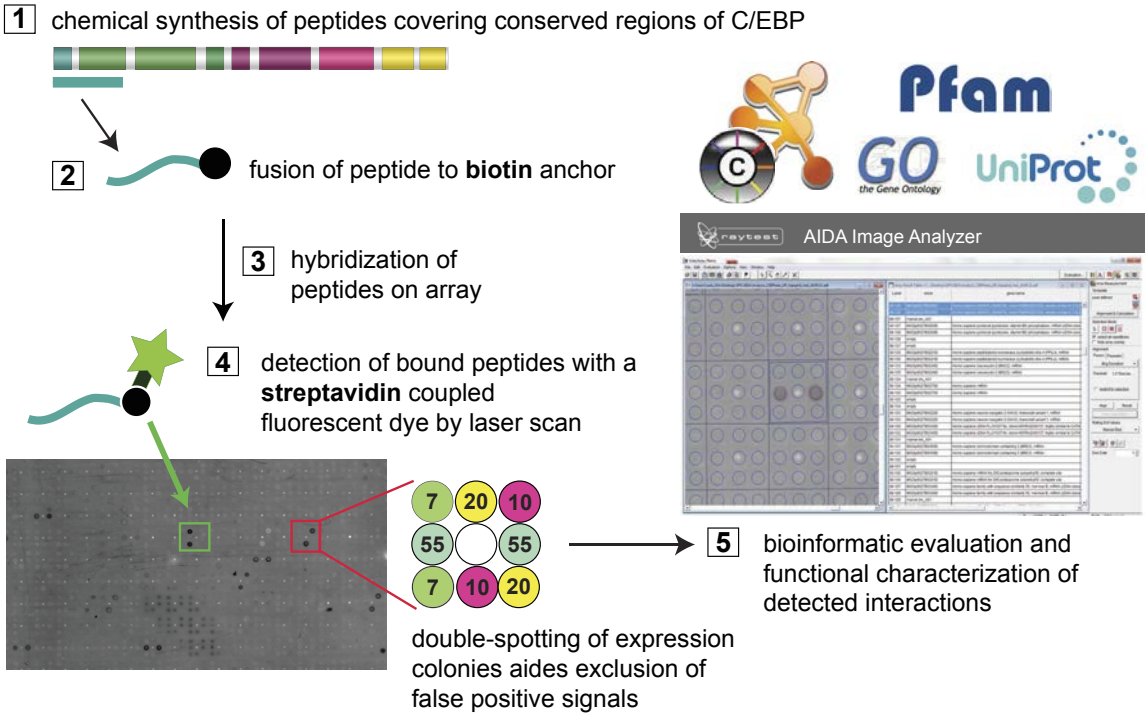

Figure 7: Workflow of the array peptide screening that was modified after Pless et al., 2011 (vide materials and methods section). Chemically synthesized and biotinylated peptides covering the conserved regions of C/EBPβ or C/EBPε (1,2) were hybridized to UniPEx protein macroarrays (3). Excess peptides were removed by washing. Peptides that interacted with the macroarray proteins were detected with streptavidin coupled fluorescent dyes and subsequent laser scanning (4). The double-spotting pattern of the macroarray- proteins enables exclusion of false positive interaction signals. The interacting proteins were identified with the AIDA Image Analyzer Software (Raytest, Straubenhardt, Germany) and characterized by subsequent bioinformatic analysis (5).

In this study we performed several APS approaches with peptides covering C/EBPβ CR1-2, C/EBPβ CR3 (partial TAD), C/EBPβ N-terminus of CR7 (partial RD), and a mixture covering C/EBPβ CR4-5 + CR 6-7 + CR 7 (complete RD; Figure 8; for further details vide material and methods section). As the entire TAD of C/EBPβ is too long for chemical synthesis we used a peptide covering the complete TAD of C/EBPε (Figure 8) for an APS screening. The C/EBPε TAD has shorter low complexity regions but shares the homologous CR2, 3 and 4 with C/EBPβ and with other C/EBP family members (Figure 1). The usage of a long C/EBP TAD sequence spanning three consecutive conserved regions aided the detection of protein interactions that require longer recognition or interaction motifs.

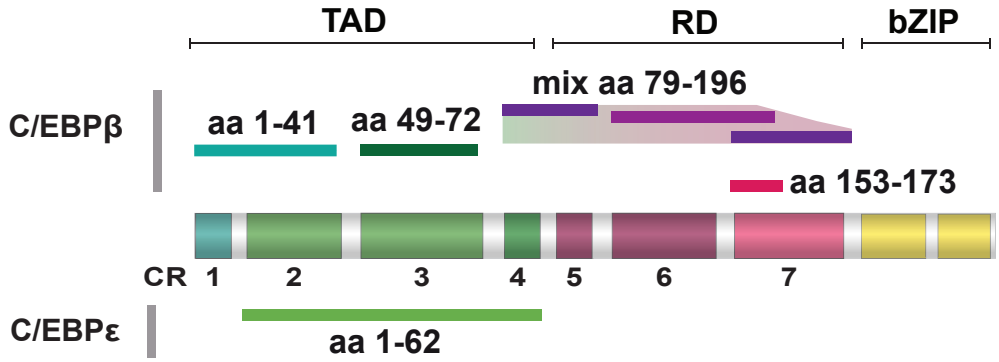

Figure 8: Array peptide screening (APS) was performed by hybridization of C/EBPβ peptides covering the conserved regions of C/EBPβ and ε (CR1-7; covering the transactivation domain (TAD) and regulatory domain (RD), but not the basic zipper domain (bZIP)) to UniPEx-peptide macroarrays. Peptides of murine C/EBPβ TAD (CR1-2, aa1-41), (CR3, aa49-72), and murine C/EBPβ RD (N-terminal part of CR7, aa153-173), (mixture of CR4-5, aa79-111; CR 6-7, aa128-172; CR 7 aa152-196), and murine C/EBPε TAD (CR2-4, aa1-61) were used for APS.

The APS screening revealed 590 proteins that interacted with C/EBPβ and ε probes. Among them were 64 proteins that have previously been found to interact with C/EBPβ (Siersbaek et al., 2014; Steinberg et al., 2012; Lee et al., 2010b; Jiang et al., 2008; Ki et al., 2005; Kowenz-Leutz and Leutz, 1999; Chang et al., 1998; Miau et al., 1998; Xia et al., 1997; LeClair et al., 1992). 492 proteins interacted with the conserved TAD regions (CR1-2 and CR3) of C/EBPβ, that are contained in the predominantly transcriptional activating LAP* and LAP isoforms. 326 proteins were found to interact with the first two conserved regions (CR1/2) and 171 with the CR3 region of the transactivation domain. The TAD of C/EBPε that structurally entails CR2, 3 and 4 exhibited only 94 interactors. The low number of C/EBPε TAD interactions might be a consequence of a more restricted accessibility of the individual CRs due to the shorter low complexity regions, subtle amino acid differences or because of specialized functions of C/EBPε. Altogether 492 proteins interacted with the conserved regions of the C/EBPε TAD and CR1/2, CR3 of the C/EBPβ TAD (Figure 9). The N-terminal part of the CR7 region (RD) interacted with 192 proteins and the CR4-7 peptide with 38 proteins (Figure 9). Approximately 10% of all identified proteins interacted with peptides covering both TAD as well as RD of C/EBPs, suggesting multiple binding to

different amino acid sequences of C/EBP or unspecific interactions.

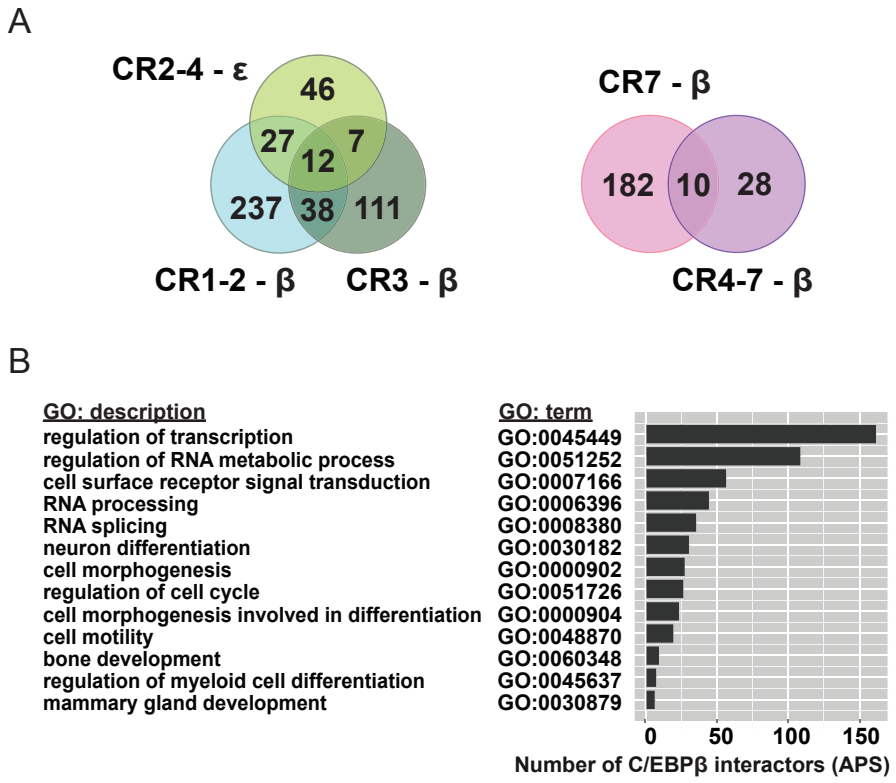

Figure 9: Data analysis of Array peptide screening that was performed with peptides covering the conserved regions of C/EBPβ and ε. A) Overlap of interactions found by APS covering the C/EBP TAD (mC/EBPβ CR1-2 and CR3; mC/EBPε CR2-4) and RD (mC/EBPβ CR4-7mix and CR 7). B) Selection of GO-terms of all interactors found by all APS approaches for all peptides of C/EBPβ and ε. Protein-interactions were analyzed with the NIH DAVID tool with GO_BP_FAT, Benjamini-Hochberg ≤ 5 ٪ (DAVID.abcc.ncifcrf.gov).

Subsequently GO:term analysis of the APS detected interactors was performed to aid initial characterization and prioritization (Figure 9). Therefore the GO-term (GO_BP_FAT) function of the DAVID online tool (DAVID.abcc.ncifcrf.gov; Huang and Berger, 2008) was applied with an exclusion rate of Benjamini-Hochberg ≤ 5 ٪ (vide material and methods section). The prime ranking GO:terms of the C/EBPβ interaction network contain the label "transcriptional regulation". The second abundant GO:terms suggested an involvement of C/EBPβ and C/EBPε interactors in RNA metabolism like splicing and RNA processing. Additionally, GO:terms showed an involvement in cell cycle regulation and myeloid functions of C/EBPβ interactors (Figure 9).

3.3 IP-MS analysis of endogenous C/EBPβ in leukemia cell lines

The advantage of the APS technique is the detection of direct protein interactions due to the lack of cellular environment. The bacterial protein expression of the APS technique is independent of cell type specific protein expression levels and facilitates the simultaneous analysis of multiple protein-protein interactions. To examine the interactions identified by APS in a leukemia specific context, immunoprecipitations against endogenous C/EBPβ followed by shotgun mass spectrometry (IP-MS) measurements (Günther Kahlert, MDC) were performed using the leukemia cell lines SU-DHL-1 (Anaplastic large cell lymphoma, ALCL), U937 (Histiocytic lymphoma/non-Hodgekin lymphoma, HL/NHL), HL60 (Acute premyelocytic leukemia, AML), JEKO-1 (Mantle cell lymphoma, MCL), OPM2 (Multiple myeloma, MM).The occurrence of the interactions in the analyzed cell lines is itemized in detail in Table S1.

The leukemia cell line SU-DHL-1 was chosen due to the before discussed association of C/EBPβ with growth and tumorigenicity of anaplastic large cell lymphomas (ALCL) and the ALCL cell line SU-DHL-1 (Jundt et al., 2005; Quintanilla-Martinez et al., 2006; Piva et al., 2006; 2010; Anastasov et al., 2010). The myeloid U937 and the premyelocytic HL60 cell line were selected because of the before described function of C/EBPβ in phorbol ester induced differentiation of U937 cells and in 1,25- dihydroxyvitamin D3 (1,25D) induced differentiation of HL60 cells (Marcinkowska et al., 2006; Ji and Studzinski, 2004; Ji et al., 2002; Chen et al., 1996). As C/EBPβ was shown to regulate the expression of transcription factors associated with proliferation and survival in multiple myeloma (Pal et al., 2009) we analyzed the OPM2 cell line (MM) as well.

Prior to anti-C/EBPβ immunoprecipitations whole cell lysates of U937, JEKO-1, HL60 and SU-DHL-1 cell lines were prepared by ultrasonic induced cell-lysis in a detergent-free buffer. Nuclear enriched cell lysates of OPM2 and SU-DHL-1 cells were prepared by lysis of the outer cell membrane in a low salt buffer followed by a lysis of the crude nuclei fraction in high salt buffer aided by ultrasonic irradiation (as described before by Schreiber et al.,

1989 and in material and methods). Immunoprecipitations of endogenous C/EBPβ (with an anti-C/EBPβ antibody) from whole cell lysates of U937, JEKO-1, HL60 and SU-DHL-1 and from nuclear enriched lysates of OPM2 and SU-DHL-1 cells were prepared as triplicates and were analyzed by shotgun mass spectrometry (Günther Kahlert, MDC) using a label free quantification approach (Hubner and Mann, 2011). The IP-MS analysis of U937 whole cell lysates revealed 132 significant interactions with endogenous C/EBPβ (p-value $\leq 2\%$) as depicted in the volcano plot in Figure 10.

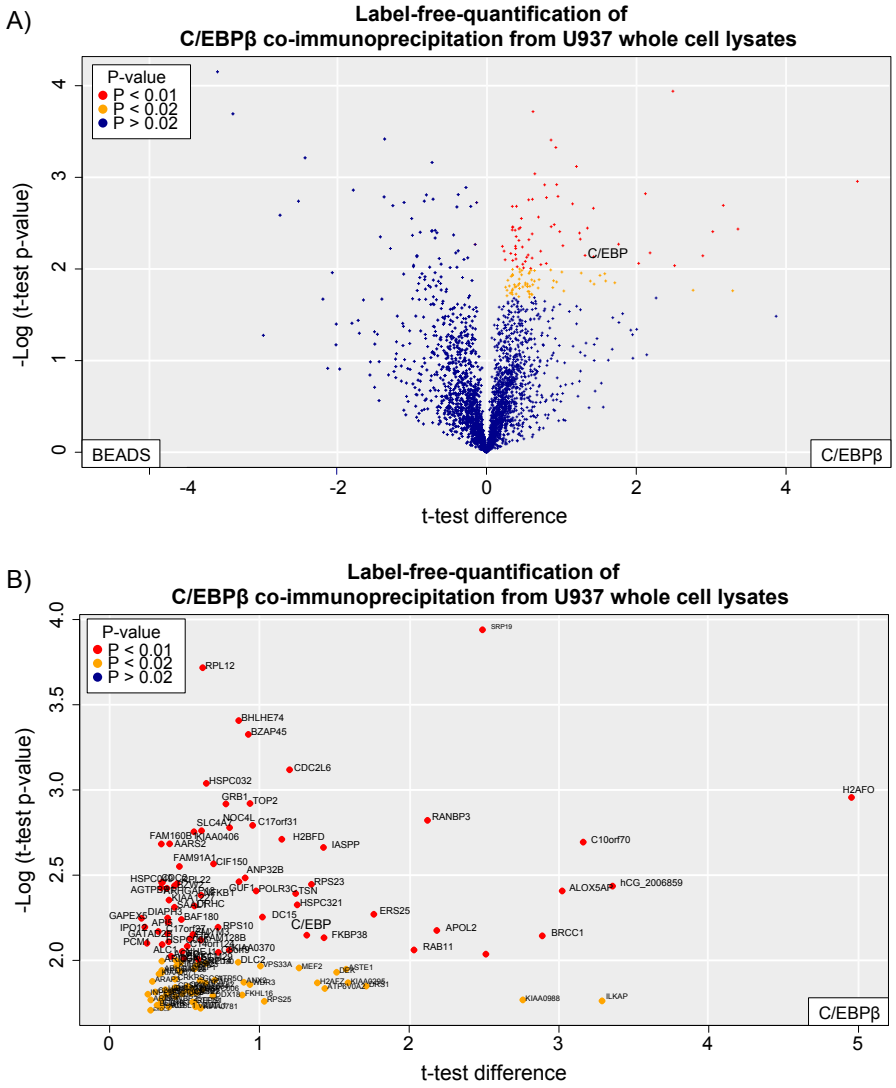

Figure 10: Volcano plot of an anti-C/EBPβ IP-MS label-free shotgun approach from U937 whole cell lysates. The x-axis shows the t-test difference of the interactions of the anti-C/EBPβ IP samples (triplicates) versus bead control (triplicates). Proteins detected either three times in the anti-C/EBPβ or three times in bead control IP probes were considered as valid and were used for the analysis. Missing values were imputated. The y-axis depicts the p-value of the t-test in a negative Log scale. Protein-protein interactions with C/EBPβ with a t-test p-value of ≤ 2 ٪ were considered as significant and are depicted in yellow. The protein-protein interactions with C/EBPβ with a t-test p-value of ≤ 1 ٪ are depicted in red. Proteins with a t-test p-value of ≥ 2 ٪ or bead control false positives are considered as insignificant and are depicted in blue (Günther Kahlert, MDC Berlin). A) Volcano plot of C/EBPβ interactions detected from U937 whole cell lysates. The significant protein interactions in the upper right corner are depicted in further detail in B. B) Volcano plot only showing the significant protein interactions of C/EBPβ. Detected proteins are colored due to their significance level and named due to the human IPI database (Günther Kahlert, MDC Berlin).

The IP-MS analysis of JEKO-1 whole cell lysates revealed 130 significant interactions with endogenous C/EBPβ (p-value ≤ 2٪) as depicted in the volcano plot in Figure 11.

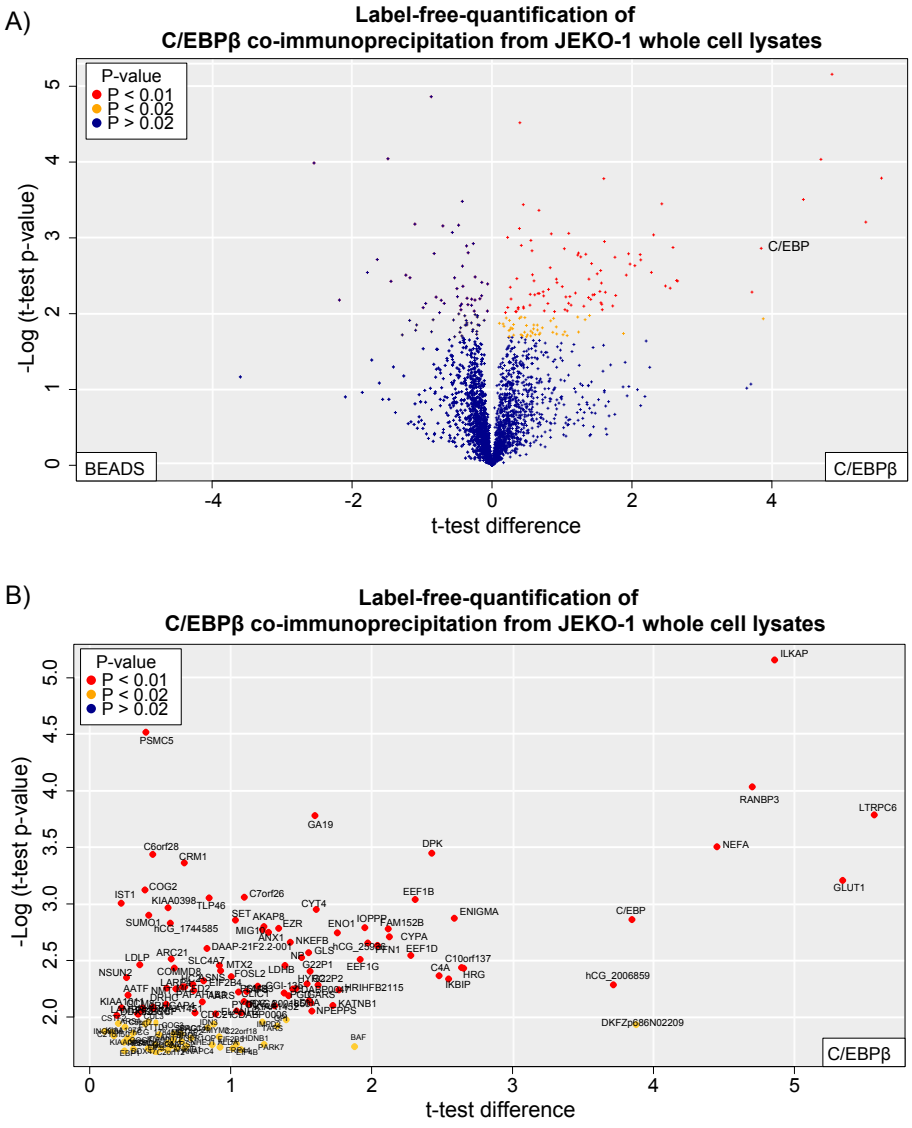

Figure 11: Volcano plot of an anti-C/EBPβ IP-MS label-free shotgun approach from JEKO-1 whole cell lysates. The x-axis shows the t-test difference of the interactions of the anti-C/EBPβ IP samples (triplicates) versus bead control (triplicates). Proteins detected either three times in the anti-C/EBPβ or three times in bead control IP probes were considered as valid and were used for the analysis. Missing values were imputated. The y-axis depicts the p-value of the t-test in a negative Log scale. Protein-protein interactions with C/EBPβ with a t-test p-value of ≤ 2 ٪ were considered as significant and are depicted in yellow. The protein-protein interactions with C/EBPβ with a t-test p-value of ≤ 1 ٪ are depicted in red. Proteins with a t-test p-value of ≥ 2 ٪ or bead control false positives are considered as insignificant and are depicted in blue (Günther Kahlert, MDC Berlin). A) Volcano plot of C/EBPβ interactions detected from JEKO-1 whole cell lysates. The significant protein interactions in the upper right corner are depicted in further detail in B. B) Volcano plot only showing the significant protein interactions of C/EBPβ. Detected proteins are colored due to their significance level and named due to the human IPI database (Günther Kahlert, MDC Berlin).

The IP-MS analysis of HL60 whole cell lysates revealed 88 significant interactions with endogenous C/EBPβ (p-value$\leq$ 2٪) as depicted in the volcano plot in Figure 12.

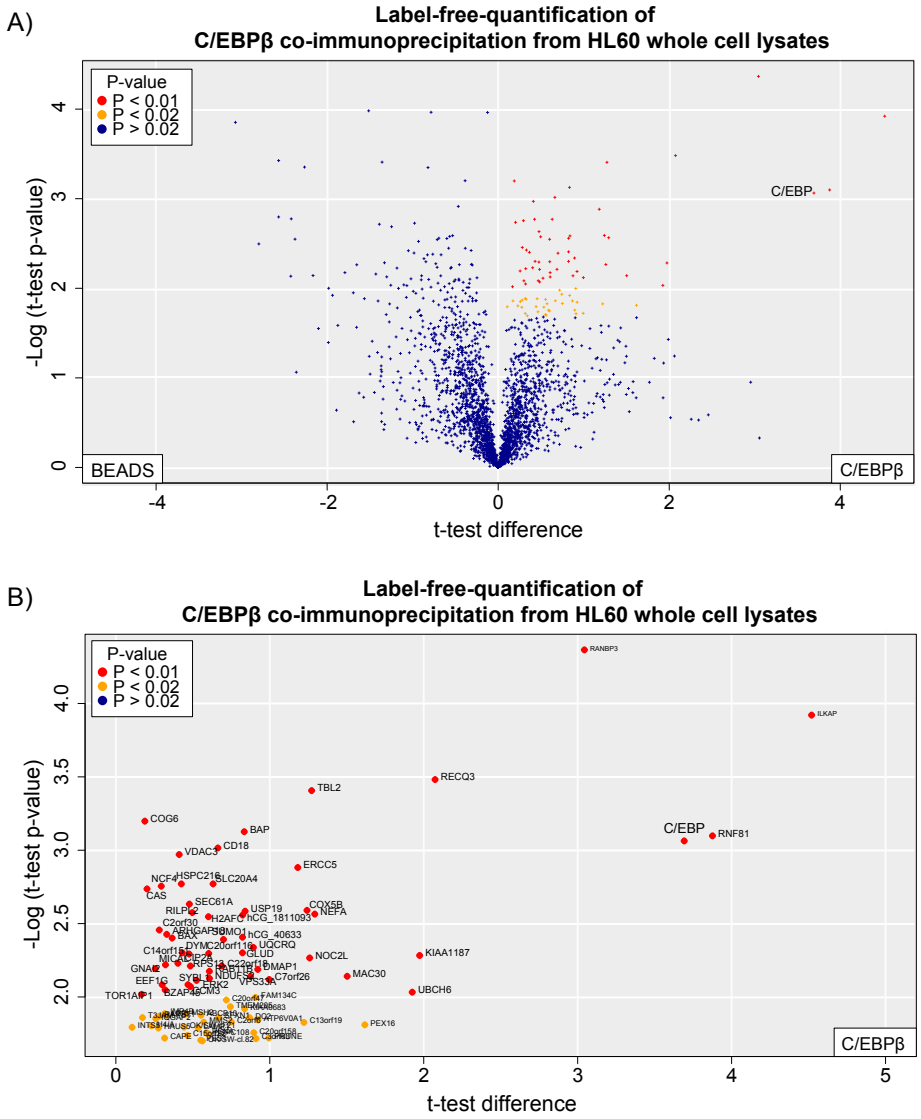

Figure 12: Volcano plot of an anti-C/EBPβ IP-MS label-free shotgun approach from HL60 whole cell lysates. The x-axis shows the t-test difference of the interactions of the anti-C/EBPβ IP samples (triplicates) versus bead control (triplicates). Proteins detected either three times in the anti-C/EBPβ or three times in bead control IP probes were considered as valid and were used for the analysis. Missing values were imputated. The y-axis depicts the p-value of the t-test in a negative Log scale. Protein-protein interactions with C/EBPβ with a t-test p-value of ≤ 2 ٪ were considered as significant and are depicted in yellow. The protein-protein interactions with C/EBPβ with a t-test p-value of ≤ 1 ٪ are depicted in red. Proteins with a t-test p-value of ≥ 2 ٪ or bead control false positives are considered as insignificant and are depicted in blue (Günther Kahlert, MDC Berlin). A) Volcano plot of C/EBPβ interactions detected from HL60 whole cell lysates. The significant protein interactions in the upper right corner are depicted in further detail in B. B) Volcano plot only showing the significant protein interactions of C/EBPβ. Detected proteins are colored due to their significance level and named due to the human IPI database (Günther Kahlert, MDC Berlin).

The IP-MS analysis of SU-DHL-1 whole cell lysates revealed 217 significant interactions with endogenous C/EBPβ (p-value≤ 2٪) as depicted in the volcano plot in Figure 13.

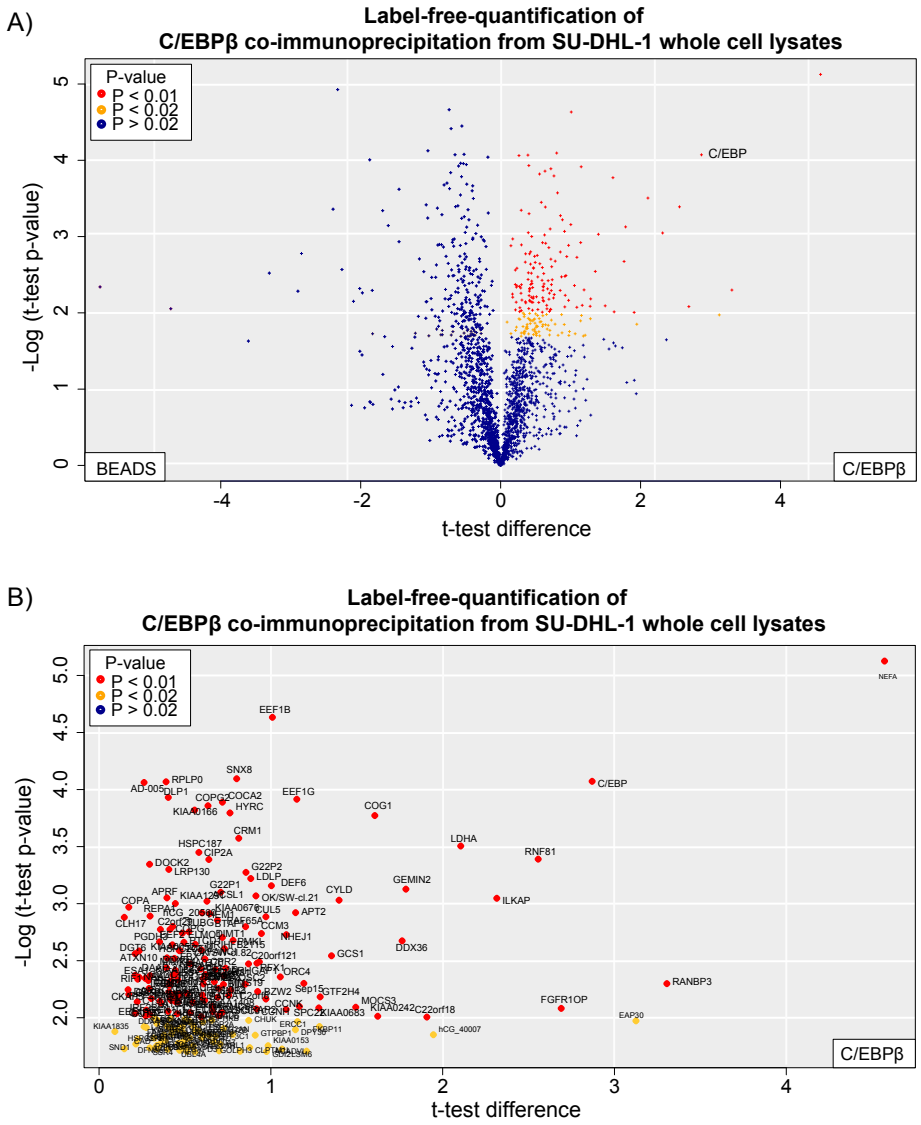

Figure 13: Volcano plot of an anti-C/EBPβ IP-MS label-free shotgun approach from SU-DHL-1 whole cell lysates. The x-axis shows the t-test difference of the interactions of the anti-C/EBPβ IP samples (triplicates) versus bead control (triplicates). Proteins detected either three times in the anti-C/EBPβ or three times in bead control IP probes were considered as valid and were used for the analysis. Missing values were imputated. The y-axis depicts the p-value of the t-test in a negative Log scale. Protein-protein interactions with C/EBPβ with a t-test p-value of ≤ 2 ٪ were considered as significant and are depicted in yellow. The protein-protein interactions with C/EBPβ with a t-test p-value of ≤ 1 ٪ are depicted in red. Proteins with a t-test p-value of ≥ 2 ٪ or bead control false positives are considered as insignificant and are depicted in blue (Günther Kahlert, MDC Berlin). A) Volcano plot of C/EBPβ interactions detected from SU-DHL-1 whole cell lysates. The significant protein interactions in the upper right corner are depicted in further detail in B. B) Volcano plot only showing the significant protein interactions of C/EBPβ. Detected proteins are colored due to their significance level and named due to the human IPI database (Günther Kahlert, MDC Berlin).

The IP-MS analysis of SU-DHL-1 nuclear enriched cell lysates revealed 163 significant interactions with endogenous C/EBPβ (FDR$\leq$ 5٪) as depicted in the volcano plot in Figure

14.

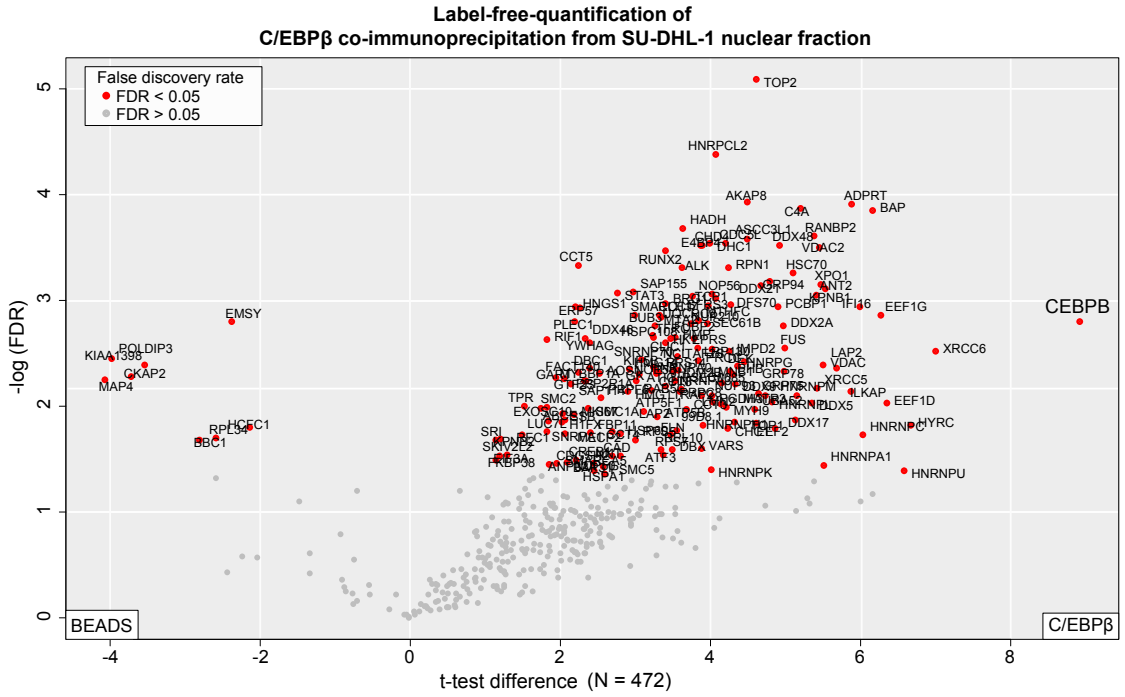

Figure 14: Volcano plot of anti-C/EBPβ IP-MS label-free shotgun approach from SU-DHL-1 nuclear enriched cell lysates. The x-axis shows the t-test difference of the interactions of the anti-C/EBPβ IP samples (triplicates) versus bead control (triplicates). Proteins that were detected at least twice in either the anti-C/EBPβ IP triplicate or the bead control triplicate were chosen for the t-test. Missing values were imputated. The y-axis depicts the FDR in a negative Log scale. Interactions with a FDR level of ≤ 5 ⁒ were considered as significant and are depicted in red. Proteins with a FDR ≥ 5⁒ are not considered as significant and are depicted in grey (Günther Kahlert, MDC Berlin). Detected proteins are colored due to their significance level and named due to the human IPI database (Günther Kahlert, MDC Berlin). The significant protein interactions with C/EBPβ are depicted and described in further detail in Figure 17.

The IP-MS analysis of OPM2 nuclear enriched cell lysates revealed 33 significant interactions with endogenous C/EBPβ (FDR≤ 5⁒) as depicted in the volcano plot in Figure 15.

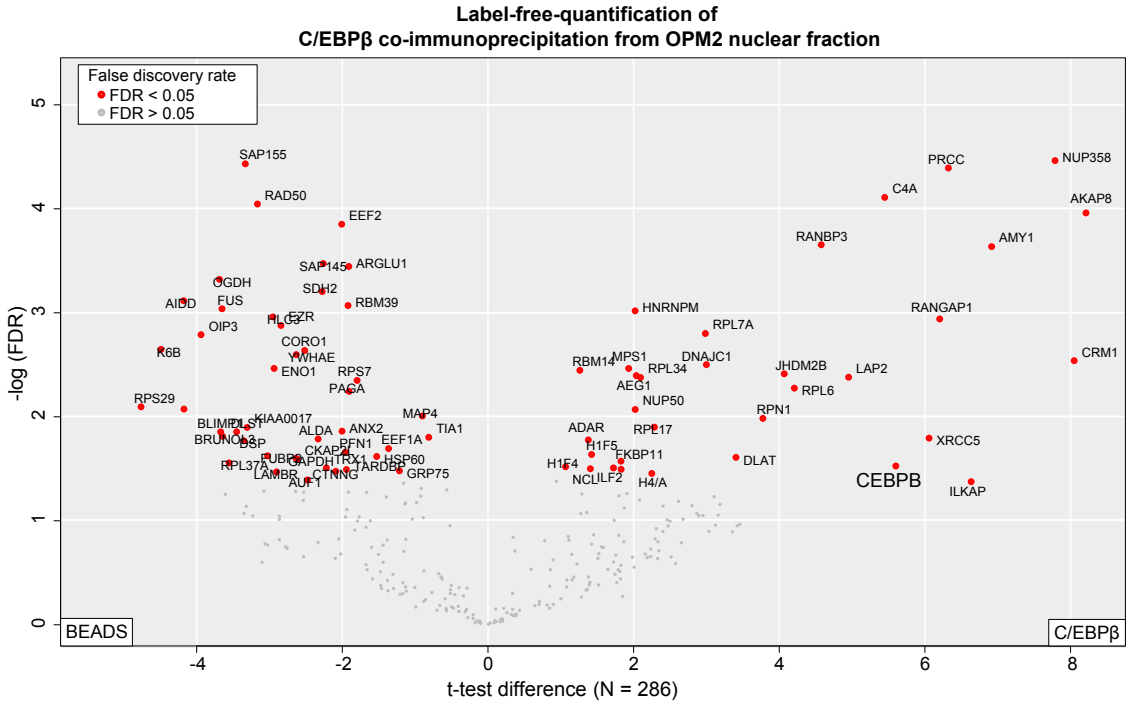

Figure 15: Volcano plot of anti-C/EBPβ IP-MS label-free shotgun approach from OPM2 nuclear enriched cell lysates. The x-axis shows the t-test difference of the interactions of the anti-C/EBPβ IP samples (triplicates) versus bead control (triplicates). Proteins that were detected at least twice in either the anti-C/EBPβ IP triplicate or the bead control triplicate were chosen for the t-test. Missing values were imputated. The y-axis depicts the FDR in a negative Log scale. Interactions with a FDR level of ≤ 5 ⁒ were considered as significant and are depicted in red. Proteins with a FDR ≥ 5⁒ are not considered as significant and are depicted in grey (Günther Kahlert, MDC Berlin). Detected proteins are colored due to their significance level and named due to the human IPI database (Günther Kahlert, MDC Berlin).

The IP-MS analysis revealed a significant overlap between the of C/EBPβ protein interaction partners in the different leukemia cell lines (Table 4). IP-MS revealed 25 interactions as overlapping between the SU-DHL-1 whole cell extract and the nuclear enriched (NE) SU-DHL-1 cell lysates and from here on the data of both IPs from SU-DHL-1 cells (whole cell lysate and nuclear enrichment) are summarized together under the name of “IP-MS from SU-DHL-1”.

As itemized in Table 4 and Figure 16 IP-MS revealed 37 proteins that interacted with C/EBPβ in both lymphocytic derived leukemia cell lines SU-DHL-1 (ALCL) and JEKO-1 (MCL). Despite the differences between the lymphocytic derived leukemia cell line SU-DHL-1 and the histiocytic cell line U937 IP-MS detected 23 proteins that interacted with C/EBPβ in both cell lines (Figure 16 and Table 4). Interestingly, only 12 proteins interactions overlap

between the IP-MS data of JEKO-1 and U937 cells and 17 overlap between IP-MS data of SU-DHL-1 and HL60 (Figure 16 and Table 4).

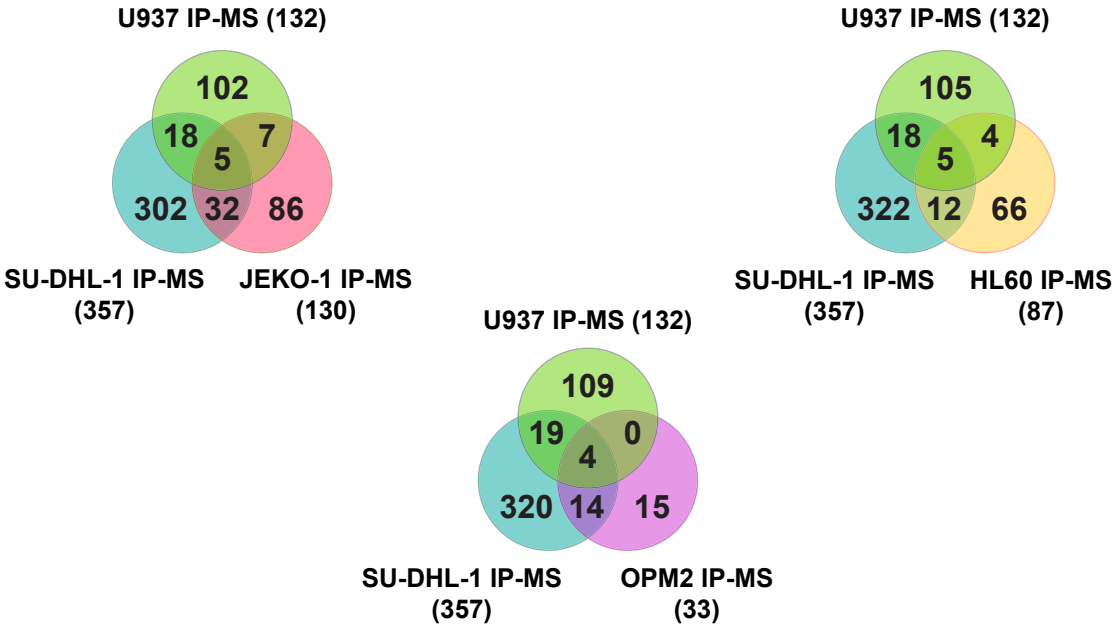

Figure 16: Venn diagrams visualizing the number of overlapping proteins detected as endogenous C/EBPβ interaction partners among the IP-MS experiments from the selected leukemia cell lines. The interaction data is itemized in detail in Table 4 and Table S1.

Subsequently the IP-MS data of endogenous C/EBPβ interactions in the leukemia cell lines was integrated with the direct protein interactions detected by APS binding to of the conserved regions of C/EBPβ. As itemized in Table S1 and for IP-MS of nuclear enriched lysates of SU-DHL-1 cells in Figure 17 the endogenous C/EBPβ immunoprecipitations revealed a wealth of significant interactions compromising 86 published protein-interactors (Siersbaek et al., 2014; Steinberg et al., 2012; Lee et al., 2010b; Jiang et al., 2008; Ki et al., 2005; Kowenz-Leutz and Leutz, 1999; Chang et al., 1998; Miau et al., 1998; Xia et al., 1997; LeClair et al., 1992) and verified 44 protein interactions detected by APS. Especially the endogenous IP of nuclear enriched SU-DHL-1 lysates verified a significant number of previously reported and/or APS detected interactions as depicted in Figure 17.

Table 4: The table on the following pages (60-61) itemizes the protein-interactions of C/EBPβ that were detected in at least two of the analyzed leukemia cell lines by IP-MS. Immunoprecipitations of endogenous C/EBPβ (with an anti-C/EBPβ antibody) from whole cell lysates of U937, JEKO-1, HL60 and SU-DHL-1 and from nuclear enriched lysates of OPM2 and SU-DHL-1 cells (column 6-11) were prepared as triplicates and were analyzed by shotgun mass spectrometry using a label-free quantification approach (Hubner and Mann, 2011). Column 2 lists the log10 of iBAQ intensity of the MS-iBAQ quantification of the SU-DHL-1 cell line (MS-analysis by Günther Kahlert, MDC; vide material and methods section).

UniProt AC	SU-DHL-1 iBAQ [log10 of iBAQ intensity]	Name	Synonyms		HL60 [whole cell lysate]	JEKO-1 [whole cell lysate]	OPM2 [nuclear enriched lysate]	U937 [whole cell lysate]	SU-DHL-1 [whole cell lysate]	SU-DHL-1 [nuclear enriched lysate]
P17676	7.5900	CEBPB	TCF5	-	Co-IP	Co-IP	Co-IP	Co-IP	Co-IP	Co-IP
Q9H0C8	7.1884	ILKAP	-	-	Co-IP	Co-IP	Co-IP	Co-IP	Co-IP	Co-IP
Q9H6Z4	7.3333	RANB3	RANBP3	-	Co-IP	Co-IP	Co-IP	Co-IP	Co-IP	0
O14980	8.0217	XPO1	CRM1	-	0	Co-IP	Co-IP	Co-IP	Co-IP	Co-IP
P13010	8.6857	XRCC5	G22P2	-	0	Co-IP	Co-IP	0	Co-IP	Co-IP
O43823	6.9873	AKAP8	AKAP95	-	0	Co-IP	Co-IP	0	0	Co-IP
P0C0L5	-	CO4B	-	-	0	Co-IP	Co-IP	0	0	Co-IP
Q7LBC6	6.6277	KDM3B	JMJD1B	-	0	Co-IP	Co-IP	0	0	Co-IP
Q92733	6.8760	PRCC	TPRC	-	0	0	Co-IP	0	Co-IP	Co-IP
P26641	8.6992	EF1G	EEF1G	-	Co-IP	Co-IP	0	0	Co-IP	Co-IP
E9PRY8	8.1325	E9PRY8	EEF1D	-	0	Co-IP	0	0	Co-IP	Co-IP
P12956	8.8269	XRCC6	G22P1	-	0	Co-IP	0	0	Co-IP	Co-IP
P78527	8.0827	PRKDC	HYRC	-	0	Co-IP	0	0	Co-IP	Co-IP
P26640	-	SYVC	VARS	G7A	0	Co-IP	0	0	Co-IP	Co-IP
P46060	7.5258	RAGP1	RANGAP1	KIAA1835	0	0	Co-IP	0	Co-IP	0
Q12905	8.6838	ILF2	NF45	-	0	0	Co-IP	0	Co-IP	0
Q9NYL4	7.8137	FKB11	FKBP11	FKBP19	0	0	Co-IP	0	Co-IP	0
P80303	7.4130	NUCB2	NEFA	-	Co-IP	Co-IP	0	0	Co-IP	0
Q9BUL8	7.5315	PDC10	PDCD10	CCM3	Co-IP	Co-IP	0	0	Co-IP	0
Q9NSP4	-	CENPM	C22orf18	-	Co-IP	Co-IP	0	0	Co-IP	0
Q9H9Q4	5.9103	NHEJ1	XLF	-	0	Co-IP	0	Co-IP	Co-IP	0
B7Z5E3	-	B7Z5E3	-	-	0	Co-IP	0	0	Co-IP	0
D3DUS9	-	D3DUS9	DNM1L	-	0	Co-IP	0	0	Co-IP	0
O60711	6.7463	LPXN	LDLP	-	0	Co-IP	0	0	Co-IP	0
O95684	7.1031	FR1OP	FOP	-	0	Co-IP	0	0	Co-IP	0
P04406	9.5663	G3P	GAPDH	GAPD	0	Co-IP	0	0	Co-IP	0
P07737	9.1337	PROF1	PFN1	-	0	Co-IP	0	0	Co-IP	0
P24534	8.2158	EF1B	EEF1B2	EEF1B	0	Co-IP	0	0	Co-IP	0
P41250	8.3967	SYG	GARS	-	0	Co-IP	0	0	Co-IP	0
P49720	8.5113	PSB3	PSMB3	-	0	Co-IP	0	0	Co-IP	0
P62306	8.7701	RUXF	SNRPF	PBSCF	0	Co-IP	0	0	Co-IP	0
P62937	9.3061	PPIA	CYPA	-	0	Co-IP	0	0	Co-IP	0
Q86UY3	-	Q86UY3	-	-	0	Co-IP	0	0	Co-IP	0
Q96JB2	6.1842	COG3	SEC34	-	0	Co-IP	0	0	Co-IP	0
Q9UBT2	7.9537	SAE2	UBA2	-	0	Co-IP	0	0	Co-IP	0
Q9UQ13	5.8638	SHOC2	KIAA0862	-	0	Co-IP	0	0	Co-IP	0
P62244	8.9113	RS15A	RPS15A	-	Co-IP	0	0	Co-IP	Co-IP	0
Q9H8S9	7.4340	MOB1A	C2orf6	-	Co-IP	0	0	Co-IP	Co-IP	0
P11172	7.5503	UMPS	-	-	Co-IP	0	0	0	Co-IP	0
P19474	-	RO52	TRIM21	RNF81	Co-IP	0	0	0	Co-IP	0
P55060	8.2769	XPO2	CSE1L	CAS	Co-IP	0	0	0	Co-IP	0
Q8TCG1	6.5320	CIP2A	KIAA1524	-	Co-IP	0	0	0	Co-IP	0
Q99623	8.6230	PHB2	BAP	-	Co-IP	0	0	0	Co-IP	0
Q9Y4R8	6.3775	TELO2	KIAA0683	-	Co-IP	0	0	0	Co-IP	0
O43156	6.9478	TTI1	-	-	0	0	0	Co-IP	Co-IP	0
P19338	8.8166	NUCL	NCL	-	0	0	Co-IP	0	0	Co-IP
P42166	7.9299	LAP2A	TMPO	LAP2	0	0	Co-IP	0	0	Co-IP
P49792	6.8798	RBP2	RANBP2	NUP358	0	0	Co-IP	0	0	Co-IP
Q9UKX7	7.0178	NUP50	NPAP60L	-	0	0	Co-IP	0	0	Co-IP
P52272	8.5349	HNRPM	HNRNPM	-	0	0	Co-IP	0	0	Co-IP
P04843	8.3652	RPN1	-	-	0	0	Co-IP	0	0	Co-IP
O00299	8.8855	CLIC1	-	G6	0	Co-IP	0	0	0	Co-IP
P12268	8.6713	IMDH2	IMPDH2	IMPD2	0	Co-IP	0	0	0	Co-IP
P22102	8.1383	PUR2	GART	PGFT	0	Co-IP	0	0	0	Co-IP
P62195	8.1190	PRS8	PSMC5	SUG1	0	Co-IP	0	0	0	Co-IP
Q13200	8.0567	PSMD2	TRAP2	-	0	Co-IP	0	0	0	Co-IP
O95347	7.5986	SMC2	CAPE	-	Co-IP	0	0	0	0	Co-IP
Q9UJZ1	8.3277	STML2	STOML2	SLP2	Co-IP	0	0	0	0	Co-IP

UniProt AC	SU-DHL-1 iBAQ [log10 of iBAQ intensity]	Name	Synonyms		HL60 [whole cell lysate]	JEKO-1 [whole cell lysate]	OPM2 [nuclear enriched lysate]	U937 [whole cell lysate]	SU-DHL-1 [whole cell lysate]	SU-DHL-1 [nuclear enriched lysate]
P62805	10.1851	H4	HIST1H4A	H4/A	Co-IP	0	Co-IP	0	0	0
B8ZZN6	7.8841	B8ZZN6	SUMO1	-	Co-IP	Co-IP	0	0	0	0
Q96N11	5.6972	CG026	C7orf26	-	Co-IP	Co-IP	0	0	0	0
A6NHB5	5.0052	A6NHB5	-	-	0	Co-IP	0	Co-IP	0	0
B5M451	-	B5M451	-	-	0	Co-IP	0	Co-IP	0	0
D3DPG0	-	D3DPG0	-	-	0	Co-IP	0	Co-IP	0	0
P42694	-	HELZ	-	-	0	Co-IP	0	Co-IP	0	0
P53990	6.7855	IST1	-	-	0	Co-IP	0	Co-IP	0	0
Q5JTZ9	5.7636	SYAM	-	-	0	Co-IP	0	Co-IP	0	0
Q7Z351	-	Q7Z351	-	-	0	Co-IP	0	Co-IP	0	0
B4DLZ8	-	B4DLZ8	-	-	Co-IP	0	0	Co-IP	0	0
Q8N392	-	RHG18	-	-	Co-IP	0	0	Co-IP	0	0
Q96AX1	5.0024	VP33A	VPS33A	-	Co-IP	0	0	Co-IP	0	0
Q9UK61	5.9612	F208A	FAM208A	C3orf63	Co-IP	0	0	Co-IP	0	0
P33121	-	ACSL1	FACL1	-	0	0	0	Co-IP	Co-IP	0
P46459	7.3631	NSF	-	-	0	0	0	Co-IP	Co-IP	0
P55160	6.3735	NCKPL	NCKAP1L	HEM1	0	0	0	Co-IP	Co-IP	0
Q13724	7.4045	MOGS	GCS1	-	0	0	0	Co-IP	Co-IP	0
Q5VYK3	-	ECM29	KIAA0368	-	0	0	0	Co-IP	Co-IP	0
Q96ER3	6.9216	SAAL1	-	-	0	0	0	Co-IP	Co-IP	0
Q96QU8	-	XPO6	KIAA0370	-	0	0	0	Co-IP	Co-IP	0
Q9BVI4	7.0331	NOC4L	-	-	0	0	0	Co-IP	Co-IP	0
Q9BXW9	6.4636	FACD2	FANCD2	FACD	0	0	0	Co-IP	Co-IP	0
Q9BZZ5	7.7939	API5	MIG8	-	0	0	0	Co-IP	Co-IP	0
Q9NV70	6.4473	EXOC1	SEC3	-	0	0	0	Co-IP	Co-IP	0
Q9UBB9	5.9354	TFP11	TFIP11	STIP	0	0	0	Co-IP	Co-IP	0
Q9Y6E2	7.6163	BZW2	HSPC028	-	0	0	0	Co-IP	Co-IP	0
P11388	7.8618	TOP2A	TOP2	-	0	0	0	Co-IP	0	Co-IP
P35659	8.1838	DEK	-	-	0	0	0	Co-IP	0	Co-IP
O43175	8.2946	SERA	PHGDH	PGDH3	0	0	0	0	Co-IP	Co-IP
P27708	7.8531	PYR1	CAD	-	0	0	0	0	Co-IP	Co-IP
P30153	8.0529	2AAA	PPP2R1A	-	0	0	0	0	Co-IP	Co-IP
P32189	7.9368	GLPK	GK	-	0	0	0	0	Co-IP	Co-IP
P35232	8.8204	PHB	-	-	0	0	0	0	Co-IP	Co-IP
P40763	7.9850	STAT3	APRF	-	0	0	0	0	Co-IP	Co-IP
P42285	7.3458	SK2L2	SKIV2L2	KIAA0052	0	0	0	0	Co-IP	Co-IP
P42704	8.1207	LPPRC	LRPPRC	LRP130	0	0	0	0	Co-IP	Co-IP
P50991	8.5139	TCPD	CCT4	CCTD	0	0	0	0	Co-IP	Co-IP
Q00610	8.2996	CLH1	CLTC	CLH17	0	0	0	0	Co-IP	Co-IP
Q9Y5B9	7.9425	SP16H	SUPT16H	FACT140	0	0	0	0	Co-IP	Co-IP
Q08211	8.4041	DHX9	DDX9	-	0	0	0	0	Co-IP	Co-IP
P13639	8.8879	EF2	EEF2	-	0	0	0	0	Co-IP	Co-IP

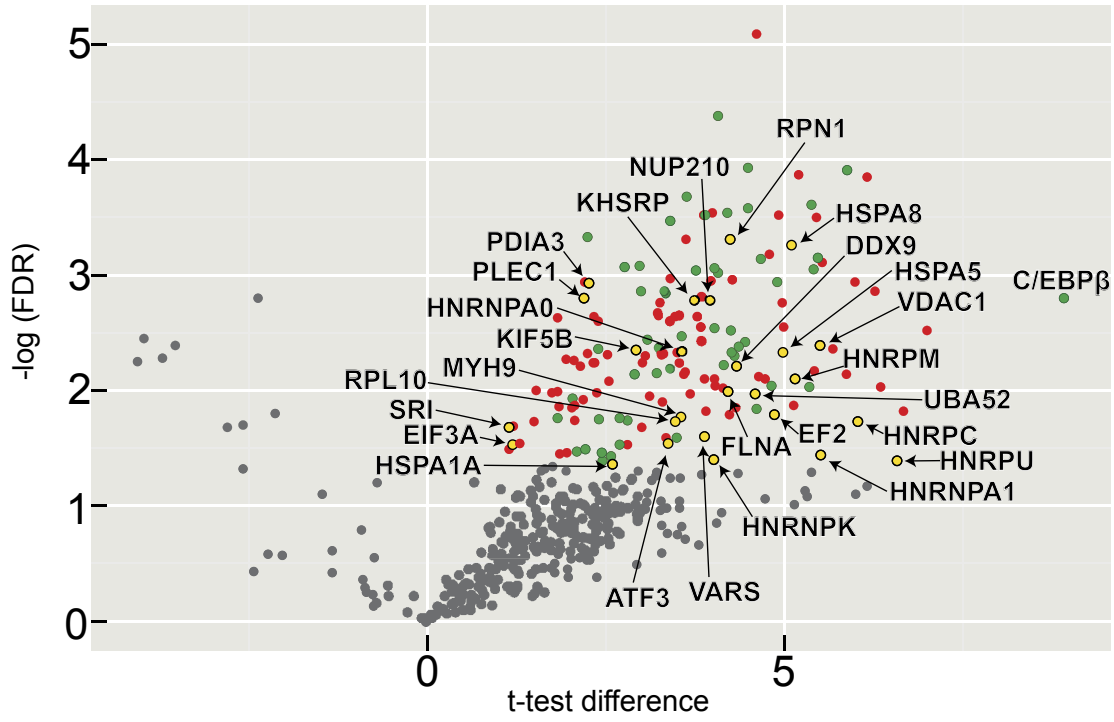

Figure 17: C/EBPβ Co-Immunoprecipitation from nuclear enriched SU-DHL-1 cell lysates revealing multiple C/EBPβ interactors that were described before and/or detected by APS. Endogenous immunoprecipitations from nuclear enriched lysates of SU-DHL-1 cell line with an anti-C/EBPβ antibody were analyzed by shotgun mass spectrometry (triplicates were used for label-free quantification, missing values were imputated (vide Figure 14), significance level: FDR$\leq$ 5 %). The x-axis shows the t-test difference of the interactions of the anti-C/EBPβ IP samples (triplicates) versus bead control (triplicates) and the y-axis presents the FDR in negative Log scale. C/EBPβ interactions with a FDR $\leq$ 5 % are depicted as red dots. Previously published C/EBPβ interactions are depicted as green dots, interactions found by APS as well as IP-MS are labeled by their protein name and depicted as yellow dots, background binding proteins and contaminants binding to the bead control are depicted as grey dots.

Extended bioinformatic analysis of the integrated APS and IP-MS data was carried out to elucidate the range of functions that C/EBPβ protein interaction network is involved in. The DAVID online tool (DAVID.abcc.ncifcrf.gov; Huang et al., 2009) was used to determine the GO:terms and the functional domains with an exclusion threshold of Benjamini-Hochberg $\leq$ 5 %. The Cytoscape software including the BisoGenet plugin (Martin et al., 2010; Shannon et al., 2003), the CORUM database (Ruepp et al., 2008; 2010), the HIPPIE database (Schaefer et al., 2011) and the STRING database (Jensen et al., 2009) were employed simultaneously to unravel the functional complexes and networks C/EBPβ interacts with. The bioinformatic

data analysis revealed a large variety of functional categories and numerous possible complexes in which the acquired C/EBPβ interactors could be grouped, such as chromatin remodeling and histone modifying complexes, as well as transcription factors and spliceosome components.

3.4 Proteomic analysis of leukemia cell lines

Despite the detection of a particular number of overlapping interactions the two detection methods revealed numerous interactions of C/EBPβ that were only detected with either the APS or the IP-MS technique. One reason could be the substantial difference in C/EBPβ protein quantities itself of either the full-length C/EBPβ in the IP-MS or C/EBPβ peptides available for interaction in APS. A cell specific minor expression pattern of C/EBPβ interaction partners detected by APS but not by IP-MS could be another possible explanation for the difference between the APS and IP-MS uncovered C/EBPβ interactors. In order to examine this theory mass spectrometry proteomics and the Intensity-Based Absolute Quantification Index (iBAQ) (Geiger et al., 2012; Schwanhäusser et al., 2011) were used for precise quantification of the SU-DHL-1 proteome, representative for all used leukemia cell lines (in cooperation with Günther Kahlert, MDC). Additionally, total C/EBPβ protein abundance was determined by MS-SRM proteomics of U937 and SU-DHL-1 cell lysates. The MS-proteomic analysis revealed that 85% of the IP-MS detected interacting proteins in SU-DHL-1 cells were also detected in the SU-DHL-1 proteome by MS-iBAQ, whereas only $\approx 20.5\%$ of all APS detected C/EBPβ interaction partners were identified within the 4533 most abundant SU-DHL-1 proteins (Figure 18). The remaining APS-derived C/EBPβ interaction partners ($\approx 79,5\%$) were neither detected in the SU-DHL-1 proteome nor identified as significant C/EBPβ interactors in the SU-DHL-1 immunoprecipitations (Figure 18), suggesting absence or low expression in the leukemia cell line, such as ZC3H3, MLL2, MEN1, NCOR2, KDM6B, L3MBT and p21/WAF1. Thus, these interacting proteins were probably detected by APS due to the bulk amounts of human proteins presented on the bacterially expressed APS macroarrays, although binding in cells awaits further validation. The data suggest that the combinatory use of expression independent in-vitro APS and endogenous IP-MS provides a powerful complementary tool to

determine a broad overview of a protein interactome.

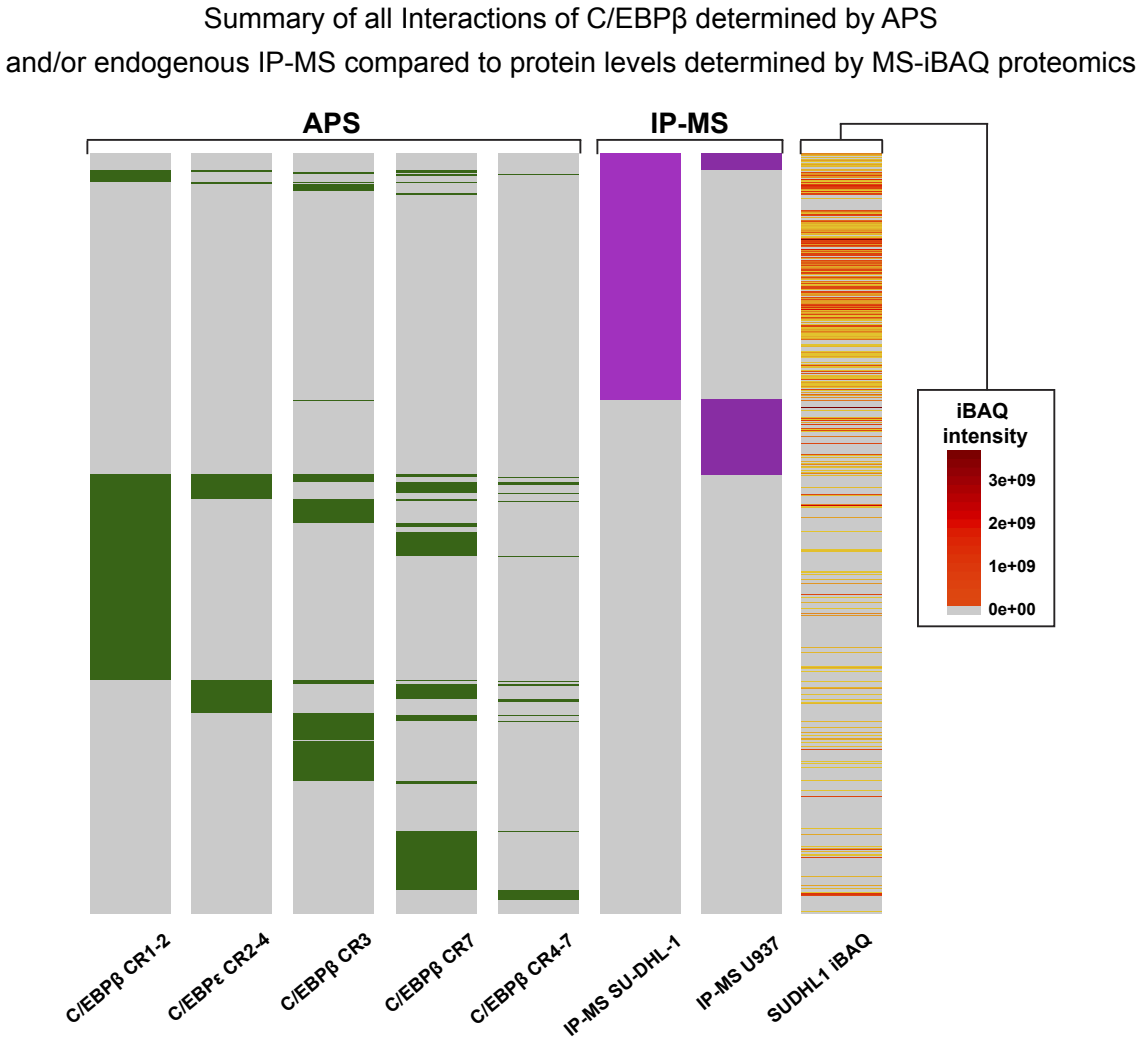

Figure 18: The heatmap depicts all C/EBPβ interactions detected by all APS experiments, by IP-MS from U937 and SU-DHL-1 (whole cell and nuclear enriched lysates) cells and the iBAQ quantification of the SU-DHL-1 proteome. The proteomic expression levels in SU-DHL-1 cells of the depicted proteins (first column from right) are presented as iBAQ intensity (grey = not detected, yellow = low, orange = medium, red = high). The positive detection of interactions in the anti C/EBPβ IP-MS approaches from U937 or SU-DHL-1 cells is marked in magenta (second and third column from right). Positive detection of interaction in APS (first 5 columns on the left) is marked in green. Proteins, which were not detected with one of the techniques, are marked in grey.

The number of C/EBPβ interactions detected in SU-DHL-1 cell lysates was larger than those detected in U937, HL60, JEKO-1 and OPM2 cells. To determine the reason of this difference the relative C/EBPβ protein abundance in SU-DHL-1 and U937 whole cell lysates was analyzed by MS-SRM proteomics (in cooperation Günther Kahlert, MDC).

SRM proteomics revealed an 18 times higher expression of C/EBPβ in the SU-DHL-1 cells compared to U937 cells (Figure 19). The results suggest that the most likely cause for the observed difference in interactions is the significantly higher expression of C/EBPβ in the SU-DHL-1 compared to the U937 cell line. The minor abundance of C/EBPβ protein IP-bait in U937 most probably leads to a shift of substantive C/EBPβ-protein interactions beneath the detection limit of mass spectrometry. The same shift in C/EBPβ abundance could also account for the reduced number of protein-protein interactions detected in the other analyzed leukemia cell lines, but needs further experimental validation.

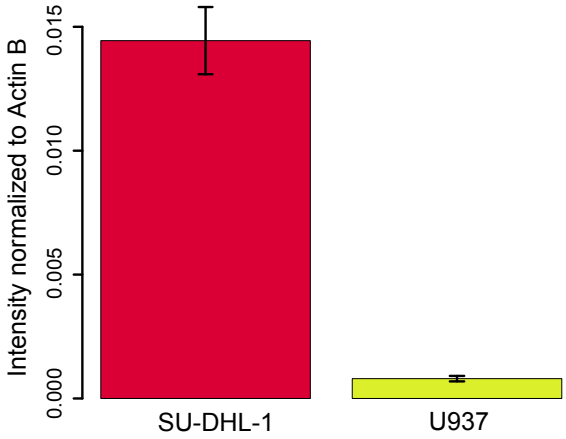

Figure 19: Abundance of C/EBPβ protein in the tested lysates of U937 and SU-DHL-1 cells determined by Selected Reaction Monitoring (SRM; Günther Kahlert, MDC). The x-axis depicts the analyzed cell lines and the y-axis shows the C/EBPβ intensity normalized to Actin B. The barplot shows an 18 times higher amount of C/EBPβ protein in SU-DHL-1 cell lysates (red) compared to U937 cell lysates (yellow).

3.5 Integration of APS and MS-data reveals a wealth of novel interaction partners of C/EBPβ

The C/EBPβ interaction data derived from APS and IP-MS approaches as well as the iBAQ proteomics data was integrated and subjected to bioinformatic analysis (vide material and methods section). The data integration of the direct and/or endogenous interactions of C/EBPβ enabled the interpretation and evaluation of the detected protein-protein interactions in a broader functional context and thereby the elucidation of potential novel roles and

functions of the transcription factor C/EBPβ.

3.6 C/EBPβ interacts with proteins associated with metabolism

GO-term analysis of the protein interactions of C/EBPβ/ε revealed by APS and/or IP-MS was performed with the DAVID online tool (DAVID.abcc.ncifcrf.gov; Huang et al., 2009). The GO analysis characterized numerous interactors as members of the glucose, the lipid or the nucleotide metabolism pathways. These results are in concordance with the proteomics results of C/EBPβ infected C/EBPβ$^{-/-}$ MEF cells. C/EBPβ infection of C/EBPβ$^{-/-}$ MEF cells induced differential expressions of proteins that could be grouped into the GO:terms GO:0055114 "oxidation-reduction process" and GO:0006091 "generation of precursor metabolites and energy". Several C/EBPβ/ε interactors from IP-MS and APS analysis are characterized by the GO-term GO:0055114 as well (Figure 20). The interacting proteins classified by this GO:term are ACADV (acyl-CoA-dehydrogenase), NDUA6 (NADH dehydrogenase (ubiquinone) 1 α subcomplex subunit 6), NB5R3 (NADH cytochrome b5 reductase 3), CYC (Cytochrome C), NNTM (nicotinamide nucleotide transhydrogenase) and QCR2 (Cytochrome b-c1 complex subunit 2; part of the mitochondrial respiratory chain). Some of the interacting proteins could additionally be grouped into the term GO:0006091 "generation of precursor metabolites and energy". C/EBPβ has been associated with glucose metabolism before (Arizmendi et al., 1999; Liu et al., 1999). In accordance with this, interactors from APS and/or IP-MS approaches could be characterized by the GO-term GO:0006006 "glucose metabolic process". These GO:term members are ATF3, ATF4, the Serine/threonine-protein phosphatase PP1-α (PP1A) and the glycerol-3-phophate dehydrogenase (GPDA). GO:0006006 encompasses members of the pentose phosphate pathway as well, namely the ribose 5-phosphate isomerase A (RPIA), the phosphogluconate dehydrogenase (6PGD) and the glucose-6-phosphate-dehydrogenase (G6PD), which interact with C/EBPβ (Figure 20). Additionally, GO:0006006 characterizes the C/EBPβ interactors glycolysis/gluconeogenesis proteins ADHX (Alcohol-dehydrogenase class 3), glyceraldehyde-3-phosphate dehydrogenase (GAPDH), pyruvate kinase (PKM) and enolase1 (ENOA) (Figure 20).

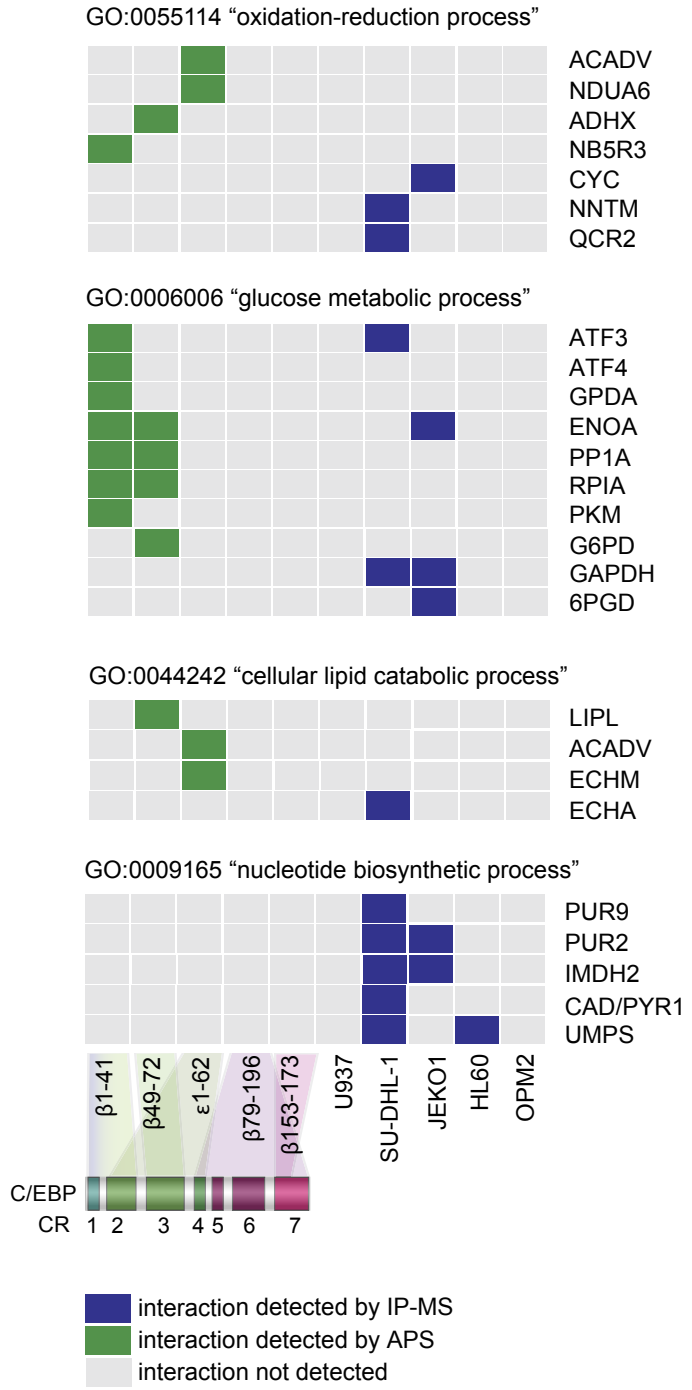

Figure 20: Selected interactions of C/EBPβ/ε that could be grouped into metabolism associated GO-terms like GO:0055114 “oxidation-reduction process”, GO:0006006 “glucose metabolic process”, GO:0044242 “cellular lipid catabolic process” and GO:0009165 “nucleotide biosynthetic process” using the DAVID online tool (DAVID.abcc.ncifcrf.gov; Huang et al., 2009). Direct interactions detected by APS with peptides of the conserved regions of C/EBPβ/ε are depicted as green squares in the heatmap. The legend below the heatmap illustrates the amino acid coverage of APS peptides of the C/EBPβ/ε protein. Interactions detected by IP-MS (anti-C/EBPβ) from cell lysates of at least one of the cell lines SU-DHL-1 (whole cell and/or nuclear enriched), U937, JEKO-1, OPM2 and HL60 are depicted in blue. Grey squares indicate not detected interaction.

Additionally, C/EBPβ/ε interactors from IP-MS and APS analysis could be grouped into the GO-term GO:0044242 “cellular lipid catabolic process” like the lipoprotein lipase (LIPL), the acyl-CoA-dehydrogenase (ACADV), the enoyl-CoA hydratase (ECHM) and the 3-hydroxyacyl-CoA-dehydrohgenase (ECHA) (Figure 20). Five interactors of C/EBPβ that were revealed by IP-MS could be characterized by GO:0009165 “nucleotide biosynthetic process”. These interactors are the purine metabolism associated PUR9, PUR2 and the inosine-5’-monophosphate dehydrogenase 2 (IMDH2), as well as the pyrimidine metabolism associated PYR1/CAD and the uridine 5’-monophosphate synthase (UMPS). In summary, this data emphasizes the involvement of C/EBPβ in metabolism in concert with previous studies (Arizmendi et al., 1999; Liu et al., 1999).

3.7 C/EBPβ interacts with proteins that regulate and participate in the gene transcription machinery

C/EBPβ locates at the CCAAT-box sequence of its target gene promoters to initiate gene transcription (Osada et al., 1996; Mahony et al., 2007, Nerlov et al., 1995). The here discussed APS and IP-MS screening data encompasses yet unknown interactions with components of the RNA-polymerase-II and III complexes. The screenings revealed a direct interaction of the C/EBPβ TAD region with ERCC3 and the general transcription factor GTF2F1 (APS) as well as GTF2B, GTF2H1 and GTF2H4 as endogenous interactions in the leukemic cell lines (IP-MS) (Figure 21). The IP-MS approaches confirmed the known C/EBPβ interactor GTF3C1 (Steinberg et al., 2012) and unraveled unknown interactions with the RNA-Polymerase III (RNA-POLIII) complex subunit POLR3C and POLR3E. The APS method detected GTF3A, a further component of this complex. In concert with this the expression of all interacting RNA-polymerase II and III complex proteins were detected in SU-DHL-1 cells by iBAQ, except for GTF3 and TFIIS. Our laboratory revealed the interaction of the Mediator complex component MED23 with the transactivation as well as the regulatory domain of C/EBPβ recently (Kowenz-Leutz et al., 2010, Mo et al., 2004). The current APS approach identified the Mediator complex member MED16 as direct interactor of the C/EBPβ TAD and MED15

of the C/EBPβ RD. On top of that, IP-MS disclosed novel interactions of endogenous C/EBPβ with the mediator complex components CDK19, MED30 and MED19 in U937 and MED16 in SU-DHL-1 (Figure 21).

3.8 C/EBPβ interacts with proteins regulating chromatin structure and organization

The SWI/SNF complex component SNF5/SMARCB1/BAF47 was shown by our lab to interact with the CR1/2 of C/EBPβ in a PTM dependent manner (Kowenz-Leutz et al., 2010). This observation could be confirmed here by APS, which revealed interaction of SNF5 with the C/EBPβ TAD peptides covering CR1-2 and CR3. Additionally, APS detected interaction of the C/EBPβ TAD with BC11A and BC11B that were recently identified as novel components of the SWI/SNF complex (Kadoch et al., 2013).
The IP-MS screenings identified interaction of C/EBPβ with the SWI/SNF component MECP2. Interestingly, IP-MS also verified the recent reported interaction with the SWI/SNF complex members BAF250 and BAF180/PB1 in U937 and SMC1A, SNF2H, BAF155 and BRG1 in SU-DHL-1 (NE) (Steinberg et al., 2012; Figure 21). The expression of SMC1A, SNF2H, BAF155 and BRG1 in SU-DHL-1 cells was verified by MS-iBAQ proteomics. Taken together these results indicate the cooperation of C/EBPβ with the SWI/SNF complex in leukemia cell lines and emphasizes the interaction of the SWI/SNF complex with the TAD region of C/EBPβ, as suggested before (Kowenz-Leutz et al., 2010).

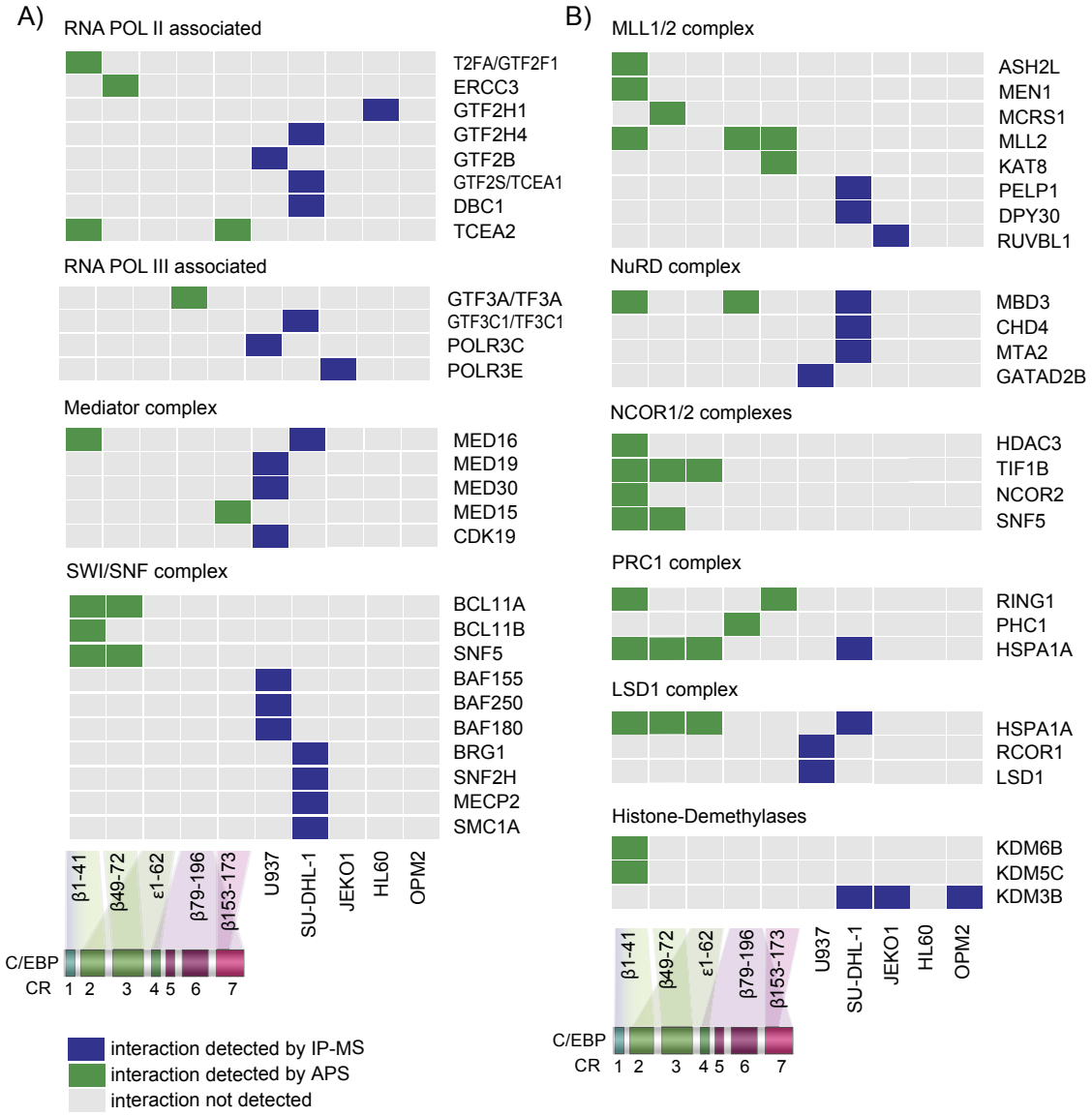

Figure 21: Selected interactions of C/EBPβ/ε that could be grouped into functional groups or published functional complexes using the CORUM database (http://mips.helmholtz-muenchen.de/genre/proj/corum; Ruepp et al., 2008; 2010). Direct interactions detected by APS with peptides of the conserved regions of C/EBPβ/ε are depicted as green squares in the heatmap. The legend below the heatmap illustrates the amino acid coverage of APS peptides of the C/EBPβ/ε protein. Interactions detected by IP-MS (anti-C/EBPβ) from cell lysates of at least one of the cell lines SU-DHL-1 (whole cell and/or nuclear enriched), U937, JEKO-1, OPM2 and HL60 are depicted in blue. Grey squares indicate not detected interaction. A) Selected interactions of C/EBPβ/ε detected by APS and/or IP-MS that could be grouped into or associated with RNA polymerase, Mediator complexes and SWI/SNF complex. B) Selected interactions of C/EBPβ/ε detected by APS and/or IP-MS that could be grouped into or associated with the MLL1/2, NuRD, NCOR, PRC1 or LSD complexes.

3.9 C/EBPβ interacts with histone modifying proteins

This survey detected C/EBPβ to interact with epigenetic and histone modifying proteins that participate in histone methyl- and acetyltransferase complexes as well as demethylase and deacetylase complexes.
The APS approaches disclosed interactions of the C/EBPβ TAD with ASH2L and MCRS1 that are understood to be components of the MLL1 histone methyltransferase complex. Moreover, IP-MS detected endogenous C/EBPβ to interact with the proposed MLL1 complex members PELP1 in SU-DHL-1 and RUVBL in JEKO-1 cells. The IP-MS data also revealed interaction of C/EBPβ with the MLL2 methyltransferase complex component DPY30, while APS reports the interaction of C/EBP TAD peptides with MEN1, ASH2L and MLL2 (also RD) (Figure 21). Furthermore, APS and IP-MS data reveal interactions of C/EBPβ with proteins of the Jumonji- histone-demethylase family. The APS screening revealed a direct interaction of the C/EBPβ CR1/2 region with the co-repressor KDM5C, known to demethylate the activating H3K4me2/3 histone mark and the coactivator KDM6B known to demethylate the repressive H3K27me2/3 signature (for overview see: Rotili and Mai, 2011; Cloos et al., 2008). IP-MS revealed the interaction of the H3K9 demethylating coactivator KDM3B with endogenous C/EBPβ in JEKO-1 and OPM2 cells.

This survey was able to identify C/EBPβ interaction with histone acetytransferases and deacetylases. The interaction of C/EBPβ with components of the NuA4/Tip-HAT complex like BRD8, RUVBL1 was revealed by IP-MS from JEKO-1 cells and APS added the complex component MRGBP. The histone acetyltransferases (HAT) CBP and p300 are well-known cooperation partners of C/EBPβ (Nerlov, 2004; Kovcs et al., 2003; Mink et al., 1996). The interaction of CBP could be verified by the APS survey. In addition, a direct interaction of C/EBPβ with TADA3 was detected by APS and IP-MS disclosed the TAF6L interaction in SU-DHL-1 cells. These two proteins are putative components of the CBP/p300 cooperating PCAF-HAT-complex (Cho et al., 1998; Korzus et al., 1998; Ogryzko et al., 1998; Vassilev et al., 1998; Chen et al., 1997). These results suggest that the here identified epigenetic modifiers could collaborate with C/EBPβ during target gene activation.

C/EBPβ is capable of both gene activation and repression (Descombes and Schibler,

1991). APS and IP-MS experiments elucidated interaction with proteins associated with negative gene regulation. IP-MS of HL60 cells revealed interaction of C/EBPβ with NOC2L, a HAT inhibitor that was also shown to inhibit p300 mediated promoter acetylation of p53 target genes (Hublitz et al., 2005). The C/EBPβ TAD is published to interact with the co-repressor NCOR2/SMRT as well as NCOR1 (Ki et al., 2005). Our APS approaches detected an interaction of the C/EBPβ TAD with NCOR2 and the C/EBPβ RD peptide interacted with the NCOR2 cooperator HDAC10 (Fischer et al., 2002; Figure 21). Additionally, the APS approaches elucidated a direct interaction of the C/EBPβ TAD with TIF1B, SNF5, SF3B3 and HDAC3 proposed components of the NCOR1-complex (Underhill et al., 2000).

The IP-MS data revealed LSD1 and RCOR (CoREST) as interaction partners of endogenous C/EBPβ in U937 cells. APS data indicates a direct interaction of the CR1/2 peptide of C/EBPβ with the REST protein, which represses neural genes in non-neural tissue in cooperation with RCOR (CoREST) and SIN3A (Grimes et al., 2000). Since the LSD1-RCOR complex as well as NCOR1/2-complexes are known to recruit HDACs to gene promoters (Lee et al., 2005; Metzger et al., 2005; Shi et al., 2005; Underhill et al., 2000; Yang et al., 2006) we hypothesize that C/EBPβ could cooperate with those complexes to silence target genes.

Intriguingly, this screening revealed interaction of C/EBPβ with the NuRD complex, a complex that is depending on its subunits, associated with transcriptional activation or repression and has been published to interact with C/EBPβ before (Günther et al., 2013; Steinberg et al., 2012). IP-MS detected interaction of endogenous C/EBPβ with the Mi2-NuRD complex components CHD4, MTA2 and MBD3 in SU-DHL-1 and GATAD2B in U937 cells. MBD3 was identified as direct C/EBPβ binder by the APS screening. Furthermore, APS revealed interaction of the C/EBPβ CR3 peptide with the co-repressor protein TIF1B/TRIM28 known to recruit CHD3 to the NuRD-complex (Schultz et al., 2001; Figure 21).

Next to the interaction of C/EBPβ TAD peptides with transcriptional repressive epigenetic modifiers APS revealed the interaction of the TAD with general transcriptional repressors like the WD-repeat protein TLE2.

3.10 C/EBPβ is cooperating with other transcription factors

C/EBPβ is known to associate and cooperate with other transcription factors like b-ZIP proteins belonging to the ATF family (Podust et al., 2001; Shuman et al., 1997; Tsukada et al., 1994; Vallejo et al., 1993). In SU-DHL-1 cells IP-MS verified the putative interaction of C/EBPβ with ATF3 (Lee et al., 2010b). The data of the combined APS and IP-MS approach revealed interaction of C/EBPβ with a multitude (>200) of zinc finger proteins containing mostly the C2H2 or LIM-zinc finger domains as derived by Pfam/InterPro analysis (via DAVID database, DAVID.abcc.ncifcrf.gov; Huang et al., 2009). The majority of zinc finger transcription factors interacted with the N-terminus of C/EBPβ in the APS approaches, which is in accordance to our previous results and suggest that C/EBPβ TAD plays an important role in the recruitment of transcriptional regulatory factors (Kowenz-Leutz et al., 2010). Interestingly, IP-MS from SU-DHL-1 cells detected interaction of STAT3 and ALK with endogenous C/EBPβ. The interaction with the transcription factor STAT3 and the regulation of C/EBPβ expression by STAT3 and the NPM-ALK-fusion kinase in the SU-DHL-1 cell line were analyzed before (Anastasov et al., 2010; Piva et al., 2006; 2010). Additionally, a high expression of C/EBPβ (Log10 of iBAQ intensity = 7.59), STAT3 (Log10 of iBAQ intensity = 7.98), ALK (Log10 of iBAQ intensity = 7.87) and NPM (Log10 of iBAQ intensity = 9.25) could be observed in SU-DHL-1 cells by MS-iBAQ proteomics. The expression of the NPM-ALK fusion gene was confirmed by the cell line provider DSMZ. Therefore a certain percentage of the by iBAQ detected ALK and NPM proteins should be present as fusion kinases.

Furthermore, this survey revealed interaction of C/EBPβ with further transcription factors like the direct interaction of the TAD (CR1/2) peptide with the eosinophil transcription factor GATA1 in APS. C/EBPβ and GATA1 are thought to cooperatively regulate eosinophil lineage genes like MBP (Yamaguchi et al., 1999). Additionally, APS detected interaction of the C/EBPβ TAD with the transcription factors MAFB and MAFF that play important roles during the development of various cells and tissues like uterus, blood cells, muscle, neurons and brain.

3.11 C/EBPβ interacts with the NFκB pathway

C/EBPβ was shown to cooperate with NF-κB p50 in order to activate NF-κB target genes and induce apoptosis (Dooher et al., 2011). Another study observed interaction of C/EBPβ with NK-kB p65/RELA, resulting in the inhibition of TNF- induced phosphorylation of p65 and loss of the transactivation capability of p65 (Zwergal et al., 2006). The APS screenings revealed RELA/p65/NFKB3 to interact directly with C/EBPβ. Moreover, IP-MS detected the interaction of endogenous C/EBPβ with NFkB1/p50 and NKIP1 in U937 cells as well as with further TNF-α/NF-κB-complex components and pathway members like SKP1, IKKA, LRPPRC and TBK1 in SU-DHL-1 and IQGAP2 in HL60 cells.

3.12 C/EBPβ interacts with SUMO and ubiquitin ligases and further factors associated with protein degradation

C/EBPβ was shown recently to interact with several components of protein ubiquitin ligase complexes (Steinberg et al., 2012). The APS approaches of the C/EBPβ TAD revealed novel interactions with proteins like Cullin1 (CUL1), ZNRF1 and TRIM37. Further ubiquitin E3-ligases complex members interacted with endogenous C/EBPβ, like CUL5, HUWE1, UBR4, HERC4 and TRIM21 in SU-DHL-1 cells, ZC3HC1 and TRIM21 in HL60 cells and CUL3 in JEKO-1 cells. Endogenous C/EBPβ interacted with the ubiquitin E2-ligases UEV2 in HL60 cells and UBE2C in SU-DHL-1 cells, as detected by IP-MS.

Moreover, IP-MS detected the interaction of endogenous C/EBPβ with the SUMO1 protein (in HL60 and JEKO-1 cells), without distinguishing between covalent or non-covalent SUMO1 interaction. Likewise, IP-MS revealed the interaction of C/EBPβ with the SUMO1-4 -E1 ligase UBA2 (in JEKO-1 and SU-DHL-1) and SUMO1-3 E1 ligase SAE1 (in SU-DHL-1). The expression of ubiquitin or SUMO pathways associated interactors could be detected by MS-iBAQ proteomics in SU-DHL-1 cells, except for TRIM21 (IP-MS), ZNRF1 (APS) and TRIM37 (APS). The in this study observed interactions provide an interesting extension

of previously reported modifications and interactions of C/EBPβ with SUMO proteins and ligases (Berberich-Siebelt et al., 2006; Eaton et al., 2003; Kim et al., 2002).

3.13 C/EBPβ interacts with cell cycle regulators and other proteins controlling proliferation

The APS and IP-MS interaction screenings elucidated prevalently novel interactions of C/EBPβ with regulators of cell proliferation and cancer progression ranging from cell cycle regulators to factors licensing and maintaining DNA replication. C/EBPβ is known to interact with the cell cycle regulator protein Cyclin-D1 and to repress Cyclin-D1 target genes as well (Lamb et al., 2003). In this screening the direct interaction with Cyclin-D1 could be verified by APS. Notably, mass spectrometry neither detected interaction of Cyclin-D1 with C/EBPβ nor the expression of Cyclin-D1 in the analyzed leukemia cell lines. Nevertheless, IP-MS detected endogenous C/EBPβ to interact with the Cyclin-D associated CDK6, the anaphase promoting complex subunit APC4, and CDK1, which promotes together with B-Cyclins the G1-S phase transition. The data also reveals interaction of C/EBPβ with Cyclin-H that was shown to regulate CDK7, a component of a complex that activates CDK1, CDK2, CDK4 and CDK6 as well as RNA polymerase II (Shiekhattar et al., 1995).

On top of that, IP-MS detected the C/EBPβ interaction with CDK6/Cyclin-D-complex inhibitor p16-INK4a in SU-DHL-1 cells and APS revealed p21-WAF1, a Cyclin-D/CDK4 inhibitor and a p53 target gene, as a direct interaction partner of C/EBPβ.

C/EBPβ and ε peptides interacted with the tumor suppressor proteins RASSF1 and RASSF2 that are also associated with negative cell cycle regulation according to GO-analysis (see material and methods section). The mitotic checkpoint proteins BUB1B (in U937) and BUB3 (in SU-DHL-1), as well as CK5P2/CDK5RAP2, a regulator of BUB1B transcription (Zhang et al., 2009) and C/EBPβ target gene (Bonzheim et al., 2013), were detected by IP-MS as novel interactors of C/EBPβ (Figure 22).

3.14 C/EBPβ interacts with proteins organizing DNA replication and mitotic chromatin structure

The IP-MS and APS data revealed interactions of C/EBPβ with components that directly facilitate, regulate and execute in DNA replication. The IP-MS screenings revealed the interaction of endogenous C/EBPβ with PCNA in HL60, RFC1, TOP1, RPA1 and TOP2 in SU-DHL-1 as well as TOP2 and RFC3 in U937 (Figure 22). Interestingly all six proteins are known to form a functional complex with the DNA-polymerases during DNA replication (Jiang et al., 2002; Coll et al., 1996). Additionally, APS data shows a direct interaction of the TAD of C/EBPβ with CDT1 and MCM5, whereas MCM4 was detected by IP-MS in JEKO-1 cells (Figure 22). Those three proteins are components of the mini-chromosome maintenance (MCM) complex, which facilitates the initiation of DNA replication and elongation in eukaryotic cells (Ishimi et al., 1996). CDT1 is one of the factors that recruits the MCM complex to the origins of replication on the DNA during the G1 phase of the cell cycle (Bochman and Schwacha, 2009). Furthermore, APS detected interaction of C/EBPβ with the polycomb group protein L3MBT, which is associated with MCM-mediated replication fork progression and p53 target gene regulation.

The interaction screenings also unraveled interactions of C/EBPβ with proteins defining mitotic chromatin structure like the centromere proteins that could be grouped into the CEN-protein-complex. IP-MS detected endogenous C/EBPβ to interact with the by Obuse and colleagues proposed CEN-complex members CENPM, NUP93, SUPT16H, HSPA5 and HSP7C in SU-DHL-1 cells (Obuse et al., 2004). A direct interaction of the TAD with the complex component HSP7C/HSPA8 was revealed by APS. Additionally, the kinetochore proteins ZW10 and KNTC1/Rod interacted with endogenous C/EBPβ in SU-DHL-1 and APS revealed the kinetochore associated kinesin KIF2C. Endogenous C/EBPβ co-precipitated from SU-DHL-1 lysates the condensin-I and -II complex components NCAPD2, NCAPG, SMC2, SMC4, CAPD3 and the before mentioned SWI/SNF complex and condensin component SMC1A. In concert with these results MS-iBAQ proteomics detected the expression of all centromeric complex components, except CENPM, in SU-DHL-1 cells.

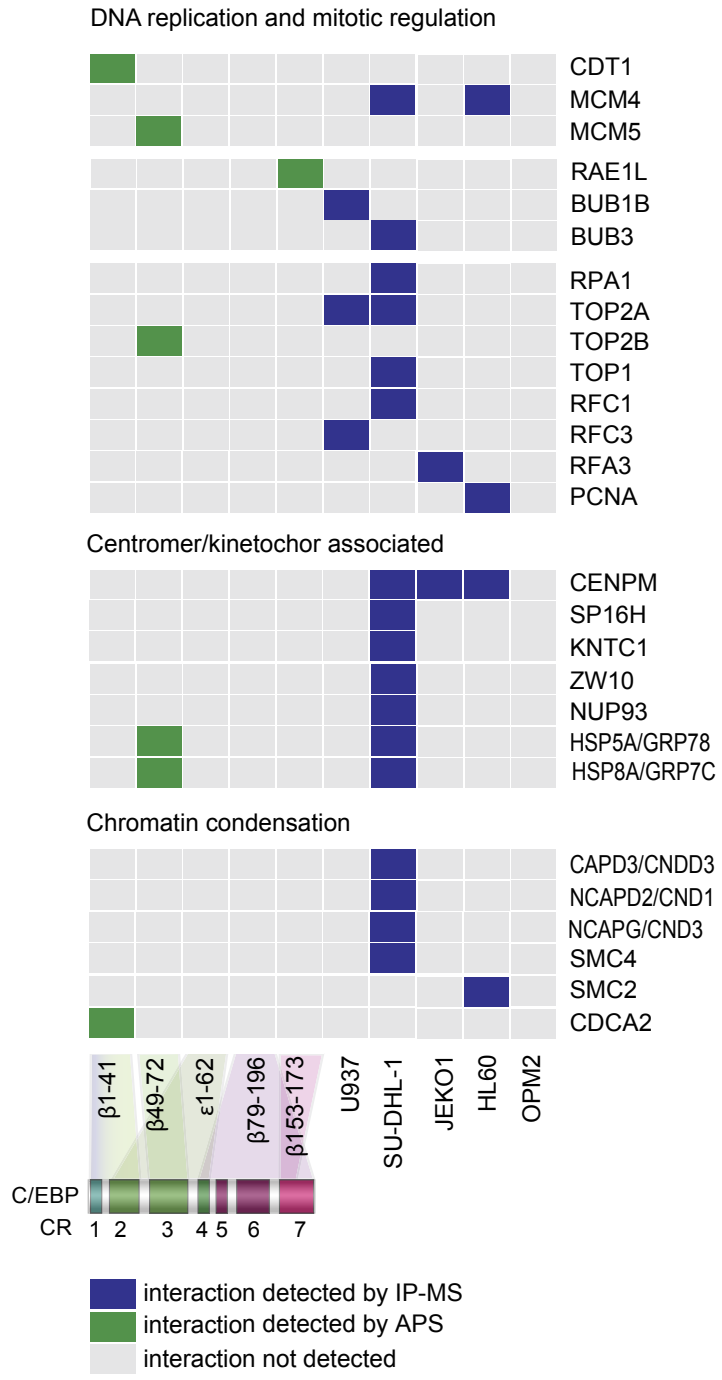

Figure 22: Selected interactions of C/EBPβ/ε detected by APS and/or IP-MS that could be grouped into functional complexes or associated with DNA replication, kinetochor/centromer functions and chromatin condensation using the CORUM database (http://mips.helmholtz-muenchen.de/genre/proj/corum; Ruepp et al., 2008; 2010). Direct interactions detected by APS with peptides of the conserved regions of C/EBPβ/ε are depicted as green squares in the heatmap. The legend below the heatmap illustrates the amino acid coverage of APS peptides of the C/EBPβ/ε protein. Interactions detected by IP-MS (anti-C/EBPβ) from cell lysates of at least one of the cell lines SU-DHL-1 (whole cell and/or nuclear enriched), U937, JEKO-1, OPM2 and HL60 are depicted in blue. Grey squares indicate not detected interaction.

Utilizing IP-MS, novel interactions of C/EBPβ were detected with several nuclear pore components in SU-DHL-1 cells. Some of these interacting proteins are known to have additional functions in mitotic spindle and chromatin organization, namely RANBP2/NUP358, NUP50 (both also in OPM2), NUP85, TPR, NUP160 and NUP210 (Figure 23). One of the most significant interactions in SU-DHL-1, JEKO-1, OPM2 and U937 were the established C/EBPβ export factor XPO1 (CRM1) (Buck et al., 2001) and its important cofactor RANBP3. IP-MS from JEKO-1 cells revealed also the initial transport protein RAN. Moreover, the GTPase activator RanGAP1, that converts Ran to the putatively inactive GDP-bound state, as well as its interactor RANBP2/NUP358 were found to interact with endogenous C/EBPβ in OPM2 and SU-DHL-1 cells. On top of this, IP-MS identified the export factors XPO2, XPO5 and XPO6 (also in U937) as interactors of endogenous C/EBPβ in SU-DHL-1. Finally, C/EBPβ interacted with the import factors IPO4 in HL60, with IPO12 in U937 and with IPO9, TRN and the importin subunit-β (KPNB1) in SU-DHL-1. Eventually all the expression of the interacting transport proteins, except for XPO6, were detected in the SU-DHL-1 cell line using MS-iBAQ proteomics.

3.15 C/EBPβ interacts with proteins associated with DNA repair and apoptosis

Interestingly, APS and IP-MS revealed the interaction of C/EBPβ with numerous proteins associated with DNA repair mechanisms like Double-strand break (DSB) repair, non homologous end joining (NHEJ) or nucleotide excision repair (NER) (Figure 23). APS detected the direct interaction of the C/EBPβ RD with the nucleotide excision repair (NER) protein RAD23A. IP-MS identified the interaction of endogenous C/EBPβ in SU-DHL-1 cells with TELO2 (and in HL60 cells) and TTI1 (and in U937 cells), which are members of the double-strand break repair triple-T (TTT) complex. The triple-T complex is considered to regulate the stability of mitotic checkpoint kinase ATR, which itself interacts with C/EBPβ in SU-DHL-1 cells (Hurov et al., 2010). Additionally, IP-MS revealed interaction of C/EBPβ with FANCD2 in U937 and SU-DHL-1 cells. The FANCD2 protein, which was recently shown

to interact with C/EBPδ is understood to have ATR target motifs and to be important for the DNA damage response (DDR) (Andreassen et al., 2004; Matsuoka et al., 2007; Moldovan and D'Andrea, 2009; Wang et al., 2010).

IP-MS detected the interactions of endogenous C/EBPβ with WRN in HL60 and PARP-1, XRCC5 (also in JEKO-1 and OPM2) and XRCC6 (also in JEKO-1) in SU-DHL-1 cells (NE) (Figure 23). The four proteins could be grouped into the Werner-syndrome complex, a complex functioning in base excision repair (BER), non-homologous end joining (NHEJ) and DNA replication (Li et al., 2004). Additionally, the Double-strand break (DSB) repair BRCA1-complex member BRE (in JEKO-1), the DSB non-homologous end joining repair protein NHEJ1 (in JEKO-1, U937 and SU-DHL-1) as well as the mismatch repair proteins MLH1 (in SU-DHL-1) and MSH2 (in HL60) interacted with the endogenous C/EBPβ (Dong et al., 2003).

C/EBPβ not only interacts with proliferation modulators. The here presented results also features novel interactions of C/EBPβ with apoptosis associated factors. Endogenous C/EBPβ interacted with the apoptosis regulators BAX, BID and Caspase 2 (CASP2). APS experiments revealed direct interactions of the C/EBPβ TAD with the positive p53 regulator ASPP2, CASP6, the TNFR1-apoptosis pathway member TRADD and the caspase independent apoptosis regulator kinase PKM. On the other hand, APS detected the anti-apoptotic factor MKL1, an inhibitor of TNF-induced caspases, and the negative ASPP2 regulator DDX42. Finally, MS-iBAQ proteomics could detect the expression of all DDR associated C/EBPβ interactors, except for UBA52, in SU-DHL-1 cells.

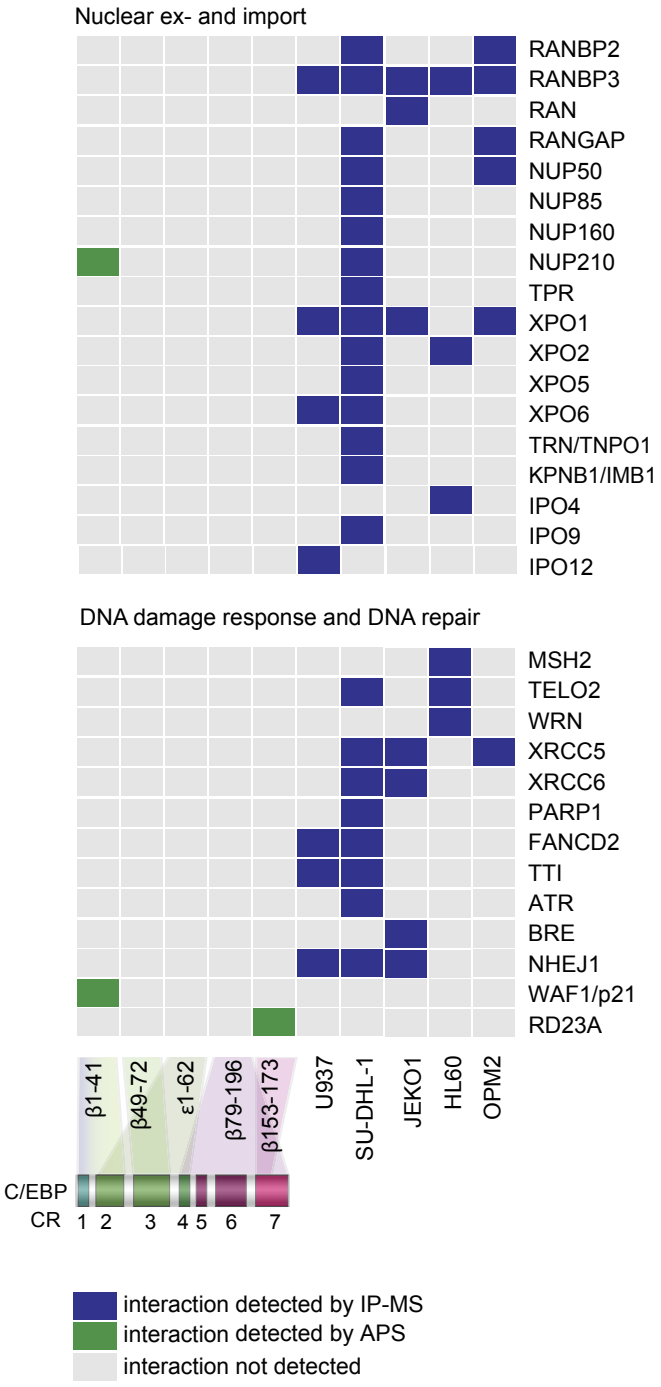

Figure 23: Selected interactions of C/EBPβ/ε detected by APS and/or IP-MS that could be grouped into functional complexes or associated with nuclear-cytoplasmic transport, DNA damage response or DNA repair functions using the CORUM database (http://mips.helmholtz-muenchen.de/genre/proj/corum; Ruepp et al., 2008; 2010). Direct interactions of peptides covering the conserved regions of C/EBPβ/ε, which were detected by APS are depicted as green squares in the heatmap. The legend below the heatmap illustrates the amino acid coverage of APS peptides of the C/EBPβ/ε protein. Interactions detected by IP-MS (anti-C/EBPβ) from cell lysates of at least one of the cell lines SU-DHL-1 (whole cell and/or nuclear enriched), U937, JEKO-1, OPM2 and HL60 are depicted in blue. Grey squares indicate not detected interaction.

3.16 RNA binding and processing proteins interact with C/EBPβ

Intriguingly, the APS and the endogenous IP-MS screenings unraveled C/EBPβ to be associated with a significant number of RNA binding proteins like components of the spliceosome, RNA processing, RNA transportation and RNA degradation associated proteins (Figure 24 and 25, Table S1). This is intriguing, as recent studies reported of the interaction of C/EBPα and C/EBPβ with RNA binding proteins and Spliceosome components (Siersbaek et al., 2014; Giambruno et al., 2013). Some of those interactions were verified by this survey (vide Table S1). Pfam and InterPro analysis revealed that numerous proteins, which were found to interact with C/EBPβ in this study, possess RNA binding motifs like the RBD/RRM or the DEAD/DEAH box (RNA) helicase domain (via DAVID database, DAVID.abcc.ncifcrf.gov; Huang et al., 2009).

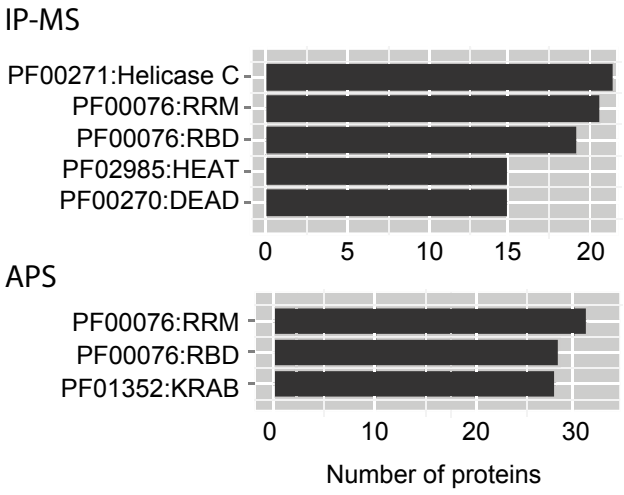

Figure 24: Illustrated is a selection of the most abundant RNA binding domains of C/EBPβ/ε interacting proteins that were found by APS and/or IP-MS (vide Supplemental Table S1). The NIH DAVID resource was used to determine PFAM domains, Benjamini-Hochberg ≤ 5 ٪ (DAVID.abcc.ncifcrf.gov; Huang et al., 2009). Depicted are the total numbers of proteins carrying the named RNA-binding domains that interacted with C/EBPβ/ε in APS and/or IP-MS.

Data analysis of the IP-MS/APS-data with either the UniProt or the GeneOntology online resources indicates RNA binding and modifying functions for more than ninety C/EBPβ/ε interacting proteins (Figure 24 and 25). A large number of those C/EBP interacting proteins are components of the spliceosome or RNA helicases like CIRBP, DHX15/9,

LSM2/6/7, PPIL1, RBM15/22/25, SNRPF, SF3B3, SKIV2L2, BCAS2, SRSF1, SRSF2/5/7 XAB2, TFIP11 and THOC5 (Jurica et al., 2002; Zhou et al., 2002; Figure 24 and 25). The interacting proteins CDC5L, SRSF2, SRSF1, ILF2, SPF27, PP1A and GCN1L could be grouped into the Spliceosome associated CDC5L-protein complex, known to promote mRNA splicing (Ajuh et al., 2000). Moreover, the RNA splicing proteins RALY, HNRPU, HNRPM, ROA3, ROA1, HNRPC and HNRPK that could be grouped into the C complex of the spliceosome (Jurica et al., 2002) were mostly simultaneously detected by APS and IP-MS from SU-DHL-1 cells (Figure 25). Eventually, MS-iBAQ proteomics revealed the expression of all spliceosome components that were detected to interact with C/EBP peptides and endogenous C/EBPβ, except for CIRBP, RALY, SRSF4, SRSF10 and DDX5.

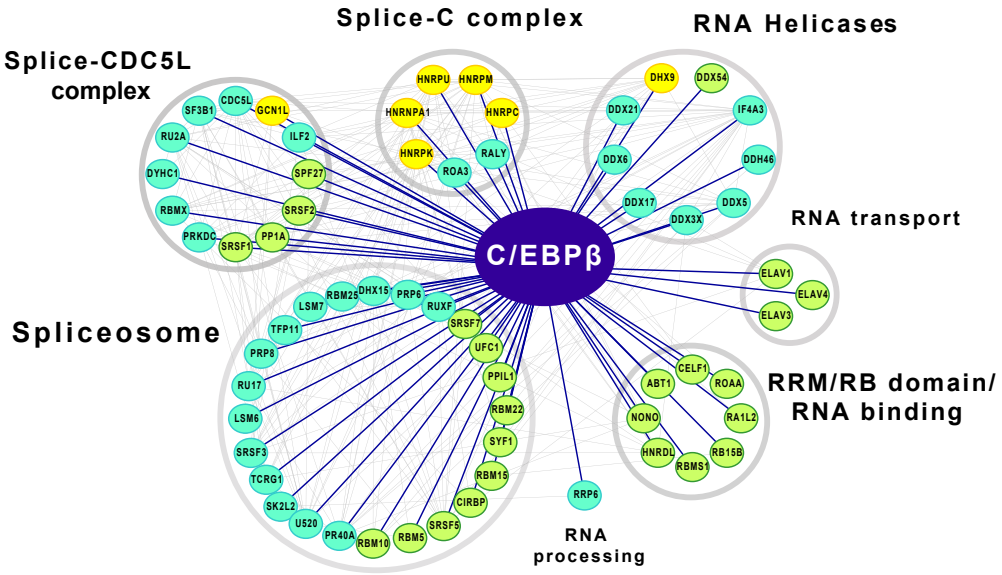

Figure 25: IP-MS and APS revealed interaction of C/EBPβ with various RNA binding and processing proteins that could be grouped into the Spliceosome, the Splice-CDC5L- and the Splice-C-complex using the CORUM database (http://mips.helmholtz-muenchen.de/genre/proj/corum; Ruepp et al., 2008; 2010). Further RNA associated proteins are grouped according to their RNA binding or helicase domains or their association with RNA transport as derived by GO analysis (NIH DAVID resource) and UniProt (vide material and methods section). The color of the nodes indicates the detection method: lime green nodes depict proteins that were detected by APS, turquois nodes indicate proteins that were detected with IP-MS and yellow nodes indicate detection with both methods. The grey edges were determined with the Cytoscape BisoGenet tool (Martin et al., 2010; Shannon et al., 2003) and depict previously reported interactions. The blue colored edges indicate interactions with C/EBPβ that were detected in this survey.

C/EBPβ was also observed in this study to interact with family members of the eukaryotic translation initiation factors. Subunits of the eIF-3 translation initiation complex were detected by IP-MS, like eIF-3A and eIF-3M in SU-DHL-1 cells and APS detected eIF-3D to directly interact with the C/EBPβ RD. The eIF-3 complex initiates the ribosome 60S-subunit dissociation and facilitates thereby the binding of eIF-4 proteins that guide the mRNA to the 40S-ribosome (Bommer et al., 1991; Hinnebusch, 2006). Additionally, IP-MS detected interactions with the eIF-4 complex subunits eIF-4A1, eIF-4A3 in SU-DHL-1 and EIF4B in JEKO-1 and APS revealed eIF-4H to interact with the C/EBPβ RD (Richter et al., 1999; Rogers et al., 2001). C/EBPβ also interacted in this survey with translation elongation factors. The APS and/or IP-MS experiments detected EEF1A1 (in SU-DHL-1 and also by APS), EEF2 (in SU-DHL-1), EEF1G (in JEKO-1, HL60 and SU-DHL-1), EEF1B2 (JEKO-1 and SU-DHL-1), EEF1D (JEKO-1 and SU-DHL-1) as interaction partners of C/EBPβ.

Noteworthy, the APS screenings also revealed C/EBPβ and ε to interact directly with the RNA binding proteins ELAVL-1/3/4 (HuR, HuC, HuD). ELAV-like proteins were until now only known to regulate C/EBPβ expression via influencing mRNA stability and degradation upon binding (Basu et al., 2011). Intriguingly, recent data describes the NPM-ALK-fusion kinase to enhance ELAVL-1/HuR-interaction with the C/EBPβ mRNA in ALCL cells (Bergalet et al., 2011).

3.17 CEBPβ is phosphorylated and interacts with kinases in leukemia / lymphoma cell lines

C/EBPβ is abundantly modified after translation. The phosphorylation of the regulatory domain by the Ras/MAPK signaling pathway associated receptor tyrosine kinase ERK1/2 was proposed to induce a conformational change enabling the interaction with transcriptional activators like the Mediator- and the SWI/SNF-complex (Kowenz-Leutz and Leutz, 1999; Mo et al., 2004; Sato et al., 2004). Notably, the IP-MS analysis of HL60 cells revealed C/EBPβ to interact with the ERK2 kinase.

Moreover, the MAPK downstream kinase RSK2 was shown before to interact with

C/EBPβ and phosphorylate Ser217 (mouse; Ser105 rat), causing an increased DNA binding ability and homodimerization (Lee et al., 2010a; Hanlon et al., 2001). Intriguingly, the IP-MS results revealed the interaction of endogenous C/EBPβ with RSK2 in SU-DHL-1 cells. C/EBPβ is known to be phosphorylated by the cycle kinases CDK1 und CDK2 (Shuman et al., 2004) and as mentioned before IP-MS detected an interaction with the CDK1 and CDK6 kinases.

Altogether, the interaction data might suggest a potentially phosphorylated and activated state of C/EBPβ in the analyzed leukemia cell lines, although this will have to be experimentally verified.

DISCUSSION

The C/EBPβ protein regulates differentiation, proliferation and survival in numerous tissues and cell types. To understand how C/EBPβ executes this diversity of functions as a pioneering transcription factor and participates in numerous biological processes it is important to determine its complete interactome. Here, we applied comprehensive array peptide screening (APS) and immune-precipitation mass-spectrometry (IP-MS) abetted by MS proteomics to unveil C/EBPβ protein-protein interactions and potential C/EBPβ regulated proteins. The APS approaches encompassed the screening of human protein expression libraries with various synthetic peptides derived from the trans-activating and regulatory regions of C/EBPβ and ε. The data derived by APS was integrated with data form IP-MS of endogenous C/EBPβ from various leukemia cell lines. The data confirmed known interactions and revealed a plenitude of novel C/EBPβ interactors that could function as components in protein complexes associated with the regulation of gene transcription, chromatin remodeling and histone modification. Other potential complexes that interacted with C/EBPβ play a part in DNA replication and cell cycle regulation, DNA-repair/DDR, nuclear transport, osteogenesis and myeloid differentiation. The involvement of C/EBPβ in energy metabolics was validated by the in this survey obtained interaction and proteomics data. In addition, components of the spliceosome and RNA-processing proteins were detected, suggesting novel functions of C/EBPβ. In conclusion, the data presented largely expands previous knowledge and discloses entirely novel areas of influence of C/EBPβ.

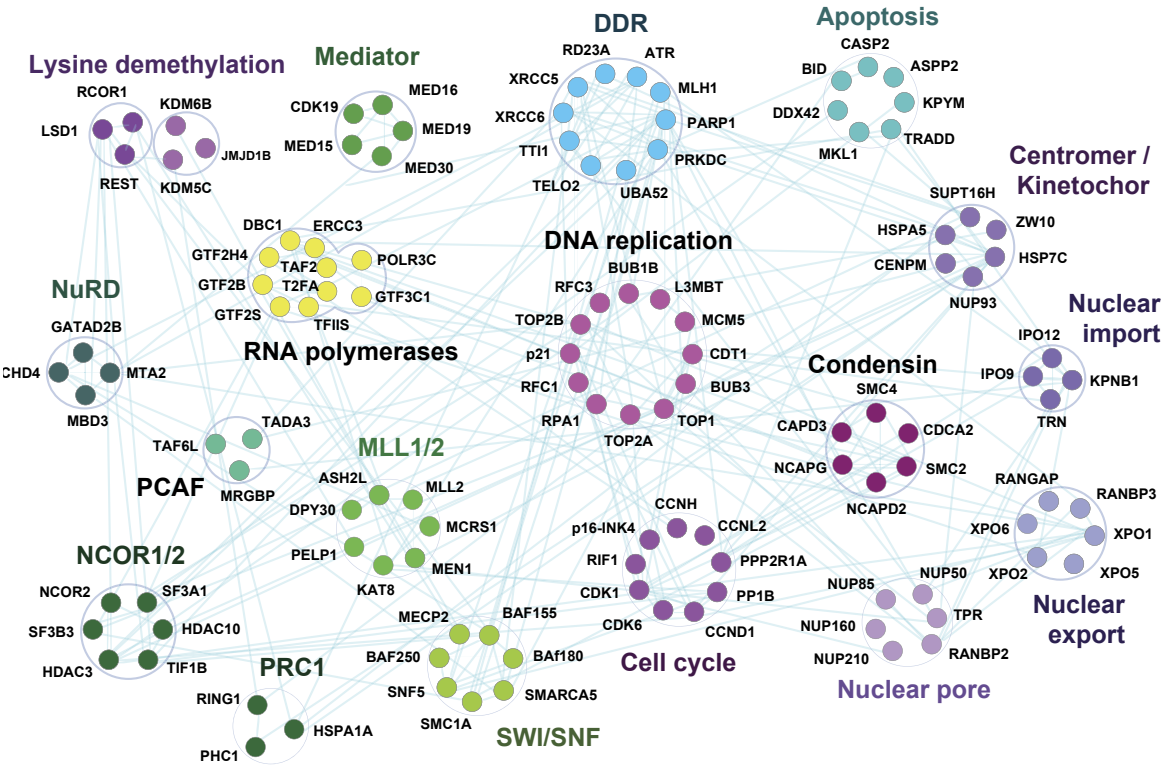

Figure 26: Selection of protein-protein interactions (nodes) of C/EBPβ that were detected in this survey by APS and/or IP-MS are visualized with Cytoscape (vide Table S1). The Cytoscape BisoGenet tool (Martin et al., 2010; Shannon et al., 2003) was used to determine previously reported protein-protein interactions (edges) between the protein nodes. Protein complex and/or functional group membership of nodes are depicted by colors and was determined by the CORUM database (http://mips.helmholtz-muenchen.de/genre/proj/corum; Ruepp et al., 2008; 2010), the Cytoscape BisoGenet plugin and the UniProt database.

4.1 Combinatory use of APS and IP-MS

In order to unravel a most detailed view of the functional network of C/EBPβ we applied two different screening methods to detect protein-protein interactions of the transcription factor. First we employed the array peptide screening (APS) that was recently developed by our group (Pless et al., 2011). The usage of short peptides in APS enabled the mapping of protein interactions to certain C/EBPβ domains that are conserved within the family of C/EBP transcription factors. But due to the usage of brief peptide sequences the APS technique is less practical for the detection of protein-interactions that require larger interaction or recognition motifs or rely on multiple contact sites. A suitable complement to this is the

immunoprecipitation of endogenous full length C/EBPβ followed by mass spectrometry measurements as it was employed in this survey. Furthermore, the APS technique enables especially the identification of direct protein interactions as a consequence of the absence of cellular cofactors and protein complexes, which naturally encompass numerous proteins in the cellular context. On the other hand the detection of protein interactions with APS depending on cofactors or a complex environment is therefore unfortunately unfeasible. Nevertheless, a further advantage of the APS technique is the possibility of simultaneous discovery of the utmost possible protein-protein interactions of a protein as the bacterial expression of human proteins on the array overcomes cell type specific protein expression or the fluctuating cellular abundance of proteins. This is underlined in this survey by the MS-iBAQ analysis of SU-DHL-1 cells, which revealed on one side that 85% of the IP-MS identified C/EBPβ interactions were also detectable analyzing the SU-DHL-1 proteome by MS-iBAQ proteomics. However, hardly ≈ 20 % of the proteins that interacted with C/EBPβ in the APS approaches were detected among the most abundant proteins of the SU-DHL-1 cell proteome (Figure 16). This observation could be one of the explanations for the considerable difference in detected C/EBPβ interactors by the endogenous IP-MS approaches and the APS technique. In conclusion, the amount of data obtained in this survey underlines the advantage of a combinatory employment of the expression independent in-vitro APS and endogenous IP-MS technique to unravel C/EBPβ protein interaction network. This is especially supported by the fact that significant numbers of known C/EBPβ interactors could be validated in by survey (Figure 15, Table S1).

A further point of discussion is the difference of C/EBPβ protein interactions that were detected by endogenous IP-MS in the different leukemia cell lines. The detection of peptides by mass spectrometry heavily relies on the amount of each individual protein per sample and the ionization properties of the measured peptides during electrospray ionization. Protein interactors of C/EBPβ that are low abundant in a cell type, or generate poorly ionizing peptides can fall below the detection limit of mass spectrometry. Therefore, cell type specific protein expression differences between the five analyzed leukemia cell lines could account for the variation of identified C/EBPβ interactions. In concert with this is the cell type specific abundance of the C/EBPβ IP-bait protein itself providing a rational for the

differential amount of detected interactions as suggested by the 18 times higher abundance of C/EBPβ protein in the SU-DHL-1 cells compared to U937 cells as determined by SRM proteomics (Figure 17). On top of that, the type of label-free IP-MS survey selected to discover C/EBPβ interactors based on a t-test only acknowledges proteins that were detected at least twice (for nuclear extract IPs) or three times (for whole cell lysate IPs) in either the IP-C/EBPβ or the bead control group. Under these statistical conditions minor changes in protein abundance are a criterion for exclusion. In summary, the here-itemized reasons can account for the differences between the protein-interactions detected for C/EBPβ by IP-MS in this study. Nevertheless, the analysis of protein-protein interactions in leukemia cell lines facilitated a crucial insight into potential cancer relevant interactions of C/EBPβ and may provide a starting point for future studies.

4.2 C/EBPβ interacts with epigenetic regulators of gene transcription

The transcription factor C/EBPβ binds the CCAAT-box sequence of the promoters of its target genes (Osada et al., 1996; Mahony et al., 2007, Nerlov et al., 1995). Transcription factors initiate gene transcription by recruiting cofactors and the polymerase complex to the transcriptional start side. The interaction of C/EBPβ with the transcription activating Mediator complex as well as the RNA-polymerase II and III complexes was described recently (Steinberg et al., 2012; Kowenz-Leutz et al., 2010, Mo et al., 2004). Intriguingly, this study was able to add a substantial number of protein components from both, the Mediator and the RNA polymerase II/III complexes to the list of C/EBPβ interaction partners. The cooperation between C/EBPβ and the Mediator and RNA polymerase complexes is most probably essential to transcriptional activation of C/EBPβ target genes, as suggested by others (Kowenz-Leutz et al., 2010, Mo et al., 2004).

4.2.1 Transcriptional activating histone methyltransfereases and demethylases

Gene transcription critically relies on the accessibility of DNA by the transcription machinery. The compaction status of the DNA can be modulated by posttranslational modifications of the histone tails (Luger et al., 1997; Kornberg and Thomas, 19974; Kornberg, 1974). Histone tail modifications are understood to provide a "histone code" determining a transcriptionally active or repressive state of gene promoters (for overview see: Strahl and Allis, 2000). The histone code attracts the chromatin remodeling and polymerase complexes or heterochromatin binding proteins (Dou et al., 2005; Hughes et al., 2004). Transcriptionally active promoters are characterized by methylation of the histone H3 at lysine 4 (H3K4) or lysine acetylation of several histone subunits. The removal of Histone H3K9 and H3K27 as well as the establishment of H3K4 methylation and histone tail acetylation is essential for the initiation of gene transcription (Jenuwein, 2001; Strahl and Allis, 2000; Turner, 2000). The methylation of lysines or arginines of histone tails is carried out by histone-methyltransferases and the acetylations of histones by histone acteyltransferases (HATs). A wealth of those proteins that either establish or read histone modifications are considered as cooperators of transcription factors or polymerases during transcriptional regulation (for overview see: Miller et al., 2009; Cheung et al., 2000; Jenuwein, 2001; Turner, 2000).

This study observed interaction of C/EBPβ with components of the MLL1 and MLL2 histone H4K4 methyltransferase complex. The histone methyltransferases of the MLL-family predominantly activate HOX gene promoters. Additionally, they are recognized to impact the transcription of non-HOX genes by methylation of histone H3K4 as well. On top of that, C/EBPβ was discovered to interact with the transcriptional co-activators KDM6B and KDM3B in this survey. These two demethylases are known to remove the repressive histone H3K9 and H3K27 methylation marks. All together the cooperation of C/EBPβ with the mentioned activating histone methyltransferases and demethylases probably aids C/EBPβ during the activation of its target genes.

4.2.2 Transcriptional repressive histone deacetylases and histone demethylases

The removal of Histone H3K4 methylation and histone tail acetylations is essential for the initiation of gene repression. The subsequent establishment of histone H3K9 and H3K27 methylation characterizes silent promoters. Several studies revealed that C/EBPβ regulates gene repression (Ki et al., 2005; Descombes and Schibler, 1991). The here presented data unravels C/EBPβ involvement in the downregulation of various proteins and shows the interplay of C/EBPβ with protein complex components associated with negative gene regulation. In the APS approaches the C/EBPβ CR1-2 interacted with the co-repressor KDM5C. KDM5C is a putative H3K4me2/3 demethylase. The IP-MS data also revealed LSD1 and RCOR (CoREST) as interaction partners of endogenous C/EBPβ in U937 cells. LSD1 is known to remove the activating histone tail methylation of H3K4 as well as the repressive methylation of H3K9 and was also suggested to form a transcriptional repressive complex with RCOR (Yang et al., 2006). Interestingly, APS showed a direct interaction of the CR1/2 domains of C/EBPβ with the REST protein, which represses neural genes in non-neural tissue in cooperation with CoREST and SIN3A (Grimes et al., 2000). C/EBPβ interacted also with members of the repressive NCOR1/2 complexes. As the LSD1-RCOR complex as well as NCOR1/2-complexes are known to recruit HDACs to gene promoters (Lee et al., 2005; Metzger et al., 2005; Shi et al., 2005; Underhill et al., 2000) it is possible that C/EBPβ cooperates with these complexes to silence target genes. Additionally, APS revealed the direct interaction of KDM5C, NCOR- and CoREST-complex components exclusively with the TAD of C/EBPβ underlining the importance of this C/EBPβ domain for gene repressive functions.

4.3 C/EBPβ interacts with proteins regulating chromatin structure

An open chromatin structure facilitates the access of the transcription machinery to gene promoters and is thereby essential for successful activation of gene expression. Chromatin remodeling complexes modulate the chromatin structure by shuffling histones along the DNA in an ATP dependent fashion. The opening of chromatin around gene promoters facilitates the binding of the RNA-polymerases and Mediator complexes that initiate transcription (Ryme et al., 2009; Nie et al., 2000). Chromatin remodeling complexes can be categorized into the SWI/SNF, ISWI, NURD/Mi-2/CHD and INO80 families and consist of numerous, highly conserved, subunits including a characteristic ATPase II helicase-related subunit (Tang et al., 2010; Singleton and Wigley, 2002). The human SWI/SNF family consists of the two subfamilies of BAF and PBAF complexes. The BAF and PBAF complexes are discriminated by their different components containing either the ATPase hBRM (BAF) or BRG1 (BAF / PBAF), the DNA binding protein BAF250 (BAF) or BAF200 (PBAF) and the bromodomain protein BAF180 (PBAF), whereas the core components BAF45, BAF47, BAF53, BAF57, BAF60, BAF155, BAF170 and β-Actin are shared by these complexes (Tang et al., 2010; Mohrmann and Verrijzer, 2005).

Several SWI/SNF complex components were previously found to interact with C/EBPβ target gene promoters and are putatively essential for successful target gene activation predominantly by interaction with the LAP* specific CR1 region (Kowenz-Leutz and Leutz, 1999; Steinberg et al., 2012). Intriguingly, the interaction of the SWI/SNF complex with the CR1/2 of C/EBPβ is regulated by posttranslational modifications (PTMs) of C/EBPβ. A methylation at the Arg3 (R3) position of the C/EBPβ CR1 region by the arginine methyltransferase PRMT4/CARM1 abrogates the interaction with the SWI/SNF and Mediator complex. The phosphorylation of the C/EBPβ RD region by the Ras/MAPK-pathway prohibits the methylation of the R3 residue by PRMT4/CARM1 and thereby facilitates the interaction of C/EBPβ with the SWI/SNF and Mediator complexes and subsequent target gene activation (Kowenz-Leutz et al., 2010). Further studies showed that a functional

SWI/SNF complex (Vradii et al., 2005) as well as its interaction with C/EBPβ TAD are essential for the differentiation of myeloid progenitor cells and transdifferentiation of B-cell progenitors into the granulocytic lineage (Stoilova et al., 2013). This study verified known and revealed novel interactions of SWI/SNF complex members with C/EBPβ by IP-MS and APS. The interactions with the recently reported C/EBPβ interactors BAF250 and BAF180/PB1 (Steinberg et al., 2012) were detected by IP-MS in the U937 lymphoma cell line. In SU-DHL-1 cells the interaction of endogenous C/EBPβ with the SWI/SNF components MECP2, SMC1A, SNF2H, BAF155 and BRG1 was discovered. Moreover, APS identified SNF5 as direct interactor of the C/EBPβ TAD. Those findings strongly emphasize C/EBPβ functional association with the SWI/SNF complex, which could assist the C/EBPβ transcription factor during target gene activation as suggested before (Stoilova et al., 2013; Kowenz-Leutz et al., 2010; Kowenz-Leutz and Leutz, 1999).

Additionally, the proteomic screening of C/EBPβ infected C/EBPβ$^{-/-}$ MEF cells revealed a significant up-regulation of the two SWI/SNF family members Baf180 and Smarcd1 (Figure 6 and Figure S1) after over-expression of both C/EBPβ LAP* and LAP isoforms. This suggests a connection between the expression levels of C/EBPβ LAP*/LAP isoforms and the availability of SWI/SNF complex components as C/EBPβ interaction partners.

C/EBPβ can be manipulated by several PTMs such as phosphorylation or methylation of the regulatory domain (RD). PTMs of the RD, positively or negatively influence the protein-protein interactions of the TAD and by that impact C/EBPβ gene regulating function (Kowenz-Leutz et al., 1994; Williams et al., 1995 Nakajima et al., 1993; Figure 4). The MAPK-downstream kinase RSK2 was shown to phosphorylate C/EBPβ on Ser105 (in rat; Thr217 in mouse) increasing DNA binding and homodimerization properties of C/EBPβ (Lee et al., 2010a; Hanlon et al., 2001; Buck et al., 1999). C/EBPβ is activated by phosphorylation of the RD by the MAPK-pathway kinases ERK1/2 prohibiting the repressive methylation of C/EBPβ K39 by the lysine-methyltransferase G9a (Pless et al., 2008). This phosphorylation is accompanied by a conformational change of C/EBPβ enabling the interaction with the transcriptional activating Mediator- and the SWI/SNF-complexes (Mo et al., 2004; Sato et al., 2004; Kowenz-Leutz and Leutz, 1999). Monocytic differentiation of the investigated lymphoma cell lines HL60 and U937 can be triggered by the MAPK-pathway activator

12-O-Tetradecanoylphorbol-13-acetate (PMA/TPA). The monocytic differentiation of these lymphoma cell lines by PMA/TPA is C/EBPβ dependent (Chen et al., 1996; Ji and Studzinski, 2004). These combined facts emphasize the here observed interactions of C/EBPβ with the SWI/SNF and Mediator complex (in SU-DHL-1 and U937) as well as with the kinases ERK2 (in HL60) and RSK2 (in SU-DHL-1), indicating a transcriptionally activate state of C/EBPβ in the examined leukemia cell lines.

The IP-MS survey of C/EBPβ protein partners in SU-DHL-1 and U937 cells revealed several kinases. The kinases encompass three MAP-kinases and one MAPK activator. It is possible to group these kinases applying the GO-term "GO:0006468 protein amino acid phosphorylation". These findings extend C/EBPβ own regulatory network and demonstrate C/EBPβ interplay with cellular signaling pathways and protein complexes in the analyzed lymphoma cell lines.

The observed protein interactions of C/EBPβ with factors regulating chromatin structure during mitosis, cell cycle and DNA replication described in this survey are most likely to expand the known protein interaction pattern of C/EBPβ significantly and suggest potential novel functions of C/EBPβ.

4.4 C/EBPβ interacts with cell cycle regulators as well as with centromere and kinetochore proteins

In the course of the cell cycle DNA is duplicated and sister chromatids are separated. The prophase marks the onset of mitosis during which chromosomes condensate. The prophase is followed by the prometaphase. The main characteristic of the prometaphase is the breakdown of the nuclear envelope and the attachment of the microtubules to the kinetochores of the compacted chromosomes (Marston and Amon, 2004; Nigg, 2001).

The organization, structure and compact state of mitotic chromosomes and the transcriptionally silenced heterochromatin intrinsically rely on condensin proteins contained in the condensin-I and -II complexes (Hirano, 2006; Ono et al., 2004; 2003; Losada and Hirano, 2001; Schmiesing et al., 2000). In this study the interaction of endogenous C/EBPβ with

six condensin-I and -II complex components was revealed by IP-MS in SU-DHL-1 cells. The condensin II complex is located in the nucleus during inter- and prophase and interacts with chromatin. In contrast to the condensing II complex the condensin I complex is cytoplasmatic and its interaction with chromatin is only possible after nuclear envelope breakdown during mitosis (Hirota et al., 2004; Ono et al., 2004). Interestingly, the condensin complex I was suggested to have additional functions during interphase where it interacts with PARP-1 and XRCC1 and translocates with those factors to DNA damage sites (Heale et al., 2006). Moreover, the condensin I complex members NCAPD2 and SMC1A were shown to be targets of the DNA damage ATR kinase (Matsuoka et al., 2007). NCAPD2 and SMC1A are novel protein partners of C/EBPβ revealed by this study.

The kinetochore is the structural component that mediates cytoskeletal interaction with the chromosomal DNA enabling the separation of sister chromatids during mitosis. This process is controlled by the spindle assembly checkpoint (SAC). The SAC prevents aneuploidy by delaying the mitotic progress until all kinetochores are attached to microtubules and subsequently initiates the separation of the sister chromatids during anaphase (Marston and Amon, 2004; Nigg, 2001). MAD2 is one of the proteins that regulates the SAC by inhibiting the anaphase-promoting complex/cyclosome (APC/C) until all kinetochores are attached (Logarinho et al., 2008; Sudakin et al., 2001; Tang et al., 2001; 2004). The kinetochores are formed at the centromeric region of chromosomes and are primarily characterized by the incorporation of the histone 3 specimen Centromere Protein A (CENP-A). CENP-A is essential for kinetochore formation. The centromeric DNA sequence consists of a large assemblage of 171-bp tandem α-satellite repeats that are recognized by the DNA-binding Centromeric Protein B (CENP-B). The incorporation of CENP-B at the centromeric α-satellite repeats of DNA is understood to foster centromere formation and recognition (Allshire and Karpen, 2008; Carroll and Straight, 2006; Westhorpe and Straight, 2013). Previous research reports up to eight repeats of consensus C/EBP binding sites in mouse centromeric α-satellite DNA and intriguingly C/EBPβ was shown to co-localize with murine centromeric α-satellite DNA and the centromeric protein CEBP-B during adipocyte differentiation (Tang et al., 2003; Tang and Lane, 1999). A survey of the centromeric proteins by the Yoda group suggested a large protein complex important for the alignment and segregation of chromosomes (Izuta

et al., 2006; Obuse et al., 2004). The Yoda group performed anti-CENP-A chromatin immunoprecipitations obtaining the interphase centromere complex (ICEN). In our study IP-MS detected endogenous C/EBPβ to interact with six proteins that are proposed members of the ICEN. Among these proteins was the PANE1/CENP-M protein, a protein that probably aids CENP-A during kinetochore assembly.

The recruitment of cytoskeletal components to the kinetochore is essential for correct chromosomal segregation during mitosis (Cleveland et al., 2003; Williams et al., 2003). During this process the bridging proteins zeste white 10 (ZW10) and rough deal (hRod/KNTC1) form a functional complex and link the microtubule motor protein dynein to the kinetochores facilitating segregation of the sister chromatids (Scaërou et al., 2001; Williams et al., 2003). The ZW10/hRod complex was suggested to exert a dual regulatory role during mitotic microtubule attachment to the kinetochore. The ZW10/hRod complex helps in the context of the SAC to delay anaphase by recruiting the Mad1-Mad2 heterodimer complex to unattached kinetochores and is required for the release of the heterodimer complex after correct microtubule attachment as well (Kops et al., 2005). In this study the IP-MS analysis of the SU-DHL-1 cell line uncovered the interaction of both proteins ZW10 and hRod/KNTC1 with endogenous C/EBPβ. Summed up, these findings suggest a possible involvement of C/EBPβ in mitotic chromatin organization and chromosome condensation.

C/EBPβ was also detected to interact with five nuclear pore complex components that are thought to play additional roles after mitotic nuclear envelope breakdown (NEBD) by regulating mitotic progress as well as functionality of the kinetochore and spindle microtubules (Sood and Brickner, 2014; Bukata et al., 2013; Drechsler and McAinsh, 2012; Dawlaty et al., 2008; Joseph et al., 2004; 2002; Salina et al., 2003). Additionally, the TPR (Megator) nucleoporin interacted with C/EBPβ in SU-DHL-1 cells. Besides TPR's function as nuclear pore component it is associated with the mitotic spindle elongation and the spindle assembly checkpoint (SAC) response as well. A study of the Maiato group reported a mitotic co-localization of Tpr with the nuclear pore until the late prometaphase during mitosis. Afterwards, Tpr partially localizes at the mitotic spindle followed by a re-localization to the reassembled nuclear membrane throughout the telophase. The authors suggested a task of Tpr during the spindle assembly checkpoint (SAC), similar to the previously mentioned

ZW10/hRod complex (Lince-Faria et al., 2009).

In addition to this, IP-MS data revealed the interaction of endogenous C/EBPβ with the nucleoporin NUP85 in SU-DHL-1 cells. NUP85 was described previously as an essential component of the Nup107-160 nucleoporin complex. The Nup107-160 complex was proposed to regulate mitotic kinetochore and spindle assembly and additionally shows similar behavior upon unattached kinetochores such as the SAC regulator Mad2 (Orjalo et al., 2006; Zuccolo et al., 2007). Furthermore, C/EBPβ interacted with the nucleoprotein and SUMOylase RANBP2 (NUP358) in SU-DHL-1 cells. The nuclear pore complex member RANBP2 is considered to play two different roles during interphase and mitosis. During interphase RANBP2 binds to RanGAP1, effectively regulating protein import and throughout mitosis both proteins translocate to kinetochores and spindle microtubules. RanBP2 was suggested to be essential for localization of RanGAP1, Mad1/2 and CENP-E/F during mitosis and for the interaction of mitotic microtubules with kinetochores (Joseph et al., 2002; 2004; Salina et al., 2003). The SUMOylase ability of RanBP2 probably plays an important role in mitotic chromosome segregation. In the study of Dawlaty et al. RanBP2 aided chromosome separation by SUMOylation of Topoisomerase II-α (TOP2A) during mitosis, which facilitated the translocation of TOP2A to centromeres where it untangles sister chromatids and prevents chromosome bridging and missegregation (Dawlaty et al., 2008). Notably, the here-described IP-MS approaches identified RANBP2 and TOP2A as interaction partners of the endogenous C/EBPβ in U937 and SU-DHL-1 cells. Additionally, APS verified TOP2B as a direct interactor of the C/EBPβ TAD. Altogether, these observations further strengthen the possibility that C/EBPβ could have unexplored functions during mitotic chromatin organization.

In agreement with this theory our study also reported interactions of the endogenous C/EBPβ with the WD40-repeat protein BUB3 and the serine/threonine-protein kinase BUBR1, two essential SAC regulators. BUBR1 is understood to supervise the CENP-E mediated kinetochore attachment to microtubules during mitosis (Chan et al., 1999). Furthermore, BUB3 and BUBR1 form a functional mitotic checkpoint complex (MCC) with further checkpoint proteins like MAD2 (Sudakin et al., 2001). Additionally, this survey detected an C/EBPβ interaction with CK5P2/CDK5RAP2, a regulator of BUB1B and MAD2 transcription (Zhang et al., 2009). Finally, APS experiments revealed interaction of C/EBPβ

RD with the mRNA transport protein RAE1, which shares high sequence similarity with the before discussed SAC protein BUB3 and supposedly has similar functions during SAC and accurate chromosome segregation (Babu et al., 2003).

These findings further expand the functional network of C/EBPβ suggesting a role in the regulation of chromatin structure throughout the cell cycle, during DNA replication and in mitotic regulation in accordance with previous results (Tang and Lane, 1999; Tang et al., 2003).

4.5 C/EBPβ interacts with proteins controlling DNA damage response and apoptosis

DNA damage, insufficient attachment of microtubules to the kinetochores or retarded chromatid segregation during mitosis induce cell cycle arrest and lead in case of an irreparable damage to apoptosis. This study revealed C/EBPβ to interact not only with proteins regulating mitotic chromatin organization and cell cycle arrest but also DNA damage response and apoptosis induction.

DNA damage response (DDR) summarizes mechanisms recognizing and repairing DNA lesions like double- or single-strand breaks, nucleotide excision or mismatch repair (Lord and Ashworth, 2012). As a result of the DDR the arrest of the cell cycle or apoptosis is initiated. The triple-T (TTT) complex is one of the DDR complexes activated by UV or ionizing radiation (IR) induced double strand breaks. Its components TTI1, TTI2 and TELO2 were indicated to play a crucial role during DDR by regulating the stability of the checkpoint kinases ATM/ATR (Hurov et al., 2010). Intriguingly, this study revealed the interaction of C/EBPβ with two TTT-complex members as well as the ATR kinase in SU-DHL-1 cells.

The Werner syndrome protein (WRN) possesses helicase and exonuclease function and participates in several DNA repair mechanisms. These repair mechanisms range from base excision repair (BER) and non-homologous end joining (NHEJ) to the untangling of loops, Holliday junctions or replication forks during DNA replication and other interfering DNA secondary structures (Rossi et al., 2010). WRN is the central component of the WRN-

DNA repair complex that encompasses also the DNA helicases XRCC5 (Ku80), XRCC6 (Ku70) as well as the ADP-ribosyltransferase PARP-1 (Li and Comai, 2001; Li et al., 2004). Our experiments revealed the interaction of C/EBPβ with all components of this complex either in the SU-DHL-1 (some in parallel also in OPM2 and/or JEKO-1 cells) or in the HL60 cell line. Moreover, the WRN protein was suggested to interact with ATR and to be posttranslationally regulated by this checkpoint kinase as well (Pichierri et al., 2011; Rossi et al., 2010), highlighting the close connection of these two C/EBPβ partners detected by IP-MS. In summary, the interaction data collected in this survey suggests a yet undescribed role of C/EBPβ in different DNA damage response pathways; however, further research is necessary to substantiate this theory.

DNA interstrand cross-links (ICLs) induced by toxic substances lead to the activation of the S-phase checkpoint and the inhibition of DNA replication and gene transcription (Noll et al., 2006). ICLs induce two DNA repair pathways, both regulated by the mitotic checkpoint kinase ATR. Noteworthy, IP-MS not only identified ATR but also FANCD2 as a C/EBPβ interaction partner in SU-DHL-1 cells. FANCD2 is part of the FACD protein family and putatively regulates the repair of ICLs (Pichierri and Rosselli, 2004) and DNA double strand breaks (Nakanishi et al., 2005). FANCD2 was revealed to have ATR target motifs (Matsuoka et al., 2007) and on top of that ATR is known to phosphorylate FANCD2. ATR is stated to be required for FANCD2 monoubiqutitinylation leading to FANCD2 translocation to DNA damage foci during the DDR (Moldovan and D'Andrea, 2009; Andreassen et al., 2004). Moreover, FANCD2 was recently shown to interact with C/EBPδ, which facilitates its nuclear import by IPO4 upon DNA damage (Wang et al., 2010). This study identified IPO4, FANCD2 and ATR as C/EBPβ interaction partners in leukemia cell lines leading to assumption that C/EBPβ could play a similar role in the DNA damage response as C/EBPδ does.

Several studies suggest that C/EBPβ impacts apoptosis and cellular survival. The phosphorylation of C/EBPβ Thr217 by RSK2 facilitates C/EBPβ interaction with the Caspases 1 and 8 (Buck et al., 2001). C/EBPβ interaction with the Caspases 1 and 8 inhibits the cleavage of both these caspases and the subsequent apoptosis of hepatic stellate cells. Another study suggested that C/EBPβ represses p53 and p18Arf, prohibiting apoptosis and

promoting cell survival and tumorigenesis after DNA damage in skin cells (Ewing et al., 2008). Supporting these previous observations, the data of this study revealed C/EBPβ to interact with apoptosis regulators like BAX, BID, TRADD, PKM, Caspase 2 and 6 and the caspase independent apoptosis regulator kinase PKM.

4.6 C/EBPβ interacts with nucleoplasmic transport factors

The nuclear export protein XPO1 (CRM1) mediates C/EBPβ nuclear export in a phosphorylation dependent manner, regulated by the MAPK-pathway (Buck et al., 2001). One of the most significant interactions in all leukemia IP-MS experiments is the export factor XPO1 (CRM1) and its important co-factor RANBP3 (Lindsay et al., 2001). Furthermore, the Ran GTPase activator RanGAP1, known to convert Ran to the putatively inactive GDP-bound state, was found to interact with C/EBPβ in the SU-DHL-1 cell line. The protein RANBP2 (NUP358) is a known interaction partner of the sumoylated RanGAP1 (Lee et al., 1998; Mahajan et al., 1997). As discussed before RANBP2 and RanGAP1 interact with C/EBPβ in the SU-DHL-1 cells. Furthermore, this survey detected endogenous C/EBPβ to interact with three nuclear exportins and five importins. The proteomics of C/EBPβ infected C/EBPβ$^{-/-}$ MEF cells revealed several protein transport factors to be upregulated after LAP* and LAP expression. In conclusion, the detected importins could aid the translocation of C/EBPβ into the nucleus and thereby foster C/EBPβ target gene regulation. Finally, the here presented data adds several potential transport factors to the already known proteins mediating C/EBPβ nucleoplasmic transport, although this theory will have to be experimentally verified.

Additionally, this study detected the interaction of C/EBPβ with five components of the nuclear pore important for the nucleoplasmic transport. Of these nuclear pore components RANBP2, TPR, NUP85 and the mRNA transport protein RAE1 are suggested to play an additional role in the kinetochore and spindle attachment during mitosis, as discussed before (Lince-Faria et al., 2009; Dawlaty et al., 2008; Zuccolo et al., 2007; Orjalo et al., 2006; Joseph et al., 2002; 2004; Salina et al., 2003).

4.7 Involvement of C/EBPβ in lipid, amino acid and glucose metabolism

C/EBPβ has been implicated to play an important role in hepatic energy metabolism including gluconeogenesis and lipid metabolism. C/EBPβ binds to the promoters of genes encoding the tyrosine aminotransferase, the acetyl-CoA carboxylase, albumin and phoenolpyruvate carboxy-kinase (PEPCK) (Arizmendi et al., 1999). The C/EBPβ transcript expression itself and C/EBPβ binding to promoters of gluconeogenesis genes is regulated by insulin and glucocorticoids (Duong et al., 2002; Ghosh et al., 2001; Guo et al., 2001; Yamada et al., 1999). Moreover, C/EBPβ serine-phosphorylation in response to cyclic adenosine monophosphate (cAMP) regulates the expression of the acetyl-CoA carboxylase gene (Tae et al., 1995). Surveys of C/EBPβ knockout mice describe two possible phenotypes of mice concerning their energy metabolism. The first phenotype is lethal only 2 hours after birth as 50% of C/EBPβ $^{-/-}$ mice are unable to maintain normal blood glucose levels. During the research on a second reported phenotype the group of J.E. Friedman observed that the viable adult C/EBPβ $^{-/-}$ mice show hypoglycemia and lower hepatic glucose production after several hours of fasting, probably due to decreased liver gluconeogenesis. Additionally, the study described a decreased release of free fatty acids from adipose tissues and reduced levels of β-hydroxybutyrate due to the knockout of C/EBPβ (Liu et al., 1999). The C/EBPβ knockout not only influences carbohydrate and lipid metabolism but also impacts amino acid metabolism. Croniger et al. observed increased levels of ammonia/urea/nitrogen, ornithine and glutamine in the blood of adult C/EBPβ $^{-/-}$ mice after several hours of fasting (Croniger et al., 2001). As a reason the authors suggested an impaired hepatic urea cycle as C/EBPβ is known to induce transcription of the arginase gene in a glucocorticoid dependent manner. Arginase is a pivotal urea cycle enzyme. In accordance with this the here presented IP-MS interaction screenings from leukemia cell lines revealed interactors involved in glucose, nucleotide and amino acid metabolism and in energy transfer. Furthermore, numerous C/EBPβ interactors involved in energy transfer, glucose and lipid metabolism were revealed by APS. These results underline the advantage of the APS screening, as several of the APS derived interactors are

predominantly expressed in liver, spleen, intestine or adipose tissue.

The interaction data is augmented by the results of the proteomics analysis of the C/EBPβ knockout MEF cells that were retrovirally infected with constructs containing the C/EBPβ LAP* or LAP isoforms. The functional GO analysis of the proteins that were at least 2 fold upregulated by infection with the LAP* and/or the LAP constructs returned GO-terms like "GO:0055114 oxidation reduction" and "GO:0006091 generation of precursor metabolites and energy". These two GO-terms comprise proteins mainly involved in carbohydrate, fatty acid and amino acid metabolism. Remarkably, these upregulated proteins also encompass several of C/EBPβ protein-interaction partners revealed by this survey. In summary, the results of this study expand the knowledge of C/EBPβ contribution to cellular energy, nucleotide and amino acid metabolism maintenance.

Concluding remarks and future directions

The transcription factor C/EBPβ is associated with tumorigenesis, the regulation of tumor cell proliferation, metastasis and tumor survival as well as senescence and apoptosis (Gutsch et al., 2011; Pal et al., 2009; Piva et al., 2006; Luedde et al., 2004; Robinson et al., 1998; Seagroves et al., 1998). The protein-interaction data of C/EBPβ revealed by this study expands the knowledge of its cellular cooperation network and offers interesting new fields for future research on the diverse functions of C/EBPβ.

APS and IP-MS interaction screenings disclosed C/EBPβ interplay with numerous RNA binding proteins, associated with RNA metabolism and splicing. The data of this survey is in concert with recent reports, which presented the interaction of C/EBPα and β with Spliceosome components and RNA binding proteins using shotgun proteomics (Siersbaek et al., 2014; Giambruno et al., 2013). This study verifies some of the previously reported interactions and extends the number of C/EBPβ partners involved in RNA processing notably, revealing numerous of them as direct interaction partners (vide Table S1). Prospective investigations are required to elucidate C/EBPβ functional relationship with these RNA binding and processing proteins in a cellular context.

The C/EBPβ protein-protein-interaction network (Table S1) and the protein abundance alteration triggered by C/EBPβ expression (Figure 6; Figure S1) investigated in this study substantiates the established functional role of C/EBPβ as a regulator of metabolic pathways. Moreover, the obtained data identifies C/EBPβ involvement in the alteration of the protein abundance of several SWI/SNF complex and MAPK pathway components. This is intriguing, as several of these proteins belong to a collection of putative and novel C/EBPβ interaction partners (Figure 21; Kowenz-Leutz et al., 2010 and 1999). Future research will have to disclose the relationship between the proteins that were upregulated by C/EBPβ expression and the proteins that are C/EBPβ interaction partners.

C/EBPβ fosters the proliferation and the survival of anaplastic large cell lymphoma

(Anastasov et al., 2010; Piva et al., 2006 and 2010; Quintanilla-Martinez et al., 2006). The collection of protein-protein interaction data put forth by this survey emphasizes the role of C/EBPβ in ALCL tumorigenicity by disclosing numerous novel C/EBPβ interaction partners responsible for executing diverse cellular functions. C/EBPβ was unveiled to interact with HuR, ALK and STAT3 in SU-DHL-1 cells by IP-MS or by APS, whereas up until now these proteins were only known to act as regulators of C/EBPβ mRNA expression in SU-DHL-1 cells (Bergalet et al., 2011; Piva et al., 2006 and 2010; Quintanilla-Martinez et al., 2006). A recent study reported numerous potential target genes of C/EBPβ in SU-DHL-1 cells (Bonzheim et al., 2013). Several of the in this survey reported interaction partners of C/EBPβ in SU-DHL-1 are regulators of gene expression and potentially aid C/EBPβ during target gene regulation.

Interestingly, the proliferation of SU-DHL-1 cells partly relies on the activating C/EBPβ Thr235 phosphorylation by the MAPK pathway kinase ERK1/2 (Anastasov et al., 2010). In addition to this, the data of this study further emphasizes the multifaceted association of C/EBPβ with the MAPK/ERK1/2 pathway and other kinase pathways suggesting potential therapeutic targets for leukemia like ALCL. This is underlined by recent studies reporting of the beneficial effects of a pharmaceutical therapy combining established ALCL therapeutics with inhibitors of the MAPK/ERK1/2- pathway in ALCL (Georgakis et al., 2006; Ito et al., 2010).

In this study the C/EBPβ protein interaction network of several distinct leukemia types was investigated. This C/EBPβ interaction network provides a solid basis for future research, for example by therapeutically targeting C/EBPβ interaction partners in leukemias and other cancer types, as C/EBPβ is also associated with aggressive types of breast tumors and high-grade colorectal cancers (Van de Vijver et al., 2002; Zahnow, 2009; Rask et al., 2000).

REFERENCES

Agre, P., Johnson, P.F., and McKnight, S.L. (1989). Cognate DNA binding specificity retained after leucine zipper exchange between GCN4 and C/EBP. Science.

Ajuh, P., Kuster, B., Panov, K., Zomerdijk, J.C., Mann, M., and Lamond, A.I. (2000). Functional analysis of the human CDC5L complex and identification of its components by mass spectrometry. The EMBO Journal *19*, 6569–6581.

Akira, S., Isshiki, H., Sugita, T., Tanabe, O., Kinoshita, S., Nishio, Y., Nakajima, T., Hirano, T., and Kishimoto, T. (1990). A nuclear factor for IL-6 expression (NF-IL6) is a member of a C/EBP family. Embo J *9*, 1897–1906.

Allshire, R.C., and Karpen, G.H. (2008). Epigenetic regulation of centromeric chromatin: old dogs, new tricks? Nature Reviews Genetics *9*, 923–937.

Anastasov, N., Bonzheim, I., Rudelius, M., Klier, M., Dau, T., Angermeier, D., Duyster, J., Pittaluga, S., Fend, F., Raffeld, M., et al. (2010). C/EBPβ expression in ALK-positive anaplastic large cell lymphomas is required for cell proliferation and is induced by the STAT3 signaling pathway. Haematologica *95*, 760–767.

Andreassen, P.R., D'Andrea, A.D., and Taniguchi, T. (2004). ATR couples FANCD2 monoubiquitination to the DNA-damage response. Genes & Development *18*, 1958–1963.

Arizmendi, C., Liu, S., Croniger, C., Poli, V., and Friedman, J.E. (1999). The Transcription Factor CCAAT/Enhancer-binding Protein Regulates Gluconeogenesis and Phosphoenolpyruvate Carboxykinase (GTP) Gene Transcription during Diabetes. Journal of Biological Chemistry *274*, 13033–13040.

Arnal-Estapé, A., Tarragona, M., Morales, M., Guiu, M., Nadal, C., Massagué, J., and Gomis, R.R. (2010). HER2 silences tumor suppression in breast cancer cells by switching expression of C/EBPβ isoforms. Cancer Research *70*, 9927–9936.

Babu, J.R., Jeganathan, K.B., Baker, D.J., Wu, X., Kang-Decker, N., and van Deursen, J.M. (2003). Rae1 is an essential mitotic checkpoint regulator that cooperates with Bub3 to prevent chromosome missegregation. J Cell Biol *160*, 341–353.

Bannister, A.J., and Kouzarides, T. (2011). Regulation of chromatin by histone modifications. Nature Publishing Group *21*, 381–395.

Basu, S.K., Malik, R., Huggins, C.J., Lee, S., Sebastian, T., Sakchaisri, K., Quiñones, O.A., Alvord, W.G., and Johnson, P.F. (2011). 3′UTR elements inhibit Ras-induced C/EBPβ post-translational activation and senescence in tumour cells. The EMBO Journal *30*, 3714–3728.

Berberich-Siebelt, F., Berberich, I., Andrulis, M., Santner-Nanan, B., Jha, M.K., Klein-Hessling, S., Schimpl, A., and Serfling, E. (2006). SUMOylation interferes with CCAAT/enhancer-binding protein beta-mediated c-myc repression, but not IL-4 activation in T cells. J Immunol *176*, 4843–4851.

Bergalet, J., Fawal, M., Lopez, C., Desjobert, C., Lamant, L., Delsol, G., Morello, D., and Espinos, E. (2011). HuR-mediated control of C/EBPbeta mRNA stability and translation in ALK-positive anaplastic large cell lymphomas. Mol. Cancer Res. *9*, 485–496.

Bégay, V., Smink, J., and Leutz, A. (2004). Essential requirement of CCAAT/enhancer binding proteins in embryogenesis. Molecular and Cellular Biology *24*, 9744–9751.

Bi, W., Wu, L., Coustry, F., de Crombrugghe, B., and Maity, S.N. (1997). DNA binding specificity of the CCAAT-binding factor CBF/NF-Y. J. Biol. Chem. *272*, 26562–26572.

Blenk, S., Engelmann, J.C., Pinkert, S., Weniger, M., Schultz, J., Rosenwald, A., Müller-Hermelink, H.K., Müller, T., and Dandekar, T. (2008). Explorative data analysis of MCL reveals gene expression networks implicated in survival and prognosis supported by explorative CGH analysis. BMC Cancer *8*, 106.

Bochman, M.L., and Schwacha, A. (2009). The Mcm Complex: Unwinding the Mechanism of a Replicative Helicase.

Microbiology and Molecular Biology Reviews *73*, 652–683.

Boersema, P.J., Raijmakers, R., Lemeer, S., Mohammed, S., and Heck, A.J.R. (2009). Multiplex peptide stable isotope dimethyl labeling for quantitative proteomics. Nature Protocols *4*, 484–494.

Bommer, U.A., Lutsch, G., Stahl, J., and Bielka, H. (1991). Eukaryotic initiation factors eIF-2 and eIF-3: interactions, structure and localization in ribosomal initiation complexes. Biochimie *73*, 1007–1019.

Bonzheim, I., Irmler, M., Klier-Richter, M., Steinhilber, J., Anastasov, N., Schäfer, S., Adam, P., Beckers, J., Raffeld, M., Fend, F., et al. (2013). Identification of C/EBPβ target genes in ALK+ anaplastic large cell lymphoma (ALCL) by gene expression profiling and chromatin immunoprecipitation. PLoS ONE *8*, e64544.

Buck, M., Poli, V., Hunter, T., and Chojkier, M. (2001a). C/EBPbeta phosphorylation by RSK creates a functional XEXD caspase inhibitory box critical for cell survival. Molecular Cell *8*, 807–816.

Buck, M., Poli, V., van der Geer, P., Chojkier, M., and Hunter, T. (1999). Phosphorylation of rat serine 105 or mouse threonine 217 in C/EBP beta is required for hepatocyte proliferation induced by TGF alpha. Molecular Cell *4*, 1087–1092.

Buck, M., Turler, H., and Chojkier, M. (1994). LAP (NF-IL-6), a tissue-specific transcriptional activator, is an inhibitor of hepatoma cell proliferation. Embo J *13*, 851–860.

Buck, M., Zhang, L., Halasz, N.A., Hunter, T., and Chojkier, M. (2001b). Nuclear export of phosphorylated C/EBPbeta mediates the inhibition of albumin expression by TNF-alpha. Embo J *20*, 6712–6723.

Bukata, L., Parker, S.L., and D'Angelo, M.A. (2013). Nuclear pore complexes in the maintenance of genome integrity. Current Opinion in Cell Biology *25*, 378–386.

Calkhoven, C.F., Muller, C., and Leutz, A. (2000). Translational control of C/EBPalpha and C/EBPbeta isoform expression. Genes & Development *14*, 1920–1932.

Carroll, C.W., and Straight, A.F. (2006). Centromere formation: from epigenetics to self-assembly. Trends in Cell Biology *16*, 70–78.

Chan, G., Jablonski, S.A., Sudakin, V., Hittle, J.C., and Yen, T.J. (1999). Human BUBR1 is a mitotic checkpoint kinase that monitors CENP-E functions at kinetochores and binds the cyclosome/APC. J Cell Biol *146*, 941–954.

Chang, C.-J., Chen, Y.-L., and Lee, S.-C. (1998). Coactivator TIF1β interacts with transcription factor C/EBPβ and glucocorticoid receptor to induce α1-acid glycoprotein gene expression. Molecular and Cellular Biology *18*, 5880–5887.

Chen, P.L., Riley, D.J., Chen-Kiang, S., and Lee, W.H. (1996). Retinoblastoma protein directly interacts with and activates the transcription factor NF-IL6. Proc. Natl. Acad. Sci. U.S.a. *93*, 465–469.

Chen, X., Liu, W., Ambrosino, C., Ruocco, M.R., Poli, V., Romani, L., Quinto, I., Barbieri, S., Holmes, K.L., Venuta, S., et al. (1997). Impaired generation of bone marrow B lymphocytes in mice deficient in C/EBPbeta. Blood *90*, 156–164.

Cheung, P., Allis, C.D., and Sassone-Corsi, P. (2000). Signaling to chromatin through histone modifications. Cell *103*, 263–271.

Chinery, R., Brockman, J.A., Dransfield, D.T., and Coffey, R.J. (1997). Antioxidant-induced nuclear translocation of CCAAT/enhancer-binding protein beta. A critical role for protein kinase A-mediated phosphorylation of Ser299. J. Biol. Chem. *272*, 30356–30361.

Cho, H., Orphanides, G., Sun, X., Yang, X.-J., Ogryzko, V., Lees, E., Nakatani, Y., and Reinberg, D. (1998). A human RNA polymerase II complex containing factors that modify chromatin structure. Molecular and Cellular Biology *18*, 5355–5363.

Chodosh, L.A., Olesen, J., Hahn, S., Baldwin, A.S., Guarente, L., and Sharp, P.A. (1988). A yeast and a human CCAAT-binding protein have heterologous subunits that are functionally interchangeable. Cell *53*, 25–35.

Cleveland, D.W., Mao, Y., and Sullivan, K.F. (2003). Centromeres and kinetochores: from epigenetics to mitotic checkpoint signaling. Cell *112*, 407–421.

Cloos, P.A., Christensen, J., Agger, K., and Helin, K. (2008). Erasing the methyl mark: histone demethylases at the center of cellular differentiation and disease. Genes & Development *22*, 1115–1140.

Coll, J.M., Sekowski, J.W., Hickey, R.J., Schnaper, L., Yue, W., Brodie, A.M., Uitto, L., Syvaoja, J.E., and Malkas,

L.H. (1996). The human breast cell DNA synthesome: its purification from tumor tissue and cell culture. Oncol Res *8*, 435–447.

Collins, S.J., Gallo, R.C., and Gallagher, R.E. (1977). Continuous growth and differentiation of human myeloid leukaemic cells in suspension culture. Nature *270*, 347–349.

Cox, J., and Mann, M. (2008). MaxQuant enables high peptide identification rates, individualized p.p.b.-range mass accuracies and proteome-wide protein quantification. Nature Biotechnology *26*, 1367–1372.

Croniger, C.M., Millward, C., Yang, J., Kawai, Y., Arinze, I.J., Liu, S., Harada-Shiba, M., Chakravarty, K., Friedman, J.E., Poli, V., et al. (2001). Mice with a deletion in the gene for CCAAT/enhancer-binding protein beta have an attenuated response to cAMP and impaired carbohydrate metabolism. J. Biol. Chem. *276*, 629–638.

Dawlaty, M.M., Malureanu, L., Jeganathan, K.B., Kao, E., Sustmann, C., Tahk, S., Shuai, K., Grosschedl, R., and van Deursen, J.M. (2008). Resolution of sister centromeres requires RanBP2-mediated SUMOylation of topoisomerase IIalpha. Cell *133*, 103–115.

Descombes, P., and Schibler, U. (1991). A liver-enriched transcriptional activator protein, LAP, and a transcriptional inhibitory protein, LIP, are translated from the sam mRNA. Cell *67*, 569–579.

Dey, S., Savant, S., Teske, B.F., Hatzoglou, M., Calkhoven, C.F., and Wek, R.C. (2012). Transcriptional repression of ATF4 gene by CCAAT/enhancer-binding protein β (C/EBPβ) differentially regulates integrated stress response. J. Biol. Chem. *287*, 21936–21949.

Di-Poi, N., Desvergne, B., Michalik, L., and Wahli, W. (2005). Transcriptional Repression of Peroxisome Proliferator-activated Receptor / in Murine Keratinocytes by CCAAT/Enhancer-binding Proteins. Journal of Biological Chemistry *280*, 38700–38710.

Dong, Y., Hakimi, M.-A., Chen, X., Kumaraswamy, E., Cooch, N.S., Godwin, A.K., and Shiekhattar, R. (2003). Regulation of BRCC, a Holoenzyme Complex Containing BRCA1 and BRCA2, by a Signalosome-like Subunit and Its Role in DNA Repair. Molecular Cell *12*, 1087–1099.

Dooher, J.E., Paz-Priel, I., Houng, S., Baldwin, A.S., and Friedman, A.D. (2011). C/EBPα, C/EBPα oncoproteins, or C/EBPβ preferentially bind NF-κB p50 compared with p65, focusing therapeutic targeting on the C/EBP:p50 interaction. Molecular Cancer Research *9*, 1395–1405.

Dorn, A., Bollekens, J., Staub, A., Benoist, C., and Mathis, D. (1987). A multiplicity of CCAAT box-binding proteins. Cell *50*, 863–872.

Dou, Y., Milne, T.A., Tackett, A.J., Smith, E.R., Fukuda, A., Wysocka, J., Allis, C.D., Chait, B.T., Hess, J.L., and Roeder, R.G. (2005). Cell - Physical Association and Coordinate Function of the H3 K4 Methyltransferase MLL1 and the H4 K16 Acetyltransferase MOF. Cell *121*, 873–885.

Drechsler, H., and McAinsh, A.D. (2012). Exotic mitotic mechanisms. Open Biology *2*, 120140.

Duong, D.T., Waltner-Law, M.E., Sears, R., Sealy, L., and Granner, D.K. (2002). Insulin inhibits hepatocellular glucose production by utilizing liver-enriched transcriptional inhibitory protein to disrupt the association of CREB-binding protein and RNA polymerase II with the phosphoenolpyruvate carboxykinase gene promoter. J. Biol. Chem. *277*, 32234–32242.

Eaton, E.M., and Sealy, L. (2003). Modification of CCAAT/enhancer-binding protein-beta by the small ubiquitin-like modifier (SUMO) family members, SUMO-2 and SUMO-3. J. Biol. Chem. *278*, 33416–33421.

Epstein, A.L., and Kaplan, H.S. (1974). Biology of the human malignant lymphomas I. Establishment in continuous cell culture and heterotransplantation of diffuse histiocytic lymphomas - Epstein - 2006 - Cancer - Wiley Online Library. Cancer.

Esteves, C.L., Kelly, V., Bégay, V., Lillico, S.G., Leutz, A., Seckl, J.R., and Chapman, K.E. (2013). Stable conditional expression and effect of C/ebpβ-LIP in adipocytes using the pSLIK system. Journal of Molecular Endocrinology *51*, 91–98.

Esteves, C.L., Kelly, V., Bégay, V., Man, T.Y., Morton, N.M., Leutz, A., Seckl, J.R., and Chapman, K.E. (2012). Regulation of adipocyte 11β-hydroxysteroid dehydrogenase type 1 (11β-HSD1) by CCAAT/enhancer-binding protein (C/EBP) β isoforms, LIP and LAP. PLoS ONE *7*, e37953–e37953.

Ewing, S.J., Zhu, S., Zhu, F., House, J.S., and Smart, R.C. (2008). C/EBPbeta represses p53 to promote cell survival downstream of DNA damage independent of oncogenic Ras and p19(Arf). Cell Death Differ *15*, 1734–

1744.

Geiger, T., Wehner, A., Schaab, C., Cox, J., and Mann, M. (2012). Comparative Proteomic Analysis of Eleven Common Cell Lines Reveals Ubiquitous but Varying Expression of Most Proteins. Molecular & Cellular Proteomics *11*, M111.014050–M111.014050.

Georgakis, G.V., Li, Y., Rassidakis, G.Z., Medeiros, L.J., and Younes, A. (2006). The HSP90 inhibitor 17-AAG synergizes with doxorubicin and U0126 in anaplastic large cell lymphoma irrespective of ALK expression. Exp. Hematol. *34*, 1670–1679.

Gery, S. (2005). Transcription profiling of C/EBP targets identifies Per2 as a gene implicated in myeloid leukemia. Blood *106*, 2827–2836.

Ghosh, A.K., Lacson, R., Liu, P., Cichy, S.B., Danilkovich, A., Guo, S., and Unterman, T.G. (2001). A Nucleoprotein Complex containing CCAAT/Enhancer-binding Protein Interacts with an Insulin Response Sequence in the Insulin-like Growth Factor-binding Protein-1 Gene and Contributes to Insulin-regulated Gene Expression. Journal of Biological Chemistry *276*, 8507–8515.

Giambruno, R., Grebien, F., Stukalov, A., Knoll, C., Planyavsky, M., Rudashevskaya, E.L., Colinge, J., Superti-Furga, G., and Bennett, K.L. (2013). Affinity purification strategies for proteomic analysis of transcription factor complexes. J. Proteome Res. *12*, 4018–4027.

Gorgoni, B., Maritano, D., Marthyn, P., Righi, M., and Poli, V. (2002). C/EBP beta gene inactivation causes both impaired and enhanced gene expression and inverse regulation of IL-12 p40 and p35 mRNAs in macrophages. J Immunol *168*, 4055–4062.

Graham, F.L., Smiley, J., Russell, W.C., and Nairn, R. (1977). Characteristics of a human cell line transformed by DNA from human adenovirus type 5. J. Gen. Virol. *36*, 59–74.

Grimes, J.A., Nielsen, S.J., Battaglioli, E., Miska, E.A., Speh, J.C., Berry, D.L., Atouf, F., Holdener, B.C., Mandel, G., and Kouzarides, T. (2000). The co-repressor mSin3A is a functional component of the REST-CoREST repressor complex. J. Biol. Chem. *275*, 9461–9467.

Guo, S., Cichy, S.B., He, X., Yang, Q., Ragland, M., Ghosh, A.K., Johnson, P.F., and Unterman, T.G. (2001). Insulin suppresses transactivation by CAAT/enhancer-binding proteins beta (C/EBPbeta). Signaling to p300/CREB-binding protein by protein kinase B disrupts interaction with the major activation domain of C/EBPbeta. J. Biol. Chem. *276*, 8516–8523.

Gutsch, R., Kandemir, J.D., Pietsch, D., Cappello, C., Meyer, J., Simanowski, K., Huber, R., and Brand, K. (2011). CCAAT/enhancer-binding protein β inhibits proliferation in monocytic cells by affecting the retinoblastoma protein/E2F/cyclin E pathway but is not directly required for macrophage morphology. J. Biol. Chem. *286*, 22716–22729.

Günther, K., Rust, M., Leers, J., Boettger, T., Scharfe, M., Jarek, M., Bartkuhn, M., and Renkawitz, R. (2013). Differential roles for MBD2 and MBD3 at methylated CpG islands, active promoters and binding to exon sequences. Nucleic Acids Research *41*, 3010–3021.

Hanlon, M., Sturgill, T.W., and Sealy, L. (2001). ERK2- and p90(Rsk2)-dependent pathways regulate the CCAAT/enhancer-binding protein-beta interaction with serum response factor. J. Biol. Chem. *276*, 38449–38456.

Hata, K., Nishimura, R., Ueda, M., Ikeda, F., Matsubara, T., Ichida, F., Hisada, K., Nokubi, T., Yamaguchi, A., and Yoneda, T. (2005). A CCAAT/enhancer binding protein beta isoform, liver-enriched inhibitory protein, regulates commitment of osteoblasts and adipocytes. Molecular and Cellular Biology *25*, 1971–1979.

Hatamochi, A., Golumbek, P.T., Van Schaftingen, E., and de Crombrugghe, B. (1988). A CCAAT DNA binding factor consisting of two different components that are both required for DNA binding. J. Biol. Chem. *263*, 5940–5947.

Heale, J.T., Ball, A.R., Schmiesing, J.A., Kim, J.-S., Kong, X., Zhou, S., Hudson, D.F., Earnshaw, W.C., and Yokomori, K. (2006). Condensin I interacts with the PARP-1-XRCC1 complex and functions in DNA single-strand break repair. Molecular Cell *21*, 837–848.

Hinnebusch, A.G. (2006). eIF3: a versatile scaffold for translation initiation complexes. Trends in Biochemical Sciences *31*, 553–562.

Hirai, H., Zhang, P., Dayaram, T., Hetherington, C.J., Mizuno, S.-I., Imanishi, J., Akashi, K., and Tenen, D.G.

(2006). C/EBPbeta is required for “emergency” granulopoiesis. Nat Immunol *7*, 732–739.

Hirano, T. (2006). At the heart of the chromosome: SMC proteins in action. Nat Rev Mol Cell Biol *7*, 311–322.

Hirota, T., Gerlich, D., Koch, B., Ellenberg, J., and Peters, J.-M. (2004). Distinct functions of condensin I and II in mitotic chromosome assembly. Journal of Cell Science *117*, 6435–6445.

Hope, I.A., and Struhl, K. (1986). Functional dissection of a eukaryotic transcriptional activator protein, GCN4 of Yeast. Cell *46*, 885–894.

Huang, D.W., Sherman, B.T., and Lempicki, R.A. (2009). Systematic and integrative analysis of large gene lists using DAVID bioinformatics resources. Nature Protocols *4*, 44–57.

Huber, R., Pietsch, D., Panterodt, T., and Brand, K. (2012). Regulation of C/EBPβ and resulting functions in cells of the monocytic lineage. Cellular Signalling *24*, 1287–1296.

Hublitz, P., Kunowska, N., Mayer, U.P., Müller, J.M., Heyne, K., Yin, N., Fritzsche, C., Poli, C., Miguet, L., and Schupp, I.W. (2005). NIR is a novel INHAT repressor that modulates the transcriptional activity of p53. Genes & Development *19*, 2912–2924.

Hubner, N.C., and Mann, M. (2011). Extracting gene function from protein-protein interactions using Quantitative BAC InteraCtomics (QUBIC). Methods *53*, 453–459.

Hughes, C.M., Rozenblatt-Rosen, O., Milne, T.A., Copeland, T.D., Levine, S.S., Lee, J.C., Hayes, D.N., Shanmugam, K.S., Bhattacharjee, A., Biondi, C.A., et al. (2004). Menin associates with a trithorax family histone methyltransferase complex and with the hoxc8 locus. Molecular Cell *13*, 587–597.

Hurov, K.E.K., Cotta-Ramusino, C.C., and Elledge, S.J.S. (2010). A genetic screen identifies the Triple T complex required for DNA damage signaling and ATM and ATR stability. Genes & Development *24*, 1939–1950.

Ishimi, Y., Ichinose, S., Omori, A., Sato, K., and Kimura, H. (1996). Binding of human minichromosome maintenance proteins with histone H3. J. Biol. Chem. *271*, 24115–24122.

Ito, M., Zhao, N., Zeng, Z., Chang, C.C., and Zu, Y. (2010). Synergistic growth inhibition of anaplastic large cell lymphoma cells by combining cellular ALK gene silencing and a low dose of the kinase inhibitor U0126. Cancer Gene Ther. *17*, 633–644.

Izuta, H., Ikeno, M., Suzuki, N., Tomonaga, T., Nozaki, N., Obuse, C., Kisu, Y., Goshima, N., Nomura, F., and Nomura, N. (2006). Comprehensive analysis of the ICEN (Interphase Centromere Complex) components enriched in the CENP-A chromatin of human cells. Genes to Cells *11*, 673–684.

Jensen, L.J., Kuhn, M., Stark, M., Chaffron, S., Creevey, C., Muller, J., Doerks, T., Julien, P., Roth, A., Simonovic, M., et al. (2009). STRING 8--a global view on proteins and their functional interactions in 630 organisms. Nucleic Acids Research *37*, D412–D416.

Jenuwein, T. (2001). Translating the Histone Code. Science *293*, 1074–1080.

Jeon, H.J., Kim, C.W., Yoshino, T., and Akagi, T. (1998). Establishment and characterization of a mantle cell lymphoma cell line. Br. J. Haematol. *102*, 1323–1326.

Ji, Y., and Studzinski, G.P. (2004). Retinoblastoma protein and CCAAT/enhancer-binding protein β are required for 1, 25-dihydroxyvitamin D3-induced monocytic differentiation of HL60 cells. Cancer Research *64*, 370–377.

Ji, Y., Kutner, A., Verstuyf, A., Verlinden, L., and Studzinski, G.P. (2002). Derivatives of vitamins D2 and D3 activate three MAPK pathways and upregulate pRb expression in differentiating HL60 cells. Cc *1*, 410–415.

Jiang, H.Y., Hickey, R.J., Abdel-Aziz, W., Tom, T.D., Wills, P.W., Liu, J., and Malkas, L.H. (2002). Human cell DNA replication is mediated by a discrete multiprotein complex. J. Cell. Biochem. *85*, 762–774.

Jiang, K., Hein, N., Eckert, K., Lüscher-Firzlaff, J., and Lüscher, B. (2008). Regulation of the MAD1 promoter by G-CSF. Nucleic Acids Research *36*, 1517–1531.

Johnson, P.F., Landschulz, W.H., Graves, B.J., and McKnight, S.L. (1987). Identification of a rat liver nuclear protein that binds to the enhancer core element of three animal viruses. Genes & Development *1*, 133–146.

Johnson, P.F. (2005). Molecular stop signs: regulation of cell-cycle arrest by C/EBP transcription factors. Journal of Cell Science *118*, 2545–2555.

Jones, L.C., Lin, M.-L., Chen, S.-S., Krug, U., Hofmann, W.-K., Lee, S., Lee, Y.-H., and Koeffler, H.P. (2002).

Expression of C/EBPβ from the C/ebpα gene locus is sufficient for normal hematopoiesis in vivo. Blood *99*, 2032–2036.

Joseph, J., Liu, S.-T., Jablonski, S.A., Yen, T.J., and Dasso, M. (2004). The RanGAP1-RanBP2 Complex Is Essential for Microtubule-Kinetochore Interactions In Vivo. Current Biology *14*, 611–617.

Joseph, J., Tan, S.-H., Karpova, T.S., McNally, J.G., and Dasso, M. (2002). SUMO-1 targets RanGAP1 to kinetochores and mitotic spindles. J Cell Biol *156*, 595–602.

Jundt, F., Raetzel, N., Müller, C., Calkhoven, C.F., Kley, K., Mathas, S., Lietz, A., Leutz, A., and Dörken, B. (2005). A rapamycin derivative (everolimus) controls proliferation through down-regulation of truncated CCAAT enhancer binding protein β and NF-kB activity in Hodgkin and anaplastic large cell lymphomas. Blood *106*, 1801–1807.

Jurica, M.S., Licklider, L.J., Gygi, S.P., Grigorieff, N., and Moore, M.J. (2002). Purification and characterization of native spliceosomes suitable for three-dimensional structural analysis. Rna *8*, 426–439.

Kadoch, C., Hargreaves, D.C., Hodges, C., Elias, L., Ho, L., Ranish, J., and Crabtree, G.R. (2013). Proteomic and bioinformatic analysis of mammalian SWI/SNF complexes identifies extensive roles in human malignancy. Nat Genet *45*, 592–601.

Kerppola, T.K., and Curran, T. (1991). Fos-Jun heterodimers and jun homodimers bend DNA in opposite orientations: Implications for transcription factor cooperativity. Cell.

Ki, S.H., Cho, I.J., Choi, D.W., and Kim, S.G. (2005). Glucocorticoid receptor (GR)-associated SMRT binding to C/EBPbeta TAD and Nrf2 Neh4/5: role of SMRT recruited to GR in GSTA2 gene repression. Molecular and Cellular Biology *25*, 4150–4165.

Kim, J. (2002). Transcriptional Activity of CCAAT/Enhancer-binding Proteins Is Controlled by a Conserved Inhibitory Domain That Is a Target for Sumoylation. Journal of Biological Chemistry *277*, 38037–38044.

Kops, G.J., Kim, Y., Weaver, B.A., Mao, Y., McLeod, I., Yates, J.R., Tagaya, M., and Cleveland, D.W. (2005). ZW10 links mitotic checkpoint signaling to the structural kinetochore. J Cell Biol *169*, 49–60.

Kornberg, R.D. (1974). Chromatin structure: a repeating unit of histones and DNA. Science *184*, 868–871.

Kornberg, R.D., and Thomas, J.O. (1974). Chromatin structure: oligomers of the histones. Science *184*, 865–868.

Korzus, E.E., Torchia, J.J., Rose, D.W.D., Xu, L.L., Kurokawa, R.R., McInerney, E.M.E., Mullen, T.M.T., Glass, C.K.C., and Rosenfeld, M.G.M. (1998). Transcription factor-specific requirements for coactivators and their acetyltransferase functions. Science *279*, 703–707.

Kovács, K.A., Steinmann, M., Magistretti, P.J., Halfon, O., and Cardinaux, J.-R. (2003). CCAAT/enhancer-binding protein family members recruit the coactivator CREB-binding protein and trigger its phosphorylation. J. Biol. Chem. *278*, 36959–36965.

Kowenz-Leutz, E., and Leutz, A. (1999). A C/EBP beta isoform recruits the SWI/SNF complex to activate myeloid genes. Molecular Cell *4*, 735–743.

Kowenz-Leutz, E., Twamley, G., Ansieau, S., and Leutz, A. (1994). Novel mechanism of C/EBP beta (NF-M) transcriptional control: activation through derepression. Genes & Development *8*, 2781–2791.

Kowenz-Leutz, E., Pless, O., Dittmar, G., Knoblich, M., and Leutz, A. (2010). Crosstalk between C/EBPbeta phosphorylation, arginine methylation, and SWI/SNF/Mediator implies an indexing transcription factor code. The EMBO Journal *29*, 1105–1115.

Lamb, J., Ramaswamy, S., Ford, H.L., Contreras, B., Martinez, R.V., Kittrell, F.S., Zahnow, C.A., Patterson, N., Golub, T.R., and Ewen, M.E. (2003). A mechanism of cyclin D1 action encoded in the patterns of gene expression in human cancer. Cell *114*, 323–334.

Landschulz, W.H., Johnson, P.F., Adashi, E.Y., Graves, B.J., and McKnight, S.L. (1988). Isolation of a recombinant copy of the gene encoding C/EBP. Genes & Development *2*, 786–800.

Landschulz, W.H., Johnson, P.F., and McKnight, S.L. (1989). The DNA binding domain of the rat liver nuclear protein C/EBP is bipartite. Science *243*, 1681–1688.

LeClair, K.P., Blanar, M.A., and Sharp, P.A. (1992). The p50 subunit of NF-kappa B associates with the NF-IL6 transcription factor. Proc. Natl. Acad. Sci. U.S.a. *89*, 8145–8149.

Lee, G.W., Melchior, F., Matunis, M.J., Mahajan, R., Tian, Q., and Anderson, P. (1998). Modification of Ran GTPase-activating protein by the small ubiquitin-related modifier SUMO-1 requires Ubc9, an E2-type ubiquitin-conjugating enzyme homologue. J. Biol. Chem. *273*, 6503–6507.

Lee, M.G., Wynder, C., Cooch, N., and Shiekhattar, R. (2005). An essential role for CoREST in nucleosomal histone 3 lysine 4 demethylation. Nature *437*, 432–435.

Lee, S., Shuman, J.D., Guszczynski, T., Sakchaisri, K., Sebastian, T., Copeland, T.D., Miller, M., Cohen, M.S., Taunton, J., Smart, R.C., et al. (2010a). RSK-Mediated Phosphorylation in the C/EBP Leucine Zipper Regulates DNA Binding, Dimerization, and Growth Arrest Activity. Molecular and Cellular Biology *30*, 2621–2635.

Lee, S.-H., Krisanapun, C., and Baek, S.J. (2010b). NSAID-activated gene-1 as a molecular target for capsaicin-induced apoptosis through a novel molecular mechanism involving GSK3beta, C/EBPbeta and ATF3. Carcinogenesis *31*, 719–728.

Leutz, A., Pless, O., Lappe, M., Dittmar, G., and Kowenz-Leutz, E. (2011). Crosstalk between phosphorylation and multi-site arginine/lysine methylation in C/EBPs. Transcription *2*, 3–8.

Li, B., and Comai, L. (2001). Requirements for the nucleolytic processing of DNA ends by the Werner syndrome protein-Ku70/80 complex. J. Biol. Chem. *276*, 9896–9902.

Li, B., Navarro, S., Kasahara, N., and Comai, L. (2004). Identification and biochemical characterization of a Werner's syndrome protein complex with Ku70/80 and poly(ADP-ribose) polymerase-1. J. Biol. Chem. *279*, 13659–13667.

Lince-Faria, M., Maffini, S., Orr, B., Ding, Y., Ding, Y., Sunkel, C.E., Tavares, A., Johansen, J., Johansen, K.M., and Maiato, H. (2009). Spatiotemporal control of mitosis by the conserved spindle matrix protein Megator. J Cell Biol *184*, 647–657.

Lindsay, M.E., Holaska, J.M., Welch, K., Paschal, B.M., and Macara, I.G. (2001). Ran-binding protein 3 is a cofactor for Crm1-mediated nuclear protein export. J Cell Biol *153*, 1391–1402.

Liu, S., Croniger, C., Arizmendi, C., Harada-Shiba, M., Ren, J., Poli, V., Hanson, R.W., and Friedman, J.E. (1999). Hypoglycemia and impaired hepatic glucose production in mice with a deletion of the C/EBPβ gene. J. Clin. Invest. *103*, 207–213.

Logarinho, E., Resende, T., Torres, C., and Bousbaa, H. (2008). The human spindle assembly checkpoint protein Bub3 is required for the establishment of efficient kinetochore-microtubule attachments. Molecular Biology of the Cell *19*, 1798–1813.

Lord, C.J., and Ashworth, A. (2012). The DNA damage response and cancer therapy. Nature *481*, 287–294.

Losada, A., and Hirano, T. (2001). Intermolecular DNA Interactions Stimulated by the Cohesin Complex in Vitro: Implications for Sister Chromatid Cohesion. Current Biology *11*, 268–272.

Luedde, T., Duderstadt, M., Streetz, K.L., Tacke, F., Kubicka, S., Manns, M.P., and Trautwein, C. (2004). C/EBP β isoforms LIP and LAP modulate progression of the cell cycle in the regenerating mouse liver. Hepatology *40*, 356–365.

Mahajan, R., Delphin, C., Guan, T., Gerace, L., and Melchior, F. (1997). A small ubiquitin-related polypeptide involved in targeting RanGAP1 to nuclear pore complex protein RanBP2. Cell *88*, 97–107.

Mahoney, C.W., Shuman, J., McKnight, S.L., Chen, H.C., and Huang, K.P. (1992). Phosphorylation of CCAAT-enhancer binding protein by protein kinase C attenuates site-selective DNA binding. J. Biol. Chem. *267*, 19396–19403.

Marcinkowska, E., Garay, E., Gocek, E., Chrobak, A., Wang, X., and Studzinski, G.P. (2006). Regulation of C/EBPβ isoforms by MAPK pathways in HL60 cells induced to differentiate by 1, 25-dihydroxyvitamin D 3. Experimental Cell Research *312*, 2054–2065.

Marston, A.L., and Amon, A. (2004). Meiosis: cell-cycle controls shuffle and deal. Nat Rev Mol Cell Biol *5*, 983–997.

Martin, A., Ochagavia, M.E., Rabasa, L.C., Miranda, J., Fernandez-de-Cossio, J., and Bringas, R. (2010). BisoGenet: a new tool for gene network building, visualization and analysis. BMC Bioinformatics *11*, 91.

Matsuoka, S., Ballif, B.A., Smogorzewska, A., McDonald, E.R., Hurov, K.E., Luo, J., Bakalarski, C.E., Zhao, Z., Solimini, N., Lerenthal, Y., et al. (2007). ATM and ATR substrate analysis reveals extensive protein networks

responsive to DNA damage. Science *316*, 1160–1166.

McKnight, S., and Tjian, R. (1986). Transcriptional selectivity of viral genes in mammalian cells. Cell *46*, 795–805.

Metzger, E., Wissmann, M., Yin, N., Müller, J.M., Schneider, R., Peters, A.H.F.M., Günther, T., Buettner, R., and Schüle, R. (2005). LSD1 demethylates repressive histone marks to promote androgen-receptor-dependent transcription. Nature *437*, 436–439.

Miau, L.H., Chang, C.J., Shen, B.J., Tsai, W.H., and Lee, S.C. (1998). Identification of heterogeneous nuclear ribonucleoprotein K (hnRNP K) as a repressor of C/EBPbeta-mediated gene activation. J. Biol. Chem. *273*, 10784–10791.

Miller, M. (2009). The importance of being flexible: the case of basic region leucine zipper transcriptional regulators. Curr Protein Pept Sci *10*, 244–269.

Miller, M., Shuman, J.D., Sebastian, T., Dauter, Z., and Johnson, P.F. (2003). Structural basis for DNA recognition by the basic region leucine zipper transcription factor CCAAT/enhancer-binding protein α. J. Biol. Chem. *278*, 15178–15184.

Mink, S., Mutschler, B., Weiskirchen, R., Bister, K., and Klempnauer, K.H. (1996). A novel function for Myc: inhibition of C/EBP-dependent gene activation. Proc. Natl. Acad. Sci. U.S.a. *93*, 6635–6640.

Mink, S., Haenig, B., and Klempnauer, K.-H. (1997). Interaction and functional collaboration of p300 and C/EBPbeta. Molecular and Cellular Biology *17*, 6609–6617.

Mo, X., Kowenz-Leutz, E., Xu, H., and Leutz, A. (2004). Ras induces mediator complex exchange on C/EBP beta. Molecular Cell *13*, 241–250.

Mohrmann, L., and Verrijzer, C.P. (2005). Composition and functional specificity of SWI2/SNF2 class chromatin remodeling complexes. Biochimica Et Biophysica Acta (BBA) - Gene Structure and Expression *1681*, 59–73.

Moldovan, G.-L., and D'Andrea, A.D. (2009). How the fanconi anemia pathway guards the genome. Annu. Rev. Genet. *43*, 223–249.

Morita, S., Kojima, T., and Kitamura, T. (2000). Plat-E: an efficient and stable system for transient packaging of retroviruses. Gene Ther *7*, 1063–1066.

Nakajima, T., Kinoshita, S., Sasagawa, T., Sasaki, K., Naruto, M., Kishimoto, T., and Akira, S. (1993). Phosphorylation at threonine-235 by a ras-dependent mitogen-activated protein kinase cascade is essential for transcription factor NF-IL6. Proc. Natl. Acad. Sci. U.S.a. *90*, 2207–2211.

Nakanishi, K., Yang, Y.-G., Pierce, A.J., Taniguchi, T., Digweed, M., D'Andrea, A.D., Wang, Z.-Q., and Jasin, M. (2005). Human Fanconi anemia monoubiquitination pathway promotes homologous DNA repair. Proc. Natl. Acad. Sci. U.S.a. *102*, 1110–1115.

Natsuka, S., Akira, S., Nishio, Y., Hashimoto, S., Sugita, T., Isshiki, H., and Kishimoto, T. (1992). Macrophage differentiation-specific expression of NF-IL6, a transcription factor for interleukin-6. Blood *79*, 460–466.

Nerlov, C. (2004). C/EBPα mutations in acute myeloid leukaemias. Nature Reviews Cancer *4*, 394–400.

Nerlov, C. (2007). The C/EBP family of transcription factors: a paradigm for interaction between gene expression and proliferation control. Trends in Cell Biology *17*, 318–324.

Nie, Z., Xue, Y., Yang, D., Zhou, S., Deroo, B.J., Archer, T.K., and Wang, W. (2000). A Specificity and Targeting Subunit of a Human SWI/SNF Family-Related Chromatin-Remodeling Complex. Molecular and Cellular Biology *20*, 8879–8888.

Nigg, E.A. (2001). Mitotic kinases as regulators of cell division and its checkpoints. Nat Rev Mol Cell Biol *2*, 21–32.

Noll, D.M., Mason, T.M., and Miller, P.S. (2006). Formation and repair of interstrand cross-links in DNA. Chemical Reviews *106*, 277–301.

Obuse, C., Yang, H., Nozaki, N., Goto, S., Okazaki, T., and Yoda, K. (2004). Proteomics analysis of the centromere complex from HeLa interphase cells: UV-damaged DNA binding protein 1 (DDB-1) is a component of the CEN-complex, while BMI-1 is transiently co-localized with the centromeric region in interphase. Genes to Cells *9*, 105–120.

Ogryzko, V.V., Kotani, T., Zhang, X., Schiltz, R.L., Howard, T., Yang, X.J., Howard, B.H., Qin, J., and Nakatani,

Y. (1998). Histone-like TAFs within the PCAF histone acetylase complex. Cell *94*, 35–44.

Ono, T., Fang, Y., Spector, D.L., and Hirano, T. (2004). Spatial and temporal regulation of Condensins I and II in mitotic chromosome assembly in human cells. Molecular Biology of the Cell *15*, 3296–3308.

Ono, T., Losada, A., Hirano, M., Myers, M.P., Neuwald, A.F., and Hirano, T. (2003). Differential contributions of condensin I and condensin II to mitotic chromosome architecture in vertebrate cells. Cell *115*, 109–121.

Orjalo, A.V., Arnaoutov, A., Shen, Z., Boyarchuk, Y., Zeitlin, S.G., Fontoura, B., Briggs, S., Dasso, M., and Forbes, D.J. (2006). The Nup107-160 nucleoporin complex is required for correct bipolar spindle assembly. Molecular Biology of the Cell *17*, 3806–3818.

Osada, S., Yamamoto, H., Nishihara, T., and Imagawa, M. (1996). DNA binding specificity of the CCAAT/enhancer-binding protein transcription factor family. J. Biol. Chem. *271*, 3891–3896.

Pabo, C.O., and Sauer, R.T. (1992). Transcription factors: structural families and principles of DNA recognition. Annu. Rev. Biochem. *61*, 1053–1095.

Pal, R., Janz, M., Galson, D.L., Gries, M., Li, S., Jöhrens, K., Anagnostopoulos, I., Dörken, B., Mapara, M.Y., Borghesi, L., et al. (2009). C/EBPbeta regulates transcription factors critical for proliferation and survival of multiple myeloma cells. Blood *114*, 3890–3898.

Pichierri, P., and Rosselli, F. (2004). The DNA crosslink-induced S-phase checkpoint depends on ATR-CHK1 and ATR-NBS1-FANCD2 pathways. Embo J *23*, 1178–1187.

Pichierri, P., Ammazzalorso, F., Bignami, M., and Franchitto, A. (2011). The Werner syndrome protein: linking the replication checkpoint response to genome stability. Aging (Albany NY) *3*, 311.

Piva, R., Agnelli, L., Pellegrino, E., Todoerti, K., Grosso, V., Tamagno, I., Fornari, A., Martinoglio, B., Medico, E., Zamò, A., et al. (2010). Gene expression profiling uncovers molecular classifiers for the recognition of anaplastic large-cell lymphoma within peripheral T-cell neoplasms. Journal of Clinical Oncology *28*, 1583–1590.

Piva, R., Pellegrino, E., Mattioli, M., Agnelli, L., Lombardi, L., Boccalatte, F., Costa, G., Ruggeri, B.A., Cheng, M., and Chiarle, R. (2006). Functional validation of the anaplastic lymphoma kinase signature identifies CEBPB and BCL2A1 as critical target genes. J. Clin. Invest. *116*, 3171–3182.

Piwien-Pilipuk, G., Van Mater, D., Ross, S.E., MacDougald, O.A., and Schwartz, J. (2001). Growth hormone regulates phosphorylation and function of CCAAT/enhancer-binding protein beta by modulating Akt and glycogen synthase kinase-3. J. Biol. Chem. *276*, 19664–19671.

Pless, O., Kowenz-Leutz, E., Dittmar, G., and Leutz, A. (2011). A differential proteome screening system for post-translational modification-dependent transcription factor interactions. Nature Protocols *6*, 359–364.

Podust, L.M., Krezel, A.M., and Kim, Y. (2001). Crystal structure of the CCAAT box/enhancer-binding protein beta activating transcription factor-4 basic leucine zipper heterodimer in the absence of DNA. J. Biol. Chem. *276*, 505–513.

Quintanilla-Martinez, L., Pittaluga, S., Miething, C., Klier, M., Rudelius, M., Davies-Hill, T., Anastasov, N., Martinez, A., Vivero, A., Duyster, J., et al. (2006). NPM-ALK-dependent expression of the transcription factor CCAAT/enhancer binding protein beta in ALK-positive anaplastic large cell lymphoma. Blood *108*, 2029–2036.

R Core Team (2013). R: A language and environment for statistical computing. R Foundation for Statistical Computing, Vienna, Austria. ISBN 3-900051-07-0, URL http://www.R-project.org/.

Ramji, D.P., and Foka, P. (2002). CCAAT/enhancer-binding proteins: structure, function and regulation. Biochem. J. *365*, 561–575.

Rappsilber, J., Mann, M., and Ishihama, Y. (2007). Protocol for micro-purification, enrichment, pre-fractionation and storage of peptides for proteomics using StageTips. Nature Protocols *2*, 1896–1906.

Rask, K., Thörn, M., Pontén, F., Kraaz, W., Sundfeldt, K., Hedin, L., and Enerbäck, S. (2000). Increased expression of the transcription factors CCAAT-enhancer binding protein-beta (C/EBBeta) and C/EBzeta (CHOP) correlate with invasiveness of human colorectal cancer. Int. J. Cancer *86*, 337–343.

Raymondjean, M., Cereghini, S., and Yaniv, M. (1988). Several distinct“ CCAAT” box binding proteins coexist in eukaryotic cells. Proc. Natl. Acad. Sci. U.S.a. *85*, 757–761.

Richter, N.J., Rogers, G.W., Hensold, J.O., and Merrick, W.C. (1999). Further biochemical and kinetic

characterization of human eukaryotic initiation factor 4H. J. Biol. Chem. *274*, 35415–35424.

Robinson, G.W., Johnson, P.F., Hennighausen, L., and Sterneck, E. (1998). The C/EBPβ transcription factor regulates epithelial cell proliferation and differentiation in the mammary gland. Genes & Development *12*, 1907–1916.

Rogers, G.W., Richter, N.J., Lima, W.F., and Merrick, W.C. (2001). Modulation of the helicase activity of eIF4A by eIF4B, eIF4H, and eIF4F. J. Biol. Chem. *276*, 30914–30922.

Rossi, M.L., Ghosh, A.K., and Bohr, V.A. (2010). Roles of Werner syndrome protein in protection of genome integrity. DNA Repair *9*, 331–344.

Rotili, D., and Mai, A. (2011). Targeting Histone Demethylases: A New Avenue for the Fight against Cancer. Genes & Cancer *2*, 663–679.

Ruepp, A., Brauner, B., Dunger-Kaltenbach, I., Frishman, G., Montrone, C., Stransky, M., Waegele, B., Schmidt, T., Doudieu, O.N., Stümpflen, V., et al. (2008). CORUM: the comprehensive resource of mammalian protein complexes. Nucleic Acids Research *36*, D646–D650.

Ruepp, A., Waegele, B., Lechner, M., Brauner, B., Dunger-Kaltenbach, I., Fobo, G., Frishman, G., Montrone, C., and Mewes, H.W. (2010). CORUM: the comprehensive resource of mammalian protein complexes--2009. Nucleic Acids Research *38*, D497–D501.

Ryden, T.A., and Beemon, K. (1989). Avian retroviral long terminal repeats bind CCAAT/enhancer-binding protein. Molecular and Cellular Biology *9*, 1155–1164.

Ryme, J., Asp, P., Böhm, S., Cavellán, E., and Farrants, A.-K.Ö. (2009). Variations in the composition of mammalian SWI/SNF chromatin remodelling complexes. J. Cell. Biochem. *108*, 565–576.

Salina, D., Enarson, P., Rattner, J.B., and Burke, B. (2003). Nup358 integrates nuclear envelope breakdown with kinetochore assembly. J Cell Biol *162*, 991–1001.

Sato, S., Tomomori-Sato, C., Parmely, T.J., Florens, L., Zybailov, B., Swanson, S.K., Banks, C.A.S., Jin, J., Cai, Y., Washburn, M.P., et al. (2004). A set of consensus mammalian mediator subunits identified by multidimensional protein identification technology. Molecular Cell *14*, 685–691.

Scaërou, F., Starr, D.A., Piano, F., Papoulas, O., Karess, R.E., and Goldberg, M.L. (2001). The ZW10 and Rough Deal checkpoint proteins function together in a large, evolutionarily conserved complex targeted to the kinetochore. Journal of Cell Science *114*, 3103–3114.

Schaefer, M.H., Fontaine, J.-F., Vinayagam, A., Porras, P., Wanker, E.E., and Andrade-Navarro, M.A. (2011). HIPPIE: Integrating protein interaction networks with experiment based quality scores. PLoS ONE *7*, e31826–e31826.

Schmiesing, J.A., Gregson, H.C., Zhou, S., and Yokomori, K. (2000). A human condensin complex containing hCAP-C–hCAP-E and CNAP1, a homolog of Xenopus XCAP-D2, colocalizes with phosphorylated histone H3 during the early stage of mitotic chromosome condensation. Molecular and Cellular Biology *20*, 6996–7006.

Schreiber, E., Matthias, P., Müller, M.M., and Schaffner, W. (1989). Rapid detection of octamer binding proteins with "mini extracts," prepared from a small number of cells. Nucleic Acids Research *17*, 6419–6419.

Schultz, D.C., Friedman, J.R., and Rauscher, F.J. (2001). Targeting histone deacetylase complexes via KRAB-zinc finger proteins: the PHD and bromodomains of KAP-1 form a cooperative unit that recruits a novel isoform of the Mi-2α subunit of NuRD. Genes & Development *15*, 428–443.

Schwanhäusser, B., Busse, D., Li, N., Dittmar, G., Schuchhardt, J., Wolf, J., Chen, W., and Selbach, M. (2011). Global analysis of cellular protein translation by pulsed SILAC. Nature *473*, 337–342.

Screpanti, I., Romani, L., Musiani, P., Modesti, A., Fattori, E., Lazzaro, D., Sellitto, C., Scarpa, S., Bellavia, D., and Lattanzio, G. (1995). Lymphoproliferative disorder and imbalanced T-helper response in C/EBP beta-deficient mice. The EMBO Journal *14*, 1932–1941.

Seagroves, T.N., Krnacik, S., Raught, B., Gay, J., Burgess-Beusse, B., Darlington, G.J., and Rosen, J.M. (1998). C/EBPbeta, but not C/EBPalpha, is essential for ductal morphogenesis, lobuloalveolar proliferation, and functional differentiation in the mouse mammary gland. Genes & Development *12*, 1917–1928.

Shannon, P., Markiel, A., Ozier, O., Baliga, N.S., Wang, J.T., Ramage, D., Amin, N., Schwikowski, B., and Ideker, T. (2003). Cytoscape: a software environment for integrated models of biomolecular interaction networks.

Genome Research *13*, 2498–2504.

Shi, Y.-J., Matson, C., Lan, F., Iwase, S., Baba, T., and Shi, Y. (2005). Regulation of LSD1 Histone Demethylase Activity by Its Associated Factors. Molecular Cell *19*, 857–864.

Shiekhattar, R., Mermelstein, F., Fisher, R.P., Drapkin, R., Dynlacht, B., Wessling, H.C., Morgan, D.O., and Reinberg, D. (1995). Cdk-activating kinase complex is a component of human transcription factor TFIIH. Nature *374*, 283–287.

Shuman, J.D., Cheong, J., and Coligan, J.E. (1997). ATF-2 and C/EBPalpha can form a heterodimeric DNA binding complex in vitro. Functional implications for transcriptional regulation. J. Biol. Chem. *272*, 12793–12800.

Shuman, J.D., Sebastian, T., Kaldis, P., Copeland, T.D., Zhu, S., Smart, R.C., and Johnson, P.F. (2004). Cell Cycle-Dependent Phosphorylation of C/EBP Mediates Oncogenic Cooperativity between C/EBP and H-RasV12. Molecular and Cellular Biology *24*, 7380–7391.

Siersbæk, R., Baek, S., Rabiee, A., Nielsen, R., Traynor, S., Clark, N., Sandelin, A., Jensen, O.N., Sung, M.-H., Hager, G.L., et al. (2014). Molecular architecture of transcription factor hotspots in early adipogenesis. CellReports *7*, 1434–1442.

Singleton, M.R., and Wigley, D.B. (2002). Modularity and specialization in superfamily 1 and 2 helicases. J. Bacteriol. *184*, 1819–1826.

Smink, J.J., and Leutz, A. (2010). Rapamycin and the transcription factor C/EBPbeta as a switch in osteoclast differentiation: implications for lytic bone diseases. J Mol Med (Berl) *88*, 227–233.

Smink, J.J., Bégay, V., Schoenmaker, T., Sterneck, E., de Vries, T.J., and Leutz, A. (2009). Transcription factor C/EBPbeta isoform ratio regulates osteoclastogenesis through MafB. The EMBO Journal *28*, 1769–1781.

Sood, V., and Brickner, J.H. (2014). Nuclear pore interactions with the genome. Current Opinion in Genetics & Development *25C*, 43–49.

Steinberg, X., Hepp, M.I., Fernández García, Y., Suganuma, T., Swanson, S.K., Washburn, M., Workman, J.L., and Gutiérrez, J.L. (2012). Human CCAAT/enhancer-binding protein β interacts with chromatin remodeling complexes of the imitation switch subfamily. Biochemistry *51*, 952–962.

Sterneck, E., Tessarollo, L., and Johnson, P.F. (1997). An essential role for C/EBPβ in female reproduction. Genes & Development *11*, 2153–2162.

Stoilova, B., Kowenz-Leutz, E., Scheller, M., and Leutz, A. (2013). Lymphoid to myeloid cell trans-differentiation is determined by C/EBPβ structure and post-translational modifications. PLoS ONE *8*, e65169.

Strahl, B.D., and Allis, C.D. (2000). The language of covalent histone modifications. Nature *403*, 41–45.

Studzinski, G.P., Brown, G., Danilenko, M., Hughes, P., and Marcinkowska, E. (2012). Differentiation and cell survival of myeloid leukemia cells. Leuk Res Treatment *2012*, 370375.

Studzinski, G.P., Wang, X., Ji, Y., Wang, Q., Zhang, Y., Kutner, A., and Harrison, J.S. (2005). The rationale for deltanoids in therapy for myeloid leukemia: Role of KSR–MAPK–C/EBP pathway. The Journal of Steroid Biochemistry and Molecular Biology *97*, 47–55.

Sudakin, V., Chan, G.K., and Yen, T.J. (2001). Checkpoint inhibition of the APC/C in HeLa cells is mediated by a complex of BUBR1, BUB3, CDC20, and MAD2. The Journal of Cell Biology *154*, 925–936.

Sundström, C., and Nilsson, K. (1976). Establishment and characterization of a human histiocytic lymphoma cell line (U-937). Int. J. Cancer *17*, 565–577.

Sury, M.D., McShane, E., Hernandez-Miranda, L.R., Birchmeier, C., and Selbach, M. (2015). Quantitative Proteomics Reveals Dynamic Interaction of c-Jun N-terminal Kinase (JNK) with RNA Transport Granule Proteins Splicing Factor Proline- and Glutamine-rich (Sfpq) and Non-POU Domain-containing Octamer-binding Protein (Nono) during Neuronal Differentiation. Molecular & Cellular Proteomics *14*, 50–65.

Tae, H.J., Zhang, S., and Kim, K.H. (1995). cAMP activation of CAAT enhancer-binding protein-beta gene expression and promoter I of acetyl-CoA carboxylase. J. Biol. Chem. *270*, 21487–21494.

Tanaka, T., Akira, S., Yoshida, K., Umemoto, M., Yoneda, Y., Shirafuji, N., Fujiwara, H., Suematsu, S., Yoshida, N., and Kishimoto, T. (1995). Targeted disruption of the NF-IL6 gene discloses its essential role in bacteria killing

and tumor cytotoxicity by macrophages. Cell *80*, 353–361.

Tang, L., Nogales, E., and Ciferri, C. (2010). Structure and function of SWI/SNF chromatin remodeling complexes and mechanistic implications for transcription. Progress in Biophysics and Molecular Biology *102*, 122–128.

Tang, Q.Q., and Lane, M.D. (1999). Activation and centromeric localization of CCAAT/enhancer-binding proteins during the mitotic clonal expansion of adipocyte differentiation. Genes & Development *13*, 2231–2241.

Tang, Q.-Q., Otto, T.C., and Lane, M.D. (2003). CCAAT/enhancer-binding protein beta is required for mitotic clonal expansion during adipogenesis. Proc. Natl. Acad. Sci. U.S.a. *100*, 850–855.

Tang, Z., Bharadwaj, R., Li, B., and Yu, H. (2001). Mad2-Independent Inhibition of APC Cdc20 by the Mitotic Checkpoint Protein BubR1. Developmental Cell *1*, 227–237.

Tang, Z., Shu, H., Oncel, D., Chen, S., and Yu, H. (2004). Phosphorylation of Cdc20 by Bub1 provides a catalytic mechanism for APC/C inhibition by the spindle checkpoint. Molecular Cell *16*, 387–397.

Tominaga, H., Maeda, S., Hayashi, M., Takeda, S., Akira, S., Komiya, S., Nakamura, T., Akiyama, H., and Imamura, T. (2008). CCAAT/enhancer-binding protein beta promotes osteoblast differentiation by enhancing Runx2 activity with ATF4. Molecular Biology of the Cell *19*, 5373–5386.

Trautwein, C., van der Geer, P., Karin, M., Hunter, T., and Chojkier, M. (1994). Protein kinase A and C site-specific phosphorylations of LAP (NF-IL6) modulate its binding affinity to DNA recognition elements. J. Clin. Invest. *93*, 2554–2561.

Trautwein, C., Caelles, C., van der Geer, P., Hunter, T., Karin, M., and Chojkier, M. (1993). Transactivation by NF-IL6/LAP is enhanced by phosphorylation of its activation domain. Nature *364*, 544–547.

Tsukada, J., Saito, K., Waterman, W.R., Webb, A.C., and Auron, P.E. (1994). Transcription factors NF-IL6 and CREB recognize a common essential site in the human prointerleukin 1 beta gene. Molecular and Cellular Biology *14*, 7285–7297.

Tsukada, J., Yoshida, Y., Kominato, Y., and Auron, P.E. (2011). The CCAAT/enhancer (C/EBP) family of basic-leucine zipper (bZIP) transcription factors is a multifaceted highly-regulated system for gene regulation. Cytokine *54*, 6–19.

Turner, B.M. (2000). Histone acetylation and an epigenetic code. Bioessays *22*, 836–845.

Uematsu, S., Kaisho, T., Tanaka, T., Matsumoto, M., Yamakami, M., Omori, H., Yamamoto, M., Yoshimori, T., and Akira, S. (2007). The C/EBP beta isoform 34-kDa LAP is responsible for NF-IL-6-mediated gene induction in activated macrophages, but is not essential for intracellular bacteria killing. J Immunol *179*, 5378–5386.

Underhill, C., Qutob, M.S., Yee, S.P., and Torchia, J. (2000). A novel nuclear receptor corepressor complex, N-CoR, contains components of the mammalian SWI/SNF complex and the corepressor KAP-1. J. Biol. Chem. *275*, 40463–40470.

UniProt Consortium (2013). Activities at the Universal Protein Resource (UniProt). Nucleic Acids Research *42*, D191–D198.

Vallejo, M., Ron, D., Miller, C.P., and Habener, J.F. (1993). C/ATF, a member of the activating transcription factor family of DNA-binding proteins, dimerizes with CAAT/enhancer-binding proteins and directs their binding to cAMP response elements. Proc. Natl. Acad. Sci. U.S.a. *90*, 4679–4683.

van de Vijver, M.J., He, Y.D., van 't Veer, L.J., Dai, H., Hart, A.A.M., Voskuil, D.W., Schreiber, G.J., Peterse, J.L., Roberts, C., Marton, M.J., et al. (2002). A Gene-Expression Signature as a Predictor of Survival in Breast Cancer. N Engl J Med *347*, 1999–2009.

Vassilev, A.A., Yamauchi, J.J., Kotani, T.T., Prives, C.C., Avantaggiati, M.L.M., Qin, J.J., and Nakatani, Y.Y. (1998). The 400 kDa subunit of the PCAF histone acetylase complex belongs to the ATM superfamily. Molecular Cell *2*, 869–875.

Vinson, C.R., Hai, T., and Boyd, S.M. (1993). Dimerization specificity of the leucine zipper-containing bZIP motif on DNA binding: prediction and rational design. Genes & Development *7*, 1047–1058.

Vradii, D., Wagner, S., Doan, D.N., Nickerson, J.A., Montecino, M., Lian, J.B., Stein, J.L., van Wijnen, A.J., Imbalzano, A.N., and Stein, G.S. (2005). Brg1, the ATPase subunit of the SWI/SNF chromatin remodeling complex, is required for myeloid differentiation to granulocytes. J. Cell. Physiol. *206*, 112–118.

Wang, J., Sarkar, T.R., Zhou, M., Sharan, S., Ritt, D.A., Veenstra, T.D., Morrison, D.K., Huang, A.-M., and Sterneck, E. (2010). CCAAT/enhancer binding protein delta (C/EBPdelta, CEBPD)-mediated nuclear import of FANCD2 by IPO4 augments cellular response to DNA damage. Proceedings of the National Academy of Sciences *107*, 16131–16136.

Westhorpe, F.G., and Straight, A.F. (2013). Functions of the centromere and kinetochore in chromosome segregation. Current Opinion in Cell Biology *25*, 334–340.

Wethmar, K., Begay, V., Smink, J.J., Zaragoza, K., Wiesenthal, V., Dorken, B., Calkhoven, C.F., and Leutz, A. (2010). C/EBP uORF mice--a genetic model for uORF-mediated translational control in mammals. Genes & Development *24*, 15–20.

Williams, B.C., Li, Z., Liu, S., Williams, E.V., Leung, G., Yen, T.J., and Goldberg, M.L. (2003). Zwilch, a new component of the ZW10/ROD complex required for kinetochore functions. Molecular Biology of the Cell *14*, 1379–1391.

Williams, D.A., Tao, W., Yang, F., Kim, C., Gu, Y., Mansfield, P., Levine, J.E., Petryniak, B., Derrow, C.W., Harris, C., et al. (2000). Dominant negative mutation of the hematopoietic-specific Rho GTPase, Rac2, is associated with a human phagocyte immunodeficiency. Blood *96*, 1646–1654.

Williams, S.C., Baer, M., Dillner, A.J., and Johnson, P.F. (1995). CRP2 (C/EBP beta) contains a bipartite regulatory domain that controls transcriptional activation, DNA binding and cell specificity. The EMBO Journal *14*, 3170.

Wisniewski, J.R., Zougman, A., and Mann, M. (2009). Combination of FASP and StageTip-based fractionation allows in-depth analysis of the hippocampal membrane proteome. J. Proteome Res. *8*, 5674–5678.

Xia, C., Cheshire, J.K., Patel, H., and Woo, P. (1997). Cross-talk between transcription factors NF-kappa B and C/EBP in the transcriptional regulation of genes. Int J Biochem Cell Biol *29*, 1525–1539.

Xie, H., Ye, M., Feng, R., and Graf, T. (2003). Stepwise Reprogramming of B Cells into Macrophages. Cell *117*, 663–676.

Xiong, W., Hsieh, C.C., Kurtz, A.J., Rabek, J.P., and Papaconstantinou, J. (2001). Regulation of CCAAT/enhancer-binding protein-beta isoform synthesis by alternative translational initiation at multiple AUG start sites. Nucleic Acids Research *29*, 3087–3098.

Yamada, K., Duong, D.T., Scott, D.K., Wang, J.C., and Granner, D.K. (1999). CCAAT/Enhancer-binding Protein Is an Accessory Factor for the Glucocorticoid Response from the cAMP Response Element in the Rat Phosphoenolpyruvate Carboxykinase Gene Promoter. Journal of Biological Chemistry *274*, 5880–5887.

Yamaguchi, Y., Nishio, H., Kishi, K., Ackerman, S.J., and Suda, T. (1999). C/EBPbeta and GATA-1 synergistically regulate activity of the eosinophil granule major basic protein promoter: implication for C/EBPbeta activity in eosinophil gene expression. Blood *94*, 1429–1439.

Yang, M., Gocke, C.B., Luo, X., Borek, D., Tomchick, D.R., Machius, M., Otwinowski, Z., and Yu, H. (2006). Structural Basis for CoREST-Dependent Demethylation of Nucleosomes by the Human LSD1 Histone Demethylase. Molecular Cell *23*, 377–387.

Zahnow, C.A., Cardiff, R.D., Laucirica, R., Medina, D., and Rosen, J.M. (2001). A role for CCAAT/enhancer binding protein beta-liver-enriched inhibitory protein in mammary epithelial cell proliferation. Cancer Research *61*, 261–269.

Zahnow, C.A. (2009). CCAAT/enhancer-binding protein beta: its role in breast cancer and associations with receptor tyrosine kinases. Expert Rev Mol Med *11*, e12.

Zhang, X., Liu, D., Lv, S., Wang, H., Zhong, X., Liu, B., Wang, B., Liao, J., Li, J., and Pfeifer, G.P. (2009). CDK5RAP2 is required for spindle checkpoint function. Cc *8*, 1206–1216.

Zhou, Z., Licklider, L.J., Gygi, S.P., and Reed, R. (2002). Comprehensive proteomic analysis of the human spliceosome. Nature *419*, 182–185.

Zhu, S., Yoon, K., Sterneck, E., Johnson, P.F., and Smart, R.C. (2002). CCAAT/enhancer binding protein-beta is a mediator of keratinocyte survival and skin tumorigenesis involving oncogenic Ras signaling. Proc. Natl. Acad. Sci. U.S.a. *99*, 207–212.

Zuccolo, M., Alves, A., Galy, V., Bolhy, S., Formstecher, E., Racine, V., Sibarita, J.B., Fukagawa, T., Shiekhattar,

R., and Yen, T. (2007). The human Nup107–160 nuclear pore subcomplex contributes to proper kinetochore functions. The EMBO Journal *26*, 1853–1864.

Zwergal, A., Quirling, M., Saugel, B., Huth, K.C., Sydlik, C., Poli, V., Neumeier, D., Ziegler-Heitbrock, H.W.L., and Brand, K. (2006). C/EBP beta blocks p65 phosphorylation and thereby NF-kappa B-mediated transcription in TNF-tolerant cells. J Immunol *177*, 665–672.

ABBREVIATIONS

aa	amino acid
ala/A	Alanine
ALCL	Anaplastic large cell lymphoma
AML	Acute myeloid leukemia
APS	array peptide screening
arg/R	Arginine
bZIP	basic leucine zipper domain
cAMP	cyclic adenosine monophosphate
C/EBP	CCAAT/enhancer-binding protein
C2H2	protein domain, Cys2-His2
CR	conserved region
Cys/C	Cysteine
DBD	DNA binding domain
ddH_2O	double deionized water
DDR	DNA damage response
DEAD	symbolizing amino acid sequence asp-glu-ala-asp
DEAH	symbolizing amino acid sequence asp-glu-ala-his
DMEM	Dulbecco's modified Eagle's medium
DNA	desoxyribonucleic acid
DSB	double strand break
EDTA	ethylenediaminetetraacetic acid
EGTA	ethylene glycol tetraacetic acid
FCS	Fetal Bovine Serum

g	gram
GO:term	gene ontology term
H3	histone H3
H4	histone H4
HAT	histone acetyltransferase
HDAC	histone deacetylase
iBAQ	Intensity-Based Absolute Quantification
ICL	(DNA) interstrand cross-links
IP	immunoprecipitation
IP-MS	immunoprecipitation followed by mass spectrometry analysis
IR	ionizing radiation
l	liter
LCR	low complexity region
LIM	protein domain named after proteins Lin11, Isl-1 and Mec-3
lys/K	Lysine
M	molar
µ	micro
MCC	mitotic checkpoint complex
me	methylation
Min	minute
MEF	mouse embryonic fibroblasts
MIEG	MSCV-IRES-EGFP retroviral vector
MM	Multiple myeloma
MSCV	Murine Stem Cell Virus
MS	mass spectrometry
NEB	nuclear envelope breakdown
NE(L)	nuclear enriched lysates

NHEJ	non-homologous end joining
PBS	phosphate buffered saline
pH	potentia Hydrogenii
PMA	phorbol 12-myristate 13-acetate
PMSF	Phenylmethylsulfonylfluorid
PTM	posttranslational modification
RBD	RNA binding domain
RD	regulatory domain
RNA	ribonucleic acid
RRM	RNA recognition motif
r.p.m.	revolutions per minute
RPMI	Roswell Park Memorial Institute
RT	room temperature (25 ℃)
SAC	spindle assembly checkpoint
SDS	Sodium dodecyl sulfate
sec	second
ser/S	Serine
SRM	selected reaction monitoring
SUMO	small ubiquitin-like modifier
TAD	transactivation domain
TF	transcription factor
thr/T	Threonine
TPA	12-O-Tetradecanoylphorbol-13-acetate
Tris	tris(hydroxymethyl)aminomethane

List of Figures

SUPPLEMENT

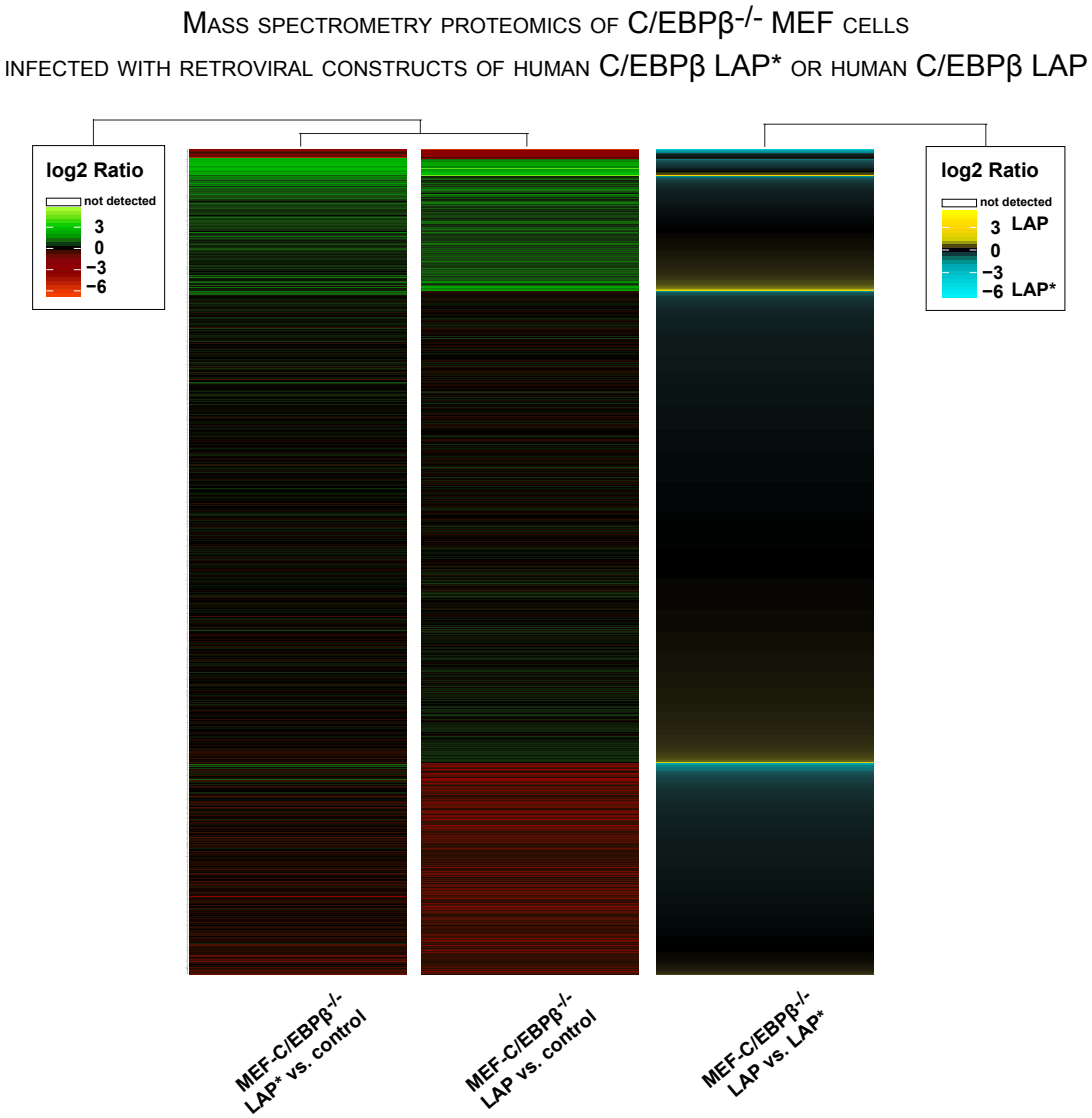

Supplemental Figure S1: Caption vide next page.

Supplemental Figure S1: The heatmap on page 123 depicts all proteins detected in the proteomics experiment with C/EBPβ$^{-/-}$ MEF cells infected with the retroviral vectors carrying either C/EBPβ LAP*, LAP or a control vector. The first two columns of the heatmap show the Log2 fold change of the detected proteins (MS analysis by Günther Kahlert, MDC) from the cells infected with C/EBPβ ("LAP*" and "LAP") constructs versus cells infected with the control construct ("control"). Signals with a Log2 fold change ≥ 1 or ≤ -1 were considered as significant. Proteins that were detected with a significant Log2 fold change of ≤ -1 after C/EBPβ infection compared to the control vector are depicted with a red scale. Proteins detected with a Log2 fold change of ≥ 1 after C/EBPβ infection compared to the control vector are depicted with a green scale. Protein signals with an insignificant Log2 fold change are depicted with a grey scale. The third column of the heatmap depicts the Log2 fold change of the cells infected with the C/EBPβ LAP isoform ("LAP") versus the cells infected with the LAP* isoform ("LAP*"). Proteins that were detected with a significant log2 fold change of ≥ 1 after LAP infection compared to the LAP* isoform are depicted with a yellow scale. Proteins detected with a Log2 fold change of ≤ -1) after LAP* infection are depicted with a blue scale. Protein signals with an insignificant Log2 fold change are depicted with a grey scale.

Supplemental Table S1: The table on the following pages (pages 125-137) itemizes the protein-interactions of C/EBPβ that were detected in the analyzed leukemia cell lines by IP-MS and by APS as well as the log10 of iBAQ intensity from iBAQ quantification of SU-DHL-1 cells (column 3). Immunoprecipitations of endogenous C/EBPβ (with an anti-C/EBPβ antibody) from whole cell lysates of U937, JEKO-1, HL60 and SU-DHL-1 and from nuclear enriched lysates of OPM2 and SU-DHL-1 cells (column 7-12) were prepared as triplicates and were analyzed by shotgun mass spectrometry (Günther Kahlert, MDC) using a label-free quantification approach (Hubner and Mann, 2011; vide material and methods section). The APS was performed by hybridization of C/EBPβ peptides covering the conserved regions of C/EBPβ and ε (CR1-7; comprising the transactivation domain (TAD) and regulatory domain (RD), but not the basic zipper domain (bZIP)) to UniPEx-peptide macroarrays (column 13-17) . Peptides of murine C/EBPβ TAD (CR1-2, aa1-41), (CR3, aa49-72), and murine C/EBPβ RD (N-terminal part of CR7, aa153-173), (mixture of CR4-5, aa79-111; CR 6-7, aa128-172; CR 7 aa152-196), and murine C/EBPε TAD (CR2-4, aa1-61) were used for APS (vide Material and methods section).

						IP-MS						APS				
UniProt AC	RefSeq ID UniPEx-library	SU-DHL-1 iBAQ [log10 of iBAQ intensity]	Name	Synonyms		HL60 [whole cell lysate]	JEKO-1 [whole cell lysate]	OPM2 [nuclear enriched lysate]	U937 [whole cell lysate]	SU-DHL-1 [whole cell lysate]	SU-DHL-1 [nuclear enriched lysate]	C/EBPβ aa1-41 [CR1-2]	C/EBPε aa1-62 [CR2-4]	C/EBPβ aa49-72 [CR3]	C/EBPβ aa153-173 [CR7]	C/EBPβ aa79-196 [CR4-7]
P17676	-	7.5900	CEBPB	TCF5	-	Co-IP	Co-IP	Co-IP	Co-IP	Co-IP	Co-IP	0	0	0	0	0
Q9H0C8	-	7.1884	ILKAP	-	-	Co-IP	Co-IP	Co-IP	Co-IP	Co-IP	Co-IP	0	0	0	0	0
O14980	-	8.0217	XPO1	CRM1	-	0	Co-IP	Co-IP	Co-IP	Co-IP	Co-IP	0	0	0	0	0
P13010	-	8.6857	XRCC5	G22P2	-	0	Co-IP	Co-IP	0	Co-IP	Co-IP	0	0	0	0	0
Q92733	-	6.8760	PRCC	TPRC	-	0	0	Co-IP	0	Co-IP	Co-IP	0	0	0	0	0
P26641	-	8.6992	EF1G	EEF1G	-	Co-IP	Co-IP	0	0	Co-IP	Co-IP	0	0	0	0	0
E9PRY8	-	8.1325	E9PRY8	EEF1D	-	0	Co-IP	0	0	Co-IP	Co-IP	0	0	0	0	0
P12956	-	8.8269	XRCC6	G22P1	-	0	Co-IP	0	0	Co-IP	Co-IP	0	0	0	0	0
P78527	-	8.0827	PRKDC	HYRC	-	0	Co-IP	0	0	Co-IP	Co-IP	0	0	0	0	0
O43175	-	8.2946	SERA	PHGDH	PGDH3	0	0	0	0	Co-IP	Co-IP	0	0	0	0	0
P27708	-	7.8531	PYR1	CAD	-	0	0	0	0	Co-IP	Co-IP	0	0	0	0	0
P30153	-	8.0529	2AAA	PPP2R1A	-	0	0	0	0	Co-IP	Co-IP	0	0	0	0	0
P32189	-	7.9368	GLPK	GK	-	0	0	0	0	Co-IP	Co-IP	0	0	0	0	0
P35232	-	8.8204	PHB	-	-	0	0	0	0	Co-IP	Co-IP	0	0	0	0	0
P40763	-	7.9850	STAT3	APRF	-	0	0	0	0	Co-IP	Co-IP	0	0	0	0	0
P42285	-	7.3458	SK2L2	SKIV2L2	KIAA0052	0	0	0	0	Co-IP	Co-IP	0	0	0	0	0
P42704	-	8.1207	LPPRC	LRPPRC	LRP130	0	0	0	0	Co-IP	Co-IP	0	0	0	0	0
P50991	-	8.5139	TCPD	CCT4	CCTD	0	0	0	0	Co-IP	Co-IP	0	0	0	0	0
Q00610	-	8.2996	CLH1	CLTC	CLH17	0	0	0	0	Co-IP	Co-IP	0	0	0	0	0
Q9Y5B9	-	7.9425	SP16H	SUPT16H	FACT140	0	0	0	0	Co-IP	Co-IP	0	0	0	0	0
P11388	-	7.8618	TOP2A	TOP2	-	0	0	0	Co-IP	0	Co-IP	0	0	0	0	0
P35659	-	8.1838	DEK	-	-	0	0	0	Co-IP	0	Co-IP	0	0	0	0	0
O43823	-	6.9873	AKAP8	AKAP95	-	0	Co-IP	Co-IP	0	0	Co-IP	0	0	0	0	0
P0C0L5	-	-	CO4B	-	-	0	Co-IP	Co-IP	0	0	Co-IP	0	0	0	0	0
Q7LBC6	-	6.6277	KDM3B	JMJD1B	-	0	Co-IP	Co-IP	0	0	Co-IP	0	0	0	0	0
P19338	-	8.8166	NUCL	NCL	-	0	0	Co-IP	0	0	Co-IP	0	0	0	0	0
P42166	-	7.9299	LAP2A	TMPO	LAP2	0	0	Co-IP	0	0	Co-IP	0	0	0	0	0
P49792	-	6.8798	RBP2	RANBP2	NUP358	0	0	Co-IP	0	0	Co-IP	0	0	0	0	0
Q9UKX7	-	7.0178	NUP50	NPAP60L	-	0	0	Co-IP	0	0	Co-IP	0	0	0	0	0
O00299	-	8.8855	CLIC1	-	G6	0	Co-IP	0	0	0	Co-IP	0	0	0	0	0
P12268	-	8.6713	IMDH2	IMPDH2	IMPD2	0	Co-IP	0	0	0	Co-IP	0	0	0	0	0
P22102	-	8.1383	PUR2	GART	PGFT	0	Co-IP	0	0	0	Co-IP	0	0	0	0	0
P62195	-	8.1190	PRS8	PSMC5	SUG1	0	Co-IP	0	0	0	Co-IP	0	0	0	0	0
Q13200	-	8.0567	PSMD2	TRAP2	-	0	Co-IP	0	0	0	Co-IP	0	0	0	0	0
O95347	-	7.5986	SMC2	CAPE	-	Co-IP	0	0	0	0	Co-IP	0	0	0	0	0
Q9UJZ1	-	8.3277	STML2	STOML2	SLP2	Co-IP	0	0	0	0	Co-IP	0	0	0	0	0
Q9H6Z4	-	7.3333	RANB3	RANBP3	-	Co-IP	Co-IP	Co-IP	Co-IP	Co-IP	0	0	0	0	0	0
P62244	-	8.9113	RS15A	RPS15A	-	Co-IP	0	0	Co-IP	Co-IP	0	0	0	0	0	0
Q9H8S9	-	7.4340	MOB1A	C2orf6	-	Co-IP	0	0	Co-IP	Co-IP	0	0	0	0	0	0
P80303	-	7.4130	NUCB2	NEFA	-	Co-IP	Co-IP	0	0	Co-IP	0	0	0	0	0	0
Q9BUL8	-	7.5315	PDC10	PDCD10	CCM3	Co-IP	Co-IP	0	0	Co-IP	0	0	0	0	0	0
Q9NSP4	-	-	CENPM	C22orf18	-	Co-IP	Co-IP	0	0	Co-IP	0	0	0	0	0	0
P11172	-	7.5503	UMPS	-	-	Co-IP	0	0	0	Co-IP	0	0	0	0	0	0
P19474	-	-	RO52	TRIM21	RNF81	Co-IP	0	0	0	Co-IP	0	0	0	0	0	0
P55060	-	8.2769	XPO2	CSE1L	CAS	Co-IP	0	0	0	Co-IP	0	0	0	0	0	0
Q8TCG1	-	6.5320	CIP2A	KIAA1524	-	Co-IP	0	0	0	Co-IP	0	0	0	0	0	0
Q99623	-	8.6230	PHB2	BAP	-	Co-IP	0	0	0	Co-IP	0	0	0	0	0	0
Q9Y4R8	-	6.3775	TELO2	KIAA0683	-	Co-IP	0	0	0	Co-IP	0	0	0	0	0	0
B4DLZ8	-	-	B4DLZ8	-	-	Co-IP	0	0	Co-IP	0	0	0	0	0	0	0
Q8N392	-	-	RHG18	-	-	Co-IP	0	0	Co-IP	0	0	0	0	0	0	0
Q96AX1	-	5.0024	VP33A	VPS33A	-	Co-IP	0	0	Co-IP	0	0	0	0	0	0	0
Q9UK61	-	5.9612	F208A	FAM208A	C3orf63	Co-IP	0	0	Co-IP	0	0	0	0	0	0	0
P62805	-	10.1851	H4	HIST1H4A	H4/A	Co-IP	0	Co-IP	0	0	0	0	0	0	0	0
B8ZZN6	-	7.8841	B8ZZN6	SUMO1	-	Co-IP	Co-IP	0	0	0	0	0	0	0	0	0
Q96N11	-	5.6972	CG026	C7orf26	-	Co-IP	Co-IP	0	0	0	0	0	0	0	0	0
Q9H9Q4	-	5.9103	NHEJ1	XLF	-	0	Co-IP	0	Co-IP	Co-IP	0	0	0	0	0	0
B7Z5E3	-	-	B7Z5E3	-	-	0	Co-IP	0	0	Co-IP	0	0	0	0	0	0
D3DUS9	-	-	D3DUS9	DNM1L	-	0	Co-IP	0	0	Co-IP	0	0	0	0	0	0
O60711	-	6.7463	LPXN	LDLP	-	0	Co-IP	0	0	Co-IP	0	0	0	0	0	0
O95684	-	7.1031	FR1OP	FOP	-	0	Co-IP	0	0	Co-IP	0	0	0	0	0	0
P04406	-	9.5663	G3P	GAPDH	GAPD	0	Co-IP	0	0	Co-IP	0	0	0	0	0	0
P07737	-	9.1337	PROF1	PFN1	-	0	Co-IP	0	0	Co-IP	0	0	0	0	0	0
P24534	-	8.2158	EF1B	EEF1B2	EEF1B	0	Co-IP	0	0	Co-IP	0	0	0	0	0	0
P41250	-	8.3967	SYG	GARS	-	0	Co-IP	0	0	Co-IP	0	0	0	0	0	0
P49720	-	8.5113	PSB3	PSMB3	-	0	Co-IP	0	0	Co-IP	0	0	0	0	0	0
P62306	-	8.7701	RUXF	SNRPF	PBSCF	0	Co-IP	0	0	Co-IP	0	0	0	0	0	0
P62937	-	9.3061	PPIA	CYPA	-	0	Co-IP	0	0	Co-IP	0	0	0	0	0	0
Q86UY3	-	-	Q86UY3	-	-	0	Co-IP	0	0	Co-IP	0	0	0	0	0	0
Q96JB2	-	6.1842	COG3	SEC34	-	0	Co-IP	0	0	Co-IP	0	0	0	0	0	0
Q9UBT2	-	7.9537	SAE2	UBA2	-	0	Co-IP	0	0	Co-IP	0	0	0	0	0	0
Q9UQ13	-	5.8638	SHOC2	KIAA0862	-	0	Co-IP	0	0	Co-IP	0	0	0	0	0	0
A6NHB5	-	5.0052	A6NHB5	-	-	0	Co-IP	0	Co-IP	0	0	0	0	0	0	0
B5M451	-	-	B5M451	-	-	0	Co-IP	0	Co-IP	0	0	0	0	0	0	0
D3DPG0	-	-	D3DPG0	-	-	0	Co-IP	0	Co-IP	0	0	0	0	0	0	0
P42694	-	-	HELZ	-	-	0	Co-IP	0	Co-IP	0	0	0	0	0	0	0
P53990	-	6.7855	IST1	-	-	0	Co-IP	0	Co-IP	0	0	0	0	0	0	0
Q5JTZ9	-	5.7636	SYAM	-	-	0	Co-IP	0	Co-IP	0	0	0	0	0	0	0
Q7Z351	-	-	Q7Z351	-	-	0	Co-IP	0	Co-IP	0	0	0	0	0	0	0
P46060	-	7.5258	RAGP1	RANGAP1	KIAA1835	0	0	Co-IP	0	Co-IP	0	0	0	0	0	0
Q12905	-	8.6838	ILF2	NF45	-	0	0	Co-IP	0	Co-IP	0	0	0	0	0	0
Q9NYL4	-	7.8137	FKB11	FKBP11	FKBP19	0	0	Co-IP	0	Co-IP	0	0	0	0	0	0
O43156	-	6.9478	TTI1	-	-	0	0	0	Co-IP	Co-IP	0	0	0	0	0	0
P33121	-	-	ACSL1	FACL1	-	0	0	0	Co-IP	Co-IP	0	0	0	0	0	0
P46459	-	7.3631	NSF	-	-	0	0	0	Co-IP	Co-IP	0	0	0	0	0	0
P55160	-	6.3735	NCKPL	NCKAP1L	HEM1	0	0	0	Co-IP	Co-IP	0	0	0	0	0	0
Q13724	-	7.4045	MOGS	GCS1	-	0	0	0	Co-IP	Co-IP	0	0	0	0	0	0
Q5VYK3	-	-	ECM29	KIAA0368	-	0	0	0	Co-IP	Co-IP	0	0	0	0	0	0
Q96ER3	-	6.9216	SAAL1	-	-	0	0	0	Co-IP	Co-IP	0	0	0	0	0	0
Q96QU8	-	-	XPO6	KIAA0370	-	0	0	0	Co-IP	Co-IP	0	0	0	0	0	0
Q9BVI4	-	7.0331	NOC4L	-	-	0	0	0	Co-IP	Co-IP	0	0	0	0	0	0
Q9BXW9	-	6.4636	FACD2	FANCD2	FACD	0	0	0	Co-IP	Co-IP	0	0	0	0	0	0

						IP-MS						APS				
UniProt AC	RefSeq ID UniPEx-library	SU-DHL-1 iBAQ [log10 of iBAQ intensity]	Name	Synonyms		HL60 [whole cell lysate]	JEKO-1 [whole cell lysate]	OPM2 [nuclear enriched lysate]	U937 [whole cell lysate]	SU-DHL-1 [whole cell lysate]	SU-DHL-1 [nuclear enriched lysate]	C/EBPβ aa1-41 [CR1-2]	C/EBPε aa1-62 [CR2-4]	C/EBPβ aa49-72 [CR3]	C/EBPβ aa153-173 [CR7]	C/EBPβ aa79-196 [CR4-7]
Q9BZZ5	-	7.7939	APIS	MIG8	-	0	0	0	Co-IP	Co-IP	0	0	0	0	0	0
Q9NV70	-	6.4473	EXOC1	SEC3	-	0	0	0	Co-IP	Co-IP	0	0	0	0	0	0
Q9UBB9	-	5.9354	TFP11	TFIP11	STIP	0	0	0	Co-IP	Co-IP	0	0	0	0	0	0
Q9Y6E2	-	7.6163	BZW2	HSPC028	-	0	0	0	Co-IP	Co-IP	0	0	0	0	0	0
P26640	-	-	SYVC	VARS	G7A	0	Co-IP	0	0	Co-IP	Co-IP	direct interact.	0	0	0	0
Q08211	AK226102	8.4041	DHX9	DDX9	-	0	0	0	0	Co-IP	Co-IP	direct interact.	direct interact.	direct interact.	direct interact.	direct interact.
P52272	NM_005968	8.5349	HNRPM	HNRNPM	-	0	0	Co-IP	0	0	Co-IP	direct interact.	0	direct interact.	0	0
P13639	NM_001961	8.8879	EF2	EEF2	-	0	0	0	0	Co-IP	Co-IP	0	0	direct interact.	0	0
P04843	NM_002950	8.3652	RPN1	-	-	0	0	Co-IP	0	0	Co-IP	0	0	direct interact.	0	0
Q3KQU3	AB033013	6.0916	MA7D1	MAP7D1	KIAA1187	Co-IP	0	0	0	0	0	0	direct interact.	direct interact.	0	0
Q8TB61	NM_178148	6.7538	S35B2	SLC35B2	PAPST1	Co-IP	0	0	0	0	0	0	0	direct interact.	0	0
B4DG73	-	-	B4DG73	-	-	Co-IP	0	0	0	0	0	0	0	0	0	0
B4DGT3	-	-	B4DGT3	-	-	Co-IP	0	0	0	0	0	0	0	0	0	0
B4DR61	-	7.2195	B4DR61	-	-	Co-IP	0	0	0	0	0	0	0	0	0	0
B7Z3B7	-	-	B7Z3B7	-	-	Co-IP	0	0	0	0	0	0	0	0	0	0
O00541	-	7.4675	PESC	PES1	-	Co-IP	0	0	0	0	0	0	0	0	0	0
O14949	-	7.5219	QCR8	UQCRQ	-	Co-IP	0	0	0	0	0	0	0	0	0	0
O75190	-	-	DNJB6	-	-	Co-IP	0	0	0	0	0	0	0	0	0	0
O75306	-	7.3115	NDUS2	NDUFS2	-	Co-IP	0	0	0	0	0	0	0	0	0	0
O94927	-	6.1444	HAUS5	-	-	Co-IP	0	0	0	0	0	0	0	0	0	0
P00367	-	8.6122	DHE3	GLUD1	GLUD	Co-IP	0	0	0	0	0	0	0	0	0	0
P05107	-	-	ITB2	ITGB2	CD18	Co-IP	0	0	0	0	0	0	0	0	0	0
P0C0S8	-	-	H2A1	H2AFP	-	Co-IP	0	0	0	0	0	0	0	0	0	0
P10606	-	7.4973	COX5B	-	-	Co-IP	0	0	0	0	0	0	0	0	0	0
P11279	-	7.5957	LAMP1	-	-	Co-IP	0	0	0	0	0	0	0	0	0	0
P12004	-	8.0876	PCNA	-	-	Co-IP	0	0	0	0	0	0	0	0	0	0
P28482	-	7.5406	MK01	MAPK1	ERK2	Co-IP	0	0	0	0	0	0	0	0	0	0
P32780	-	6.3460	TF2H1	GTF2H1	-	Co-IP	0	0	0	0	0	0	0	0	0	0
P43246	-	7.5119	MSH2	-	-	Co-IP	0	0	0	0	0	0	0	0	0	0
P48378	-	-	RFX2	-	-	Co-IP	0	0	0	0	0	0	0	0	0	0
P51809	-	-	VAMP7	SYBL1	-	Co-IP	0	0	0	0	0	0	0	0	0	0
P62277	-	8.9080	RS13	RPS13	-	Co-IP	0	0	0	0	0	0	0	0	0	0
Q02978	-	7.5380	M2OM	SLC25A11	SLC20A4	Co-IP	0	0	0	0	0	0	0	0	0	0
Q07812	-	7.8180	BAX	BCL2L4	-	Co-IP	0	0	0	0	0	0	0	0	0	0
Q13576	-	-	IQGA2	IQGAP2	-	Co-IP	0	0	0	0	0	0	0	0	0	0
Q14191	-	5.7970	WRN	RECQ3	-	Co-IP	0	0	0	0	0	0	0	0	0	0
Q14739	-	7.6779	LBR	-	-	Co-IP	0	0	0	0	0	0	0	0	0	0
Q15080	-	-	NCF4	SH3PXD4	-	Co-IP	0	0	0	0	0	0	0	0	0	0
Q15819	-	7.7901	UB2V2	UBE2V2	MMS2	Co-IP	0	0	0	0	0	0	0	0	0	0
Q15907	-	8.1941	RB11B	RAB11B	YPT3	Co-IP	0	0	0	0	0	0	0	0	0	0
Q27J81	-	5.3039	INF2	C14orf151	-	Co-IP	0	0	0	0	0	0	0	0	0	0
Q546F9	-	-	Q546F9	-	-	Co-IP	0	0	0	0	0	0	0	0	0	0
Q5BJF2	-	-	TMM97	TMEM97	MAC30	Co-IP	0	0	0	0	0	0	0	0	0	0
Q5JTV8	-	7.8452	TOIP1	TOR1AIP1	-	Co-IP	0	0	0	0	0	0	0	0	0	0
Q6B6N3	-	-	Q6B6N3	-	-	Co-IP	0	0	0	0	0	0	0	0	0	0
Q6P9B9	-	6.2978	INT5	INTS5	KIAA1698	Co-IP	0	0	0	0	0	0	0	0	0	0
Q6UW68	-	7.0464	TM205	TMEM205	-	Co-IP	0	0	0	0	0	0	0	0	0	0
Q7RTS9	-	6.0730	DYM	-	-	Co-IP	0	0	0	0	0	0	0	0	0	0
Q86TP1	-	6.4830	PRUNE	-	-	Co-IP	0	0	0	0	0	0	0	0	0	0
Q86VR2	-	7.1670	F134C	FAM134C	-	Co-IP	0	0	0	0	0	0	0	0	0	0
Q86WB0	-	6.4909	NIPA	ZC3HC1	-	Co-IP	0	0	0	0	0	0	0	0	0	0
Q8NEM7	-	-	SP20H	-	-	Co-IP	0	0	0	0	0	0	0	0	0	0
Q8TDZ2	-	-	MICA1	MICAL1	MICAL	Co-IP	0	0	0	0	0	0	0	0	0	0
Q8TEX9	-	7.4716	IPO4	IMP4B	-	Co-IP	0	0	0	0	0	0	0	0	0	0
Q969X0	-	-	RIPL2	RILPL2	RLP2	Co-IP	0	0	0	0	0	0	0	0	0	0
Q96AN2	-	6.8618	Q96AN2	NRF1	-	Co-IP	0	0	0	0	0	0	0	0	0	0
Q96DZ1	-	6.0765	ERLEC	ERLEC1	C2orf30	Co-IP	0	0	0	0	0	0	0	0	0	0
Q96HY6	-	7.1156	DDRGK	DDRGK1	C20orf116	Co-IP	0	0	0	0	0	0	0	0	0	0
Q9BTC0	-	6.2940	DIDO1	C20orf158	-	Co-IP	0	0	0	0	0	0	0	0	0	0
Q9H836	-	-	Q9H836	-	-	Co-IP	0	0	0	0	0	0	0	0	0	0
Q9H9B4	-	8.2961	SFXN1	-	-	Co-IP	0	0	0	0	0	0	0	0	0	0
Q9NRK6	-	6.3375	ABCBA	ABCB10	-	Co-IP	0	0	0	0	0	0	0	0	0	0
Q9NRP0	-	7.1681	OSTC	DC2	-	Co-IP	0	0	0	0	0	0	0	0	0	0
Q9NV66	-	6.1987	TYW1	RSAFD1	-	Co-IP	0	0	0	0	0	0	0	0	0	0
Q9UKE5	-	-	TNIK	-	-	Co-IP	0	0	0	0	0	0	0	0	0	0
Q9Y228	-	-	T3JAM	TRAF3IP3	-	Co-IP	0	0	0	0	0	0	0	0	0	0
Q9Y277	-	-	VDAC3	-	-	Co-IP	0	0	0	0	0	0	0	0	0	0
Q9Y282	-	-	ERGI3	ERGIC3	C20orf47	Co-IP	0	0	0	0	0	0	0	0	0	0
Q9Y3Q3	-	-	TMED3	C15orf22	-	Co-IP	0	0	0	0	0	0	0	0	0	0
Q9Y3T9	-	7.2186	NOC2L	NIR	-	Co-IP	0	0	0	0	0	0	0	0	0	0
Q9Y4P3	-	6.7928	TBL2	WBSCR13	-	Co-IP	0	0	0	0	0	0	0	0	0	0
Q9Y5Y5	-	5.9031	PEX16	-	-	Co-IP	0	0	0	0	0	0	0	0	0	0
P06733	AL833741	9.3449	ENOA	ENO1	ENO1L1	0	Co-IP	0	0	0	0	direct interact.	0	direct interact.	0	0
P29558	NM_016839	6.9589	RBMS1	C2orf12	-	0	Co-IP	0	0	0	0	direct interact.	0	direct interact.	0	0
P23588	NM_001417	-	IF4B	-	-	0	Co-IP	0	0	0	0	0	0	direct interact.	0	0
Q9NY61	NM_012138	7.7516	AATF	CHE1	-	0	Co-IP	0	0	0	0	0	0	0	direct interact.	0
A8MQB6	-	-	A8MQB6	-	-	0	Co-IP	0	0	0	0	0	0	0	0	0
B3KSH1	-	8.3032	B3KSH1	-	-	0	Co-IP	0	0	0	0	0	0	0	0	0
B3V096	-	-	B3V096	-	-	0	Co-IP	0	0	0	0	0	0	0	0	0
B4DF70	-	-	B4DF70	-	-	0	Co-IP	0	0	0	0	0	0	0	0	0
B5MDF5	-	9.0468	B5MDF5	RAN	-	0	Co-IP	0	0	0	0	0	0	0	0	0
O15145	-	7.8994	ARPC3	-	-	0	Co-IP	0	0	0	0	0	0	0	0	0
O43681	-	7.7166	ASNA	-	-	0	Co-IP	0	0	0	0	0	0	0	0	0
O75431	-	7.5319	MTX2	-	-	0	Co-IP	0	0	0	0	0	0	0	0	0
O75531	-	8.4100	BAF	-	-	0	Co-IP	0	0	0	0	0	0	0	0	0
O94925	-	7.0974	GLSK	-	-	0	Co-IP	0	0	0	0	0	0	0	0	0
P00491	-	8.5555	PNPH	-	-	0	Co-IP	0	0	0	0	0	0	0	0	0
P00558	-	8.9335	PGK1	-	-	0	Co-IP	0	0	0	0	0	0	0	0	0
P04075	-	9.1471	ALDOA	-	-	0	Co-IP	0	0	0	0	0	0	0	0	0
P04083	-	8.7710	ANXA1	-	-	0	Co-IP	0	0	0	0	0	0	0	0	0
P06737	-	8.3841	PYGL	-	-	0	Co-IP	0	0	0	0	0	0	0	0	0

						IP-MS						APS				
UniProt AC	RefSeq ID UniPEx-library	SU-DHL-1 iBAQ [log10 of iBAQ intensity]	Name	Synonyms		HL60 [whole cell lysate]	JEKO-1 [whole cell lysate]	OPM2 [nuclear enriched lysate]	U937 [whole cell lysate]	SU-DHL-1 [whole cell lysate]	SU-DHL-1 [nuclear enriched lysate]	C/EBPβ aa1-41 [CR1-2]	C/EBPε aa1-62 [CR2-4]	C/EBPβ aa49-72 [CR3]	C/EBPβ aa153-173 [CR7]	C/EBPβ aa79-196 [CR4-7]
P06744	-	8.9083	G6PI	-	-	0	Co-IP	0	0	0	0	0	0	0	0	0
P07195	-	8.9149	LDHB	-	-	0	Co-IP	0	0	0	0	0	0	0	0	0
P08243	-	7.7987	ASNS	-	-	0	Co-IP	0	0	0	0	0	0	0	0	0
P08865	-	8.7790	RSSA	RPSA	-	0	Co-IP	0	0	0	0	0	0	0	0	0
P15311	-	7.6361	EZRI	-	-	0	Co-IP	0	0	0	0	0	0	0	0	0
P15408	-	7.2466	FOSL2	-	-	0	Co-IP	0	0	0	0	0	0	0	0	0
P18583	-	7.0724	SON	-	-	0	Co-IP	0	0	0	0	0	0	0	0	0
P18669	-	8.9269	PGAM1	-	-	0	Co-IP	0	0	0	0	0	0	0	0	0
P25786	-	8.3825	PSA1	PSMA1	-	0	Co-IP	0	0	0	0	0	0	0	0	0
P30419	-	8.1241	NMT1	-	-	0	Co-IP	0	0	0	0	0	0	0	0	0
P30740	-	8.8102	ILEU	-	-	0	Co-IP	0	0	0	0	0	0	0	0	0
P33991	-	7.7942	MCM4	-	-	0	Co-IP	0	0	0	0	0	0	0	0	0
P35244	-	7.8212	RFA3	RPA3	-	0	Co-IP	0	0	0	0	0	0	0	0	0
P49588	-	7.8792	SYAC	-	-	0	Co-IP	0	0	0	0	0	0	0	0	0
P50579	-	7.3099	MAP2	-	-	0	Co-IP	0	0	0	0	0	0	0	0	0
P52209	-	8.2765	6PGD	-	-	0	Co-IP	0	0	0	0	0	0	0	0	0
P55010	-	7.9429	IF5	eIF5	-	0	Co-IP	0	0	0	0	0	0	0	0	0
P55786	-	8.0811	PSA	-	-	0	Co-IP	0	0	0	0	0	0	0	0	0
P83436	-	6.0419	COG7	-	-	0	Co-IP	0	0	0	0	0	0	0	0	0
P99999	-	8.9317	CYC	-	-	0	Co-IP	0	0	0	0	0	0	0	0	0
Q01105	-	8.4653	SET	-	-	0	Co-IP	0	0	0	0	0	0	0	0	0
Q06830	-	8.8777	PRDX1	-	-	0	Co-IP	0	0	0	0	0	0	0	0	0
Q07617	-	-	SPAG1	-	-	0	Co-IP	0	0	0	0	0	0	0	0	0
Q08J23	-	7.8352	NSUN2	-	-	0	Co-IP	0	0	0	0	0	0	0	0	0
Q13144	-	7.1162	EI2BE	-	-	0	Co-IP	0	0	0	0	0	0	0	0	0
Q13618	-	7.1829	CUL3	-	-	0	Co-IP	0	0	0	0	0	0	0	0	0
Q14746	-	6.0859	COG2	-	-	0	Co-IP	0	0	0	0	0	0	0	0	0
Q15102	-	8.5729	PA1B3	-	-	0	Co-IP	0	0	0	0	0	0	0	0	0
Q15181	-	8.6352	IPYR	-	-	0	Co-IP	0	0	0	0	0	0	0	0	0
Q16401	-	7.5026	PSMD5	-	-	0	Co-IP	0	0	0	0	0	0	0	0	0
Q32Q12	-	8.8573	Q32Q12	-	-	0	Co-IP	0	0	0	0	0	0	0	0	0
Q3B7T1	-	-	EDRF1	-	-	0	Co-IP	0	0	0	0	0	0	0	0	0
Q59GX2	-	-	Q59GX2	-	-	0	Co-IP	0	0	0	0	0	0	0	0	0
Q6ICB0	-	-	DESI1	-	-	0	Co-IP	0	0	0	0	0	0	0	0	0
Q6KC79	-	5.7978	NIPBL	-	-	0	Co-IP	0	0	0	0	0	0	0	0	0
Q70UQ0	-	7.0012	IKIP	-	-	0	Co-IP	0	0	0	0	0	0	0	0	0
Q71RC2	-	6.2261	LARP4	-	-	0	Co-IP	0	0	0	0	0	0	0	0	0
Q7Z2W7	-	-	TRPM8	-	-	0	Co-IP	0	0	0	0	0	0	0	0	0
Q7Z7G8	-	-	VP13B	-	-	0	Co-IP	0	0	0	0	0	0	0	0	0
Q8IU60	-	-	DCP2	-	-	0	Co-IP	0	0	0	0	0	0	0	0	0
Q8IY67	-	6.1188	RAVR1	-	-	0	Co-IP	0	0	0	0	0	0	0	0	0
Q8N6G5	-	6.3463	CGAT2	-	-	0	Co-IP	0	0	0	0	0	0	0	0	0
Q8NBS9	-	7.8742	TXND5	-	-	0	Co-IP	0	0	0	0	0	0	0	0	0
Q8NI22	-	7.0737	MCFD2	-	-	0	Co-IP	0	0	0	0	0	0	0	0	0
Q8WXH0	-	5.2997	SYNE2	-	-	0	Co-IP	0	0	0	0	0	0	0	0	0
Q9BS26	-	7.6013	ERP44	-	-	0	Co-IP	0	0	0	0	0	0	0	0	0
Q9BVA0	-	-	KTNB1	-	-	0	Co-IP	0	0	0	0	0	0	0	0	0
Q9BZF1	-	6.7799	OSBL8	-	-	0	Co-IP	0	0	0	0	0	0	0	0	0
Q9H0E9	-	-	BRD8	-	-	0	Co-IP	0	0	0	0	0	0	0	0	0
Q9H0S4	-	7.4640	DDX47	-	-	0	Co-IP	0	0	0	0	0	0	0	0	0
Q9H270	-	6.2231	VPS11	-	-	0	Co-IP	0	0	0	0	0	0	0	0	0
Q9H2K8	-	6.0370	TAOK3	-	-	0	Co-IP	0	0	0	0	0	0	0	0	0
Q9NR12	-	7.0860	PDLI7	-	-	0	Co-IP	0	0	0	0	0	0	0	0	0
Q9NVU0	-	5.8427	RPC5	POLR3E	-	0	Co-IP	0	0	0	0	0	0	0	0	0
Q9NXR7	-	7.2440	BRE	-	-	0	Co-IP	0	0	0	0	0	0	0	0	0
Q9NXW1	-	-	Q9NXW1	-	-	0	Co-IP	0	0	0	0	0	0	0	0	0
Q9P2G1	-	-	AKIB1	-	-	0	Co-IP	0	0	0	0	0	0	0	0	0
Q9UI10	-	7.2696	EI2BD	-	-	0	Co-IP	0	0	0	0	0	0	0	0	0
Q9UIA0	-	-	CYH4	-	-	0	Co-IP	0	0	0	0	0	0	0	0	0
Q9UJX5	-	-	APC4	-	-	0	Co-IP	0	0	0	0	0	0	0	0	0
Q9UQ80	-	8.6168	PA2G4	-	-	0	Co-IP	0	0	0	0	0	0	0	0	0
Q9Y265	-	8.4005	RUVB1	RUVBL1	-	0	Co-IP	0	0	0	0	0	0	0	0	0
Q9Y2R4	-	7.1330	DDX52	-	-	0	Co-IP	0	0	0	0	0	0	0	0	0
Q9Y333	-	8.2776	LSM2	-	-	0	Co-IP	0	0	0	0	0	0	0	0	0
Q9Y3D6	-	7.7176	FIS1	-	-	0	Co-IP	0	0	0	0	0	0	0	0	0
P33176	NM_004521	7.4971	KINH	KIF5B	KNS	0	0	0	0	0	Co-IP	direct interact.	direct interact.	0	direct interact.	0
P62987	NM_001033930	-	RL40	UBA52	UBCEP2	0	0	0	0	0	Co-IP	direct interact.	direct interact.	0	direct interact.	0
P61978	NM_002140	8.5239	HNRPK	HNRNPK	-	0	0	0	0	0	Co-IP	direct interact.	0	direct interact.	direct interact.	0
P35579	NM_002473	7.9494	MYH9	-	-	0	0	0	0	0	Co-IP	direct interact.	0	0	direct interact.	direct interact.
P07910	BC103758	8.8378	HNRPC	HNRNPC	-	0	0	0	0	0	Co-IP	direct interact.	0	0	direct interact.	0
P27635	NM_006013	8.9099	RL10	RPL10	-	0	0	0	0	0	Co-IP	direct interact.	0	0	direct interact.	0
P18847	NM_001040619	-	ATF3	-	-	0	0	0	0	0	Co-IP	direct interact.	0	0	0	0
P21333	X53416	7.9224	FLNA	FLN	-	0	0	0	0	0	Co-IP	direct interact.	0	0	0	0
P30626	NM_003130	8.7059	SORCN	SRI	-	0	0	0	0	0	Co-IP	direct interact.	0	0	0	0
Q8TEM1	NM_024923	7.4334	PO210	NUP210	KIAA0906	0	0	0	0	0	Co-IP	direct interact.	0	0	0	0
Q00839	NM_031844	8.6520	HNRPU	HNRNPU	-	0	0	0	0	0	Co-IP	0	direct interact.	direct interact.	direct interact.	0
P09651	NM_031157	9.2385	ROA1	HNRPA1	-	0	0	0	0	0	Co-IP	0	0	direct interact.	0	0
P11021	NM_005347	8.9411	GRP78	HSPA5	-	0	0	0	0	0	Co-IP	0	0	direct interact.	0	0
P11142	NM_006597	9.0335	HSP7C	HSPA8	HSC70	0	0	0	0	0	Co-IP	0	0	direct interact.	0	0
P21796	AK122953	8.7486	VDAC1	VDAC	-	0	0	0	0	0	Co-IP	0	0	direct interact.	0	0
P30101	NM_005313	8.8459	PDIA3	ERP57	-	0	0	0	0	0	Co-IP	0	0	direct interact.	0	0
Q14152	NM_003750	7.7567	EIF3A	EIF3S10	-	0	0	0	0	0	Co-IP	0	0	direct interact.	0	0
Q13151	NM_006805	8.4866	ROA0	HNRNPA0	HNRPA0	0	0	0	0	0	Co-IP	0	0	0	direct interact.	0
A8MXP9	-	8.3681	A8MXP9	MATR3	-	0	0	0	0	0	Co-IP	0	0	0	0	0
B3KTC7	-	7.2817	B3KTC7	MRE11A	-	0	0	0	0	0	Co-IP	0	0	0	0	0
E7ENR4	-	-	E7ENR4	HK1	-	0	0	0	0	0	Co-IP	0	0	0	0	0
F5H2F4	-	6.3998	F5H2F4	MTHFD1	-	0	0	0	0	0	Co-IP	0	0	0	0	0
G8JLB6	-	8.3817	G8JLB6	HNRNPH1	-	0	0	0	0	0	Co-IP	0	0	0	0	0
H3BLZ8	-	-	H3BLZ8	DDX17	-	0	0	0	0	0	Co-IP	0	0	0	0	0
H3BPE7	-	8.1516	H3BPE7	FUS	-	0	0	0	0	0	Co-IP	0	0	0	0	0
J3KPX7	-	-	J3KPX7	PHB2	-	0	0	0	0	0	Co-IP	0	0	0	0	0

						IP-MS						APS				
UniProt AC	RefSeq ID UniPEx-library	SU-DHL-1 iBAQ [log10 of iBAQ intensity]	Name	Synonyms		HL60 [whole cell lysate]	JEKO-1 [whole cell lysate]	OPM2 [nuclear enriched lysate]	U937 [whole cell lysate]	SU-DHL-1 [whole cell lysate]	SU-DHL-1 [nuclear enriched lysate]	C/EBPβ aa1-41 [CR1-2]	C/EBPε aa1-62 [CR2-4]	C/EBPβ aa49-72 [CR3]	C/EBPβ aa153-173 [CR7]	C/EBPβ aa79-196 [CR4-7]
J3KQ73	-	7.8794	J3KQ73	FKBP8	-	0	0	0	0	0	Co-IP	0	0	0	0	0
J9JID7	-	7.6930	J9JID7	LMNB2	-	0	0	0	0	0	Co-IP	0	0	0	0	0
M0R0R2	-	-	M0R0R2	RPS5	-	0	0	0	0	0	Co-IP	0	0	0	0	0
O00567	-	8.2986	NOP56	NOL5A	-	0	0	0	0	0	Co-IP	0	0	0	0	0
O00571	-	8.1034	DDX3X	DBX	-	0	0	0	0	0	Co-IP	0	0	0	0	0
O14776	-	7.5497	TCRG1	TCERG1	CA150	0	0	0	0	0	Co-IP	0	0	0	0	0
O43684	-	7.7139	BUB3	-	-	0	0	0	0	0	Co-IP	0	0	0	0	0
O60264	-	7.5611	SMCA5	SMARCA5	SNF2H	0	0	0	0	0	Co-IP	0	0	0	0	0
O75400	-	7.4539	PR40A	FBP11	-	0	0	0	0	0	Co-IP	0	0	0	0	0
O75475	-	7.6965	PSIP1	DFS70	-	0	0	0	0	0	Co-IP	0	0	0	0	0
O75533	-	8.0133	SF3B1	SAP155	-	0	0	0	0	0	Co-IP	0	0	0	0	0
O75643	-	7.7762	U520	-	-	0	0	0	0	0	Co-IP	0	0	0	0	0
O94776	-	7.2959	MTA2	MTA1L1	-	0	0	0	0	0	Co-IP	0	0	0	0	0
O94906	-	7.1980	PRP6	PRPF6	C20orf14	0	0	0	0	0	Co-IP	0	0	0	0	0
P02786	-	8.3614	TFR1	TFRC	-	0	0	0	0	0	Co-IP	0	0	0	0	0
P05114	-	7.9492	HMGN1	HMG14	-	0	0	0	0	0	Co-IP	0	0	0	0	0
P05141	-	8.6246	ADT2	SLC25A5	ANT2	0	0	0	0	0	Co-IP	0	0	0	0	0
P05455	-	8.3147	LA	SSB	-	0	0	0	0	0	Co-IP	0	0	0	0	0
P06576	-	8.7587	ATPB	ATP5B	ATPMB	0	0	0	0	0	Co-IP	0	0	0	0	0
P07814	-	7.8517	SYEP	EPRS	GLNS	0	0	0	0	0	Co-IP	0	0	0	0	0
P08107	-	9.1218	HSP71	HSPA1A	HSPA1	0	0	0	0	0	Co-IP	0	0	0	0	0
P08621	-	8.2245	RU17	RNPU1Z	-	0	0	0	0	0	Co-IP	0	0	0	0	0
P09429	-	8.9782	HMGB1	HMG1	-	0	0	0	0	0	Co-IP	0	0	0	0	0
P09661	-	8.2094	RU2A	SNRPA1	-	0	0	0	0	0	Co-IP	0	0	0	0	0
P09874	-	8.3864	PARP1	ADPRT	-	0	0	0	0	0	Co-IP	0	0	0	0	0
P10809	-	9.2729	CH60	HSPD1	HSP60	0	0	0	0	0	Co-IP	0	0	0	0	0
P11387	-	8.2252	TOP1	-	-	0	0	0	0	0	Co-IP	0	0	0	0	0
P12270	-	7.5366	TPR	Megator	-	0	0	0	0	0	Co-IP	0	0	0	0	0
P14625	-	8.6960	ENPL	GRP94	-	0	0	0	0	0	Co-IP	0	0	0	0	0
P14866	-	8.8144	HNRPL	HNRNPL	-	0	0	0	0	0	Co-IP	0	0	0	0	0
P16220	-	7.2644	CREB1	-	-	0	0	0	0	0	Co-IP	0	0	0	0	0
P17844	-	-	DDX5	G17P1	-	0	0	0	0	0	Co-IP	0	0	0	0	0
P17987	-	8.4731	TCPA	TCP1	CCT1	0	0	0	0	0	Co-IP	0	0	0	0	0
P18754	-	7.7185	RCC1	CHC1	-	0	0	0	0	0	Co-IP	0	0	0	0	0
P20700	-	8.5378	LMNB1	LMN2	-	0	0	0	0	0	Co-IP	0	0	0	0	0
P22695	-	8.1384	QCR2	UQCRC2	-	0	0	0	0	0	Co-IP	0	0	0	0	0
P23193	-	8.2005	TCEA1	GTF2S	-	0	0	0	0	0	Co-IP	0	0	0	0	0
P24539	-	8.0119	AT5F1	ATP5F1	-	0	0	0	0	0	Co-IP	0	0	0	0	0
P31939	-	8.5118	PUR9	ATIC	PURH	0	0	0	0	0	Co-IP	0	0	0	0	0
P35251	-	6.7624	RFC1	RFC140	-	0	0	0	0	0	Co-IP	0	0	0	0	0
P38159	-	8.2315	RBMX	HNRPG	-	0	0	0	0	0	Co-IP	0	0	0	0	0
P38646	-	8.8713	GRP75	HSPA9	-	0	0	0	0	0	Co-IP	0	0	0	0	0
P38919	-	8.2801	IF4A3	EIF4A3	DDX48	0	0	0	0	0	Co-IP	0	0	0	0	0
P39687	-	8.5587	AN32A	ANP32A	C15orf1	0	0	0	0	0	Co-IP	0	0	0	0	0
P40939	-	8.0267	ECHA	HADHA	HADH	0	0	0	0	0	Co-IP	0	0	0	0	0
P42167	-	7.6168	LAP2B	TMPO	LAP2	0	0	0	0	0	Co-IP	0	0	0	0	0
P45880	-	8.5352	VDAC2	-	-	0	0	0	0	0	Co-IP	0	0	0	0	0
P46013	-	6.8371	KI67	MKI67	-	0	0	0	0	0	Co-IP	0	0	0	0	0
P48643	-	8.5240	TCPE	CCT5	CCTE	0	0	0	0	0	Co-IP	0	0	0	0	0
P49368	-	8.5472	TCPG	CCT3	CCTG	0	0	0	0	0	Co-IP	0	0	0	0	0
P50990	-	8.7306	TCPQ	CCT8	C21orf112	0	0	0	0	0	Co-IP	0	0	0	0	0
P51148	-	8.4868	RAB5C	RABL	-	0	0	0	0	0	Co-IP	0	0	0	0	0
P51572	-	7.8745	BAP31	BCAP31	-	0	0	0	0	0	Co-IP	0	0	0	0	0
P51608	-	6.8308	MECP2	-	-	0	0	0	0	0	Co-IP	0	0	0	0	0
P51991	-	8.4869	ROA3	HNRNPA3	HNRPA3	0	0	0	0	0	Co-IP	0	0	0	0	0
P60468	-	7.8280	SC61B	SEC61B	-	0	0	0	0	0	Co-IP	0	0	0	0	0
P60842	-	8.8379	IF4A1	EIF4A1	DDX2A	0	0	0	0	0	Co-IP	0	0	0	0	0
P61221	-	7.9643	ABCE1	RLI	-	0	0	0	0	0	Co-IP	0	0	0	0	0
P61981	-	8.5366	1433G	YWHA	-	0	0	0	0	0	Co-IP	0	0	0	0	0
P62081	-	9.0781	RS7	RPS7	-	0	0	0	0	0	Co-IP	0	0	0	0	0
P62263	-	9.1293	RS14	RPS14	PRO2640	0	0	0	0	0	Co-IP	0	0	0	0	0
P78371	-	8.6480	TCPB	CCT2	-	0	0	0	0	0	Co-IP	0	0	0	0	0
P84103	-	8.6480	SRSF3	SFRS3	-	0	0	0	0	0	Co-IP	0	0	0	0	0
Q01780	-	7.0423	EXOSX	EXOSC10	PMSCL	0	0	0	0	0	Co-IP	0	0	0	0	0
Q13423	-	7.2995	NNTM	NNT	-	0	0	0	0	0	Co-IP	0	0	0	0	0
Q13950	-	-	RUNX2	-	-	0	0	0	0	0	Co-IP	0	0	0	0	0
Q14204	-	7.7668	DYHC1	DYNC1H1	DHC1	0	0	0	0	0	Co-IP	0	0	0	0	0
Q14683	-	6.9590	SMC1A	DXS423E	-	0	0	0	0	0	Co-IP	0	0	0	0	0
Q14839	-	7.5089	CHD4	-	-	0	0	0	0	0	Co-IP	0	0	0	0	0
Q14974	-	8.6996	IMB1	KPNB1	NTF97	0	0	0	0	0	Co-IP	0	0	0	0	0
Q15149	-	7.1737	PLEC	PLEC1	-	0	0	0	0	0	Co-IP	0	0	0	0	0
Q15365	-	8.3672	PCBP1	-	-	0	0	0	0	0	Co-IP	0	0	0	0	0
Q15459	-	7.7969	SF3A1	SAP114	-	0	0	0	0	0	Co-IP	0	0	0	0	0
Q16649	-	6.8000	NFIL3	E4BP4	-	0	0	0	0	0	Co-IP	0	0	0	0	0
Q16666	-	8.0618	IF16	IFI16	-	0	0	0	0	0	Co-IP	0	0	0	0	0
Q16891	-	7.8753	MIC60	IMMT	HMP	0	0	0	0	0	Co-IP	0	0	0	0	0
Q5UIP0	-	6.6469	RIF1	-	-	0	0	0	0	0	Co-IP	0	0	0	0	0
Q6P2Q9	-	7.6838	PRP8	PRPF8	PRPC8	0	0	0	0	0	Co-IP	0	0	0	0	0
Q7L014	-	7.6680	DDX46	KIAA0801	-	0	0	0	0	0	Co-IP	0	0	0	0	0
Q8N163	-	7.5161	CCAR2	DBC1	-	0	0	0	0	0	Co-IP	0	0	0	0	0
Q8N1F7	-	7.5658	NUP93	KIAA0095	-	0	0	0	0	0	Co-IP	0	0	0	0	0
Q8N5K1	-	7.7667	CISD2	CDGSH2	-	0	0	0	0	0	Co-IP	0	0	0	0	0
Q92522	-	7.9290	H1X	H1FX	-	0	0	0	0	0	Co-IP	0	0	0	0	0
Q92922	-	6.9859	SMRC1	SMARCC1	BAF155	0	0	0	0	0	Co-IP	0	0	0	0	0
Q92945	-	8.0816	FUBP2	KHSRP	-	0	0	0	0	0	Co-IP	0	0	0	0	0
Q92973	-	7.7489	TNPO1	KPNB2	-	0	0	0	0	0	Co-IP	0	0	0	0	0
Q99459	-	7.5146	CDC5L	KIAA0432	-	0	0	0	0	0	Co-IP	0	0	0	0	0
Q9BQG0	-	7.5587	MBB1A	MYBBP1A	P160	0	0	0	0	0	Co-IP	0	0	0	0	0
Q9H3N1	-	8.2156	TMX1	TMX	-	0	0	0	0	0	Co-IP	0	0	0	0	0
Q9HBD4	-	6.9299	Q9HBD4	SMARCA4	BRG1	0	0	0	0	0	Co-IP	0	0	0	0	0
Q9NR30	-	8.4495	DDX21	-	-	0	0	0	0	0	Co-IP	0	0	0	0	0

						IP-MS						APS				
UniProt AC	RefSeq ID UniPEx-library	SU-DHL-1 iBAQ [log10 of iBAQ intensity]	Name	Synonyms		HL60 [whole cell lysate]	JEKO-1 [whole cell lysate]	OPM2 [nuclear enriched lysate]	U937 [whole cell lysate]	SU-DHL-1 [whole cell lysate]	SU-DHL-1 [nuclear enriched lysate]	C/EBPβ aa1-41 [CR1-2]	C/EBPε aa1-62 [CR2-4]	C/EBPβ aa49-72 [CR3]	C/EBPβ aa153-173 [CR7]	C/EBPβ aa79-196 [CR4-7]
Q9UBE0	-	8.0953	SAE1	AOS1	-	0	0	0	0	0	Co-IP	0	0	0	0	0
Q9UKM9	-	-	RALY	HNRPCL2	-	0	0	0	0	0	Co-IP	0	0	0	0	0
Q9UM73	-	7.8718	ALK	-	-	0	0	0	0	0	Co-IP	0	0	0	0	0
Q9Y2X3	-	8.1875	NOP58	NOL5	-	0	0	0	0	0	Co-IP	0	0	0	0	0
Q9Y383	-	7.7274	LC7L2	LUC7L2	-	0	0	0	0	0	Co-IP	0	0	0	0	0
Q9Y678	NM_016128	7.8706	COPG1	COPG	-	0	0	0	0	Co-IP	0	direct interact.	0	direct interact.	0	0
O95983	NM_003926	6.5042	MBD3	-	-	0	0	0	0	Co-IP	0	direct interact.	0	0	direct interact.	0
P68104	-	9.2142	EF1A1	EEF1A1	EEF1A	0	0	0	0	Co-IP	0	direct interact.	0	0	0	0
Q92556	AL136787	7.0135	ELMO1	KIAA0281	-	0	0	0	0	Co-IP	0	direct interact.	0	0	0	0
Q9Y2X0	AF106934	5.9797	MED16	DRIP92	-	0	0	0	0	Co-IP	0	direct interact.	0	0	0	0
Q14008	NM_001008938	7.1800	CKAP5	KIAA0097	-	0	0	0	0	Co-IP	0	0	direct interact.	0	0	0
Q92616	NM_006836	7.5075	GCN1L	GCN1L1	KIAA0219	0	0	0	0	Co-IP	0	0	direct interact.	0	0	0
P22670	NM_002918	6.8528	RFX1	-	-	0	0	0	0	Co-IP	0	0	0	direct interact.	0	0
Q5GLZ8	NM_022079	6.7220	HERC4	KIAA1593	-	0	0	0	0	Co-IP	0	0	0	direct interact.	0	0
A5YKK6	-	6.9198	CNOT1	CDC39	-	0	0	0	0	Co-IP	0	0	0	0	0	0
A8K0K1	-	-	A8K0K1	-	-	0	0	0	0	Co-IP	0	0	0	0	0	0
A8K8W9	-	-	A8K8W9	-	-	0	0	0	0	Co-IP	0	0	0	0	0	0
B3KT11	-	-	B3KT11	-	-	0	0	0	0	Co-IP	0	0	0	0	0	0
B4DEA8	-	-	B4DEA8	-	-	0	0	0	0	Co-IP	0	0	0	0	0	0
B4DJ38	-	-	B4DJ38	-	-	0	0	0	0	Co-IP	0	0	0	0	0	0
B4DJV9	-	-	B4DJV9	-	-	0	0	0	0	Co-IP	0	0	0	0	0	0
B4DLV7	-	-	B4DLV7	-	-	0	0	0	0	Co-IP	0	0	0	0	0	0
B4DQX2	-	-	B4DQX2	-	-	0	0	0	0	Co-IP	0	0	0	0	0	0
B4DSU8	-	-	B4DSU8	-	-	0	0	0	0	Co-IP	0	0	0	0	0	0
B4DTS2	-	-	B4DTS2	-	-	0	0	0	0	Co-IP	0	0	0	0	0	0
B4DU42	-	-	B4DU42	-	-	0	0	0	0	Co-IP	0	0	0	0	0	0
B4DZ73	-	-	B4DZ73	-	-	0	0	0	0	Co-IP	0	0	0	0	0	0
B7Z7L3	-	-	B7Z7L3	-	-	0	0	0	0	Co-IP	0	0	0	0	0	0
C9J4C3	-	-	C9J4C3	-	-	0	0	0	0	Co-IP	0	0	0	0	0	0
C9JI13	-	-	C9JI13	-	-	0	0	0	0	Co-IP	0	0	0	0	0	0
C9JI70	-	-	C9JI70	-	-	0	0	0	0	Co-IP	0	0	0	0	0	0
O00178	-	7.1738	GTPB1	GTPBP1	-	0	0	0	0	Co-IP	0	0	0	0	0	0
O00762	-	6.5299	UBE2C	UBCH10	-	0	0	0	0	Co-IP	0	0	0	0	0	0
O14893	-	-	GEMI2	GEMIN2	SIP1	0	0	0	0	Co-IP	0	0	0	0	0	0
O14981	-	5.8696	BTAF1	TAF172	-	0	0	0	0	Co-IP	0	0	0	0	0	0
O15111	-	6.2621	IKKA	CHUK	-	0	0	0	0	Co-IP	0	0	0	0	0	0
O15260	-	8.4156	SURF4	-	-	0	0	0	0	Co-IP	0	0	0	0	0	0
O43143	-	8.1480	DHX15	DBP1	-	0	0	0	0	Co-IP	0	0	0	0	0	0
O43264	-	6.8555	ZW10	-	-	0	0	0	0	Co-IP	0	0	0	0	0	0
O43615	-	7.6814	TIM44	TIMM44	MIMT44	0	0	0	0	Co-IP	0	0	0	0	0	0
O43929	-	-	ORC4	ORC4L	-	0	0	0	0	Co-IP	0	0	0	0	0	0
O60443	-	7.3314	DFNA5	ICERE1	-	0	0	0	0	Co-IP	0	0	0	0	0	0
O60613	-	7.0594	41897	-	-	0	0	0	0	Co-IP	0	0	0	0	0	0
O60749	-	7.4188	SNX2	TRG9	-	0	0	0	0	Co-IP	0	0	0	0	0	0
O75494	-	7.9445	SRS10	SRSF10	FUSIP1	0	0	0	0	Co-IP	0	0	0	0	0	0
O75955	-	8.2233	FLOT1	-	-	0	0	0	0	Co-IP	0	0	0	0	0	0
O95372	-	-	LYPA2	LYPLA2	APT2	0	0	0	0	Co-IP	0	0	0	0	0	0
O95487	-	-	SC24B	SEC24B	-	0	0	0	0	Co-IP	0	0	0	0	0	0
O96005	-	7.3051	CLPT1	CLPTM1	-	0	0	0	0	Co-IP	0	0	0	0	0	0
O96008	-	8.4218	TOM40	TOMM40	C19orf1	0	0	0	0	Co-IP	0	0	0	0	0	0
P05388	-	8.8975	RLA0	RPLP0	-	0	0	0	0	Co-IP	0	0	0	0	0	0
P0CB44	-	-	SKA2L	-	-	0	0	0	0	Co-IP	0	0	0	0	0	0
P11177	-	7.9089	ODPB	PHE1B	-	0	0	0	0	Co-IP	0	0	0	0	0	0
P23258	-	7.3651	TBG1	TUBG1	TUBG	0	0	0	0	Co-IP	0	0	0	0	0	0
P26196	-	7.8555	DDX6	HLR2	-	0	0	0	0	Co-IP	0	0	0	0	0	0
P27694	-	7.7242	RFA1	RPA1	REPA1	0	0	0	0	Co-IP	0	0	0	0	0	0
P40616	-	7.4741	ARL1	-	-	0	0	0	0	Co-IP	0	0	0	0	0	0
P40692	-	5.8790	MLH1	COCA2	-	0	0	0	0	Co-IP	0	0	0	0	0	0
P42345	-	6.0189	MTOR	FRAP	-	0	0	0	0	Co-IP	0	0	0	0	0	0
P42695	-	6.1419	CNDD3	NCAPD3	CAPD3	0	0	0	0	Co-IP	0	0	0	0	0	0
P42771	-	7.3792	CD2A1	p16	CDKN2A	0	0	0	0	Co-IP	0	0	0	0	0	0
P43490	-	9.1935	NAMPT	PBEF	-	0	0	0	0	Co-IP	0	0	0	0	0	0
P49411	-	8.4337	EFTU	TUFM	-	0	0	0	0	Co-IP	0	0	0	0	0	0
P49643	-	7.3657	PRI2	PRIM2	PRIM2A	0	0	0	0	Co-IP	0	0	0	0	0	0
P49756	-	7.5260	RBM25	RNPC7	-	0	0	0	0	Co-IP	0	0	0	0	0	0
P50748	-	5.8816	KNTC1	KIAA0166	-	0	0	0	0	Co-IP	0	0	0	0	0	0
P51571	-	7.7945	SSRD	SSR4	TRAPD	0	0	0	0	Co-IP	0	0	0	0	0	0
P51812	-	7.8994	KS6A3	RPS6KA3	ISPK1	0	0	0	0	Co-IP	0	0	0	0	0	0
P51946	-	-	CCNH	-	-	0	0	0	0	Co-IP	0	0	0	0	0	0
P53396	-	8.4787	ACLY	-	-	0	0	0	0	Co-IP	0	0	0	0	0	0
P53621	-	7.7538	COPA	-	-	0	0	0	0	Co-IP	0	0	0	0	0	0
P54886	-	7.7946	P5CS	ALDH18A1	GSAS	0	0	0	0	Co-IP	0	0	0	0	0	0
P55957	-	7.8724	BID	-	-	0	0	0	0	Co-IP	0	0	0	0	0	0
P61019	-	7.7870	RAB2A	RAB2	-	0	0	0	0	Co-IP	0	0	0	0	0	0
P61106	-	7.8971	RAB14	-	-	0	0	0	0	Co-IP	0	0	0	0	0	0
P62140	-	7.0172	PP1B	PPP1CB	-	0	0	0	0	Co-IP	0	0	0	0	0	0
P62312	-	7.9051	LSM6	-	-	0	0	0	0	Co-IP	0	0	0	0	0	0
P63208	-	7.5148	SKP1	EMC19	-	0	0	0	0	Co-IP	0	0	0	0	0	0
Q00534	-	7.8883	CDK6	CDKN6	-	0	0	0	0	Co-IP	0	0	0	0	0	0
Q07960	-	7.2411	RHG01	ARHGAP1	CDC42GAP	0	0	0	0	Co-IP	0	0	0	0	0	0
Q12769	-	6.9414	NU160	NUP160	KIAA0197	0	0	0	0	Co-IP	0	0	0	0	0	0
Q12789	-	5.9314	TF3C1	GTF3C1	-	0	0	0	0	Co-IP	0	0	0	0	0	0
Q13535	-	5.7407	ATR	FRP1	-	0	0	0	0	Co-IP	0	0	0	0	0	0
Q13868	-	7.1850	EXOS2	EXOSC2	RRP4	0	0	0	0	Co-IP	0	0	0	0	0	0
Q14166	-	7.5434	TTL12	TTLL12	KIAA0153	0	0	0	0	Co-IP	0	0	0	0	0	0
Q14254	-	-	FLOT2	ESA1	-	0	0	0	0	Co-IP	0	0	0	0	0	0
Q14674	-	-	ESPL1	ESP1	-	0	0	0	0	Co-IP	0	0	0	0	0	0
Q14697	-	8.3607	GANAB	G2AN	-	0	0	0	0	Co-IP	0	0	0	0	0	0
Q15021	-	7.2261	CND1	NCAPD2	CAPD2	0	0	0	0	Co-IP	0	0	0	0	0	0
Q15126	-	7.3335	PMVK	PMKI	-	0	0	0	0	Co-IP	0	0	0	0	0	0
Q15645	-	7.5911	PCH2	TRIP13	-	0	0	0	0	Co-IP	0	0	0	0	0	0

						IP-MS						APS				
UniProt AC	RefSeq ID UniPEx-library	SU-DHL-1 iBAQ [log10 of iBAQ intensity]	Name	Synonyms		HL60 [whole cell lysate]	JEKO-1 [whole cell lysate]	OPM2 [nuclear enriched lysate]	U937 [whole cell lysate]	SU-DHL-1 [whole cell lysate]	SU-DHL-1 [nuclear enriched lysate]	C/EBPβ aa1-41 [CR1-2]	C/EBPε aa1-62 [CR2-4]	C/EBPβ aa49-72 [CR3]	C/EBPβ aa153-173 [CR7]	C/EBPβ aa79-196 [CR4-7]
Q5HY81	-	-	Q5HY81	UBL4A	-	0	0	0	0	Co-IP	0	0	0	0	0	0
Q5T4S7	-	6.9405	UBR4	KIAA0462	-	0	0	0	0	Co-IP	0	0	0	0	0	0
Q5VIR6	-	6.6225	VPS53	PP13624	-	0	0	0	0	Co-IP	0	0	0	0	0	0
Q66K14	-	-	TBC9B	TBC1D9B	KIAA0676	0	0	0	0	Co-IP	0	0	0	0	0	0
Q6YN16	-	7.0345	HSDL2	C9orf99	-	0	0	0	0	Co-IP	0	0	0	0	0	0
Q7KZF4	-	7.9211	SND1	TDRD11	-	0	0	0	0	Co-IP	0	0	0	0	0	0
Q7L2H7	-	8.1415	EIF3M	HFLB5	-	0	0	0	0	Co-IP	0	0	0	0	0	0
Q7Z3E5	-	5.5983	ARMC9	KIAA1868	-	0	0	0	0	Co-IP	0	0	0	0	0	0
Q7Z4H7	-	6.3597	HAUS6	DGT6	-	0	0	0	0	Co-IP	0	0	0	0	0	0
Q7Z6Z7	-	7.2223	HUWE1	KIAA0312	-	0	0	0	0	Co-IP	0	0	0	0	0	0
Q7Z7F5	-	-	Q7Z7F5	-	-	0	0	0	0	Co-IP	0	0	0	0	0	0
Q8IU81	-	6.7595	I2BP1	IRF2BP1	-	0	0	0	0	Co-IP	0	0	0	0	0	0
Q8IZL8	-	-	PELP1	HMX3	-	0	0	0	0	Co-IP	0	0	0	0	0	0
Q8N0X7	-	6.6067	SPG20	KIAA0610	-	0	0	0	0	Co-IP	0	0	0	0	0	0
Q8N3C0	-	5.9154	ASCC3	HELIC1	-	0	0	0	0	Co-IP	0	0	0	0	0	0
Q8N3D4	-	5.3977	EH1L1	EHBP1L1	-	0	0	0	0	Co-IP	0	0	0	0	0	0
Q8TE02	-	6.3345	ELP5	C17orf81	-	0	0	0	0	Co-IP	0	0	0	0	0	0
Q8WTW3	-	5.9911	COG1	KIAA1381	-	0	0	0	0	Co-IP	0	0	0	0	0	0
Q8WUX9	-	6.6172	CHMP7	-	-	0	0	0	0	Co-IP	0	0	0	0	0	0
Q92575	-	6.9097	UBXN4	KIAA0242	-	0	0	0	0	Co-IP	0	0	0	0	0	0
Q92608	-	7.0604	DOCK2	KIAA0209	-	0	0	0	0	Co-IP	0	0	0	0	0	0
Q92759	-	6.7907	TF2H4	GTF2H4	-	0	0	0	0	Co-IP	0	0	0	0	0	0
Q93008	-	6.6307	USP9X	DFFRX	-	0	0	0	0	Co-IP	0	0	0	0	0	0
Q93034	-	6.8595	CUL5	VACM1	-	0	0	0	0	Co-IP	0	0	0	0	0	0
Q93100	-	5.8963	KPBB	PHKB	-	0	0	0	0	Co-IP	0	0	0	0	0	0
Q96BY7	-	-	ATG2B	C14orf103	-	0	0	0	0	Co-IP	0	0	0	0	0	0
Q96H20	-	7.0328	SNF8	EAP30	-	0	0	0	0	Co-IP	0	0	0	0	0	0
Q96JG6	-	6.2632	CC132	CCDC132	KIAA1861	0	0	0	0	Co-IP	0	0	0	0	0	0
Q96KA5	-	7.2258	CLP1L	CLPTM1L	CRR9	0	0	0	0	Co-IP	0	0	0	0	0	0
Q96P70	-	7.5440	IPO9	IMP9	-	0	0	0	0	Co-IP	0	0	0	0	0	0
Q96SN8	-	-	CK5P2	CEP215	-	0	0	0	0	Co-IP	0	0	0	0	0	0
Q99832	-	8.5071	TCPH	CCT7	CCTH	0	0	0	0	Co-IP	0	0	0	0	0	0
Q9BPX3	-	7.2037	CND3	NCAPG	CAPG	0	0	0	0	Co-IP	0	0	0	0	0	0
Q9BSJ8	-	7.3817	ESYT1	FAM62A	-	0	0	0	0	Co-IP	0	0	0	0	0	0
Q9BTX7	-	6.2348	TTPAL	C20orf121	-	0	0	0	0	Co-IP	0	0	0	0	0	0
Q9BUQ0	-	-	Q9BUQ0	-	-	0	0	0	0	Co-IP	0	0	0	0	0	0
Q9BW27	-	7.1505	NUP85	NUP75	-	0	0	0	0	Co-IP	0	0	0	0	0	0
Q9C005	-	8.2500	DPY30	-	-	0	0	0	0	Co-IP	0	0	0	0	0	0
Q9H0W8	-	6.3226	SMG9	C19orf61	-	0	0	0	0	Co-IP	0	0	0	0	0	0
Q9H269	-	6.3655	VPS16	-	-	0	0	0	0	Co-IP	0	0	0	0	0	0
Q9H4A6	-	6.7172	GOLP3	GOLPH3	GPP34	0	0	0	0	Co-IP	0	0	0	0	0	0
Q9H4E7	-	-	DEFI6	DEF6	IBP	0	0	0	0	Co-IP	0	0	0	0	0	0
Q9H9A6	-	7.0926	LRC40	LRRC40	-	0	0	0	0	Co-IP	0	0	0	0	0	0
Q9HAU5	-	6.4215	RENT2	UPF2	KIAA1408	0	0	0	0	Co-IP	0	0	0	0	0	0
Q9HAV4	-	7.4547	XPO5	KIAA1291	-	0	0	0	0	Co-IP	0	0	0	0	0	0
Q9HCU5	-	7.0744	PREB	SEC12	-	0	0	0	0	Co-IP	0	0	0	0	0	0
Q9NQC7	-	-	CYLD	CYLD1	-	0	0	0	0	Co-IP	0	0	0	0	0	0
Q9NTJ3	-	7.3118	SMC4	CAPC	-	0	0	0	0	Co-IP	0	0	0	0	0	0
Q9NVI1	-	6.7026	FANCI	KIAA1794	-	0	0	0	0	Co-IP	0	0	0	0	0	0
Q9P2A4	-	6.9038	ABI3	NESH	-	0	0	0	0	Co-IP	0	0	0	0	0	0
Q9UBB4	-	7.1520	ATX10	ATXN10	SCA10	0	0	0	0	Co-IP	0	0	0	0	0	0
Q9UBD5	-	6.8643	ORC3	LATHEO	-	0	0	0	0	Co-IP	0	0	0	0	0	0
Q9UBF2	-	7.2423	COPG2	-	-	0	0	0	0	Co-IP	0	0	0	0	0	0
Q9UHD2	-	6.7905	TBK1	NAK	-	0	0	0	0	Co-IP	0	0	0	0	0	0
Q9UI12	-	6.8282	VATH	ATP6V1H	-	0	0	0	0	Co-IP	0	0	0	0	0	0
Q9UJY4	-	5.7374	GGA2	KIAA1080	-	0	0	0	0	Co-IP	0	0	0	0	0	0
Q9UKZ1	-	6.4089	CNO11	CNOT11	C2orf29	0	0	0	0	Co-IP	0	0	0	0	0	0
Q9UNQ2	-	7.7014	DIM1	DIMT1	DIMT1L	0	0	0	0	Co-IP	0	0	0	0	0	0
Q9UNY4	-	-	TTF2	-	-	0	0	0	0	Co-IP	0	0	0	0	0	0
Q9Y3I1	-	6.5433	FBX7	FBXO7	-	0	0	0	0	Co-IP	0	0	0	0	0	0
Q9Y5X2	-	6.3875	SNX8	-	-	0	0	0	0	Co-IP	0	0	0	0	0	0
Q9Y679	-	6.7884	AUP1	-	-	0	0	0	0	Co-IP	0	0	0	0	0	0
Q9Y6J9	-	5.6499	TAF6L	PAF65A	-	0	0	0	0	Co-IP	0	0	0	0	0	0
Q99536	NM_006373	8.1292	VAT1	-	-	0	0	0	Co-IP	0	0	0	0	direct interact.	0	0
P35268	NM_000983	8.9112	RL22	RPL22	-	0	0	0	Co-IP	0	0	0	0	0	direct interact.	0
A0JLT2	-	6.1788	MED19	-	-	0	0	0	Co-IP	0	0	0	0	0	0	0
A4D1P6	-	-	WDR91	-	-	0	0	0	Co-IP	0	0	0	0	0	0	0
A6NNN6	-	-	A6NNN6	-	-	0	0	0	Co-IP	0	0	0	0	0	0	0
A8K2S4	-	-	A8K2S4	-	-	0	0	0	Co-IP	0	0	0	0	0	0	0
B4DMN1	-	-	B4DMN1	-	-	0	0	0	Co-IP	0	0	0	0	0	0	0
B4DN86	-	-	B4DN86	-	-	0	0	0	Co-IP	0	0	0	0	0	0	0
B4DR52	-	9.5559	B4DR52	-	-	0	0	0	Co-IP	0	0	0	0	0	0	0
B4DRD7	-	-	B4DRD7	-	-	0	0	0	Co-IP	0	0	0	0	0	0	0
B4E1T5	-	-	B4E1T5	-	-	0	0	0	Co-IP	0	0	0	0	0	0	0
B7Z2R8	-	-	B7Z2R8	-	-	0	0	0	Co-IP	0	0	0	0	0	0	0
B8ZZ87	-	7.0705	B8ZZ87	-	-	0	0	0	Co-IP	0	0	0	0	0	0	0
B9EIQ6	-	-	B9EIQ6	-	-	0	0	0	Co-IP	0	0	0	0	0	0	0
C9JDG0	-	-	C9JDG0	-	-	0	0	0	Co-IP	0	0	0	0	0	0	0
O14497	-	6.0197	ARI1A	BAF250	ARID1A	0	0	0	Co-IP	0	0	0	0	0	0	0
O15014	-	-	ZN609	-	-	0	0	0	Co-IP	0	0	0	0	0	0	0
O60341	-	6.7713	KDM1A	LSD1	-	0	0	0	Co-IP	0	0	0	0	0	0	0
O60566	-	-	BUB1B	BUBR1	-	0	0	0	Co-IP	0	0	0	0	0	0	0
O60645	-	6.2066	EXOC3	-	-	0	0	0	Co-IP	0	0	0	0	0	0	0
O95163	-	7.0360	ELP1	IKBKAP	-	0	0	0	Co-IP	0	0	0	0	0	0	0
P06493	-	7.4226	CDK1	CDC2	-	0	0	0	Co-IP	0	0	0	0	0	0	0
P07355	-	8.5841	ANXA2	-	-	0	0	0	Co-IP	0	0	0	0	0	0	0
P08574	-	7.9485	CY1	-	-	0	0	0	Co-IP	0	0	0	0	0	0	0
P09132	-	6.9514	SRP19	-	-	0	0	0	Co-IP	0	0	0	0	0	0	0
P0C0S5	-	8.9918	H2AZ	-	-	0	0	0	Co-IP	0	0	0	0	0	0	0
P17029	-	5.7225	ZKSC1	-	-	0	0	0	Co-IP	0	0	0	0	0	0	0
P19838	-	6.3254	NFKB1	-	-	0	0	0	Co-IP	0	0	0	0	0	0	0

						IP-MS						APS				
UniProt AC	RefSeq ID UniPEx-library	SU-DHL-1 iBAQ [log10 of iBAQ intensity]	Name	Synonyms		HL60 [whole cell lysate]	JEKO-1 [whole cell lysate]	OPM2 [nuclear enriched lysate]	U937 [whole cell lysate]	SU-DHL-1 [whole cell lysate]	SU-DHL-1 [nuclear enriched lysate]	C/EBPβ aa1-41 [CR1-2]	C/EBPε aa1-62 [CR2-4]	C/EBPβ aa49-72 [CR3]	C/EBPβ aa153-173 [CR7]	C/EBPβ aa79-196 [CR4-7]
P20292	-	7.7305	AL5AP	-	-	0	0	0	Co-IP	0	0	0	0	0	0	0
P27986	-	-	P85A	-	-	0	0	0	Co-IP	0	0	0	0	0	0	0
P30050	-	8.6834	RL12	RPL12	-	0	0	0	Co-IP	0	0	0	0	0	0	0
P37108	-	8.8960	SRP14	-	-	0	0	0	Co-IP	0	0	0	0	0	0	0
P39880	-	5.5297	CUX1	CUTL1	-	0	0	0	Co-IP	0	0	0	0	0	0	0
P40938	-	7.1797	RFC3	-	-	0	0	0	Co-IP	0	0	0	0	0	0	0
P42575	-	-	CASP2	-	-	0	0	0	Co-IP	0	0	0	0	0	0	0
P46783	-	8.5852	RS10	RPS10	-	0	0	0	Co-IP	0	0	0	0	0	0	0
P48047	-	8.2477	ATPO	-	-	0	0	0	Co-IP	0	0	0	0	0	0	0
P62266	-	8.3081	RS23	-	-	0	0	0	Co-IP	0	0	0	0	0	0	0
P62851	-	8.8036	RS25	-	-	0	0	0	Co-IP	0	0	0	0	0	0	0
Q00403	-	6.8163	TF2B	GTF2B	TFIIB	0	0	0	Co-IP	0	0	0	0	0	0	0
Q08050	-	-	FOXM1	-	-	0	0	0	Co-IP	0	0	0	0	0	0	0
Q08AM6	-	6.5511	VAC14	-	-	0	0	0	Co-IP	0	0	0	0	0	0	0
Q12851	-	-	M4K2	MAP4K2	M2K4	0	0	0	Co-IP	0	0	0	0	0	0	0
Q14318	-	-	FKBP8	-	-	0	0	0	Co-IP	0	0	0	0	0	0	0
Q14C86	-	6.3308	GAPD1	-	-	0	0	0	Co-IP	0	0	0	0	0	0	0
Q15013	-	-	MD2BP	-	-	0	0	0	Co-IP	0	0	0	0	0	0	0
Q15058	-	-	KIF14	-	-	0	0	0	Co-IP	0	0	0	0	0	0	0
Q15631	-	8.1004	TSN	-	-	0	0	0	Co-IP	0	0	0	0	0	0	0
Q15788	-	-	NCOA1	-	-	0	0	0	Co-IP	0	0	0	0	0	0	0
Q2TB18	-	-	ASTE1	-	-	0	0	0	Co-IP	0	0	0	0	0	0	0
Q32NF0	-	-	Q32NF0	-	-	0	0	0	Co-IP	0	0	0	0	0	0	0
Q5TA45	-	-	INT11	-	-	0	0	0	Co-IP	0	0	0	0	0	0	0
Q5W0V3	-	-	F16B1	-	-	0	0	0	Co-IP	0	0	0	0	0	0	0
Q63HN8	-	6.3871	RN213	RNF213	-	0	0	0	Co-IP	0	0	0	0	0	0	0
Q658Y4	-	6.1181	F91A1	-	-	0	0	0	Co-IP	0	0	0	0	0	0	0
Q659A1	-	-	ICE2	NARG2	-	0	0	0	Co-IP	0	0	0	0	0	0	0
Q6FI13	-	8.3413	H2A2A	-	-	0	0	0	Co-IP	0	0	0	0	0	0	0
Q6P1X5	-	5.2037	TAF2	TFIID	-	0	0	0	Co-IP	0	0	0	0	0	0	0
Q7Z6I6	-	5.7853	RHG30	-	-	0	0	0	Co-IP	0	0	0	0	0	0	0
Q7Z7H5	-	7.0363	TMED4	-	-	0	0	0	Co-IP	0	0	0	0	0	0	0
Q86U86	-	6.3430	PB1	BAF180	-	0	0	0	Co-IP	0	0	0	0	0	0	0
Q86US8	-	-	EST1A	-	-	0	0	0	Co-IP	0	0	0	0	0	0	0
Q86WJ1	-	6.3051	CHD1L	-	-	0	0	0	Co-IP	0	0	0	0	0	0	0
Q8IUD2	-	5.5241	RB6I2	-	-	0	0	0	Co-IP	0	0	0	0	0	0	0
Q8IWR0	-	-	Z3H7A	-	-	0	0	0	Co-IP	0	0	0	0	0	0	0
Q8N442	-	5.7559	GUF1	-	-	0	0	0	Co-IP	0	0	0	0	0	0	0
Q8TAF3	-	-	WDR48	-	-	0	0	0	Co-IP	0	0	0	0	0	0	0
Q8WUF5	-	5.7487	IASPP	-	-	0	0	0	Co-IP	0	0	0	0	0	0	0
Q8WWN8	-	-	ARAP3	-	-	0	0	0	Co-IP	0	0	0	0	0	0	0
Q8WXI9	-	6.4019	P66B	GATAD2B	-	0	0	0	Co-IP	0	0	0	0	0	0	0
Q92688	-	8.2484	AN32B	-	-	0	0	0	Co-IP	0	0	0	0	0	0	0
Q969U7	-	7.1002	PSMG2	-	-	0	0	0	Co-IP	0	0	0	0	0	0	0
Q96D71	-	6.3771	REPS1	-	-	0	0	0	Co-IP	0	0	0	0	0	0	0
Q96FJ2	-	7.4893	DYL2	-	-	0	0	0	Co-IP	0	0	0	0	0	0	0
Q96HR3	-	-	MED30	-	-	0	0	0	Co-IP	0	0	0	0	0	0	0
Q96Q15	-	-	SMG1	-	-	0	0	0	Co-IP	0	0	0	0	0	0	0
Q96QG7	-	-	MTMR9	-	-	0	0	0	Co-IP	0	0	0	0	0	0	0
Q99856	-	7.0662	ARI3A	-	-	0	0	0	Co-IP	0	0	0	0	0	0	0
Q9BUI4	-	6.3430	RPC3	POLR3C	-	0	0	0	Co-IP	0	0	0	0	0	0	0
Q9BWU1	-	5.5598	CDK19	CDC2L6	-	0	0	0	Co-IP	0	0	0	0	0	0	0
Q9H583	-	7.6247	HEAT1	-	-	0	0	0	Co-IP	0	0	0	0	0	0	0
Q9H5X1	-	6.9063	FA96A	-	-	0	0	0	Co-IP	0	0	0	0	0	0	0
Q9NRG7	-	5.7589	D39U1	-	-	0	0	0	Co-IP	0	0	0	0	0	0	0
Q9NVI7	-	7.2418	ATD3A	-	-	0	0	0	Co-IP	0	0	0	0	0	0	0
Q9NVP1	-	8.0194	DDX18	-	-	0	0	0	Co-IP	0	0	0	0	0	0	0
Q9NZ45	-	7.8771	CISD1	-	-	0	0	0	Co-IP	0	0	0	0	0	0	0
Q9UBP0	-	5.7916	SPAST	-	-	0	0	0	Co-IP	0	0	0	0	0	0	0
Q9UBQ0	-	7.5689	VPS29	-	-	0	0	0	Co-IP	0	0	0	0	0	0	0
Q9UH65	-	-	SWP70	-	-	0	0	0	Co-IP	0	0	0	0	0	0	0
Q9UK45	-	7.2428	LSM7	-	-	0	0	0	Co-IP	0	0	0	0	0	0	0
Q9UKL0	-	-	RCOR1	-	-	0	0	0	Co-IP	0	0	0	0	0	0	0
Q9ULJ3	-	5.7651	ZBT21	-	-	0	0	0	Co-IP	0	0	0	0	0	0	0
Q9UNX4	-	7.2388	WDR3	-	-	0	0	0	Co-IP	0	0	0	0	0	0	0
Q9UPW5	-	6.2017	CBPC1	-	-	0	0	0	Co-IP	0	0	0	0	0	0	0
Q9Y2H2	-	5.6213	SAC2	-	-	0	0	0	Co-IP	0	0	0	0	0	0	0
Q9Y5L0	-	7.1374	TNPO3	IPO12	-	0	0	0	Co-IP	0	0	0	0	0	0	0
Q9Y6C9	-	8.0461	MTCH2	-	-	0	0	0	Co-IP	0	0	0	0	0	0	0
Q9Y6M1	-	-	IF2B2	-	-	0	0	0	Co-IP	0	0	0	0	0	0	0
Q96PK6	BC000488	7.8405	RBM14	SIP	-	0	0	Co-IP	0	0	0	direct interact.	0	direct interact.	0	0
C9JYP6	-	-	C9JYP6	-	-	0	0	Co-IP	0	0	0	0	0	0	0	0
E7ENU4	-	7.2887	E7ENU4	ADAR	-	0	0	Co-IP	0	0	0	0	0	0	0	0
P10412	-	8.3776	H14	H1F4	-	0	0	Co-IP	0	0	0	0	0	0	0	0
P10515	-	7.4802	ODP2	DLAT	DLTA	0	0	Co-IP	0	0	0	0	0	0	0	0
P16401	-	9.2269	H15	H1F5	-	0	0	Co-IP	0	0	0	0	0	0	0	0
P18621	-	8.7622	RL17	RPL17	-	0	0	Co-IP	0	0	0	0	0	0	0	0
P42677	-	8.3097	RS27	RPS27	MPS1	0	0	Co-IP	0	0	0	0	0	0	0	0
P49207	-	8.5371	RL34	RPL34	-	0	0	Co-IP	0	0	0	0	0	0	0	0
P62424	-	8.9776	RL7A	RPL7A	SURF-3	0	0	Co-IP	0	0	0	0	0	0	0	0
Q02878	-	8.9842	RL6	RPL6	TXREB1	0	0	Co-IP	0	0	0	0	0	0	0	0
Q86UE4	-	7.4200	LYRIC	MTDH	AEG1	0	0	Co-IP	0	0	0	0	0	0	0	0
Q96KC8	-	5.5509	DNJC1	DNAJC1	HTJ1	0	0	Co-IP	0	0	0	0	0	0	0	0
Q99417	-	7.5967	MYCBP	AMY1	-	0	0	Co-IP	0	0	0	0	0	0	0	0
Q6PKG0	NM_033551	7.3704	LARP1	KIAA0731	-	0	0	0	0	0	0	direct interact.	direct interact.	direct interact.	direct interact.	0
Q86XP3	NM_007372	6.9329	DDX42	-	-	0	0	0	0	0	0	direct interact.	direct interact.	direct interact.	direct interact.	0
Q96S94	NM_001039577	-	CCNL2	SB138	-	0	0	0	0	0	0	direct interact.	direct interact.	direct interact.	direct interact.	0
Q9NSD4	NM_001080485	-	ZN275	ZNF275	-	0	0	0	0	0	0	direct interact.	direct interact.	direct interact.	direct interact.	0
O60765	NM_005649	-	Z354A	ZNF354A	EZNF	0	0	0	0	0	0	direct interact.	direct interact.	direct interact.	0	direct interact.
Q5M8T3	BC087840	-	Q5M8T3	HES5	-	0	0	0	0	0	0	direct interact.	direct interact.	direct interact.	0	direct interact.
P81877	NM_012446	-	SSBP2	SSDP2	-	0	0	0	0	0	0	direct interact.	direct interact.	direct interact.	0	0

						IP-MS						APS				
UniProt AC	RefSeq ID UniPEx-library	SU-DHL-1 iBAQ [log10 of iBAQ intensity]	Name	Synonyms		HL60 [whole cell lysate]	JEKO-1 [whole cell lysate]	OPM2 [nuclear enriched lysate]	U937 [whole cell lysate]	SU-DHL-1 [whole cell lysate]	SU-DHL-1 [nuclear enriched lysate]	C/EBPβ aa1-41 [CR1-2]	C/EBPε aa1-62 [CR2-4]	C/EBPβ aa49-72 [CR3]	C/EBPβ aa153-173 [CR7]	C/EBPβ aa79-196 [CR4-7]
Q14576	NM_001420	-	ELAV3	ELAVL3	HUC	0	0	0	0	0	0	direct interact.	direct interact.	direct interact.	0	0
Q15388	NM_014765	7.6932	TOM20	TOMM20	KIAA0016	0	0	0	0	0	0	direct interact.	direct interact.	direct interact.	0	0
Q86XZ4	NM_023071	-	SPAS2	SPATS2	SCR59	0	0	0	0	0	0	direct interact.	direct interact.	direct interact.	0	0
Q9H0M5	AK126871	-	ZN700	ZNF700	-	0	0	0	0	0	0	direct interact.	direct interact.	direct interact.	0	0
O14640	NM_004421	-	DVL1	-	-	0	0	0	0	0	0	direct interact.	direct interact.	0	direct interact.	direct interact.
P52824	BC063801	-	DGKQ	DAGK4	-	0	0	0	0	0	0	direct interact.	direct interact.	0	direct interact.	direct interact.
Q92793	NM_004380	5.3233	CBP	CREBBP	-	0	0	0	0	0	0	direct interact.	direct interact.	0	direct interact.	direct interact.
Q9BT23	NM_030576	-	LIMD2	SB143	-	0	0	0	0	0	0	direct interact.	direct interact.	0	direct interact.	direct interact.
O14686	NM_003482	-	KMT2D	MLL2	ALR	0	0	0	0	0	0	direct interact.	direct interact.	0	direct interact.	0
O94910	NM_001008701	-	LPHN1	-	-	0	0	0	0	0	0	direct interact.	direct interact.	0	direct interact.	0
P10588	BC002669	-	NR2F6	EAR2	-	0	0	0	0	0	0	direct interact.	direct interact.	0	direct interact.	0
P43699	NM_003317	-	NKX21	NKX201	NKX2A	0	0	0	0	0	0	direct interact.	direct interact.	0	direct interact.	0
P78543	NM_006763	-	BTG2	PC3	-	0	0	0	0	0	0	direct interact.	direct interact.	0	direct interact.	0
Q13835	NM_000299	-	PKP1	-	-	0	0	0	0	0	0	direct interact.	direct interact.	0	direct interact.	0
Q1KMD3	DQ470474	7.3715	HNRL2	HNRPUL2	-	0	0	0	0	0	0	direct interact.	direct interact.	0	direct interact.	0
Q6DD87	BC077728	-	ZN787	ZNF787	-	0	0	0	0	0	0	direct interact.	direct interact.	0	direct interact.	0
Q8NDT2	NM_013286	5.6036	RB15B	RBM15B	OTT3	0	0	0	0	0	0	direct interact.	direct interact.	0	direct interact.	0
Q8TBZ5	NM_033210	-	ZN502	ZNF502	-	0	0	0	0	0	0	direct interact.	direct interact.	0	direct interact.	0
Q96MS0	AY509035	-	ROBO3	-	-	0	0	0	0	0	0	direct interact.	direct interact.	0	direct interact.	0
Q9UL40	NM_012279	-	ZN346	ZNF346	JAZ	0	0	0	0	0	0	direct interact.	direct interact.	0	direct interact.	0
P62979	BE875057	9.0349	RS27A	-	-	0	0	0	0	0	0	direct interact.	direct interact.	0	0	direct interact.
Q00604	X65724	-	NDP	EVR2	-	0	0	0	0	0	0	direct interact.	direct interact.	0	0	direct interact.
B2R4W8	AK054921	-	B2R4W8	-	-	0	0	0	0	0	0	direct interact.	direct interact.	0	0	0
P69905	BQ709225	8.6265	HBA	HBA1	HBA2	0	0	0	0	0	0	direct interact.	direct interact.	0	0	0
Q01844	BX648769	7.4015	EWS	EWSR1	-	0	0	0	0	0	0	direct interact.	direct interact.	0	0	0
Q15717	NM_001419	-	ELAV1	ELAVL1	HUR	0	0	0	0	0	0	direct interact.	direct interact.	0	0	0
Q7L190	NM_018189	-	DPPA4	-	-	0	0	0	0	0	0	direct interact.	direct interact.	0	0	0
Q8N9T8	NM_023008	6.3754	KRI1	-	-	0	0	0	0	0	0	direct interact.	direct interact.	0	0	0
Q99729	NM_031266	-	ROAA	HNRNPAB	ABBP1	0	0	0	0	0	0	direct interact.	direct interact.	0	0	0
Q9UK76	BC039343	7.6306	HN1	ARM2	-	0	0	0	0	0	0	direct interact.	direct interact.	0	0	0
Q14011	AK095781	-	CIRBP	-	-	0	0	0	0	0	0	direct interact.	0	direct interact.	direct interact.	direct interact.
B3KPK9	AK056467	-	B3KPK9	-	-	0	0	0	0	0	0	direct interact.	0	direct interact.	direct interact.	0
P79522	NM_025263	6.3581	PRR3	CAT56	-	0	0	0	0	0	0	direct interact.	0	direct interact.	direct interact.	0
Q8NEZ9	AK090484	-	Q8NEZ9	FLJ00406	-	0	0	0	0	0	0	direct interact.	0	direct interact.	direct interact.	0
Q92614	D86970	-	MY18A	MYO18A	KIAA0216	0	0	0	0	0	0	direct interact.	0	direct interact.	direct interact.	0
P61204	NM_001659	-	ARF3	-	-	0	0	0	0	0	0	direct interact.	0	direct interact.	0	direct interact.
B3KTY1	NM_138356	-	B3KTY1	-	-	0	0	0	0	0	0	direct interact.	0	direct interact.	0	0
B3KY12	AK128438	-	B3KY12	-	-	0	0	0	0	0	0	direct interact.	0	direct interact.	0	0
D6W5D9	NM_022893	-	D6W5D9	BCL11A	-	0	0	0	0	0	0	direct interact.	0	direct interact.	0	0
O14979	NM_031372	8.0489	HNRDL	HNRPDL	JKTBP	0	0	0	0	0	0	direct interact.	0	direct interact.	0	0
O43776	NM_004539	7.5364	SYNC	NARS	-	0	0	0	0	0	0	direct interact.	0	direct interact.	0	0
P49247	NM_144563	7.3865	RPIA	RPI	-	0	0	0	0	0	0	direct interact.	0	direct interact.	0	0
P62136	AK098311	8.3001	PP1A	PPP1CA	PPP1A	0	0	0	0	0	0	direct interact.	0	direct interact.	0	0
Q06945	NM_003107	-	SOX4	-	-	0	0	0	0	0	0	direct interact.	0	direct interact.	0	0
Q12824	NM_003073	-	SNF5	SMARCB1	BAF47	0	0	0	0	0	0	direct interact.	0	direct interact.	0	0
Q15059	NM_007371	5.6380	BRD3	KIAA0043	-	0	0	0	0	0	0	direct interact.	0	direct interact.	0	0
Q15784	NM_006160	-	NDF2	NEUROD2	BHLHA1	0	0	0	0	0	0	direct interact.	0	direct interact.	0	0
Q2QGD7	NM_001040653	-	ZXDC	ZXDL	-	0	0	0	0	0	0	direct interact.	0	direct interact.	0	0
Q6ZS47	AK127739	-	Q6ZS47	-	-	0	0	0	0	0	0	direct interact.	0	direct interact.	0	0
Q8IZ52	AB095813	-	CHSS2	CHPF	CSS2	0	0	0	0	0	0	direct interact.	0	direct interact.	0	0
Q8NF73	AK090406	-	Q8NF73	FLJ00296	-	0	0	0	0	0	0	direct interact.	0	direct interact.	0	0
Q92576	BX648268	5.5810	PHF3	KIAA0244	-	0	0	0	0	0	0	direct interact.	0	direct interact.	0	0
Q92913	BC012347	-	FGF13	FHF2	-	0	0	0	0	0	0	direct interact.	0	direct interact.	0	0
Q969T9	NM_012478	-	WBP2	-	-	0	0	0	0	0	0	direct interact.	0	direct interact.	0	0
Q96G74	NM_017602	-	OTUD5	-	-	0	0	0	0	0	0	direct interact.	0	direct interact.	0	0
Q96JB5	AF217982	-	CK5P3	CDK5RAP3	IC53	0	0	0	0	0	0	direct interact.	0	direct interact.	0	0
Q9H813	AK001736	-	TM206	TMEM206	C1orf75	0	0	0	0	0	0	direct interact.	0	direct interact.	0	0
Q9H8M2	BC007217	-	BRD9	UNQ3040	-	0	0	0	0	0	0	direct interact.	0	direct interact.	0	0
Q9NW64	AL136933	6.3840	RBM22	ZC3H16	-	0	0	0	0	0	0	direct interact.	0	direct interact.	0	0
Q9NWF9	NM_207111	-	RN216	RNF216	TRIAD3	0	0	0	0	0	0	direct interact.	0	direct interact.	0	0
Q9UBG0	NM_006039	5.3243	MRC2	CLEC13E	-	0	0	0	0	0	0	direct interact.	0	direct interact.	0	0
Q9UBL0	NM_016300	-	ARP21	ARPP21	TARPP	0	0	0	0	0	0	direct interact.	0	direct interact.	0	0
Q9UL33	AK126779	-	TPC2L	TRAPPC2L	HSPC126	0	0	0	0	0	0	direct interact.	0	direct interact.	0	0
Q9Y508	NM_018683	-	RN114	RNF114	ZNF228	0	0	0	0	0	0	direct interact.	0	direct interact.	0	0
Q59F65	AB209596	-	Q59F65	-	-	0	0	0	0	0	0	direct interact.	0	0	direct interact.	0
O00468	AB191264	5.4766	AGRIN	AGRN	-	0	0	0	0	0	0	direct interact.	0	0	direct interact.	0
O14730	NM_003831	-	RIOK3	SUDD	-	0	0	0	0	0	0	direct interact.	0	0	direct interact.	0
O14978	NM_005741	-	ZN263	ZNF263	FPM315	0	0	0	0	0	0	direct interact.	0	0	direct interact.	0
O15428	U82382	-	PINL	PIN1L	-	0	0	0	0	0	0	direct interact.	0	0	direct interact.	0
O43159	AB007869	6.5605	RRP8	-	-	0	0	0	0	0	0	direct interact.	0	0	direct interact.	0
O75325	AF030435	-	LRRN2	GAC1	-	0	0	0	0	0	0	direct interact.	0	0	direct interact.	0
O95248	BC087612	-	MTMR5	SBF1	-	0	0	0	0	0	0	direct interact.	0	0	direct interact.	0
P01137	X02812	-	TGFB1	TGFB	-	0	0	0	0	0	0	direct interact.	0	0	direct interact.	0
P25774	NM_004079	-	CATS	CTSS	-	0	0	0	0	0	0	direct interact.	0	0	direct interact.	0
P29590	NM_033238	5.3306	PML	MYL	-	0	0	0	0	0	0	direct interact.	0	0	direct interact.	0
P51911	BC036307	-	CNN1	-	-	0	0	0	0	0	0	direct interact.	0	0	direct interact.	0
P56270	NM_001042539	-	MAZ	ZNF801	-	0	0	0	0	0	0	direct interact.	0	0	direct interact.	0
Q04206	BC110830	6.5697	TF65	RELA	NFKB3	0	0	0	0	0	0	direct interact.	0	0	direct interact.	0
Q06587	BC002922	5.9522	RING1	RNF1	-	0	0	0	0	0	0	direct interact.	0	0	direct interact.	0
Q13685	NM_001087	-	AAMP	-	-	0	0	0	0	0	0	direct interact.	0	0	direct interact.	0
Q14160	NM_182706	6.1380	SCRIB	CRIB1	-	0	0	0	0	0	0	direct interact.	0	0	direct interact.	0
Q14584	AB095928	-	ZN266	ZNF266	KIAA2007	0	0	0	0	0	0	direct interact.	0	0	direct interact.	0
Q15560	AK226140	-	TCEA2	-	-	0	0	0	0	0	0	direct interact.	0	0	direct interact.	0
Q25QX8	AB065282	-	Q25QX8	TIPUH1	-	0	0	0	0	0	0	direct interact.	0	0	direct interact.	0
Q3T8J9	AY335491	-	GON4L	GON4	-	0	0	0	0	0	0	direct interact.	0	0	direct interact.	0
Q499Z4	BC035140	-	ZN672	ZNF672	-	0	0	0	0	0	0	direct interact.	0	0	direct interact.	0
Q4LE74	AB209997	-	Q4LE74	MYO9B	-	0	0	0	0	0	0	direct interact.	0	0	direct interact.	0
Q59F37	AB209624	-	Q59F37	-	-	0	0	0	0	0	0	direct interact.	0	0	direct interact.	0
Q59FF1	AB209509	-	Q59FF1	-	-	0	0	0	0	0	0	direct interact.	0	0	direct interact.	0
Q59FY8	AB209321	-	Q59FY8	-	-	0	0	0	0	0	0	direct interact.	0	0	direct interact.	0
Q59H57	AB208902	-	Q59H57	-	-	0	0	0	0	0	0	direct interact.	0	0	direct interact.	0

						IP-MS						APS				
UniProt AC	RefSeq ID UniPEx-library	SU-DHL-1 iBAQ [log10 of iBAQ intensity]	Name	Synonyms		HL60 [whole cell lysate]	JEKO-1 [whole cell lysate]	OPM2 [nuclear enriched lysate]	U937 [whole cell lysate]	SU-DHL-1 [whole cell lysate]	SU-DHL-1 [nuclear enriched lysate]	C/EBPβ aa1-41 [CR1-2]	C/EBPε aa1-62 [CR2-4]	C/EBPβ aa49-72 [CR3]	C/EBPβ aa153-173 [CR7]	C/EBPβ aa79-196 [CR4-7]
Q5SWA1	BC065280	-	PR15B	PPP1R15B	-	0	0	0	0	0	0	direct interact.	0	0	direct interact.	0
Q5T9A4	AB033099	6.2726	ATD3B	ATAD3B	KIAA1273	0	0	0	0	0	0	direct interact.	0	0	direct interact.	0
Q6P597	BC073841	-	KLC3	KLC2	-	0	0	0	0	0	0	direct interact.	0	0	direct interact.	0
Q6P6B7	BC067892	-	ANR16	ANKRD16	-	0	0	0	0	0	0	direct interact.	0	0	direct interact.	0
Q8IWT6	NM_019594	-	LRC8A	LRRC8A	KIAA1437	0	0	0	0	0	0	direct interact.	0	0	direct interact.	0
Q8N3V7	AB028952	6.4326	SYNPO	KIAA1029	-	0	0	0	0	0	0	direct interact.	0	0	direct interact.	0
Q8WW22	NM_018602	6.7323	DNJA4	DNAJA4	-	0	0	0	0	0	0	direct interact.	0	0	direct interact.	0
Q969Z0	AB023165	7.1716	TBRG4	CPR2	-	0	0	0	0	0	0	direct interact.	0	0	direct interact.	0
Q96B54	NM_182498	-	ZN428	ZNF428	C19orf37	0	0	0	0	0	0	direct interact.	0	0	direct interact.	0
Q99661	NM_006845	7.1920	KIF2C	KNSL6	-	0	0	0	0	0	0	direct interact.	0	0	direct interact.	0
Q99941	NM_004381	-	ATF6B	CREBL1	-	0	0	0	0	0	0	direct interact.	0	0	direct interact.	0
Q9BZR9	NM_030912	-	TRIM8	GERP	-	0	0	0	0	0	0	direct interact.	0	0	direct interact.	0
Q9C0C2	NM_033396	5.4274	TB182	TNKS1BP1	KIAA1741	0	0	0	0	0	0	direct interact.	0	0	direct interact.	0
Q9NV56	NM_018270	6.7385	MRGBP	C20orf20	-	0	0	0	0	0	0	direct interact.	0	0	direct interact.	0
Q9UIS9	NM_015846	-	MBD1	CXXC3	-	0	0	0	0	0	0	direct interact.	0	0	direct interact.	0
Q9Y468	AB014581	-	LMBL1	L3MBTL1	KIAA0681	0	0	0	0	0	0	direct interact.	0	0	direct interact.	0
Q9Y5S2	AF128625	-	MRCKB	CDC42BPB	KIAA1124	0	0	0	0	0	0	direct interact.	0	0	direct interact.	0
Q0664	BC018898	-	-	-	-	0	0	0	0	0	0	direct interact.	0	0	0	direct interact.
Q15773	BM919311	-	MLF2	-	-	0	0	0	0	0	0	direct interact.	0	0	0	direct interact.
Q9P253	AL713725	6.2793	VPS18	KIAA1475	-	0	0	0	0	0	0	direct interact.	0	0	0	direct interact.
A6NDC7	AK092882	-	A6NDC7	-	-	0	0	0	0	0	0	direct interact.	0	0	0	0
B3KNA8	AK024202	-	B3KNA8	-	-	0	0	0	0	0	0	direct interact.	0	0	0	0
B3KNS9	AK054888	-	B3KNS9	-	-	0	0	0	0	0	0	direct interact.	0	0	0	0
B3KQ39	AK057302	-	B3KQ39	-	-	0	0	0	0	0	0	direct interact.	0	0	0	0
B3KQE6	AK074821	-	B3KQE6	-	-	0	0	0	0	0	0	direct interact.	0	0	0	0
B3KR73	AK091118	-	B3KR73	-	-	0	0	0	0	0	0	direct interact.	0	0	0	0
B3KSB0	AK093216	-	B3KSB0	NCBP2	-	0	0	0	0	0	0	direct interact.	0	0	0	0
B3KUN3	AK097610	-	B3KUN3	-	-	0	0	0	0	0	0	direct interact.	0	0	0	0
B3KW85	AK124526	-	B3KW85	BCAR1	-	0	0	0	0	0	0	direct interact.	0	0	0	0
B3KWB2	AK124709	-	B3KWB2	-	-	0	0	0	0	0	0	direct interact.	0	0	0	0
B3KWN0	AK125379	-	B3KWN0	-	-	0	0	0	0	0	0	direct interact.	0	0	0	0
B5B2S0	NM_004555	-	B5B2S0	NFATC3	-	0	0	0	0	0	0	direct interact.	0	0	0	0
D9ZGF1	NM_006079	-	D9ZGF1	CITED2	-	0	0	0	0	0	0	direct interact.	0	0	0	0
O00255	NM_130803	-	MEN1	-	SCG2	0	0	0	0	0	0	direct interact.	0	0	0	0
O00622	Y11307	-	CYR61	CCN1	-	0	0	0	0	0	0	direct interact.	0	0	0	0
O14492	NM_020979	-	SH2B2	APS	-	0	0	0	0	0	0	direct interact.	0	0	0	0
O14986	BC030587	-	PI51B	PIP5K1B	STM7	0	0	0	0	0	0	direct interact.	0	0	0	0
O15054	NM_001080424	-	KDM6B	JMJD3	-	0	0	0	0	0	0	direct interact.	0	0	0	0
O15209	NM_005453	-	ZBT22	ZBTB22	BING1	0	0	0	0	0	0	direct interact.	0	0	0	0
O15230	NM_005560	-	LAMA5	-	-	0	0	0	0	0	0	direct interact.	0	0	0	0
O15379	AF005482	6.0241	HDAC3	-	-	0	0	0	0	0	0	direct interact.	0	0	0	0
O43474	NM_004235	-	KLF4	EZF	-	0	0	0	0	0	0	direct interact.	0	0	0	0
O43768	NM_207043	-	ENSA	-	-	0	0	0	0	0	0	direct interact.	0	0	0	0
O60499	BQ057394	6.5230	STX10	SYN10	-	0	0	0	0	0	0	direct interact.	0	0	0	0
O60547	AK130651	6.8815	GMDS	-	-	0	0	0	0	0	0	direct interact.	0	0	0	0
O60828	BM909365	6.7803	PQBP1	NPW38	-	0	0	0	0	0	0	direct interact.	0	0	0	0
O75110	NM_006045	-	ATP9A	ATPIIA	-	0	0	0	0	0	0	direct interact.	0	0	0	0
O75509	AB209394	-	TNR21	TNFRSF21	DR6	0	0	0	0	0	0	direct interact.	0	0	0	0
O75832	NM_002814	7.1072	PSD10	PSMD10	-	0	0	0	0	0	0	direct interact.	0	0	0	0
O76003	AK021926	8.0572	GLRX3	PICOT	-	0	0	0	0	0	0	direct interact.	0	0	0	0
O94941	NM_014948	-	RNF37	UBOX5	-	0	0	0	0	0	0	direct interact.	0	0	0	0
O94972	NM_015294	-	TRI37	TRIM37	-	0	0	0	0	0	0	direct interact.	0	0	0	0
O94985	AB020718	-	CSTN1	CLSTN1	-	0	0	0	0	0	0	direct interact.	0	0	0	0
O95125	NM_003455	-	ZN202	ZNF202	-	0	0	0	0	0	0	direct interact.	0	0	0	0
O95376	NM_006321	-	ARI2	ARIH2	-	0	0	0	0	0	0	direct interact.	0	0	0	0
O95793	NM_017453	7.4571	STAU1	STAU	-	0	0	0	0	0	0	direct interact.	0	0	0	0
P00387	NM_007326	7.8604	NB5R3	CYB5R3	DIA1	0	0	0	0	0	0	direct interact.	0	0	0	0
P01023	CR749334	-	A2MG	A2M	CPAMD5	0	0	0	0	0	0	direct interact.	0	0	0	0
P02461	NM_000090	-	CO3A1	COL3A1	-	0	0	0	0	0	0	direct interact.	0	0	0	0
P02749	BC026283	-	APOH	B2G1	-	0	0	0	0	0	0	direct interact.	0	0	0	0
P02768	AF130077	-	ALBU	ALB	GIG20	0	0	0	0	0	0	direct interact.	0	0	0	0
P04049	NM_002880	-	RAF1	-	-	0	0	0	0	0	0	direct interact.	0	0	0	0
P07858	NM_147780	7.9285	CATB	CTSB	CPSB	0	0	0	0	0	0	direct interact.	0	0	0	0
P07996	NM_003246	-	TSP1	THBS1	TSP	0	0	0	0	0	0	direct interact.	0	0	0	0
P08047	NM_138473	-	SP1	TSFP1	-	0	0	0	0	0	0	direct interact.	0	0	0	0
P08253	NM_004530	-	MMP2	CLG4A	-	0	0	0	0	0	0	direct interact.	0	0	0	0
P14649	BQ673169	5.9642	MYL6B	MLC1SA	-	0	0	0	0	0	0	direct interact.	0	0	0	0
P14921	NM_005238	-	ETS1	EWSR2	-	0	0	0	0	0	0	direct interact.	0	0	0	0
P15976	NM_002049	-	GATA1	ERYF1	-	0	0	0	0	0	0	direct interact.	0	0	0	0
P17026	NM_006963	6.3086	ZNF22	KOX15	-	0	0	0	0	0	0	direct interact.	0	0	0	0
P18848	NM_001675	-	ATF4	CREB2	-	0	0	0	0	0	0	direct interact.	0	0	0	0
P21695	NM_005276	-	GPDA	GPD1	-	0	0	0	0	0	0	direct interact.	0	0	0	0
P24593	NM_000599	-	IBP5	IGFBP5	-	0	0	0	0	0	0	direct interact.	0	0	0	0
P25791	NM_005574	-	RBTN2	LMO2	-	0	0	0	0	0	0	direct interact.	0	0	0	0
P26378	BC036071	-	ELAV4	ELAVL4	HUD	0	0	0	0	0	0	direct interact.	0	0	0	0
P27918	AK122955	-	PROP	CFP	PFC	0	0	0	0	0	0	direct interact.	0	0	0	0
P29279	NM_001901	-	CTGF	CCN2	-	0	0	0	0	0	0	direct interact.	0	0	0	0
P29597	NM_003331	-	TYK2	-	-	0	0	0	0	0	0	direct interact.	0	0	0	0
P30040	NM_006817	8.2806	ERP29	C12orf8	-	0	0	0	0	0	0	direct interact.	0	0	0	0
P35080	BC043646	-	PROF2	PFN2	-	0	0	0	0	0	0	direct interact.	0	0	0	0
P35269	NM_002096	7.4058	T2FA	GTF2F1	RAP74	0	0	0	0	0	0	direct interact.	0	0	0	0
P35442	NM_003247	-	TSP2	THBS2	-	0	0	0	0	0	0	direct interact.	0	0	0	0
P38936	NM_078467	-	CDN1A	p21	CDKN1A	0	0	0	0	0	0	direct interact.	0	0	0	0
P40855	NM_002857	6.8640	PEX19	HK33	-	0	0	0	0	0	0	direct interact.	0	0	0	0
P41221	NM_003392	-	WNT5A	-	-	0	0	0	0	0	0	direct interact.	0	0	0	0
P41229	NM_004187	-	KDM5C	JARID1C	-	0	0	0	0	0	0	direct interact.	0	0	0	0
P51523	BC036656	-	ZNF84	-	-	0	0	0	0	0	0	direct interact.	0	0	0	0
P51693	NM_001024807	-	APLP1	-	-	0	0	0	0	0	0	direct interact.	0	0	0	0
P52737	AK123008	-	ZN136	ZNF136	-	0	0	0	0	0	0	direct interact.	0	0	0	0
P53804	D84294	-	TTC3	DCRR1	-	0	0	0	0	0	0	direct interact.	0	0	0	0
P54105	NM_001293	7.5603	ICLN	CLNS1A	CLCI	0	0	0	0	0	0	direct interact.	0	0	0	0

						IP-MS						APS				
UniProt AC	RefSeq ID UniPEx-library	SU-DHL-1 iBAQ [log10 of iBAQ intensity]	Name	Synonyms		HL60 [whole cell lysate]	JEKO-1 [whole cell lysate]	OPM2 [nuclear enriched lysate]	U937 [whole cell lysate]	SU-DHL-1 [whole cell lysate]	SU-DHL-1 [nuclear enriched lysate]	C/EBPβ aa1-41 [CR1-2]	C/EBPε aa1-62 [CR2-4]	C/EBPβ aa49-72 [CR3]	C/EBPβ aa153-173 [CR7]	C/EBPβ aa79-196 [CR4-7]
P61968	NM_006769	-	LMO4	-	-	0	0	0	0	0	0	direct interact.	0	0	0	0
P62841	BM923584	-	RS15	RPS15	RIG	0	0	0	0	0	0	direct interact.	0	0	0	0
P68133	BC012597	-	ACTS	ACTA1	ACTA	0	0	0	0	0	0	direct interact.	0	0	0	0
P98175	NM_005676	6.6396	RBM10	DXS8237E	-	0	0	0	0	0	0	direct interact.	0	0	0	0
Q04725	NM_003260	-	TLE2	-	-	0	0	0	0	0	0	direct interact.	0	0	0	0
Q05923	L11329	-	DUS2	DUSP2	PAC1	0	0	0	0	0	0	direct interact.	0	0	0	0
Q06889	NM_004430	-	EGR3	PILOT	-	0	0	0	0	0	0	direct interact.	0	0	0	0
Q13127	NM_005612	-	REST	NRSF	-	0	0	0	0	0	0	direct interact.	0	0	0	0
Q13616	NM_003592	6.9944	CUL1	-	-	0	0	0	0	0	0	direct interact.	0	0	0	0
Q13625	NM_005426	-	ASPP2	TP53BP2	-	0	0	0	0	0	0	direct interact.	0	0	0	0
Q13642	AK122708	-	FHL1	SLIM1	-	0	0	0	0	0	0	direct interact.	0	0	0	0
Q13751	NM_001025598	-	LAMB3	LAMNB1	-	0	0	0	0	0	0	direct interact.	0	0	0	0
Q14201	BC011957	-	BTG3	ANA	-	0	0	0	0	0	0	direct interact.	0	0	0	0
Q14C66	NM_001109	-	Q14C66	ADAM8	-	0	0	0	0	0	0	direct interact.	0	0	0	0
Q14CW9	NM_020218	-	AT7L3	ATXN7L3	-	0	0	0	0	0	0	direct interact.	0	0	0	0
Q15070	BX248001	-	OXA1L	-	-	0	0	0	0	0	0	direct interact.	0	0	0	0
Q15334	NM_004140	-	L2GL1	LLGL1	DLG4	0	0	0	0	0	0	direct interact.	0	0	0	0
Q15393	D13642	8.0127	SF3B3	KIAA0017	-	0	0	0	0	0	0	direct interact.	0	0	0	0
Q15628	AK090673	6.9764	TRADD	-	-	0	0	0	0	0	0	direct interact.	0	0	0	0
Q15935	BC043354	-	ZNF77	-	-	0	0	0	0	0	0	direct interact.	0	0	0	0
Q16881	NM_003330	7.9267	TRXR1	TXNRD1	GRIM12	0	0	0	0	0	0	direct interact.	0	0	0	0
Q2TAZ0	BC110650	-	ATG2A	KIAA0404	-	0	0	0	0	0	0	direct interact.	0	0	0	0
Q2YDX2	NM_014643	-	Q2YDX2	ZNF516	-	0	0	0	0	0	0	direct interact.	0	0	0	0
Q32P51	AK126454	-	RA1L2	HNRNPA1L	-	0	0	0	0	0	0	direct interact.	0	0	0	0
Q3KQV3	NM_175872	-	ZN792	ZNF792	-	0	0	0	0	0	0	direct interact.	0	0	0	0
Q3V5L5	AB235153	-	MGT5B	MGAT5B	KIAA2008	0	0	0	0	0	0	direct interact.	0	0	0	0
Q3ZCU9	BC039299	-	Q3ZCU9	STIP1	-	0	0	0	0	0	0	direct interact.	0	0	0	0
Q4VBQ6	NM_016162	-	Q4VBQ6	-	-	0	0	0	0	0	0	direct interact.	0	0	0	0
Q53EL4	AK223625	-	Q53EL4	-	-	0	0	0	0	0	0	direct interact.	0	0	0	0
Q59F46	AB209615	-	Q59F46	-	-	0	0	0	0	0	0	direct interact.	0	0	0	0
Q59FM7	AB209433	-	Q59FM7	-	-	0	0	0	0	0	0	direct interact.	0	0	0	0
Q59FW3	AB209346	-	Q59FW3	-	-	0	0	0	0	0	0	direct interact.	0	0	0	0
Q59HB4	AB208845	-	Q59HB4	-	-	0	0	0	0	0	0	direct interact.	0	0	0	0
Q5MNZ6	NM_019613	-	WIPI3	WDR45B	WDR45L	0	0	0	0	0	0	direct interact.	0	0	0	0
Q5TGY3	NM_001029882	-	AHDC1	-	-	0	0	0	0	0	0	direct interact.	0	0	0	0
Q5VUD6	AF318355	-	FA69B	FAM69B	C9orf136	0	0	0	0	0	0	direct interact.	0	0	0	0
Q63HK3	CA434734	-	ZKSC2	ZKSCAN2	ZNF694	0	0	0	0	0	0	direct interact.	0	0	0	0
Q676U5	NM_030803	-	A16L1	ATG16L1	APG16L	0	0	0	0	0	0	direct interact.	0	0	0	0
Q69YH5	NM_152562	5.7600	CDCA2	-	-	0	0	0	0	0	0	direct interact.	0	0	0	0
Q6NTE8	BX537968	-	CE045	C5orf45	-	0	0	0	0	0	0	direct interact.	0	0	0	0
Q6P0P0	NM_052897	-	Q6P0P0	MBD6	-	0	0	0	0	0	0	direct interact.	0	0	0	0
Q6P4A8	NM_024829	-	PLBL1	PLBD1	-	0	0	0	0	0	0	direct interact.	0	0	0	0
Q6ZN04	AK131424	-	MEX3B	KIAA2009	-	0	0	0	0	0	0	direct interact.	0	0	0	0
Q6ZNI9	AK131106	-	Q6ZNI9	FLJ00395	-	0	0	0	0	0	0	direct interact.	0	0	0	0
Q6ZQU7	AK128712	-	Q6ZQU7	-	-	0	0	0	0	0	0	direct interact.	0	0	0	0
Q7Z5J4	NM_030665	-	RAI1	KIAA1820	-	0	0	0	0	0	0	direct interact.	0	0	0	0
Q7Z7K2	AK131441	-	ZN467	ZNF467	-	0	0	0	0	0	0	direct interact.	0	0	0	0
Q86V38	BC051795	-	Q86V38	ATN1	-	0	0	0	0	0	0	direct interact.	0	0	0	0
Q86WZ6	BC047570	-	ZN227	ZNF227	-	0	0	0	0	0	0	direct interact.	0	0	0	0
Q86YR5	AL117478	-	GPSM1	AGS3	-	0	0	0	0	0	0	direct interact.	0	0	0	0
Q8IVM0	AJ557013	6.1927	CCD50	CCDC50	C3orf6	0	0	0	0	0	0	direct interact.	0	0	0	0
Q8IWC1	AL832120	-	MA7D3	MAP7D3	-	0	0	0	0	0	0	direct interact.	0	0	0	0
Q8IWT3	CR749511	-	CUL9	H7AP1	-	0	0	0	0	0	0	direct interact.	0	0	0	0
Q8IXK2	NM_024642	-	GLT12	GALNT12	-	0	0	0	0	0	0	direct interact.	0	0	0	0
Q8IXR4	BC039496	-	Q8IXR4	-	-	0	0	0	0	0	0	direct interact.	0	0	0	0
Q8IXW5	AK023212	-	RPAP2	C1orf82	-	0	0	0	0	0	0	direct interact.	0	0	0	0
Q8IY17	BC050553	6.1829	PLPL6	PNPLA6	NTE	0	0	0	0	0	0	direct interact.	0	0	0	0
Q8IYI8	AK095252	-	ZN440	ZNF440	-	0	0	0	0	0	0	direct interact.	0	0	0	0
Q8N1G0	AB037862	-	ZN687	ZNF687	KIAA1441	0	0	0	0	0	0	direct interact.	0	0	0	0
Q8N3F0	NM_152793	-	MTURN	C7orf41	-	0	0	0	0	0	0	direct interact.	0	0	0	0
Q8N567	AL512712	-	ZCHC9	ZCCHC9	-	0	0	0	0	0	0	direct interact.	0	0	0	0
Q8NB37	NM_182612	-	PDDC1	-	-	0	0	0	0	0	0	direct interact.	0	0	0	0
Q8ND25	NM_032268	-	ZNRF1	NIN283	-	0	0	0	0	0	0	direct interact.	0	0	0	0
Q8NDP4	AL833935	-	ZN439	ZNF439	-	0	0	0	0	0	0	direct interact.	0	0	0	0
Q8NE65	BC034499	-	ZN738	ZNF738	-	0	0	0	0	0	0	direct interact.	0	0	0	0
Q8NEB1	NM_033141	-	Q8NEB1	-	-	0	0	0	0	0	0	direct interact.	0	0	0	0
Q8TAP4	NM_018640	-	LMO3	RBTN3	-	0	0	0	0	0	0	direct interact.	0	0	0	0
Q8TAS9	BC025971	-	Q8TAS9	C7orf50	-	0	0	0	0	0	0	direct interact.	0	0	0	0
Q8TEK3	AB058717	-	DOT1L	KIAA1814	-	0	0	0	0	0	0	direct interact.	0	0	0	0
Q8WYH8	NM_032329	-	ING5	-	-	0	0	0	0	0	0	direct interact.	0	0	0	0
Q969K4	AF447886	-	ABTB1	BPOZ	-	0	0	0	0	0	0	direct interact.	0	0	0	0
Q96BJ3	BC015535	-	AIDA	C1orf80	-	0	0	0	0	0	0	direct interact.	0	0	0	0
Q96C19	NM_024329	7.5948	EFHD2	SWS1	-	0	0	0	0	0	0	direct interact.	0	0	0	0
Q96EP1	BC012072	-	CHFR	RNF196	-	0	0	0	0	0	0	direct interact.	0	0	0	0
Q96GP6	NM_153334	-	SREC2	SCARF2	-	0	0	0	0	0	0	direct interact.	0	0	0	0
Q96HZ4	AK075040	-	HES6	BHLHB41	-	0	0	0	0	0	0	direct interact.	0	0	0	0
Q96JF6	AB058774	-	ZN594	ZNF594	KIAA1871	0	0	0	0	0	0	direct interact.	0	0	0	0
Q96JW5	AK027837	-	Q96JW5	BZW2	-	0	0	0	0	0	0	direct interact.	0	0	0	0
Q96K62	NM_032792	-	ZBT45	ZBTB45	ZNF499	0	0	0	0	0	0	direct interact.	0	0	0	0
Q96MT1	BC042684	-	RN145	RNF145	-	0	0	0	0	0	0	direct interact.	0	0	0	0
Q96NM4	AK055135	-	TOX2	C20orf100	-	0	0	0	0	0	0	direct interact.	0	0	0	0
Q96PE2	NM_014786	-	ARHGH	KIAA0337	-	0	0	0	0	0	0	direct interact.	0	0	0	0
Q96RP9	AF309777	7.4132	EFGM	GFM1	EFG	0	0	0	0	0	0	direct interact.	0	0	0	0
Q96ST2	AK027561	6.6758	IWS1	IWS1L	-	0	0	0	0	0	0	direct interact.	0	0	0	0
Q96T37	BC042587	6.4774	RBM15	OTT	-	0	0	0	0	0	0	direct interact.	0	0	0	0
Q99439	NM_004368	-	CNN2	-	-	0	0	0	0	0	0	direct interact.	0	0	0	0
Q99543	NM_014377	7.0904	DNJC2	DNAJC2	1	0	0	0	0	0	0	direct interact.	0	0	0	0
Q99750	CR594049	-	MDFI	-	-	0	0	0	0	0	0	direct interact.	0	0	0	0
Q9BWG4	NM_033044	-	SSBP4	-	-	0	0	0	0	0	0	direct interact.	0	0	0	0
Q9BWG6	AK056322	-	SCNM1	-	-	0	0	0	0	0	0	direct interact.	0	0	0	0
Q9C0K0	NM_138576	-	BC11B	BCL11B	CTIP2	0	0	0	0	0	0	direct interact.	0	0	0	0

						IP-MS						APS				
UniProt AC	RefSeq ID UniPEx-library	SU-DHL-1 iBAQ [log10 of iBAQ intensity]	Name	Synonyms		HL60 [whole cell lysate]	JEKO-1 [whole cell lysate]	OPM2 [nuclear enriched lysate]	U937 [whole cell lysate]	SU-DHL-1 [whole cell lysate]	SU-DHL-1 [nuclear enriched lysate]	C/EBPβ aa1-41 [CR1-2]	C/EBPε aa1-62 [CR2-4]	C/EBPβ aa49-72 [CR3]	C/EBPβ aa153-173 [CR7]	C/EBPβ aa79-196 [CR4-7]
Q9H211	AB053172	-	CDT1	-	-	0	0	0	0	0	0	direct interact.	0	0	0	0
Q9H3P2	AK126056	7.0487	NELFA	WHSC2	-	0	0	0	0	0	0	direct interact.	0	0	0	0
Q9H4M3	CR749368	-	FBX44	FBXO44	FBG3	0	0	0	0	0	0	direct interact.	0	0	0	0
Q9HBE1	NM_014323	-	PATZ1	PATZ	-	0	0	0	0	0	0	direct interact.	0	0	0	0
Q9HCS7	AK074035	7.0928	SYF1	XAB2	HCNP	0	0	0	0	0	0	direct interact.	0	0	0	0
Q9NR46	AL832592	-	SHLB2	SH3GLB2	KIAA1848	0	0	0	0	0	0	direct interact.	0	0	0	0
Q9NSK0	AK055293	5.5281	KLC4	KNSL8	-	0	0	0	0	0	0	direct interact.	0	0	0	0
Q9NSV7	AL137714	-	Q9NSV7	1323	-	0	0	0	0	0	0	direct interact.	0	0	0	0
Q9NUL5	AK096142	-	CS066	C19orf66	-	0	0	0	0	0	0	direct interact.	0	0	0	0
Q9NYZ3	NM_016426	-	GTSE1	-	-	0	0	0	0	0	0	direct interact.	0	0	0	0
Q9P0J7	NM_020122	-	KCMF1	FIGC	-	0	0	0	0	0	0	direct interact.	0	0	0	0
Q9P219	NM_001080414	-	DAPLE	CCDC88C	-	0	0	0	0	0	0	direct interact.	0	0	0	0
Q9UBL3	BC015936	6.9553	ASH2L	ASH2L1	-	0	0	0	0	0	0	direct interact.	0	0	0	0
Q9UBQ7	AK024386	7.6289	GRHPR	GLXR	-	0	0	0	0	0	0	direct interact.	0	0	0	0
Q9UHF1	AK091964	-	EGFL7	MEGF7	-	0	0	0	0	0	0	direct interact.	0	0	0	0
Q9UHY1	AK122664	6.9663	NRBP	NRBP1	BCON3	0	0	0	0	0	0	direct interact.	0	0	0	0
Q9UJ88	Y12395	6.2046	Q9UJ88	IFRD2	hCG	0	0	0	0	0	0	direct interact.	0	0	0	0
Q9UNE7	NM_005861	6.4561	CHIP	STUB1	-	0	0	0	0	0	0	direct interact.	0	0	0	0
Q9Y3C6	AY359032	7.2984	PPIL1	CYPL1	-	0	0	0	0	0	0	direct interact.	0	0	0	0
Q9Y3X0	AL050284	6.6634	CCDC9	-	-	0	0	0	0	0	0	direct interact.	0	0	0	0
Q9Y534	NM_014460	-	CSDC2	PIPPIN	-	0	0	0	0	0	0	direct interact.	0	0	0	0
Q9Y5A6	NM_145914	-	ZSC21	ZSCAN21	ZFP38	0	0	0	0	0	0	direct interact.	0	0	0	0
Q9Y5Q3	NM_005461	-	MAFB	KRML	-	0	0	0	0	0	0	direct interact.	0	0	0	0
Q9Y6J0	AB002328	-	CABIN	CABIN1	KIAA0330	0	0	0	0	0	0	direct interact.	0	0	0	0
Q9Y6R7	NM_003890	-	FCGBP	-	-	0	0	0	0	0	0	direct interact.	0	0	0	0
Q7Z5L9	NM_182972	6.3165	I2BP2	IRF2BP2	-	0	0	0	0	0	0	0	direct interact.	direct interact.	direct interact.	0
Q9P2K9	NM_020780	-	PTHD2	PTCHD2	DISP3	0	0	0	0	0	0	0	direct interact.	direct interact.	direct interact.	0
P13196	NM_000688	6.8970	HEM1	-	-	0	0	0	0	0	0	0	direct interact.	direct interact.	0	direct interact.
P17038	NM_003423	-	ZNF43	KOX27	-	0	0	0	0	0	0	0	direct interact.	direct interact.	0	0
Q6NYC5	NM_002374	-	Q6NYC5	-	-	0	0	0	0	0	0	0	direct interact.	direct interact.	0	0
O95613	NM_006031	-	PCNT	PCNT2	-	0	0	0	0	0	0	0	direct interact.	0	direct interact.	direct interact.
Q9NS23	NM_170714	-	RASF1	RASSF1	RDA32	0	0	0	0	0	0	0	direct interact.	0	direct interact.	direct interact.
O60331	NM_012398	-	PI51C	PIP5K1C	KIAA0589	0	0	0	0	0	0	0	direct interact.	0	direct interact.	0
P15621	NM_016264	-	ZNF44	GIOT2	-	0	0	0	0	0	0	0	direct interact.	0	direct interact.	0
P17480	NM_001076683	7.4080	UBF1	UBTF	UBF	0	0	0	0	0	0	0	direct interact.	0	direct interact.	0
P30405	NM_005729	7.8572	PPIF	CYP3	-	0	0	0	0	0	0	0	direct interact.	0	direct interact.	0
P52756	AB208813	6.0664	RBM5	H37	-	0	0	0	0	0	0	0	direct interact.	0	direct interact.	0
Q16478	NM_002088	-	GRIK5	GRIK2	-	0	0	0	0	0	0	0	direct interact.	0	direct interact.	0
Q59GA1	AB209208	-	Q59GA1	-	-	0	0	0	0	0	0	0	direct interact.	0	direct interact.	0
Q59H49	AB208910	-	Q59H49	-	-	0	0	0	0	0	0	0	direct interact.	0	direct interact.	0
Q7L945	BC098416	-	ZN627	ZNF627	-	0	0	0	0	0	0	0	direct interact.	0	direct interact.	0
Q8IUX7	NM_001129	-	AEBP1	ACLP	-	0	0	0	0	0	0	0	direct interact.	0	direct interact.	0
Q92879	AB210019	-	CELF1	BRUNOL2	-	0	0	0	0	0	0	0	direct interact.	0	direct interact.	0
Q969V6	BC115039	5.5105	MKL1	KIAA1438	-	0	0	0	0	0	0	0	direct interact.	0	direct interact.	0
Q96CW1	NM_004068	7.2405	AP2M1	CLAPM1	-	0	0	0	0	0	0	0	direct interact.	0	direct interact.	0
Q96PV7	AB067518	-	F193B	FAM193B	KIAA1931	0	0	0	0	0	0	0	direct interact.	0	direct interact.	0
Q9BV10	NM_024105	-	ALG12	PP14673	-	0	0	0	0	0	0	0	direct interact.	0	direct interact.	0
Q9NQV8	NM_020226	-	PRDM8	PFM5	-	0	0	0	0	0	0	0	direct interact.	0	direct interact.	0
Q9NUD5	BC069238	-	ZCHC3	ZCCHC3	C20orf99	0	0	0	0	0	0	0	direct interact.	0	direct interact.	0
Q9NW07	NM_018083	-	ZN358	ZNF358	-	0	0	0	0	0	0	0	direct interact.	0	direct interact.	0
Q9UBN1	NM_014405	-	CCG4	CACNG4	-	0	0	0	0	0	0	0	direct interact.	0	direct interact.	0
P56556	NM_002490	7.0935	NDUA6	-	-	0	0	0	0	0	0	0	direct interact.	0	0	direct interact.
P61353	BF219474	9.0689	RL27	-	-	0	0	0	0	0	0	0	direct interact.	0	0	direct interact.
Q15697	NM_003450	-	ZN174	ZNF174	ZSCAN8	0	0	0	0	0	0	0	direct interact.	0	0	direct interact.
Q6PJ21	BC041897	-	SPSB3	C16orf31	-	0	0	0	0	0	0	0	direct interact.	0	0	direct interact.
Q96G42	BC009980	-	KLD7B	-	-	0	0	0	0	0	0	0	direct interact.	0	0	direct interact.
-	XR_019643	-	-	-	-	0	0	0	0	0	0	0	direct interact.	0	0	0
O15169	AB208876	-	AXIN1	AXIN	-	0	0	0	0	0	0	0	direct interact.	0	0	0
P05412	NM_002228	6.6522	JUN	AP-1	-	0	0	0	0	0	0	0	direct interact.	0	0	0
P30084	NM_004092	7.4695	ECHM	-	-	0	0	0	0	0	0	0	direct interact.	0	0	0
P49674	NM_152221	-	KC1E	-	-	0	0	0	0	0	0	0	direct interact.	0	0	0
P49748	NM_000018	7.4713	ACADV	ACADVL	VLCAD	0	0	0	0	0	0	0	direct interact.	0	0	0
P50749	AY154470	-	RASF2	RASSF2	KIAA0168	0	0	0	0	0	0	0	direct interact.	0	0	0
Q15025	NM_006058	-	TNIP1	KIAA0113	-	0	0	0	0	0	0	0	direct interact.	0	0	0
Q4V348	NM_001032297	-	Z658B	ZNF658B	-	0	0	0	0	0	0	0	direct interact.	0	0	0
Q76LX8	AB069698	-	ATS13	C9orf8	-	0	0	0	0	0	0	0	direct interact.	0	0	0
Q8TF20	NM_133474	-	ZN721	-	-	0	0	0	0	0	0	0	direct interact.	0	0	0
Q8WTV1	NM_138350	-	THAP3	-	-	0	0	0	0	0	0	0	direct interact.	0	0	0
Q96EZ8	NM_006337	-	MCRS1	INO80Q	-	0	0	0	0	0	0	0	direct interact.	0	0	0
Q96JG8	NM_001098800	-	MAGD4	MAGED4	KIAA1859	0	0	0	0	0	0	0	direct interact.	0	0	0
Q9BU23	BC014652	-	LMF2	TMEM112B	-	0	0	0	0	0	0	0	direct interact.	0	0	0
Q9NV79	AB028973	-	PCMD2	PCMTD2	C20orf36	0	0	0	0	0	0	0	direct interact.	0	0	0
Q9P1Y5	NM_001080429	-	CAMP3	CAMSAP3	KIAA1543	0	0	0	0	0	0	0	direct interact.	0	0	0
Q9UK11	BC022466	-	ZN223	ZNF223	-	0	0	0	0	0	0	0	direct interact.	0	0	0
Q9ULX9	NM_001161572-4	6.4362	MAFF	-	-	0	0	0	0	0	0	0	direct interact.	0	0	0
O00459	NM_005027	-	P85B	PIK3R2	-	0	0	0	0	0	0	0	0	direct interact.	direct interact.	0
P08247	BC064550	-	SYPH	SYP	-	0	0	0	0	0	0	0	0	direct interact.	direct interact.	0
P51674	NM_201591	-	GPM6A	M6A	-	0	0	0	0	0	0	0	0	direct interact.	direct interact.	0
P98161	NM_001009944	-	PKD1	-	-	0	0	0	0	0	0	0	0	direct interact.	direct interact.	0
Q01814	AB210008	-	AT2B2	ATP2B2	PMCA2	0	0	0	0	0	0	0	0	direct interact.	direct interact.	0
Q8IWZ8	AY072916	6.3029	SUGP1	SF4	-	0	0	0	0	0	0	0	0	direct interact.	direct interact.	0
Q8IZD0	AK094209	-	SAM14	SAMD14	-	0	0	0	0	0	0	0	0	direct interact.	direct interact.	0
P48509	AK130369	-	CD151	-	-	0	0	0	0	0	0	0	0	direct interact.	0	direct interact.
P62993	NM_002086	7.4483	GRB2	ASH	-	0	0	0	0	0	0	0	0	direct interact.	0	direct interact.
Q68CR1	BC060867	-	SE1L3	-	-	0	0	0	0	0	0	0	0	direct interact.	0	direct interact.
A0AUZ9	NM_152519	-	KAL1L	-	-	0	0	0	0	0	0	0	0	direct interact.	0	0
A6NHR9	NM_015295	7.0601	SMHD1	-	-	0	0	0	0	0	0	0	0	direct interact.	0	0
A8KAG1	NM_182679	-	A8KAG1	-	-	0	0	0	0	0	0	0	0	direct interact.	0	0
AK226126	-	-	-	-	-	0	0	0	0	0	0	0	0	direct interact.	0	0
B3KXJ0	NM_006158	-	B3KXJ0	-	-	0	0	0	0	0	0	0	0	direct interact.	0	0
B9A6J5	NM_015705	-	B9A6J5	-	-	0	0	0	0	0	0	0	0	direct interact.	0	0

						IP-MS						APS				
UniProt AC	RefSeq ID UniPEx-library	SU-DHL-1 iBAQ [log10 of iBAQ intensity]	Name	Synonyms		HL60 [whole cell lysate]	JEKO-1 [whole cell lysate]	OPM2 [nuclear enriched lysate]	U937 [whole cell lysate]	SU-DHL-1 [whole cell lysate]	SU-DHL-1 [nuclear enriched lysate]	C/EBPβ aa1-41 [CR1-2]	C/EBPε aa1-62 [CR2-4]	C/EBPβ aa49-72 [CR3]	C/EBPβ aa153-173 [CR7]	C/EBPβ aa79-196 [CR4-7]
E9KL44	NM_000182	-	E9KL44	-	-	0	0	0	0	0	0	0	0	direct interact.	0	0
O14683	BC045666	-	P5I11	TP53I11	PIG11	0	0	0	0	0	0	0	0	direct interact.	0	0
O60688	CR933630	-	YPEL1	FKSG3	-	0	0	0	0	0	0	0	0	direct interact.	0	0
O75051	NM_025179	-	PLXA2	PLXNA2	-	0	0	0	0	0	0	0	0	direct interact.	0	0
O75934	BC022880	7.4510	SPF27	BCAS2	DAM1	0	0	0	0	0	0	0	0	direct interact.	0	0
O95201	NM_003456	-	ZN205	ZNF205	ZNF210	0	0	0	0	0	0	0	0	direct interact.	0	0
O95721	NM_004782	6.3671	SNP29	SNAP29	-	0	0	0	0	0	0	0	0	direct interact.	0	0
P05060	BC000375	-	SCG1	CHGB	-	0	0	0	0	0	0	0	0	direct interact.	0	0
P06858	NM_000237	-	LIPL	LPL	LIPD	0	0	0	0	0	0	0	0	direct interact.	0	0
P0CG48	-	-	UBC	-	-	0	0	0	0	0	0	0	0	direct interact.	0	0
P10586	NM_002840	-	PTPRF	LAR	-	0	0	0	0	0	0	0	0	direct interact.	0	0
P11413	X03674	7.5171	G6PD	-	-	0	0	0	0	0	0	0	0	direct interact.	0	0
P11766	-	7.7121	ADHX	ADH5	-	0	0	0	0	0	0	0	0	direct interact.	0	0
P13501	-	-	CCL5	-	-	0	0	0	0	0	0	0	0	direct interact.	0	0
P14618	NM_182470	8.9310	KPYM	PKM	OIP3	0	0	0	0	0	0	0	0	direct interact.	0	0
P15923	NM_003200	-	TFE2	TCF3	-	0	0	0	0	0	0	0	0	direct interact.	0	0
P19447	AK127469	6.6059	ERCC3	XPB	-	0	0	0	0	0	0	0	0	direct interact.	0	0
P22607	AB209441	-	FGFR3	JTK4	-	0	0	0	0	0	0	0	0	direct interact.	0	0
P23471	NM_002851	-	PTPRZ	-	-	0	0	0	0	0	0	0	0	direct interact.	0	0
P26232	AK127226	6.0950	CTNA2	CTNNA2	CAPR	0	0	0	0	0	0	0	0	direct interact.	0	0
P33316	NM_001025248	7.7482	DUT	-	-	0	0	0	0	0	0	0	0	direct interact.	0	0
P33992	NM_006739	7.6536	MCM5	CDC46	-	0	0	0	0	0	0	0	0	direct interact.	0	0
P39656	NM_005216	7.8912	OST48	-	-	0	0	0	0	0	0	0	0	direct interact.	0	0
P48147	NM_002726	6.6387	PPCE	-	-	0	0	0	0	0	0	0	0	direct interact.	0	0
P49448	BC050732	-	DHE4	GLUD2	GLUDP1	0	0	0	0	0	0	0	0	direct interact.	0	0
P53365	NM_012402	6.5863	ARFP2	ARFIP2	POR1	0	0	0	0	0	0	0	0	direct interact.	0	0
P54920	NM_003827	7.4669	SNAA	-	-	0	0	0	0	0	0	0	0	direct interact.	0	0
P55212	NM_001226	6.3496	CASP6	-	-	0	0	0	0	0	0	0	0	direct interact.	0	0
P56202	BC048255	-	CATW	CTSW	-	0	0	0	0	0	0	0	0	direct interact.	0	0
P56211	AL833077	-	ARP19	ARPP19	-	0	0	0	0	0	0	0	0	direct interact.	0	0
P60660	-	-	MYL6	-	-	0	0	0	0	0	0	0	0	direct interact.	0	0
Q02880	NM_001068	7.2709	TOP2B	-	-	0	0	0	0	0	0	0	0	direct interact.	0	0
Q07343	NM_001037341	-	PDE4B	-	-	0	0	0	0	0	0	0	0	direct interact.	0	0
Q08117	-	-	AES	GRG	-	0	0	0	0	0	0	0	0	direct interact.	0	0
Q13263	X97548	8.2502	TIF1B	TRIM28	KAP1	0	0	0	0	0	0	0	0	direct interact.	0	0
Q13519	NM_006228	-	PNOC	-	-	0	0	0	0	0	0	0	0	direct interact.	0	0
Q15233	NM_007363	8.6193	NONO	NRB54	-	0	0	0	0	0	0	0	0	direct interact.	0	0
Q15853	NM_003367	-	USF2	-	-	0	0	0	0	0	0	0	0	direct interact.	0	0
Q504Y2	BC094697	-	PKDCC	SGK493	-	0	0	0	0	0	0	0	0	direct interact.	0	0
Q53ET0	BC053562	-	CRTC2	TORC2	-	0	0	0	0	0	0	0	0	direct interact.	0	0
Q53EV1	NM_002871	-	Q53EV1	-	-	0	0	0	0	0	0	0	0	direct interact.	0	0
Q59EQ8	AB209753	-	Q59EQ8	-	-	0	0	0	0	0	0	0	0	direct interact.	0	0
Q59FX6	NM_002850	-	Q59FX6	-	-	0	0	0	0	0	0	0	0	direct interact.	0	0
Q59GG0	AB209149	-	Q59GG0	-	-	0	0	0	0	0	0	0	0	direct interact.	0	0
Q6IQ23	NM_175058	-	PKHA7	PLEKHA7	-	0	0	0	0	0	0	0	0	direct interact.	0	0
Q6NXG8	NM_003959	-	Q6NXG8	HIP1R	-	0	0	0	0	0	0	0	0	direct interact.	0	0
Q6ZMJ6	AK160386	-	Q6ZMJ6	FLJ00420	-	0	0	0	0	0	0	0	0	direct interact.	0	0
Q6ZP65	NM_207311	-	BICR1	-	-	0	0	0	0	0	0	0	0	direct interact.	0	0
Q6ZQU3	AK128722	-	Q6ZQU3	-	-	0	0	0	0	0	0	0	0	direct interact.	0	0
Q7Z3E2	NM_018017	-	CC186	C10orf118	-	0	0	0	0	0	0	0	0	direct interact.	0	0
Q7Z429	AK127640	-	LFG1	GRINA	-	0	0	0	0	0	0	0	0	direct interact.	0	0
Q86Y91	BC044933	5.9745	KI18B	KIF18B	-	0	0	0	0	0	0	0	0	direct interact.	0	0
Q86YD1	NM_017432	-	PTOV1	ACID2	-	0	0	0	0	0	0	0	0	direct interact.	0	0
Q86Z22	AF466367	-	Q86Z22	-	-	0	0	0	0	0	0	0	0	direct interact.	0	0
Q8IVD9	NM_015332	6.5850	NUDC3	NUDCD3	KIAA1068	0	0	0	0	0	0	0	0	direct interact.	0	0
Q8N2K0	NM_001042472	5.8024	ABD12	-	-	0	0	0	0	0	0	0	0	direct interact.	0	0
Q8N5U6	NM_014868	-	RNF10	-	-	0	0	0	0	0	0	0	0	direct interact.	0	0
Q8TBC5	NM_023926	-	ZSC18	-	-	0	0	0	0	0	0	0	0	direct interact.	0	0
Q8WXG9	AF435925	-	GPR98	KIAA0686	-	0	0	0	0	0	0	0	0	direct interact.	0	0
Q92900	NM_002911	7.4770	RENT1	UPF1	KIAA0221	0	0	0	0	0	0	0	0	direct interact.	0	0
Q93063	-	-	EXT2	-	-	0	0	0	0	0	0	0	0	direct interact.	0	0
Q969N2	NM_015937	6.8633	PIGT	-	-	0	0	0	0	0	0	0	0	direct interact.	0	0
Q96HW7	BC015664	6.1340	INT4	INTS4	MSTP093	0	0	0	0	0	0	0	0	direct interact.	0	0
Q96RT7	NM_020461	5.7975	GCP6	TUBGCP6	-	0	0	0	0	0	0	0	0	direct interact.	0	0
Q99569	NM_003628	-	PKP4	-	-	0	0	0	0	0	0	0	0	direct interact.	0	0
Q99608	NM_002487	-	NECD	-	-	0	0	0	0	0	0	0	0	direct interact.	0	0
Q99963	NM_003027	-	SH3G3	-	-	0	0	0	0	0	0	0	0	direct interact.	0	0
Q9BTT6	NM_018214	-	LRRC1	-	-	0	0	0	0	0	0	0	0	direct interact.	0	0
Q9BU62	NM_013318	-	Q9BU62	BAT2L	-	0	0	0	0	0	0	0	0	direct interact.	0	0
Q9BZL6	NM_016457	-	KPCD2	PRKD2	PKD2	0	0	0	0	0	0	0	0	direct interact.	0	0
Q9H0J4	AL136774	-	QRIC2	QRICH2	-	0	0	0	0	0	0	0	0	direct interact.	0	0
Q9H2D6	NM_001039141	-	TARA	TRIOBP	KIAA1662	0	0	0	0	0	0	0	0	direct interact.	0	0
Q9H3T2	NM_030913	-	SEM6C	-	-	0	0	0	0	0	0	0	0	direct interact.	0	0
Q9NP58	BC043423	-	ABCB6	MTABC3	-	0	0	0	0	0	0	0	0	direct interact.	0	0
Q9NPA5	NM_018197	-	ZF64A	ZFP64	ZNF338	0	0	0	0	0	0	0	0	direct interact.	0	0
Q9NT68	-	-	TEN2	TENM2	KIAA1127	0	0	0	0	0	0	0	0	direct interact.	0	0
Q9NXR8	NM_019071	-	ING3	-	-	0	0	0	0	0	0	0	0	direct interact.	0	0
Q9P0L9	NM_016112	-	PK2L1	PKD2L1	PKD2L	0	0	0	0	0	0	0	0	direct interact.	0	0
Q9ULD4	NM_015695	-	BRPF3	-	-	0	0	0	0	0	0	0	0	direct interact.	0	0
Q9Y2Q5	LAMTOR2	-	LTOR2	LAMTOR2	MAPBPIP	0	0	0	0	0	0	0	0	direct interact.	0	0
Q9Y3C8	BC005187	7.2328	UFC1	CGI0126	-	0	0	0	0	0	0	0	0	direct interact.	0	0
Q9Y618	NM_012112	-	NCOR2	SMRT	CTG26	0	0	0	0	0	0	0	0	direct interact.	0	0
Q9Y6X7	AB020671	-	Q9Y6X7	KIAA0864	-	0	0	0	0	0	0	0	0	direct interact.	0	0
P14598	BC002816	-	NCF1	NOXO2	-	0	0	0	0	0	0	0	0	0	direct interact..	0
P78364	NM_004426	-	PHC1	EDR1	-	0	0	0	0	0	0	0	0	0	direct interact..	0
Q9BWG0	AB210026	-	Q9BWG0	MYH10	-	0	0	0	0	0	0	0	0	0	direct interact..	0
Q9H6S3	AK122903	-	ES8L2	EPS8L2	EPS8R2	0	0	0	0	0	0	0	0	0	direct interact..	0
Q8IY33	BC037988	-	MILK2	MICALL2	-	0	0	0	0	0	0	0	0	0	direct interact.	direct interact.
A6NC98	NM_032251	-	CC88B	BRLZ	-	0	0	0	0	0	0	0	0	0	direct interact.	0
A7J992	NM_017934	-	A7J992	PHIP	-	0	0	0	0	0	0	0	0	0	direct interact.	0
O14641	NM_004422	-	DVL2	-	-	0	0	0	0	0	0	0	0	0	direct interact.	0

						IP-MS						APS				
UniProt AC	RefSeq ID UniPEx-library	SU-DHL-1 iBAQ [log10 of iBAQ intensity]	Name	Synonyms		HL60 [whole cell lysate]	JEKO-1 [whole cell lysate]	OPM2 [nuclear enriched lysate]	U937 [whole cell lysate]	SU-DHL-1 [whole cell lysate]	SU-DHL-1 [nuclear enriched lysate]	C/EBPβ aa1-41 [CR1-2]	C/EBPε aa1-62 [CR2-4]	C/EBPβ aa49-72 [CR3]	C/EBPβ aa153-173 [CR7]	C/EBPβ aa79-196 [CR4-7]
O15371	NM_003753	7.6876	EIF3D	EIF3S7	-	0	0	0	0	0	0	0	0	0	direct interact.	0
O43566	NM_006480	6.0393	RGS14	-	-	0	0	0	0	0	0	0	0	0	direct interact.	0
O43896	AB014606	-	KIF1C	-	-	0	0	0	0	0	0	0	0	0	direct interact.	0
O60239	NM_004844	-	3BP5	SH3BP5	SAB	0	0	0	0	0	0	0	0	0	direct interact.	0
O75528	BC009240	6.1765	TADA3	ADA3	-	0	0	0	0	0	0	0	0	0	direct interact.	0
O95157	AB032985	-	NXPH3	-	-	0	0	0	0	0	0	0	0	0	direct interact.	0
P08572	NM_001846	-	CO4A2	COL4A2	-	0	0	0	0	0	0	0	0	0	direct interact.	0
P10072	AK128116	-	HKR1	ZNF875	-	0	0	0	0	0	0	0	0	0	direct interact.	0
P10645	NM_001275	-	CMGA	CHGA	-	0	0	0	0	0	0	0	0	0	direct interact.	0
P19532	NM_006521	-	TFE3	-	-	0	0	0	0	0	0	0	0	0	direct interact.	0
P21810	BC004244	-	PGS1	BGN	SLRR1A	0	0	0	0	0	0	0	0	0	direct interact.	0
P21860	NM_001982	-	ERBB3	HER3	-	0	0	0	0	0	0	0	0	0	direct interact.	0
P24385	NM_053056	-	CCND1	BCL1	-	0	0	0	0	0	0	0	0	0	direct interact.	0
P25098	NM_001619	6.0836	ARBK1	ADRBK1	BARK	0	0	0	0	0	0	0	0	0	direct interact.	0
P42229	NM_003152	-	STA5A	STAT5A	STAT5	0	0	0	0	0	0	0	0	0	direct interact.	0
P43250	NM_002082	-	GRK6	GPRK6	-	0	0	0	0	0	0	0	0	0	direct interact.	0
P48634	NM_080686	7.1212	PRC2A	PRRC2A	BAT2	0	0	0	0	0	0	0	0	0	direct interact.	0
P50281	NM_004995	-	MMP14	-	-	0	0	0	0	0	0	0	0	0	direct interact.	0
P50548	AB209271	-	ERF	-	-	0	0	0	0	0	0	0	0	0	direct interact.	0
P53007	L75823	7.6229	TXTP	SLC25A1	SLC20A3	0	0	0	0	0	0	0	0	0	direct interact.	0
P54725	NM_005053	7.4935	RD23A	RAD23A	-	0	0	0	0	0	0	0	0	0	direct interact.	0
P55072	BC110913	8.3107	TERA	VCP	-	0	0	0	0	0	0	0	0	0	direct interact.	0
P78406	AY349350	7.5120	RAE1L	RAE1	MRNP41	0	0	0	0	0	0	0	0	0	direct interact.	0
Q01130	BC070086	8.4192	SRSF2	SFRS2	-	0	0	0	0	0	0	0	0	0	direct interact.	0
Q02641	BC037311	-	CACB1	CACNB1	CACNLB1	0	0	0	0	0	0	0	0	0	direct interact.	0
Q07955	NM_001078166	-	SRSF1	ASF	-	0	0	0	0	0	0	0	0	0	direct interact.	0
Q12972	NM_138558	7.1746	PP1R8	PPP1R8	ARD1	0	0	0	0	0	0	0	0	0	direct interact.	0
Q13243	BC040209	7.0695	SRSF5	HRS	-	0	0	0	0	0	0	0	0	0	direct interact.	0
Q13867	NM_000386	7.1172	BLMH	-	-	0	0	0	0	0	0	0	0	0	direct interact.	0
Q15056	NM_022170	8.2690	IF4H	EIF4H	KIAA0038	0	0	0	0	0	0	0	0	0	direct interact.	0
Q15758	U53347	8.6190	AAAT	SLC1A5	ASCT2	0	0	0	0	0	0	0	0	0	direct interact.	0
Q16629	AK091425	8.5128	SRSF7	SFRS7	-	0	0	0	0	0	0	0	0	0	direct interact.	0
Q16760	NM_152879	-	DGKD	KIAA0145	-	0	0	0	0	0	0	0	0	0	direct interact.	0
Q1ED39	NM_001012991	-	KNOP1	C16orf88	-	0	0	0	0	0	0	0	0	0	direct interact.	0
Q2L4Q9	NM_001039503	-	PRS53	PRSS53	-	0	0	0	0	0	0	0	0	0	direct interact.	0
Q59EF5	AB209856	-	Q59EF5	-	-	0	0	0	0	0	0	0	0	0	direct interact.	0
Q59FG1	AB209499	-	Q59FG1	-	-	0	0	0	0	0	0	0	0	0	direct interact.	0
Q59G26	AB209283	-	Q59G26	-	-	0	0	0	0	0	0	0	0	0	direct interact.	0
Q59GG3	AB209146	-	Q59GG3	-	-	0	0	0	0	0	0	0	0	0	direct interact.	0
Q5TH69	NM_020340	5.3945	BIG3	ARFGEF3	-	0	0	0	0	0	0	0	0	0	direct interact.	0
Q5XKG8	BC026321	-	Q5XKG8	ZNF334	-	0	0	0	0	0	0	0	0	0	direct interact.	0
Q6VY07	NM_018026	6.2393	PACS1	KIAA1175	-	0	0	0	0	0	0	0	0	0	direct interact.	0
Q7Z2K8	BC052950	-	GRIN1	GPRIN1	KIAA1893	0	0	0	0	0	0	0	0	0	direct interact.	0
Q86V15	DQ217660	-	CASZ1	CST	-	0	0	0	0	0	0	0	0	0	direct interact.	0
Q8IVH2	NM_001012426	-	FOXP4	FKHLA	-	0	0	0	0	0	0	0	0	0	direct interact.	0
Q8IW90	BC040659	-	Q8IW90	MTCH1	-	0	0	0	0	0	0	0	0	0	direct interact.	0
Q8N2S1	NM_001042544	-	LTBP4	-	-	0	0	0	0	0	0	0	0	0	direct interact.	0
Q8N5D0	AB028960	-	WDTC1	KIAA1037	-	0	0	0	0	0	0	0	0	0	direct interact.	0
Q8N5V2	NM_019850	-	NGEF	-	-	0	0	0	0	0	0	0	0	0	direct interact.	0
Q8NDH3	NM_024663	5.9436	PEPL1	NPEPL1	KIAA1974	0	0	0	0	0	0	0	0	0	direct interact.	0
Q8TBB7	NM_003861	-	Q8TBB7	WDR22	DCAF5	0	0	0	0	0	0	0	0	0	direct interact.	0
Q8TCX5	NM_052924	-	RHPN1	KIAA1929	-	0	0	0	0	0	0	0	0	0	direct interact.	0
Q8TDD1	NM_024072	6.4960	DDX54	-	-	0	0	0	0	0	0	0	0	0	direct interact.	0
Q8TEW0	AF196185	5.6315	PARD3	PAR3	-	0	0	0	0	0	0	0	0	0	direct interact.	0
Q8TF61	NM_001080410	-	FBX41	FBXO41	-	0	0	0	0	0	0	0	0	0	direct interact.	0
Q969S8	NM_032019	-	HDA10	HDAC10	-	0	0	0	0	0	0	0	0	0	direct interact.	0
Q96BM9	NM_138795	7.5800	ARL8A	ARL10B	-	0	0	0	0	0	0	0	0	0	direct interact.	0
Q96F46	NM_014339	-	I17RA	IL17RA	IL17R	0	0	0	0	0	0	0	0	0	direct interact.	0
Q96FE7	BC041903	-	P3IP1	PIK3IP1	HGFL	0	0	0	0	0	0	0	0	0	direct interact.	0
Q96GS6	AK090438	-	AB17A	ABHD17A	C19orf27	0	0	0	0	0	0	0	0	0	direct interact.	0
Q96RN5	NM_001003891	6.4106	MED15	ARC105	-	0	0	0	0	0	0	0	0	0	direct interact.	0
Q99758	NM_001089	-	ABCA3	ABC3	-	0	0	0	0	0	0	0	0	0	direct interact.	0
Q9C0B0	NM_001080419	-	UNK	KIAA1753	-	0	0	0	0	0	0	0	0	0	direct interact.	0
Q9H7Z6	M98343	6.0028	KAT8	MOF	-	0	0	0	0	0	0	0	0	0	direct interact.	0
Q9HBL0	NM_022648	-	TENS1	TNS1	TNS	0	0	0	0	0	0	0	0	0	direct interact.	0
Q9NPA3	NM_021242	-	M1IP1	MID1IP1	MIG12	0	0	0	0	0	0	0	0	0	direct interact.	0
Q9NSY0	BC071605	-	NRBP2	PP9320	-	0	0	0	0	0	0	0	0	0	direct interact.	0
Q9NYQ6	AF231024	-	CELR1	CELSR1	CDHF9	0	0	0	0	0	0	0	0	0	direct interact.	0
Q9UEG4	NM_001080417	-	ZN629	ZNF629	KIAA0326	0	0	0	0	0	0	0	0	0	direct interact.	0
Q9UG56	NM_014338	-	PISD	-	-	0	0	0	0	0	0	0	0	0	direct interact.	0
Q9ULW3	NM_013375	7.3073	ABT1	-	-	0	0	0	0	0	0	0	0	0	direct interact.	0
Q9Y2V2	NM_001042476	7.4938	CHSP1	CARHSP1	-	0	0	0	0	0	0	0	0	0	direct interact.	0
Q9Y520	NM_015172	6.5005	PRC2C	PRRC2C	BAT2D1	0	0	0	0	0	0	0	0	0	direct interact.	0
O14908	NM_005716	6.6038	GIPC1	-	-	0	0	0	0	0	0	0	0	0	0	direct interact.
O43296	NM_003417	-	ZN264	ZNF264	-	0	0	0	0	0	0	0	0	0	0	direct interact.
P50502	NM_003932	8.0970	F10A1	-	-	0	0	0	0	0	0	0	0	0	0	direct interact.
P57678	AF177341	6.5901	GEMI4	-	-	0	0	0	0	0	0	0	0	0	0	direct interact.
P80404	NM_000663	-	GABT	-	-	0	0	0	0	0	0	0	0	0	0	direct interact.
P84098	BF698920	8.7034	RL19	-	-	0	0	0	0	0	0	0	0	0	0	direct interact.
Q86V86	NM_001001852	-	PIM3	-	-	0	0	0	0	0	0	0	0	0	0	direct interact.
Q92664	AK057993	-	TF3A	-	-	0	0	0	0	0	0	0	0	0	0	direct interact.
Q96FF9	BC011000	-	CDCA5	-	-	0	0	0	0	0	0	0	0	0	0	direct interact.
Q9BUJ2	NM_007040	7.7783	HNRL1	-	-	0	0	0	0	0	0	0	0	0	0	direct interact.
Q9UKS6	AF130979	-	PACN3	SH3	-	0	0	0	0	0	0	0	0	0	0	direct interact.

PUBLICATIONS

Böhm, Julia Wiebke*, Kahlert, G.*, Kowenz-Leutz, E., Pless, O., Dittmar, G., and Leutz,A. (2014). "A comprehensive C/EBPβ interactome". *these authors contributed equally to this work

IN RESUBMISSION PROCESS

Grimm, C., Chavez, L., Vilardell, M., Farrall, A.L., Tierling, S., Böhm, Julia Wiebke, Grote, P., Lienhard, M., Dietrich, J., Timmermann, B., et al. (2013). "DNA-Methylome Analysis of Mouse Intestinal Adenoma Identifies a Tumour-Specific Signature That Is Partly Conserved in Human Colon Cancer". PLoS Genet 9, e1003250.

Berlin, 25th January 2015

ACKNOWLEDGEMENTS

I would like to greatly thank Prof. Dr. Achim Leutz for giving me the opportunity to work as a member of his research group at the Max Delbrück Center for Molecular Medicine (MDC).
My thank goes to the Max-Delbrück-Centre for Molecular Medicine (MDC) and the Helmholtz-Zentrum Geesthacht / Berlin-Brandenburg Center for Regenerative Therapies (BCRT) for the financing of this PhD thesis.
I would like to thank Dr. Gunnar Dittmar and Günther Kahlert for the pleasant cooperation, assistance and helpful discussions concerning mass spectrometry analysis.
I would like to thank Maria Hofstätter for the kind cooperation in connection with the APS screening. I would like to thank Dr. Elisabeth Kowenz-Leutz, Dr. Bilyana Stoilova and Dr. Jörg Schönheit for providing the C/EBPβ retroviral constructs, the C/EBPβ$^{-/-}$ MEF cells and the associated protocols. Additional thanks goes to Dr. Elisabeth Kowenz-Leutz and Maria Knoblich for assistance concerning any kind of laboratory problems.
I would like to thank all lab members of the Leutz lab at the MDC and BCRT and the members of the Dittmar lab for the pleasant time during the 3 years of my PhD thesis.
Thanks goes to Dr. Hans-Peter Rahn from the MDC Flow Cytomerty facility for FACS cell sorting and advice.
Thanks goes to the MDC PhD office and Sylvia Sibilak for assistance with administrative issues.
Furthermore, I would like to thank Prof. Dr. Matthias Selbach and Prof. Dr. Udo Heinemann for acting as referees of this thesis.
A special thanks goes to my family, my parents Martina and Gerhard Böhm, my grandparents, my godparent Andreas, to my precious long-standing friends and not least to Charlie for continually supporting and encouraging me.

Julia Wiebke Böhm
Berlin, 25th January 2015

SELBSTSTÄNDIGKEITSERKLÄRUNG

Hiermit erkläre ich, die vorliegende Arbeit selbstständig und nur unter Zuhilfenahme der angegebenen Quellen und Hilfsmittel verfasst zu haben.

Ich erkläre mich nicht anderwärtig um einen Doktorgrad beworben zu haben bzw. einen entsprechenden Doktorgrad zu besitzen.

Ich habe die dem Verfahren zugrunde liegende Promotionsordnung der Mathematisch-Naturwissenschaftlichen Fakultät I / der Lebenswissenschaftlichen Fakultät der Humboldt-Universität zu Berlin zur Kenntnis genommen.

Julia Wiebke Böhm

Berlin, den